Investigation and GIS Development of the Buried Holocene-Pleistocene Surface in the Louisiana Coastal Plain

A technical report to accompany final digital deliverables for contract
CPRA-2013-TO11SBO1-DR
Prepared for and submitted to the
Coastal Protection and Restoration Authority of Louisiana

Paul Heinrich, Robert Paulsell, Riley Milner, John Snead, and Hampton Peele

November 2015

Louisiana Geological Survey
Louisiana State University
Baton Rouge, Louisiana

Recommended Citation:

Heinrich, Paul, Robert Paulsell, Riley Milner, John Snead and Hampton Peele, 2015, Investigation and GIS development of the buried Holocene-Pleistocene surface in the Louisiana coastal plain: Baton Rouge, LA, Louisiana Geological Survey-Louisiana State University *for* Coastal Protection and Restoration Authority of Louisiana, 140 p., 3 pls.

Table of Contents

List of figures

List of tables

List of map plates

Adobe portable document format (.pdf)

Abstract

The Louisiana Geological Survey was contracted by The Water Institute of Gulf on behalf of Coastal Protection and Restoration Authority of Louisiana to investigate, assess, and develop a three-dimensional GIS dataset of the buried Holocene-Pleistocene surface, a regional unconformity sometimes known as the "base of the Holocene", for coastal Louisiana.

This investigation was undertaken because of a lack of a single comprehensive map delineating the Holocene-Pleistocene surface that covers the entire Louisiana coastal plain and coastal waters. Rather, the available data consisted of maps created by various authors at different times in different study areas and using different criteria. As a result, many gaps exist in the coverage of these maps as well as conflicts in their interpretation.

The technical work conducted for this project consisted of: (1) a search and investigation of 15,863 existing published and unpublished boring locations; (2) an assessment of the effectiveness of the source data; (3) data development and compilation of 3,012 useful H-P data points; (4) the development of a GIS dataset of the Holocene-Pleistocene surface; and (5) the preparation of deliverable GIS datasets, digital maps, and a final report with an interpretation of the data.

It is intended that the Holocene-Pleistocene surface model of the entire Louisiana coastal plain will offer improvement in understanding geologic variables in engineering design for coastal restoration projects, reduce uncertainties in accessing future geo-environmental conditions, support decision-making on coastal issues, and help improve data and assumptions used in predictive subsidence modeling.

Introduction

The geology of the Louisiana coastal plain has been much studied since the early 20th century. A large number of existing geologic maps and textual data exist. However most such maps are very small-scale paper prints and many are now obsolete with the existence of newer data. Scale and detail level vary dramatically and few of the legacy maps cover the entire coastal plain. Surface geology sources have been synthesized several times in recent years but subsurface data is sparse in the Quaternary Period, most of the drilling having been done by oil exploration searching for far older and deeper geologic units.

As part of a two-year project for the Coastal Protection and Restoration Authority (CPRA), under a contract from The Water Institute of the Gulf (TWIG), the Louisiana Geological Survey (LGS) undertook research involving the compilation and development of a geographic information system (GIS) dataset of a regional unconformity commonly known as the "Base of the Holocene" of the Louisiana coastal plain and coastal waters.

In this report, the term "Holocene-Pleistocene surface" (or H-P surface) will be used because the unconformity is time-transgressive in nature and can be old as the Late Wisconsinan period, about 20,000 years ago during the end of the last period of continental glaciation in North America. The H-P surface depicts the elevation relative to mean sea level and the general topography of the three-dimensional contact surface now buried beneath the Louisiana coastal plain. From this, the relative thickness of the Holocene stratigraphic interval above can be determined which is of great interest in subsidence modeling.

In a previous study for the CPRA (*Heinrich et al., 2011a)*, this team investigated and digitized 23 original maps from 18 previous studies of Holocene and Pleistocene stratigraphy in southern Louisiana that could give data useful for determining the H-P surface. As a result, it was determined that the small study areas, large coverage gaps, and differing mapping criteria over time would make it impossible to compile this data into a regional coverage. More problematic was that the source data mostly consisted of isopleth maps of the authors personal interpretation of the surfaces, often mapped with little or no included references to the original data used to determine the depth and topography of the surface.

These interpretations ranged from conservative trend slopes to highly imaginative contouring with an extensive network of detailed paleochannels. It was clear that previous interpretations could not be effectively assessed for accuracy nor be properly compiled together with other sources. Extracting data from the legacy isopleths would result in an interpolation of interpolations. It was necessary to return to original samples, boring logs, and tabular bore hole data in order to create a consistent surface over the entire Louisiana coastal plain.

The objectives of this study were to locate, investigate and compile these records into a dataset and prepare a GIS of the Holocene-Pleistocene surface suitable for use by coastal scientists for research, planning and assessment of coastal restoration and protection studies and projects. Data is delivered as a GIS dataset with 3-D surface interpolations, and also as cartographically developed maps and PDF files.

The study area can be characterized as the Louisiana coastal plain and the adjacent portion of the continental shelf, roughly the area between 88.5° and 94° West Longitude and between 28.5° and 31° North Latitude. The boundaries of the developed H-P surface map area are smaller, being bounded landward by the exposed Pleistocene formations and seaward by the extent of the useable source data.

The Holocene-Pleistocene surface is a geologic element of value for coastal protection and restoration planning within the Louisiana Coastal Zone for two primary reasons. The first is better knowledge of the geologic structures related to coastal subsidence. The overlying topstratum deposits (mostly Holocene) compact with time. It has been estimated that processes within the topstratum deposits (notably sediment compaction) typically account for at least 80% of the subsidence as measured at the land surface *(Törnqvist, 2013)*. Better mapping of the H-P surface enables better understanding of the thickness of the Holocene interval. Better awareness of the thickness of this interval offers insight into significant coastal subsidence that is related to Holocene compaction.

Secondly, better knowledge of the Holocene-Pleistocene surface provides planners with data for considering coastal engineering structures requiring stable sediment bases or pilings reaching to stable Pleistocene sediments that immediately underlie this contact.

The target user groups for this research and development project are the geologists, engineers, and environmental scientists involved in coastal protection and restoration investigations. The datasets help provide the geologic framework needed to make geologic assessments in a GIS format that can be used with physical, environmental, socio-political, engineering, and other GIS data appropriate to coastal planning and decision-making. It is understood that many non-geologists will be interested in this information, so a glossary of terms is included.

Regional geology

The modern Louisiana coastal plain was largely formed in the geologically recent Quaternary period (2.58 million years ago to present), which is divided into the Pleistocene and Holocene Epochs. The Pleistocene is the geologic time interval spanning the world's most recent period of repeated glaciations, colloquially known as the “Ice Age”. The Holocene is the time following the last glaciation and is the geologic time in which we live (11,700 years ago to present). Geologically speaking, all of the Quaternary is composed of relatively young geologic deposits.

The coalescing alluvial and deltaic deposits of many coastal rivers and streams formed the northern Gulf of Mexico coastal plain. These deposits are composed of gravel, sand, silt, and clay particles lain down by streams of various size, velocities, and sediment loads as they cross the coastal plain to reach the sea. The Louisiana coastal plain itself is distinguished by the presence of the massive alluvial and deltaic deposits of the Mississippi River, the continent’s largest river system.

In reaching the sea, some of these riverine deposits have been reworked by marine processes into headland, barrier island, chenier, and lagoon deposits. But sea level has not been static. During Pleistocene glacial advances, sea levels were at times significantly lower due to much of the world’s water being frozen in giant continental glaciers. Coastal streams were forced to erode their valleys down to meet a lower mean sea level and also to extend their courses a greater distance to meet a shoreline further offshore than present. At other times during interglacial periods, sea level was higher than at present leaving relict coastal barrier landforms and other deposits high on the coastal plain when the ocean again retreated. The sea is described as having transgressed landward in this case ***(Figure 1)***.

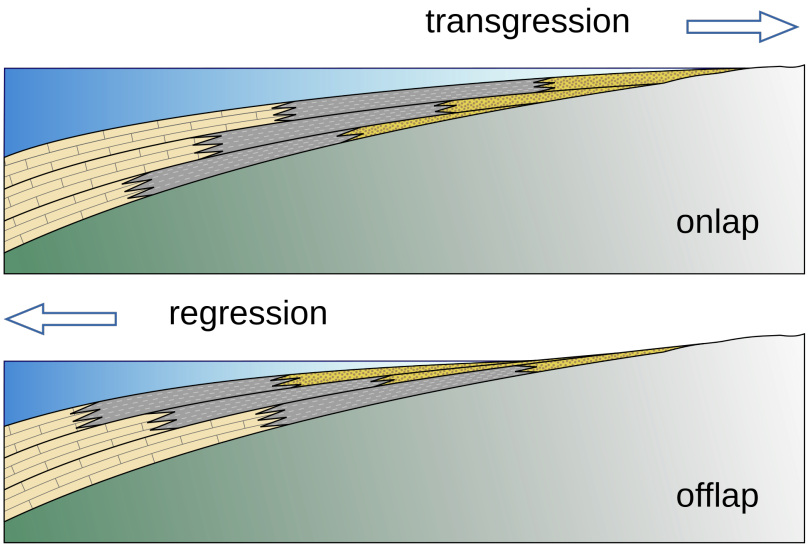

Figure 1 – Marine Transgression. *Two diagrams illustrating the shift of sedimentary facies during regression and transgression. (Woudloper, 2009).*

The process has resulted in the creation of a regional geologic contact surface between the Pleistocene and Holocene deposits. In most places, this contact is an unconformity, indicating that sediment deposition was not continuous. The older layer was exposed to erosion for an interval of time before deposition of the younger. This type of erosion can leave channels and paleosols (fossil soils) in the sediment record, which can help identify the Holocene-Pleistocene surface.

During the last marine transgression, starting during terminal Pleistocene time and continuing through the Holocene Epoch to the present, large quantities of fluvial, deltaic, and marine sediments were deposited within the Louisiana coastal plain to form the sedimentary units beneath the Mississippi River alluvial valley, the delta plain and adjacent Louisiana chenier plain *(**Figure 2**).*

***Figure 2 –Surface geology and geographic regions of the Louisiana coastal plain**. Locations of the cross section in figures 3 and 4 are shown. Adapted from Snead and McCulloh (1984) and Spearing (1995).*

The delta was formed by the Mississippi River as its channels regularly shifted through time to deposit its sediment in a rough fan where it meets the Gulf of Mexico. The chenier plain was formed when longshore marine currents re-deposited Mississippi River sediment westward forming a series of signature coast-parallel ridges known as cheniers along the western Louisiana coastal plain.

The surficial geologic deposits of the Louisiana coastal plain can be differentiated into three major sedimentary units ***(Figures 2, 3, and 4)***. The oldest of these deposits consist of

sediments of the Prairie allogroup that were deposited during the last interglacial stage, known as the Sangamon interglacial. They comprise the lowest of the terraced Pleistocene deposits that stand landward above the modern coastal marshes and alluvial bottomland. But they also extend gulfward beneath these Holocene deposits. They underlie what was the surface (now buried) of the Late Pleistocene coastal plain during the lowstand of sea level that occurred during the last glacial maximum about 29,000 to 11,000 years ago ***(Figure 5)***, known as the Wisconsin glaciation.

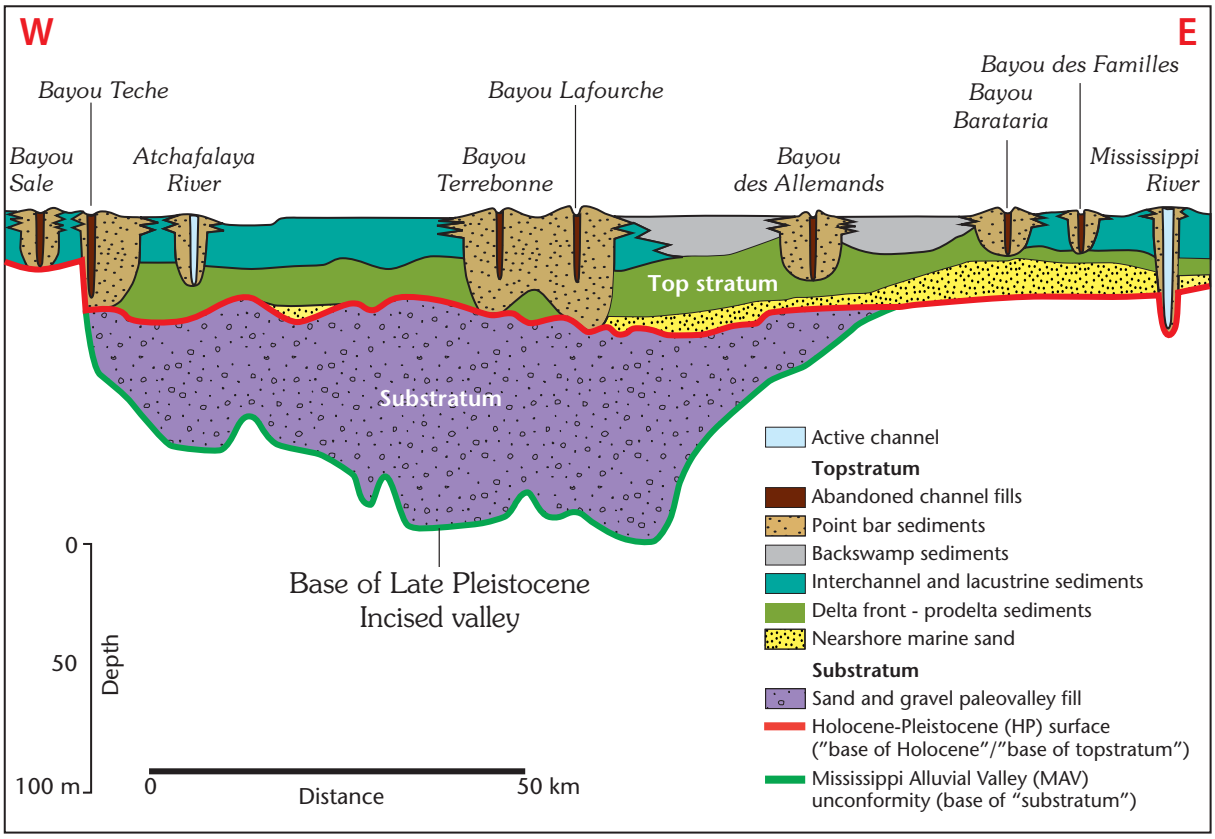

Figure 3 – West-East cross-section across the Mississippi River Delta *showing stratigraphic units. Adapted from Autin et al. (1991).*

The second set of stratigraphic units consist of the Wisconsin valley fills of the Mississippi Alluvial Valley, which is informally known as the "substratum" ***(Figure 3)***, within the Mississippi Alluvial Valley and the Wisconsin valley fills of the Deweyville allogroup within the valleys of smaller rivers that empty into the Gulf of Mexico. Although exposed as braid belts in north Louisiana where it forms the Macon Ridge alloformation, the Wisconsin valley fill is an entirely buried substratum in the study area.

Overlying both the Prairie allogroup and the substratum is the third major stratigraphic unit, the Holocene, comprised of river alluvium, and deltaic deposits now surfaced with backwamps, coastal marshes and natural levees. Some terminal Pleistocene sediments of the Mississippi River (informally known as the "topstratum") are included within the Mississippi Alluvial Valley.

The topstratum is separated from the underlying substratum and Late Pleistocene deposits of the Prairie allogroup by a regional unconformity, which is informally and commonly known as the "Base of the Holocene" and by Quaternary geologists as the "Holocene-Pleistocene surface" ***(Figures 3 and 4)***.

Within the Louisiana Chenier Plain, the Holocene-Pleistocene surface separates the Holocene Mermentau alloformation from the underlying Deweyville and Prairie allogroups of the Pleistocene ***(Figure 4)***. There are fewer and smaller substratum deposits in the Chenier Plain and they are separated by the "Sabine-Trinity unconformity".

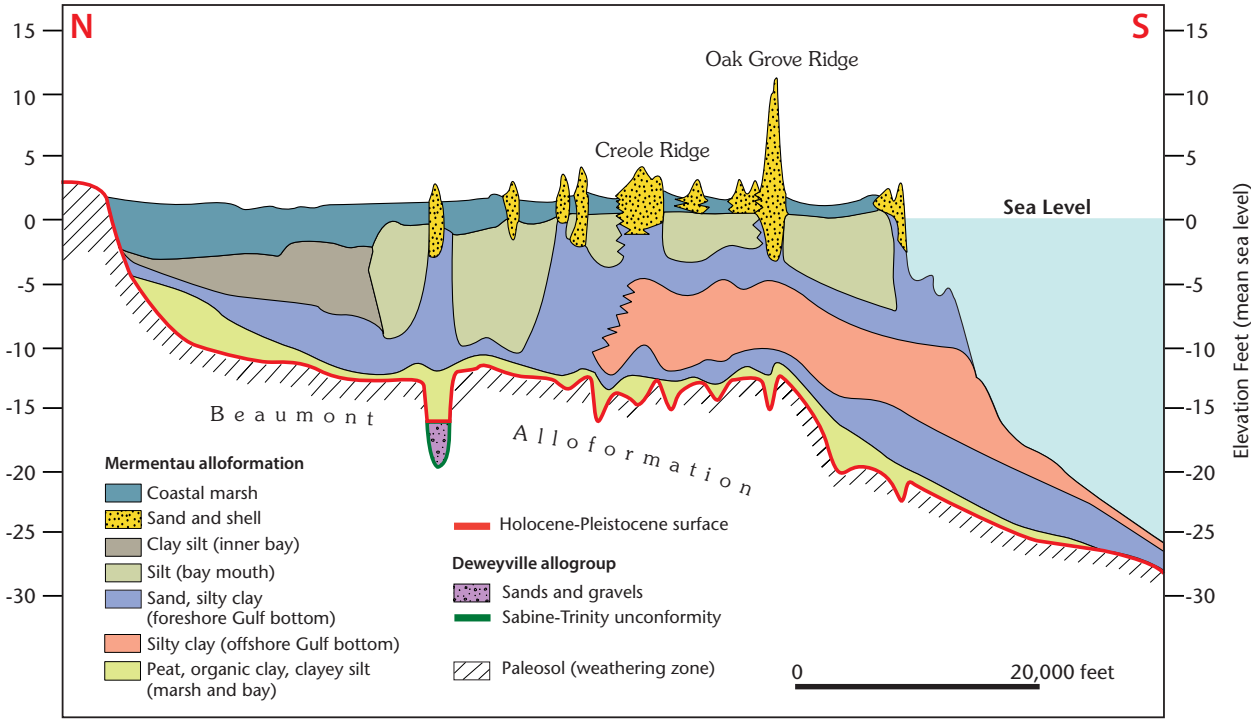

Figure 4 – *North-South cross-section across the Louisiana Chenier Plain showing sedimentary facies and bounding unconformities of Mermentau alloformation. The Holocene-Pleistocene surface is the bottom bounding unconformity of the Mermentau alloformation. Adapted from Gould and McFarlan (1959).*

The Holocene deposits and the substratum are separated from the older deposits of the Prairie allogroup by distinct unconformities created by the entrenchment of fluvial systems during the Late Wisconsin. Within the Mississippi alluvial valley, this unconformity is informally called the "Mississippi Alluvial Valley unconformity."

These surfaces have been confused and conflated by different investigators in the past and remain a complication in determining the H-P surface using data from previous reports without access to their original boring logs.

Traditional sedimentary units in geology are defined by their stratigraphic position and their lithology. This is effective in older hard-rock geology with extensive beds of consistent rock types. But the largely unconsolidated and recent riverine deposits of the coastal plain are laid down by dynamic and shifting rivers and leave small and widely varying packages of sediment juxtaposed among each other.

All of these depositional units are composed of gravel, sand, silt and clay sediments in varying portions and sometimes in complex interfingering facies. Traditional lithologic formation descriptions are of less value here and Quaternary geologists must often use other distinguishing criteria. For surface geologic units, morphologic criteria are useful and units can be described by their characteristic landforms (terraces, natural levees, backswamp, etc.).

But when assessing these units in the subsurface, it becomes useful to define them as alloformations, where the lens of sediment is described by its bounding unconformities. Several related alloformations can be considered together as an allogroup.

1. Sangamonian sediments (Prairie allogroup)

The oldest sediments exposed within the study area are those of the Hammond, Avoyelles, and Beaumont alloformations of the Prairie allogroup deposited during the Sangamon interglacial. They underlie the coast-parallel Prairie terrace and are onlapped by Holocene marsh and other sediments. The fluvial-deltaic sediments of the Hammond alloformation are found east of the Mississippi Alluvial Valley and the fluvial-deltaic sediments of the Beaumont and Avoyelles alloformations are found to the west.

Hammond alloformation **–** East of the Mississippi Alluvial Valley, sediments of the Hammond alloformation underlie the Prairie terraces that form the northern border of marshes and swamps bordering Lake Pontchartrain and extend seaward beneath them. The Hammond alloformation underlies 10 to 25 mi (16 to 40 km) wide coast-parallel terrace, which extends eastward from the eastern valley wall of Mississippi Alluvial Valley across the Feliciana parishes to the Pearl River valley.

This is the lowest and best preserved of the coast-parallel terraces that occur within eastern Louisiana. The surface of this relict coastal plain exhibits moderately to poorly preserved relict constructional landforms, which include relict river courses, meander loops, ridge and swale topography, coastal ridges, and beach ridges. In some areas, the valley walls and floodplains of paleovalleys incised into this surface can be seen. In places, faulting has displaced the surface of this coast-parallel terrace creating numerous fault-line scarps.

The sediments that comprise the Hammond alloformation accumulated within a diverse suite of coastal plain settings, i.e., fluvial (meander-belt and backswamp), colluvial, estuarine, deltaic, and shallow marine environments as indicated by the relict landforms associated with them. These sediments and relict landforms date to the high sea levels of the Marine Isotope Stage 5 that existed prior to 82,000 years ago *(**Figure 5**)(Mossa and Autin 1989; Autin et al. 1991; McCulloh et al. 2003; Heinrich and McCulloh 2004, Heinrich 2006a).*

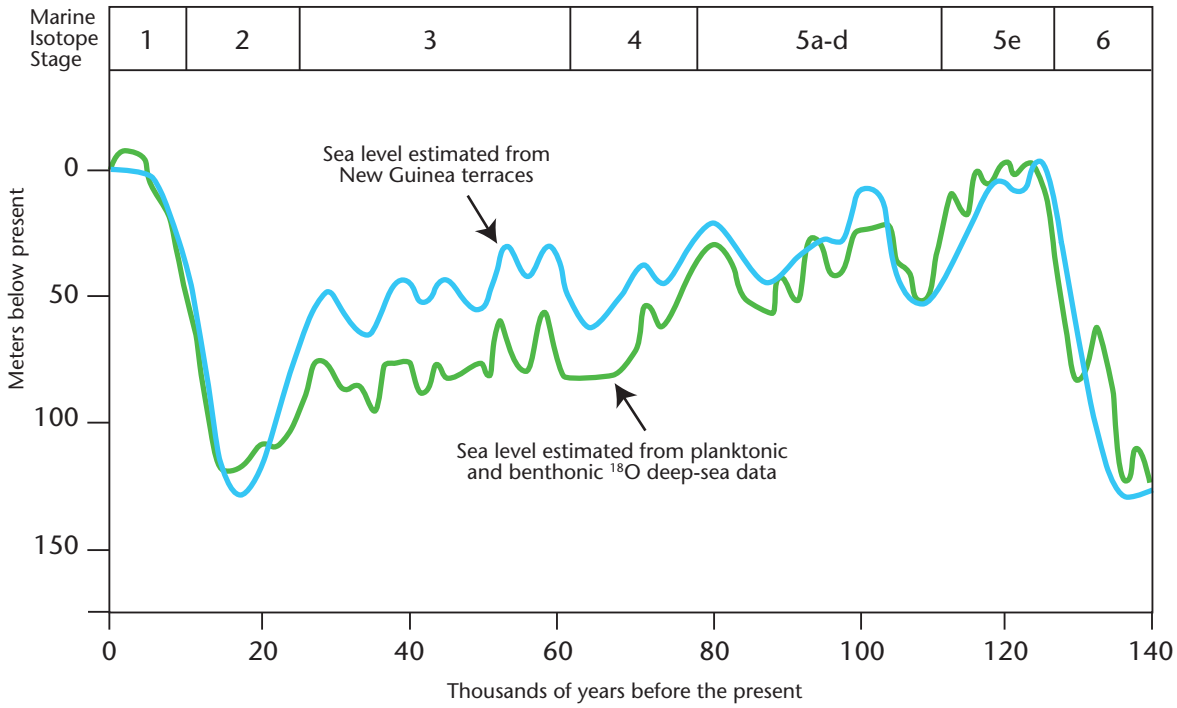

Figure 5 – Global sea level changes over the last 140,000 years, *according to the isotopic record of deep-sea cores and New Guinea marine terraces.*

Further south within the New Orleans region and buried beneath the deltaic sediments of the topstratum, younger Pleistocene deposits underlie the surface of the regional Late Pleistocene coastal plain of the Last Glacial Maximum. These also consist of sediments that accumulated within a diverse suite of coastal plain settings, i.e., fluvial (meander-belt and backswamp), colluvial, estuarine, deltaic, and shallow marine environments. These sediments overlie the sediments of the Hammond alloformation *(Kolb et al. 1975; Miller 1983; Saucier and Snowden 1995)*.

Avoyelles alloformation – Immediately west of the Mississippi alluvial valley, sediments of the Avoyelles alloformation underlie a Pleistocene surface that forms the southernmost segment of the western valley wall of the Mississippi Alluvial Valley. The Avoyelles alloformation underlies a triangular 0 to 22 mi (0 to 35 km) wide surface, which extends eastward from the western valley wall of Mississippi Alluvial Valley from New Iberia, Louisiana to Abbeville, Louisiana, and just west of Intracoastal City, Louisiana *(Heinrich, 2006b; Heinrich et al 2003)*. This surface crosscuts older, loess-covered fluvial-deltaic plains of the Red River, which are underlain by the Beaumont alloformation *(Saucier, 1994; Shen et al., 2012)*.

This is the lowest and best preserved of the coast-parallel terraces that occur within western Louisiana. The surface of this terrace exhibits moderately to poorly preserved relict constructional landforms relict river courses, meander loops, and ridge and swale topography that are comparable in size to those of the modern Mississippi River. These relict fluvial landforms comprise an ancient Late Pleistocene Mississippi River meander belt, which is known as the "Lafayette Meander Belt" *(Fisk, 1940; Saucier, 1994; Shen et al., 2012)*. In places, the surface of this relict meander belt has been displaced by faulting to form fault-line scarps. The sediments that comprise the Avoyelles alloformation accumulated within the Late Pleistocene Lafayette meander belt *(Heinrich, 2005a).* As illustrated by *Wellner et al., (2004),* the ancient delta associated with this meander belt now lies underwater and offshore of Cameron Parish where it forms the part of the southern edge of the Louisiana Continental Shelf.

The Avoyelles alloformation consists largely of thick point bar, crevasse, and overbank sediments. The channel deposits are overlain by 2–4 m of Mississippi River overbank deposits. In turn, the overbank sediments are veneered by 2–5 m of Peoria Loess *(Saucier, 1994; Shen et al., 2012)*. The base of this allostratigraphic unit is a time-transgressive, compound unconformity created by the slight incision and lateral migration of the ancient Mississippi River into the Beaumont alloformation and older units.

Beaumont alloformation – West of the Lafayette meander belt and associated alluvial plain, lays an extensive coast-parallel terrace that forms the surface of the Beaumont alloformation. Except where cut by valleys formed during sea level lowstands of the last glacial stage, this surface and upper boundary of the Beaumont alloformation within the

study area consists of the surface of the Gulf of Mexico coastal plain from Mississippi River Valley to the valley of the Rio Grande *(Winker, 1991)*. The surface of Beaumont alloformation exhibits moderately well preserved relict depositional topography of the Red and Calcasieu Rivers and small streams *(Aronow, 1986; Winker, 1991; Saucier and Snead, 1989)*.

The Beaumont alloformation consists of 30 to 60 m of clay-rich sediments enclosing dip-oriented fluvial sands, sandy fluvial, and deltaic-distributary channels. It also includes an isolated segment of a coast-parallel, sandy beach ridge known as the Ingleside barrier/strandplain system *(Barrilleaux, 1986).* These sediments accumulated as short depositional episodes during multiple high-frequency glacio-eustatic sea-level fluctuations. According to downdip correlations by *Young et al. (2012)*, the Beaumont alloformation began accumulating 600,000 years ago.

The Beaumont alloformation is an unconformity bounded stratigraphic unit. As defined and mapped by *Young et al. (2012),* it is separated from the underlying Lissie Formation by a regional unconformity. This regional unconformity is an extensive flooding surface that is correlated with micropaleontological zones offshore and a well-defined regional terrace surface updip. This flooding surface is correlated northward along the bases of major channel sands to where the Beaumont alloformation onlaps onto the surface of the Lissie Formation *(Young et al. 2012).*

2. Wisconsinan sediments (substratum and Deweyville allogroup)

Within the Louisiana Coastal zone, Wisconsinan-age sediments are preserved within valleys cut into the strata of the Prairie allogroup. Within the Mississippi Alluvial Valley, its bottom is filled with Wisconsin sand and gravels deposited by glacial meltwaters that traveled down it. In the Lower Mississippi River valley north of the study area, these glacial outwash sediments form extensive terraced braid belts at the surface. Within the study area, younger, largely Holocene, fluvial-deltaic deposits bury these sediments. In smaller river systems, down which glacial meltwaters did not flow, Wisconsin-age fluvial sands and gravels of the Deweyville allogroup fill the bottom of the entrenched valleys to lower, contemporaneous sea levels.

The Substratum– Beneath the Mississippi River floodplain and delta, the late Pleistocene paleovalley of the Mississippi River is filled by a thick sequence of fluvial sands and gravelly sand ***(Figure 3)***. They rest within the paleovalley formed by the Mississippi Alluvial Valley unconformity and separate from younger, typically finer-grained sediments by the Holocene-Pleistocene surface. These sediments were first recognized and named the "substratum" by *Fisk (1944)*. They consist largely of sands and gravels which were deposited by a series of braided meltwater river systems that were fed by North American ice sheet and large proglacial lakes during Marine Isotope Stages 2, 3, and 4 from about

80,000 to 11,000 years ago ***(Figure 5)***. These river systems occupied a paleovalley that was incised through the terrace surfaces of the Prairie allogroup to a shoreline that was located at the continental shelf-margin and as much as 120 m lower in elevation than present *(Fisk 1944; Saucier 1994; Rittenour et al. 2007; Blum and Roberts 2012)*.

An unconformity, informally designated for this study as the "Mississippi Alluvial Valley unconformity", separates the substratum that underlies the floor of the Mississippi River Valley from older Pleistocene deposits of the Hammond alloformation ***(Figure 3)***. It is an unconformity that forms the base of a deep Late Pleistocene paleovalley of the Mississippi River. This unconformity was first illustrated by *Fisk (1944)* and later mapped in more detail by *May et al. (1984), Saucier (1994)*, and others. In their mapping of the Louisiana Coastal Zone, they tend to conflate the Mississippi Alluvial Valley unconformity and the Holocene-Pleistocene surface. Although widely regarded to have been once the subaerially exposed as the surface of the Mississippi Alluvial Valley during the Last Glacial Maximum (Marine Isotope Stage 2) lowstand of sea level, it is likely a polygenetic unconformity created by both subaqueous channel and subaerial erosion at different periods of time during Wisconsin Age.

The Deweyville allogroup – The Deweyville allogroup lies largely buried beneath the Mermentau alloformation within the Louisiana Chenier Plain. Where exposed, it forms prominent terraces along the major rivers north of the Louisiana Chenier Plain (*Heinrich, 2005b; Heinrich 2006a*). There is no identified coastwise equivalent to the alluvial Deweyville unit.

The Deweyville allogroup consists of largely coarse-grained fluvial sediments that fill the valleys of the Calcasieu, Sabine, and Houston rivers and their tributaries. It consists of separate unconformity-bounded allostratigraphic units with terraces as their upper boundaries and fluvial entrenchment surfaces as their lower boundaries ***(Figure 4)***. The coarse-grained valley fills of the Deweyville allogroup represents; (a) the abandonment and entrenchment of valleys within the Beaumont alluvial plains by river systems about 100,000 years ago; and (b) multiple episodes of lateral migration, aggradation, and/or degradation within those valleys during the Marine Isotope Stages 4, 3, and 2. These fluvial systems were graded to shorelines at midshelf or farther south (*Blum et al. 1995*).

Where buried at the base of the Calcasieu River Valley, the sediments of the Deweyville alloformation are separated by the Holocene-Pleistocene surface created by flooding of the coastal plain by sea level rise and the postglacial lateral migration of streams and rivers from younger undifferentiated Holocene fluvial, estuarine, and chenier plain sediments. The exposed surface of the Deweyville exhibits well-preserved oversized fluvial features.

3. The Holocene-Pleistocene surface

Separating the Late Pleistocene sediments of the substratum and Prairie allogroups from younger terminal Pleistocene and Holocene fluvial and deltaic deposits of the topstratum is an unconformity that can be referred to as "base of the Holocene" or the "top of the Pleistocene"(***Figures 3 and 4***). For this study it is called the "Holocene-Pleistocene surface" (or H-P surface) because in the gulfward portions of its extent, it is as old as Late Wisconsin and is in places described as the "Late Wisconsin unconformity." This is a regional unconformity that extends along the Gulf of Mexico coast from at least the Central Texas continental shelf, where it is known as the "Holocene-Pleistocene exposure surface," across the Louisiana coastal plain and continental shelf and eastward of the Chandeleur Islands, where it is known as the "Late Wisconsin unconformity."

Overall, the Holocene-Pleistocene surface represents the former Late Pleistocene coastal plain during last lowstand of sea level that occurred during the Last Glacial Maximum of Marine Isotope Stage 2 about 29,000 to 11,000 years ago. The gulfward portion of this former coastal plain was flooded from about 18,000 to 4,000 years ago as deglaciation led to a rapid rise in sea level across this low relief coastal plain *(**Figure 4**)*. As the Mississippi River filled its alluvial valley and its delta built gulfward across this surface, it was buried by shallow marine, fluvial, and deltaic sediments of the topstratum as sea level stabilized *(Siringan 1993; Saucier 1994; Kulp et al. 2002; Milliken et al. 2008; Blum and Roberts 2012)*

In soil borings, the position of the Holocene-Pleistocene surface is often, but not always, readily determinable. Outside of the Mississippi Alluvial Valley, there exists a sharp change at this contact between the typically dark gray or blue gray to fairly black topstratum deposits and the characteristically oxidized yellow, tan, and orange or greenish gray paleosols of Late Pleistocene deposits where they lie at a depths of 15 m (50 ft.) or less below sea level. At depths greater than 15 m (50 ft.), the tan oxidized coloring is often absent and is replaced entirely by a greenish-gray cast. Then the contact is not as readily determined by color and other characteristics of Pleistocene deposits distinguishing them from overlying topstratum. These characteristics include a marked decrease in water content; a distinctive stiffening of soil consistency; a decrease in rate of penetration of sampling devices; an increase in soil strength; and the occurrence of calcareous concretions. Within the Mississippi Alluvial Valley, the contact is generally marked by a change from fine-grained flood basin sediments to coarse-grained braided stream sediments *(Kolb and Van Lopik 1958; Saucier 1994).*

4. The Holocene topstratum

Overlying the Holocene-Pleistocene surface and immediately underlying the surface of the modern Mississippi Alluvial Valley is a largely Holocene stratigraphic unit that is informally known as the "topstratum" by numerous investigators starting with *Fisk (1944)*.

Underlying the Mississippi River Delta, the topstratum consists of a sequence of deltaic and underlying shallow marine sediments that largely accumulated after sea-level rise decelerated about 7,000 to 6,000 years ago *(**Figure 3**)*. However, the gulfward edge of the topstratum contains at its base, deltaic and shallow marine sediments that started accumulating on the gulfward edge of the Marine Isotope Stage 2 coastal plain as soon as sea level started rising over 14,000 years ago. In all, the thickness of the topstratum exceeds 60 m (200 ft.) under the Lafourche delta and is >100 m (330 ft.) beneath the Plaquemines-Balize delta *(Frazier 1967; Coleman 1988; Roberts and Coleman 1996; Kulp et al. 2005; Blum and Roberts 2012).*

This Holocene interval is the geologic unit that the study attempts to map consistently from the best original boring records available. The compaction of the largely Holocene topstratum sediments overlying the Holocene-Pleistocene contact is a dominant component of subsidence over the past century and will remain a significant component of it in the future. This compaction is the result of physical, biological, and chemical processes acting on these geologically recent sediments, as opposed to the more consolidated older sediments found beneath the H-P surface (*McCulloh et al., 2006; Reed and Yuill, 2009; van Asselen et al., 2009*).

Riverine and deltaic deposits – Within the topstratum of the Mississippi Alluvial Valley, the deltaic sediments grade laterally into Holocene natural levee, lacustrine and floodplain muds that overlie the Holocene-Pleistocene surface and point bar and other meander-belt sediments that cut into it. The Holocene floodplain deposits that occur between meander belts taper in thickness from less than 40 m (130 ft.) thick at the latitude of New Orleans to a thin veneer ~500 km (310 miles) upstream. These sediments reflect the transformation of the lower Mississippi as it transformed back to a meandering system after glacial meltwaters were diverted to the north and east and sea level rose *(Fisk 1944; Saucier 1994; Blum et al. 2000; Kesel 2008; Blum and Roberts 2012)*. The base of these riverine and deltaic deposits is the Holocene-Pleistocene surface *(**Figure 3**)*.

Mermentau alloformation – The Mermentau alloformation is a lithologically heterogeneous stratigraphic unit that lacks what can be considered a characteristic lithology. As discussed *by Byrne et al. (1959), Gould and McFarlan (1959),* the Mermentau alloformation consists from bottom to top of (1) basal transgressive deposits, (2) gulf-bottom sand and silty clay, (3) gulf-bottom silty clay, (4) bay-bottom and mud flat and clayey silt, (5) bay mouth silt, (6) marsh organic clay and silt, and (7) distinct chenier ridges of sand and shell hash. Estuarine deposits are also present within paleovalleys buried beneath the Louisiana Chenier Plain. The base of the Mermentau alloformation is the Holocene-Pleistocene surface *(**Figure 4**)*.

Technical approach

The methodology for this project consisted of five major tasks:

Task 1. Geologic investigation and data acquisition

The nature of the original source data – Although new 3-D seismic data is starting to become available, most of it is proprietary oil and gas company data aimed at far deeper strata. The depth to the Holocene-Pleistocene surface has traditionally been determined by drilling. Many thousands of holes have been drilled into the subsurface of Louisiana in search of deep oil and gas resources and also for shallow environmental sampling. As they explore the subsurface, geologists record the sediment types to find the lithologic break between the different geologic units represented. Samples are systematically collected or entire sections of intact core can be extracted with hollow drill bits or vibracore technology, but it is rare for these original field samples to have been archived for subsequent research.

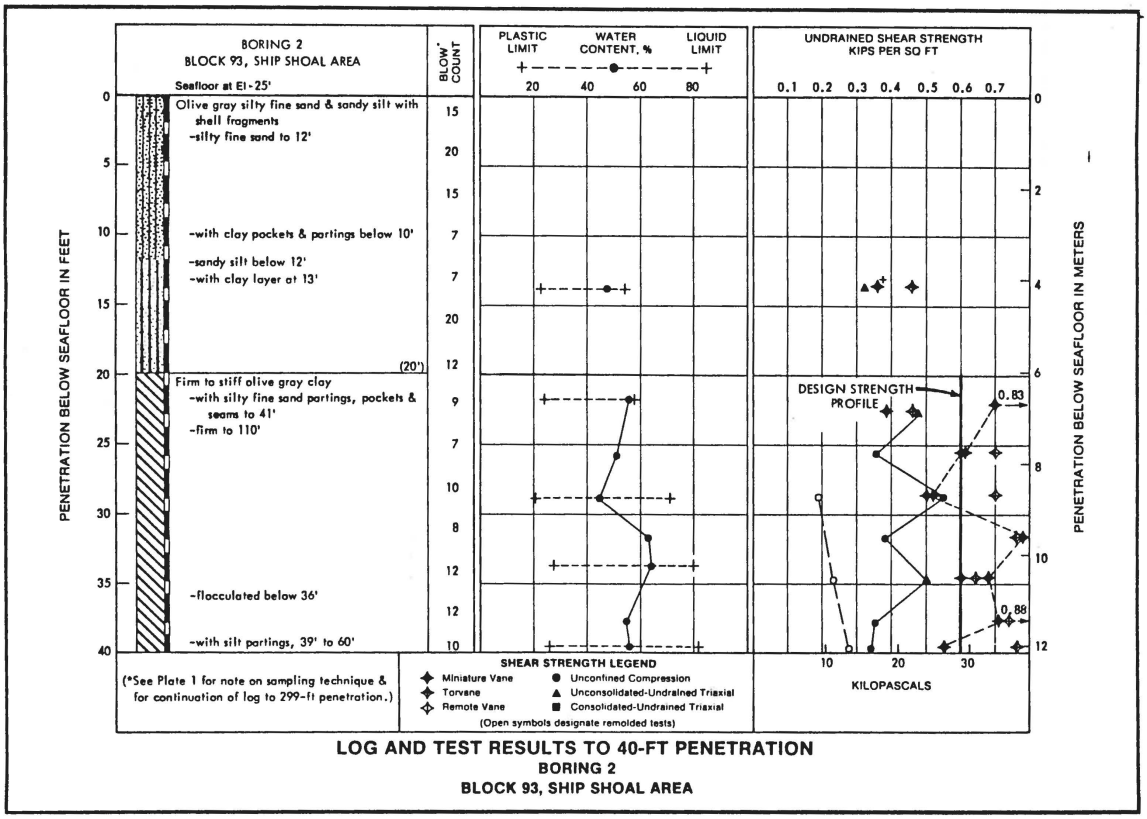

Figure 6 – Example of an offshore soil boring log *showing use of graphic symbols and text to describe physical properties and illustrate thickness of sediments penetrated by boring. As is common with many offshore soil borings that are available to researchers, the exact coordinates are lacking and exact location of the boring within a 9 square mile offshore block is indeterminable. From Cuomo (1984).*

The best records generally available for determining subsurface geology are the logs created by the geologist who evaluates the cores and samples ***(Figures 6 and 7)***. A boring log is a systematic and sequential text and graphic description of the geologic units encountered. Samples are collected as material is removed from the ground by the drill and described with the corresponding depth associated with the recovered material. Sometimes a length of intact core is collected to preserve an actual sample of the subsurface for a very detailed study. These original logs are often the best source for x-y-z coordinate data for the H-P surface along with a description of the material.

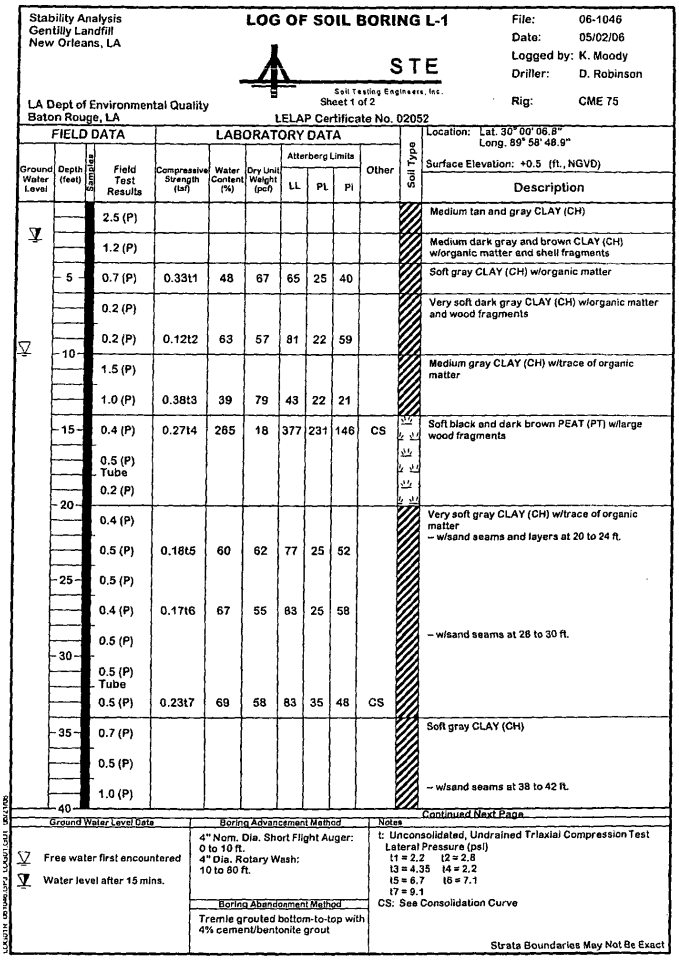

Stability Analysis
Gentilly Landfill
New Orleans, LA

LOG OF SOIL BORING L-1

STE
Soil Testing Engineers, Inc.
Sheet 1 of 2

File: 06-1046
Date: 05/02/06
Logged by: K. Moody
Driller: D. Robinson
Rig: CME 75

LA Dept of Environmental Quality
Baton Rouge, LA

LELAP Certificate No. 02052

Location: Lat. 30° 00' 06.8"
Long. 89° 58' 48.9"
Surface Elevation: +0.5 (ft., NGVD)

FIELD DATA				LABORATORY DATA								
Ground Water Level	Depth (feet)	Samples	Field Test Results	Compressive Strength (taf)	Water Content (%)	Dry Unit Weight (pcf)	Atterberg Limits LL	Atterberg Limits PL	Atterberg Limits PI	Other	Soil Type	Description
			2.5 (P)									Medium tan and gray CLAY (CH)
▽			1.2 (P)									Medium dark gray and brown CLAY (CH) w/organic matter and shell fragments
	5		0.7 (P)	0.33t1	48	67	65	25	40			Soft gray CLAY (CH) w/organic matter
			0.2 (P)									Very soft dark gray CLAY (CH) w/organic matter and wood fragments
▽			0.2 (P)	0.12t2	63	57	81	22	59			
	10		1.5 (P)									Medium gray CLAY (CH) w/trace of organic matter
			1.0 (P)	0.38t3	39	79	43	22	21			
	15		0.4 (P)	0.27t4	265	18	377	231	146	CS		Soft black and dark brown PEAT (PT) w/large wood fragments
			0.5 (P) Tube									
			0.2 (P)									
	20		0.4 (P)									Very soft gray CLAY (CH) w/trace of organic matter – w/sand seams and layers at 20 to 24 ft.
			0.5 (P)	0.18t5	60	62	77	25	52			
	25		0.5 (P)									
			0.4 (P)	0.17t6	67	55	83	25	58			
			0.5 (P)									– w/sand seams at 28 to 30 ft.
	30		0.5 (P)									
			0.5 (P) Tube									
			0.5 (P)	0.23t7	69	58	83	35	48	CS		
	35		0.7 (P)									Soft gray CLAY (CH)
			0.5 (P)									
			1.0 (P)									– w/sand seams at 38 to 42 ft.
	40											Continued Next Page

Ground Water Level Data
▽ Free water first encountered
▽ Water level after 15 mins.

Boring Advancement Method
4" Nom. Dia. Short Flight Auger: 0 to 10 ft.
4" Dia. Rotary Wash: 10 to 80 ft.

Boring Abandonment Method
Tremie grouted bottom-to-top with 4% cement/bentonite grout

Notes
t: Unconsolidated, Undrained Triaxial Compression Test
Lateral Pressure (psi)
t1 = 2.2 t2 = 2.8
t3 = 4.35 t4 = 2.2
t5 = 6.7 t6 = 7.1
t7 = 9.1
CS: See Consolidation Curve

Strata Boundaries May Not Be Exact

Figure 7 – Example of a partial onshore soil boring *showing use of graphic symbols and text to describe physical properties and illustrate thickness of sediments penetrated by boring. As is typical of paper or scanned copies of such logs, the best available copy that can be accessed is either a second, third, or greater generation copy of the original or, in some cases, microfilm or microfiche. Log from Soil Testing Engineers, Inc., 2006.*

A geophysical resistivity log is often recorded for an oil and gas well or water well. Probes that measure different physical properties are lowered into the borehole to collect continuous data that is graphically displayed as a geophysical log. The technique measures electrical resistance of the different sediments in the subsurface. Each material type (i.e. sand, clay, rock, etc.) will provide a different electrical resistance signal and generate a signature profile in the continuous graph of the logged interval *(**Figure 8**).*

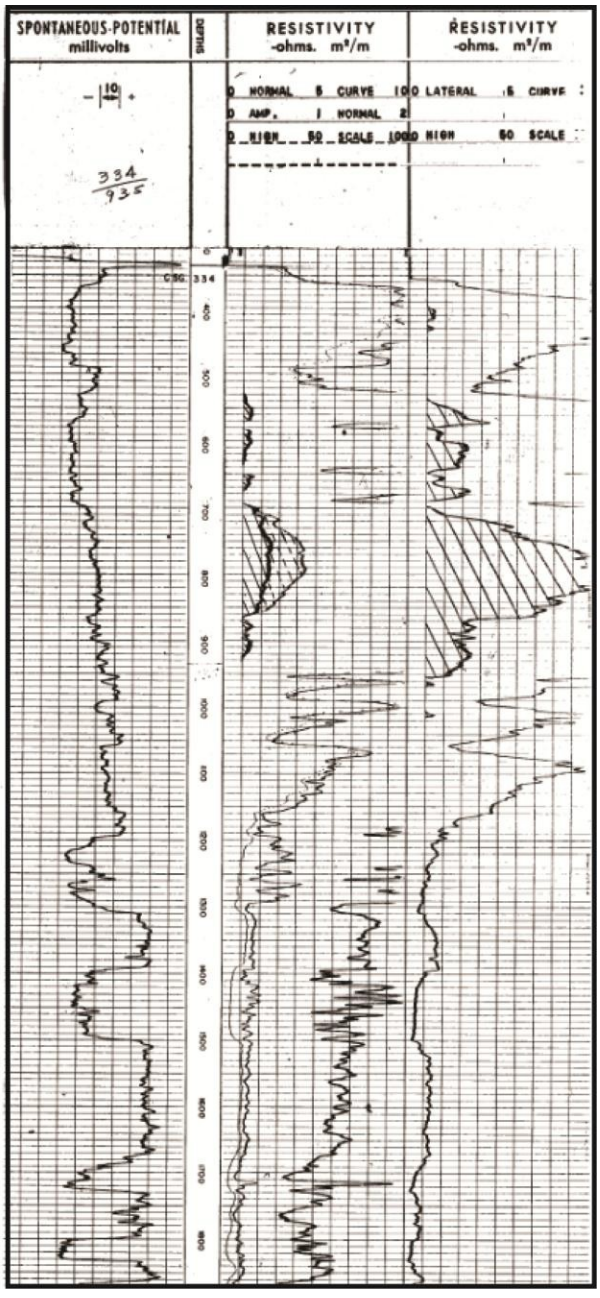

Figure 8 – A geophysical well log interval for a borehole *showing normal resistivity, lateral resistivity, and spontaneous potential curves. From Ayrer, 2010.*

Geophysical resistivity logs were sought to identify the H-P surface. However, petroleum exploration logs are typically logged only at deeper depths than the H-P surface. Water wells in the study area were typically logged too shallow to reach the H-P surface.

Unfortunately, the indexing and preservation of all logs is haphazard and much data has been lost. Often the best source for these data are maps and cross-sections created from the original fieldwork. Positional information can be gathered from the mapped boring locations and depth information from the cross-sections, often with the lithology indicated as well. But sometimes these documents are not created for the desired interval or are proprietary.

Most of the boring and core data obtained for this study were previously collected and compiled in tabular form by the original geologists in their reports, professional publications, theses, and dissertations. The x-y-z locational data is usually adequate, but there are often no lithological descriptions or any way to corroborate the interpretations that the geologists made in determining the surfaces they encountered.

Efforts were made to gather the best available boring log data from a wide variety of potential sources. They included a variety of publications, which included peer-reviewed professional papers, PhD dissertations, MS theses, state and federal agency publications and contract reports, scientific periodicals, and published maps. In addition, a number of government databases were investigated for the boring logs of engineering, sand resource, oil and gas, and other boring data. These databases included the digital files of the U.S. Army Corps of Engineers, the Louisiana Department of Natural Resources' (DNR) Strategic Online Natural Resources Information System (SONRIS), CPRA's Louisiana Sand Resource Database (LASARD), the files and databases of the Louisiana Department of Transportation and Development (DOTD), and the Electronic Document Management System of the Louisiana Department of Environmental Quality (LDEQ).

Individual researchers at the Louisiana State University (LSU) Coastal Studies Institute, the Louisiana Water Resources Research Institute, and the St. Petersburg Coastal and Marine Science Center of the U.S. Geological Survey were contacted in attempts to acquire borings logs and other data for this study. Finally, various private companies and parish agencies were contacted in the search for boring logs.

For each of these data sources, the borings data was collected and assessed for any issues that would exclude it for this investigation:

- located outside the potential H-P map area
- logged too deep to record the H-P surface
- logged too shallow to record the H-P surface
- inadequate H-P depth information
- inadequate geographic location information
- suspicious H-P determination criteria

Professional publications – The professional, non-governmental, peer-reviewed literature, including many publications listed in "Bibliography of Louisiana Coastal Plain and Continental Shelf Geology" (*Heinrich et al., 2011b)*, was searched for logs and other data that could be used in creating a map of the Holocene-Pleistocene surface. Although some of these papers, i.e. *Frazier (1967, 1974*) for the Mississippi Delta, *Gould and McFarlan (1959)* and *Leblanc (1949)* for the Louisiana Chenier Plain, contain cross-sections that depict borings that penetrated the Holocene-Pleistocene surface, the figures typically lacked the detail in their location maps and cross-sections required to extract useful data through georeferencing and digitization.

For these publications, attempts were made to find the original geological data, including boring logs, on which they are based. Staff at Shell Oil Company were contacted about the original borings logs acquired for and used in *Leblanc (1949)* and staff at ExxonMobil were contacted for information about the original borings logs acquired for and used in *Gould and McFarlan (1959).* Despite these efforts, nobody at either at Shell or ExxonMobil responded to any of the inquiries for the data of either *Leblanc (1949)* or *Gould and McFarlan (1959).* It remains unknown whether these data still exist, where they are archived, and how they can be accessed.

Within the Mississippi River Delta region of the study area, some exceptions were found. One such exception is *Morgan (1963*), which contained maps and cross-sections of sufficient detail that data could be extracted. Another exception, Table 1 of *Stanley et al. (1996)* contains subsurface data for 92 engineering borings from a variety of public and private sources. Unfortunately, this table lacks coordinates for the locations of these borings. These boring locations had to be either determined by georeferencing their figures and digitizing the boring locations or from other sources from the U.S. Army Corps of Engineers listed within. Although, *Stanley et al. (1996)* states that the well logs are on file with the Geotechnical and Structures Laboratory in Vicksburg, Mississippi, they have been misplaced within their massive collections of well logs, reports, manuscripts, and material and could not be located.

A few papers were found to contain precise digital data concerning the depth of the Holocene–Pleistocene surface and information was extracted. These papers included *Gonzalez and Törnqvist (2009), Törnqvist et al. (2004), and Yu et al. (2012).* From these sources, data from a total of 78 borings were obtained. Unfortunately, many of these borings lay very close to others within study areas of restricted size. As a result, they provided data for only very localized parts of the entire Louisiana coastal zone.

Dissertations and theses – A number of PhD. dissertations and MS theses were examined. They included *Roth (1999), Kulp (2000), Kuecher (1994), and Wessel (2010).* Both *Roth (1999)*, and *Kulp (2000)* contain lengthy tables of subsurface data extracted from a variety of public and private sources. These sources include U.S. Army Corps of Engineers

publications and files, Louisiana Department of Transportation and Development engineering borings, and assorted private borings. For Lake Pontchartrain, the tables of *Roth (1999)* also contain subsurface data derived from seismic profiles. The data from these tables were transcribed into Microsoft Excel spreadsheets. Although data could not be extracted from the cross-sections of *Wessel (2010),* its appendix contained detailed graphic logs of 10 borings from Terrebonne Parish. The coordinates of these borings are given by *Wessel (2010)* or were obtained from the St. Petersburg Coastal and Marine Science Center of the U.S. Geological Survey *(Flocks 2013).*

Only one of these borings, the P-I-90 boring of *Kuecher (1994*), is deep enough to penetrate the substratum. *Kuecher et al. (2001)* illustrated a number of cores that penetrated the substratum. Of these borings, core descriptions and locational data sufficiently detailed to be of use could only be located for the P-I-90 boring. In case of the Louisiana Chenier Plain, useful data that were not available from or duplicated by other sources were not found in any PhD. dissertation or MS thesis examined.

US Army Corps of Engineers (USACE) publications – A rich source of subsurface data for the Louisiana Coastal Zone are the USACE geomorphic maps of the Mississippi River Delta by *Dunbar et al. (1994, 1995)* and *May et al. (1984)*. A set of files containing these data was acquired from Jim Flock of the USGS St. Petersburg Coastal and Marine Science Center. The data consisted of the latitude and longitude of boring locations shown on the maps and, for many borings, the depths of contact for geologic units shown in the cross-section associated with each geomorphic map. To supplement and cross-check these data, the maps were georeferenced and the locations of borings were extracted from the maps and the depths of the Mississippi Alluvial Valley and Holocene-Pleistocene surface were extracted from their cross-sections.

Other U.S. Army Corps of Engineers publications, i.e. *Kolb (1962), Kolb and Van Lopik (1958)* and *Kolb et al. (1975)* contain a wealth of subsurface data. Their maps were not digitized and the data in them were not extracted because the bulk of these data was incorporated into and duplicated by *Dunbar et al. (1994, 1995), May et al. (1984), Roth (1999),* and *Kulp (2000).*

Extensive correspondence and conversations were conducted with John M. Anderson of the Cartographic Information Center, LSU Department of Geography and Anthropology and Joseph B. Dunbar of the USACE Geotechnical and Structures Laboratory, Vicksburg, Mississippi, in an attempt to locate the databases and engineering boring logs used to construct the configuration of sub-alluvial surface maps of *Saucier (1994).* None of the data and documentation associated with these sub-alluvial surface maps were found in the archives of Roger T. Saucier that are curated by the LSU Cartographic Information Center. This effort established that, if they still exist, the databases and original boring logs and maps Dr. Saucier used to construct the sub-alluvial surface maps would be archived in the

files of the U.S. Army Geotechnical and Structures Laboratory, Vicksburg, Mississippi. Despite the efforts of Dr. Dunbar and associates, only a couple of low-resolution SURFER digital elevation models (DEM) related to the sub-alluvial surface maps of *Saucier (1994)* could be located. These DEMs were found to lack both specific locational and stratigraphic data for individual borings.

Harold Fisk *(1948a)*, whose structural maps are a primary source material for the digital elevation of *Milliken et al. (2008)*'s model of the Holocene-Pleistocene surface, was found to contain a wealth of subsurface data for the Louisiana Chenier Plain. However, despite a lengthy search, the only copies of this report that could be found in both the U.S. Army Corps of Engineers and university libraries are copies of copies and, as a result, typically contained maps that exhibited poor resolution. Although the locations of many of the borings could still be digitized, it was often difficult or impossible to read the depths to the Holocene-Pleistocene surface associated with each boring location. This report also contains several cross-sections from which depths could be estimated. A related report, *Fisk (1948b)* contains the same type of data for the Calcasieu Lock area*. Fisk (1948b)* has the same limitations in terms of compiling data from it as *Fisk (1948a)*.

Given that Dr. Fisk was working for Humble Oil and Refining Company at the time he prepared both reports, it was presumed that the ExxonMobil research laboratory might have the original data, including thousands of boring logs, on which *Fisk (1948a, 1948b)*, were based. Various attempts to contact the appropriate staff at ExxonMobil in Houston about this material failed to receive any replies.

US Army Corps of Engineers (USACE), New Orleans District – Early in this study, inquiries were made with Del Britsch of the USACE New Orleans District about obtaining access to their boring database. It was determined that the database could not be accessed directly. Instead any requests for the logs of engineering boring had to be made through their Freedom of Information Act officer. As a result, only a limited number of boring logs could be requested for examination. For this reason, the boring logs requested were restricted to post-1985 boring logs not already incorporated into the geological mapping and cross-sections of *Dunbar et al. (1994, 1995)* and *May et al. (1984)*. In addition, it was discovered that since 1985, there have been few projects that have engineering borings that penetrate the Holocene-Pleistocene surface and many of these engineering borings occur in areas in which pre-1985 boring data exists. As a result, the requested logs of engineering borings were restricted to those deep enough to penetrate the Holocene-Pleistocene surface and occur in areas lacking existing pre-1985 coverage. A number of logs were requested and received. If they penetrated the Holocene-Pleistocene surface, they were incorporated into the current data set.

US Army Corps of Engineers, Geotechnical and Structures Laboratory, Vicksburg, Mississippi – At the beginning of this study, inquiries were made with Joseph B. Dunbar about obtaining access to the USACE Geotechnical and Structures Laboratory files in Vicksburg, Mississippi. It quickly became obvious that obtaining permission from U.S. Army Corps of Engineers to personally work with these files would not be possible. In addition, Dr. Dunbar felt that was highly unlikely that any search of their files by Louisiana Geological Survey personnel for this study would yield any useful information. These inquiries did indicate that the logs of private engineering borings and other related data used by *Stanley et al. (1996)* in their mapping might be archived in the files of the U.S. Army Geotechnical and Structures Laboratory. However, by the end of the project, neither the data nor related material could be located despite the best efforts of Dr. Dunbar and his staff.

US Geological Survey, St. Petersburg Coastal and Marine Science Center – Inquiries were made with Jim Flock of the USGS St. Petersburg Coastal and Marine Science Center, St. Petersburg, Florida. He was able to provide the official coordinates for the locations of borings within Terrebonne Parish that are mentioned in *Wessel (2010).*

Louisiana Department of Environmental Quality (LDEQ)– A parish-by-parish search was made of the files within the Electronic Document Management System of the LDEQ. Because of the sheer volume of files and the rudimentary index system, searching these files for the logs of engineering borings and water monitoring wells was quite time-consuming and labor intensive. Examination of the files had to be restricted to facilities most likely to have required soil borings and monitoring wells in their environmental and geotechnical studies. By trial and error, it was discovered that the documents most likely to contain useful subsurface data were the permit applications for these facilities that consisted of more than 150-200 pages. Unfortunately, any specific information about which documents contain logs of engineering borings and other useful subsurface information is completely absent in the very rudimentary and often cryptic indexing.

Louisiana Department of Transportation and Development – A search for usable subsurface data was made of the general files and GIS Geotechnical website of the Louisiana DOTD. Searching their general files proved quite time-consuming as locating usable subsurface data involved a labor-intensive number of steps. First, bridges and other structures of a size and nature to have required the drilling of sufficiently deep engineering borings within the study area needed to be located. Second, after such a structure has been located, a search had to be made for the project number of the structure. Third, if the project number can be found, then it was used to locate the appropriate microfilm files, which have to be requested and an appointment made to view them. Finally, one must look through tens to over a hundred pages of documents to find one to five pages of engineering boring logs and location maps.

Even when the actual engineering boring logs are in hand, the coordinates of the associated borings have to be determined using whatever maps can be found. In case of their GIS Geotechnical Website, the boring logs have been gathered in one archive. However, they often have been separated from their associated maps and lack any coordinate data that can be used in a GIS system, In order to use these logs in a GIS database, the location of the boring needs to be determined for each boring log.

Louisiana Department of Wildlife and Fisheries – Staff at the Louisiana Department of Wildlife and Fisheries (LDWF) were contacted for boring information. This resulted in the acquisition of two sets of recent soil borings, *Breaux and McDowell (2014)*, and *Poche and Vutera (2014)*, from projects in Marsh Island and Vermilion Bay, Louisiana. Both reports provided useful subsurface data for mapping the Holocene-Pleistocene surface. In addition, they provided a copy of *Orten (1959*) and associated plates. These borings either are too shallow or the boring logs lack the needed detail to determine the Holocene-Pleistocene surface.

Louisiana Sand Resources Database (LASARD) – The Louisiana Sand Resources Database of the CPRA was examined for useful subsurface information. Although well organized, readily searchable, and well documented as to source and location, limited useful information was found. The majority of the borings were too shallow to provide information that could be used in mapping the Holocene-Pleistocene surface.

Strategic Online Natural Resources Information System (SONRIS) – The SONRIS database of the Louisiana Department of Natural Resources was examined for useful geophysical logs. The logs of oil and gas well were found to begin too deep to be of much use in mapping the Holocene-Pleistocene surface. Only the geophysical logs of salt-water disposal wells are shallow enough to the surface to be useful in mapping it. The criteria for recognizing the paleosols associated with the contact of the Holocene-Pleistocene surface was found in cross-sections and other material in *McFarlan and LeRoy (1988a, 1988b).*

Ground Water Resources Program, Louisiana Department of Natural Resources – The water files of the DNR Ground Water Resources Program were examined. Although this source contains an abundance of well-documented data, the water well logs could not be used to recognize and map the Holocene-Pleistocene surface because the few wells in the coastal study area mostly pump from very shallow Holocene aquifers. In the lower coastal marshes, water wells generally do not exist.

The Coastal Studies Institute, Louisiana State University – Harry H. Roberts of the LSU Coastal Studies Institute was consulted about subsurface data within the study area. With Dr. Robert's permission, searches were made of specific collections. These searches yielded a small collection of potentially useful geological and engineering borings and information about the location of borings discussed by *Kuecher (2001).*

Department of Geology and Geophysics, Louisiana State University – Inquiries were made with the faculty and staff of the LSU Department of Geology and Geophysics concerning subsurface data that they might have. It was determined that at one time Arnold H. Bouma had a massive library of engineering and soil borings for locations all over the Louisiana Costal Zone and Offshore Continental Shelf. Efforts were made to locate and access this collection. Although the room that once housed it in the old Geology Building at one time could be located, the collection itself had disappeared. Attempts were made to contact and determine if this collection might be part of Dr. Bouma's papers or other collections that are curated at Texas A&M University, College Station, Texas. Unfortunately, despite the best of efforts, none of the various staff contacted at Texas A&M University ever responded to any of these inquiries. As a result, what happened to this collection of boring logs remains unknown.

Louisiana Water Resources Research Institute – Contacts were made with the faculty and staff of the Louisiana Water Resources Research Institute in Baton Rouge, Louisiana concerning subsurface data that they might have. As a result of these inquiries, Joseph N. Suhayda provided a large collection of logs and data for cone penetrometer test borings located within the Mississippi River Delta region. Because of the lack of precise locational data, they were not used in this study.

Legacy oil and gas lawsuits – For both the Mississippi River Delta and Louisiana Chenier Plain, the available files for a number of Oil & Gas Exploration Waste and Oilfield Legacy cases were examined at the Louisiana Department of Natural Resources. An examination of the environmental data associated with these lawsuits proved disappointing because, although well locations and groundwater analyses associated with these borings was reported in detail, lithologic logs and other descriptions of the borings were typically lacking. Well logs, often-uninformative geophysical logs, of any sort were rarely found. A couple of geologic cross-sections were found, but they were so generalized and lacking in detail as to be un-interpretable in terms of the depth of the Holocene-Pleistocene surface.

Private sources – A number of private companies were contacted about acquiring copies of engineering borings for their structures within the study area. Many failed to answer such inquiries and most declined to share data. Oil companies were reluctant to even discuss the matter because of legal matters involving state boards. Only a handful of engineering boring logs were acquired from private sources.

Task 2. Assessment of the source data

An assessment of the limitations and effectiveness of the source data was undertaken. Early in the project it was recognized that there were several major hurdles to be dealt with in order to acquire useable original boring data points needed to create the desired surface.

Limited access to original boring logs. A major problem encountered in this study was the limited access to original logs and other data relating to soil and geophysical borings. Access to data held by private consulting companies was severely restricted and efforts to obtain the data were typically ignored. Often this is because the individual report belongs to clients. Regarding their subsurface data as proprietary and confidential also provides them with a competitive advantage in their market.

The private companies that commissioned and owned these studies and the subsurface data that they contained exhibited lack of interest for releasing it for research, likely because they saw no benefit for the costs and risks of making efforts to do so. At that time, given the ongoing Southeast Louisiana Flood Protection Authority-East suit, the release of any information might have seemed to be a legally unwise and risky act regardless of the reasons for doing so. Even when subsurface data were collected by state agencies using state funds for public projects, the requests for what was public data involved lengthy correspondence involving the state agency, the consulting companies who conducted the investigations, and in one case even the Federal Emergency Management Agency (FEMA) was consulted about whether the borings might be released.

Another factor that limited access to subsurface data was that there is no official database of what studies contained either the logs of soil borings or other subsurface data. Advice as to what specific reports in which to find such data depended largely on the memories of state employees and consulting firms as to when and where they remembered having seen a report containing such data. Both the Louisiana DOTD and DNR have created such databases, but both databases need more effort towards collecting existing surface data and capturing new data as it is created.

Finally, significant collections of soil borings and other subsurface data have reportedly been compiled either for personal research, e.g. by Arnold Bouma; as a part of regional geotechnical studies, e.g. *Fisk (1948a, 1948b)*; and as official archives of data used in published research, e.g. *Stanley and Warne (1993)*. Access is limited to this material because these data have been either misplaced or discarded. This limitation greatly restricts how older interpretations could be re-evaluated.

Insufficient information on soil boring logs. Some of the soil borings that could be found and examined lacked sufficient information to make a determination of the Holocene-Pleistocene contact. Some soil borings provided only the simplest descriptions, e.g. only gross lithology and sparse geotechnical data, and lacked critical information such as if

either shell, slickensides, or organic matter was present. In case of many water wells logs, the lithologic descriptions were either too generalized or of too questionable reliability to be of any use. In some cases, they consisted only of geophysical logs that lacked any criteria from which the Holocene-Pleistocene boundary could be determined. In addition, the digital versions of some soil borings seemed to be only brief summaries of what was seen, in which case criteria used to differentiate Pleistocene from Holocene sediments in the field were not recorded. As a result, they could not be used to re-evaluate field identification using the available subsurface data.

Geophysical logs are rarely recorded at shallow depths. Although numerous oil and gas geophysical logs are archived in the Department of Natural Resources SONRIS database system, the relatively shallow interval sought in this study is largely missing. The geologic unit or target of the petroleum industry is much deeper and older than the Holocene-Pleistocene surface target of this study.

It is the petroleum industry's prerogative whether to log the shallower subsurface, typically in the order of 100s to 1000s of feet to deep. Generally this interval is cased with concrete lining. Salt-water disposal wells were the only geophysical logs that were logged to near surface position, and only 29 of those logs archived were identified that recorded the Holocene-Pleistocene Surface. Salt-water disposal wells are considered an injection well and are regulated differently than the oil and gas exploration and production wells requiring a much shallower logged depth to near surface.

Water well data are largely lacking in the study area. The water well log records have been recently moved from the DOTD to the DNR. A search through the water well logs was for the most part unsuccessful because much of the study area is either in open water or marsh where no water wells exist. In a few areas in the coastal zone where domestic water wells exist, they were accessing shallow Holocene aquifers and were all too shallow to record the H-P surface. In some cases, the federal Department of Homeland Security restricted information on municipal wells in the towns and communities in the study area.

Uneven distribution of data. An abundance of soils borings were available in places, such as the New Orleans metropolitan area and strips along major waterways and elsewhere where engineered levees had been built. In sharp contrast, suitable soil borings and other subsurface data was found to be virtually absent within the deltaic plains lying between these waterways. Sparseness of data in large areas limits the accuracy of the predictive H-P surface model.

For the Louisiana Chenier Plain, the LASARD data contains an abundance of soil borings. However, the vast majority of these borings are too shallow to have penetrated the full thickness of Holocene sediments underlying the Louisiana Chenier Plain. As a result, there is a lack of data concerning of the depth of the Holocene-Pleistocene surface. Similarly, the Texas Coastal Sediment Geodatabase, which was created and is maintained by the Texas

General Land Office, contains a number of the logs and descriptions of soil and geologic borings within southwestern Louisiana and adjacent parts of southeastern Texas. Again, the vast majority of these borings also are too shallow to have penetrated the full thickness of Holocene sediments underlying the chenier plain in Louisiana and Texas.

Insufficient geographic control. A major problem encountered in acquiring usable data is the lack of accurate geographic control on many source maps and cross sections. The soil borings that were acquired from the Louisiana DOTD lacked any coordinates that could be used to incorporate them into a GIS database. To have acquired this information would have required a very time-consuming and cost-prohibitive search of the original paper documents from which they came to locate the plans showing the locations of the soil boring and georeferencing plan and the boring locations within them. Many of these engineering plans still lacked proper geodetic control for georeferencing in the GIS.

In another case, a large set of cone-penetrometer data for numerous locations within the Mississippi River delta plain was provided by Joseph N. Suhayda of the Louisiana Water Resources Research Institute. However, the boring data had become separated from field notes that contained the locational information. Given that these field notes are yet to be located and may be lost, this data set lacks the coordinates that are needed to georeference them. The lack of suitable locational data can be a problem in incorporating otherwise quite usable data into the GIS database.

Task 3. Data development and digital compilation

The data used for the final Holocene-Pleistocene surface map are a compilation of data from multiple sources ***(Table 1)***. A total of 15,863 known boring locations in the study area were identified for assessment ***(Figure 9)***.

Much of the existing GIS boring/core data reviewed for the project did not identify the Holocene-Pleistocene target surface and could not be utilized. Others did not extend to the depth necessary. USACE core data contained 3,254 points for the Mississippi Alluvial Valley that were unable to be used. There is adequate spatial control on these data but there is no Holocene-Pleistocene surface information in the attribute tables. The same issues were found with the LASARD geotechnical borings downloaded from SONRIS (7,247 points) and the CPRA borings data (165 points) also downloaded from the DNR website. In all, 10,666 archived GIS boring locations could not be considered for further investigation because of a lack of attribute data or from insufficient depth recorded to be of use to this project.

Some data were derived from DNR's SONRIS online database. After extensive research into the oil and gas well data, only 26 borings were derived from SONRIS. This is due to the lack of core sample records shallow enough to penetrate the HP surface. Most geotechnical logs start well below our target interval because oil and gas prospect strata are typically well below the H-P surface.

The remaining data needed digital development for input into a GIS. Text file data were available from Flock, Roth, and Kulp. Flock's data came as 71 tables formatted as .txt. The text files were converted and merged into a spreadsheet file that was imported to ArcGIS and saved as a shapefile. The Roth and Kulp data were received in image format. Automated character reading techniques failed to produce reliable files so the team manually entered each record.

Most of the digital tabular borings source data contained adequate spatial control for use in the production of a regional surface model. The Kulp and Stanley data had lesser spatial accuracy. For these source data, the precision of the horizontal accuracy of the boring coordinates could be improved by digitizing from scanned USACE engineering geology "Distribution of Alluvial Deposits" 15-minute maps and associated cross-sections. The H-P surface and the MAV surface elevations were taken from the USACE cross-sections. The resulting database was then joined to the digitized borings shapefile. This effort improved the spatial accuracy of some 121 attributes while adding 211 additional points that were not included in any original data source.

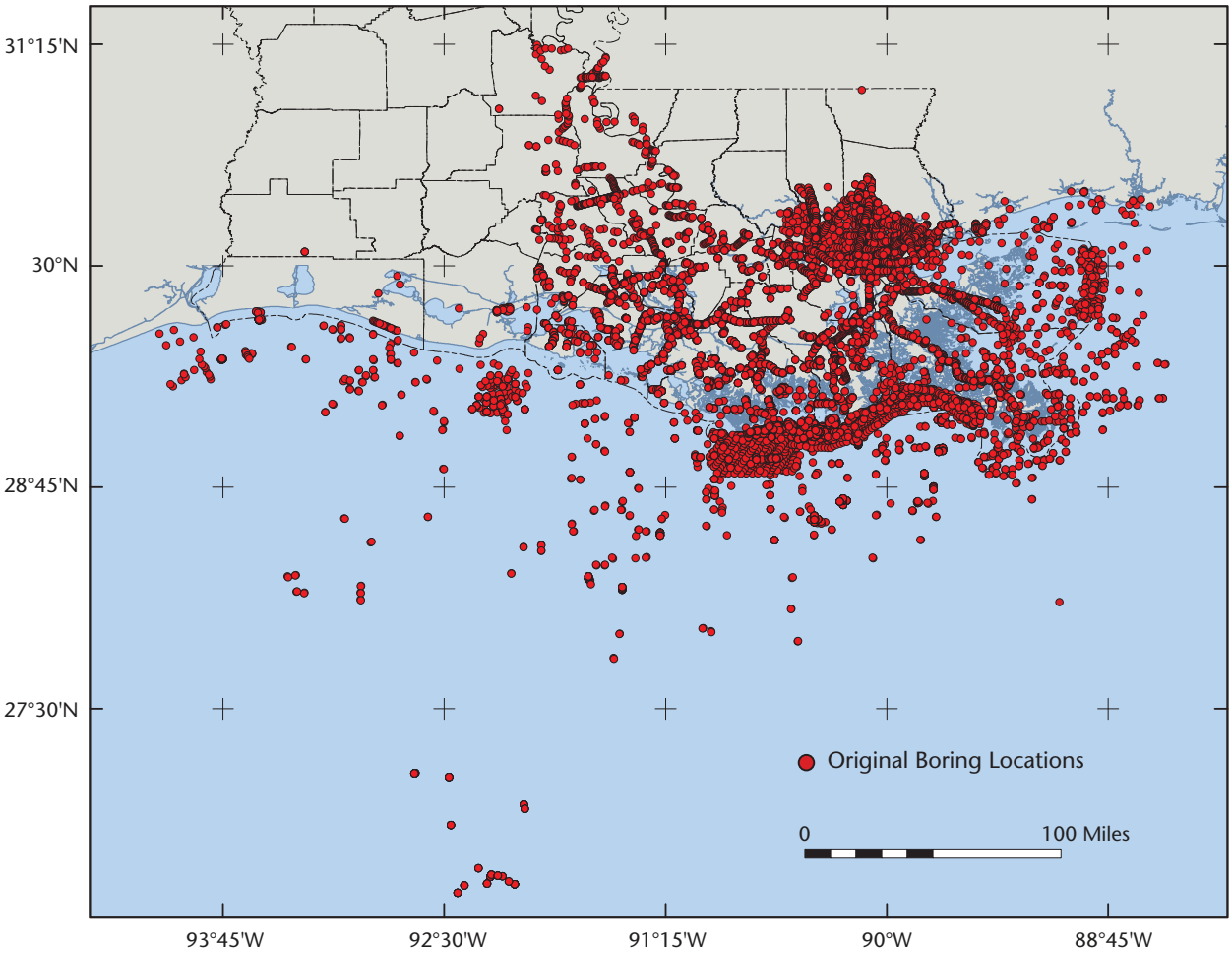

Figure 9 – Original boring locations investigated in this study *(15,863).*

Other data were digitized using heads-up technology in the GIS environment. Fisk data obtained for the project were hardcopy maps. These were scanned, georeferenced, and digitized using ArcMap 10.2. Attribute tables were populated using a template developed for the borings data. The same techniques were used to develop the legacy lawsuit data. Arabie Environmental Solutions, Inc. data were in a PDF document with scanned well logs and soil horizons well depicted. The data from *Yu, Gonzales, and Törnqvist (2012)*, and *Törnqvist et al. (2013)* were also in PDF documents of a scanned original publication. These tables were manually entered into a spreadsheet.

All data were developed and merged into a master shapefile that was thoroughly reviewed. There were many duplicate core records, a result of different researchers examining the same samples but making different interpretations. These differences were usually minor. Most of the discarded data were the result of duplicate records and better spatial positioning of a corresponding duplicate. Legacy lawsuit data were reviewed and

are included with the final data. Few points were derived from these data, often located in data dense areas.

Several maps depicting core sample locations were digitized. One source came on USGS 15-minute quad maps that have good spatial control. The cores on these maps had cross sections that were used to determine the H-P surface. USACE and LaDOT maps were utilized in this fashion. Stanley's Balize cores were digitized from a small-scale map. This small scale introduces a great deal of uncertainty with the spatial quality of the data. Duplicate data locations were first removed from the least spatially accurate data sources.

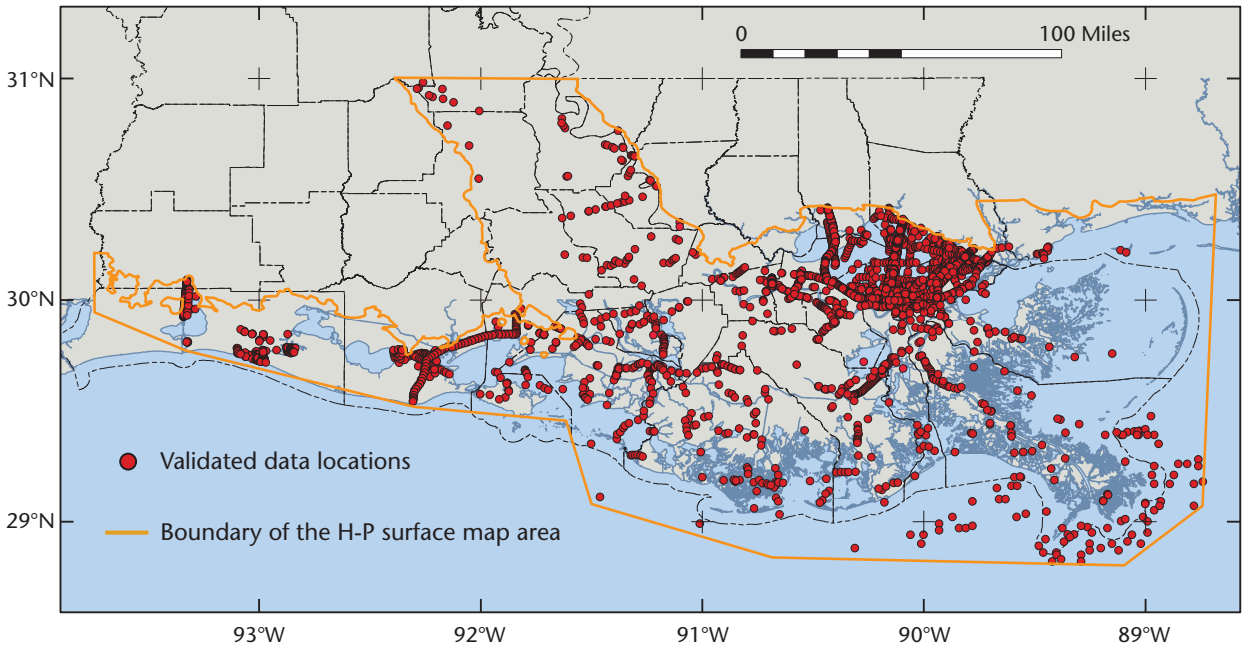

Figure 10 – Validated data locations utilized in the interpolation of the H-P surface *(3,012). Also depicted is the boundary of the H-P surface map area.*

As a result of the process, 3,012 validated data location were utilized to interpolate the final Holocene-Pleistocene surface dataset ***(Figure 10, Appendix)***.

A Pleistocene exposure area barrier file was created to act as an inland spatial boundary for the surface modeling. The 1:100,000 geology GIS data of the area was selected with the Pleistocene units identified and their gulfward limits were delineated. This polyline shapefile serves as a barrier to restrict the software from modeling the exposed Pleistocene outcrop. The polyline barrier was also used to derive 5,084 elevation points from the topographic/bathymetric DEM data. These elevation data were merged with the 3,012 selected HP surface points for the final 8,096 total HP surface data points to represent the inland edge of the buried H-P surface, where it is exposed as a weathered surface formation ***(Figure 10)***.

Data Source	*Initial Data Format*	*Initial Points*	*Resulting Points*
Arabie Environmental	digital log (.pdf)	5	5
CPRA	digital data (.shp)	165	0
Digital Elevation Model*	image (raster)	N/A	5,084 *
Fisk	hard copy map	410	266
Flock	text document (.txt)	2,932	500
Flock and Stanley	digital map (.pdf)	36	31
Gonzalez and Törnqvist	text table (.pdf)	18	18
Kulp	digital (.xls)	801	76
DOTD	digital map (.pdf)	64	64
LASARD	digital data (.shp)	7,247	0
Poche and Ventura	digital table (.pdf)	6	6
Roth Geotechnical	digital (.pdf)	1,837	1,251
Roth Seismic	digital (.pdf)	475	307
Roth Vibracore	digital (.pdf)	95	64
SONRIS	visual (web site)	30	26
Stanley	digital image (.pdf)	82	39
Törnqvist *et al.*	digital table (.pdf)	36	36
USACE	digital map (.pdf)	2115	310
USACE (Dunbar *et al.*)	digital data (.shp)	2487	0
USACE (Saucier)	digital data (.shp)	867	0
Yu *et al.*	digital table (.pdf)	13	13
TOTAL	N/A	15,863	3,012

Table 1 – Sources of the boring data utilized in this study. ** = Data source not from researched material. Used as a Pleistocene outcrop interpolation barrier and not included in the total.*

Task 4. GIS and surface model development

Once compiled, the HP surface data were loaded into ArcGIS v10.3. Initial compiled data totaled 15,863 records*. (**Figure 9, Table 1**)*. These came from multiple sources and were compiled from different formats. The geologists systematically eliminated the many borings that did not include the Holocene-Pleistocene surface as described in Task 1. Data development was performed to compile the final dataset, as described in Task 2.

After the processes of investigating and compiling the H-P surface data, 3,012 data locations were selected for surface model development ***(Figure 10).*** This is a sufficient number of data points for a predictive surface development; however, the spatial distribution of these data contains areas in which predictive surface interpolation is less confident.

Additional points were added from topographic digital elevation models and surface geologic maps to define the location and elevation of the Pleistocene exposure areas that form the inland boundary of the buried H-P surface.

Several interpolation methods were investigated to develop an effective surface model that produced the best results. Surfaces have been created using both ArcMap 10.3 and Surfer 12.0 to find the most effective surface model for the project data. Surfer 12.0 was superior for the 3-D renderings.

The original study area was modified to eliminate a very large area of no data in the southwest and a small area off the continental shelf in the southeast.

Many potential users will wish to use the data provided to create their own surface models, but one has been developed for use in this project. A number of surface modeling algorithms were investigated. All showed similar surface trends however Spline (ArcMap 10.3) and Minimum Curvature (Surfer 12.0) showed the most consistent surfaces. Empirical Bayesian Kriging (ArcMap 10.3) depicts better detail in certain areas but also displays a number of digital artifacts that are unrepresentative of the surface.

Other modeling algorithms investigated were Inverse Direct Weighting (ArcMap), Natural Neighbor (ArcMap, Surfer), Inverse Distance to a Power (Surfer), Modified Shepard's Method (Surfer), Polynomial Regression (Surfer), Nearest Neighbor (Surfer), Local Polynomial (Surfer), and Radial Basis Function (Surfer).

Inverse Direct Weighting showed good results but displayed an irregular surface. Kriging surface interpolation techniques have shown good results, but with some annoying digital artifacts that confuse the surface. The Natural Neighbor method created polygonal stair step effects that are not representative of the HP surface. The Spline interpolation method showed the best surface especially when combined with the Pleistocene outcrop interpolation barrier. Other methods showed no promise of better results.

The Spline with Barrier interpolation method was used to create the H-P surface for the project. Contours created are smooth and display fewer digital artifacts than those of any other interpolative techniques *(**Figure 11**)*.

The inconsistent spatial distribution of the data has caused many problems with the creation of a good surface model. All modeling techniques displayed problems with interpolation. The poor spatial distribution encompasses areas with sparse data and areas with tight data. Some data was randomly arranged and others in a linear fashion. The Anisotropy settings were increased slightly to help address the spatial linear nature of such data. This increases the lateral search radius to adjust for the linear nature of the data in certain areas. In general, eastern Louisiana is better represented with more and better-distributed data points than western Louisiana *(**figures 12 and 13**)*.

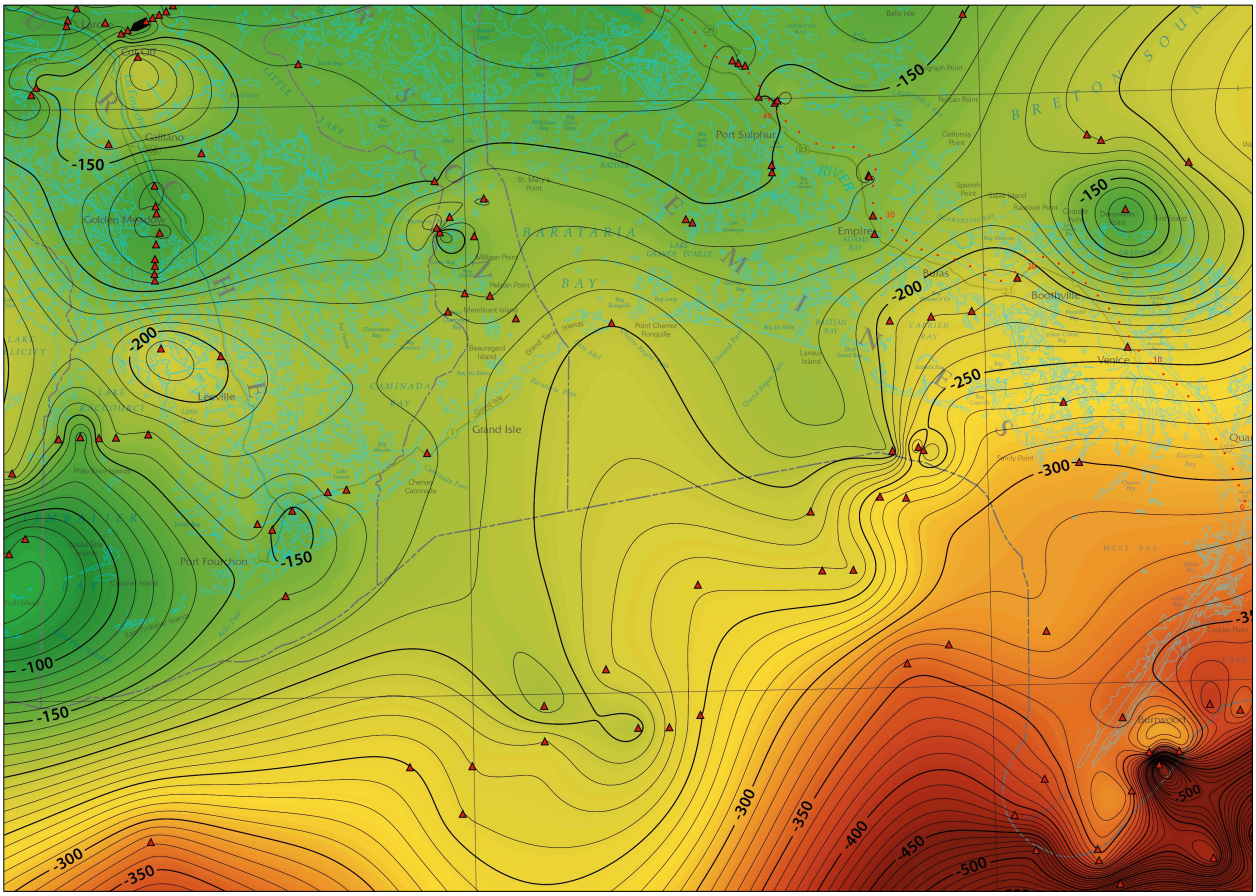

Figure 11 – Detail of structure using Spline predictive surface interpolation *with contours using depicting the depth of the H-P surface below mean sea level.*

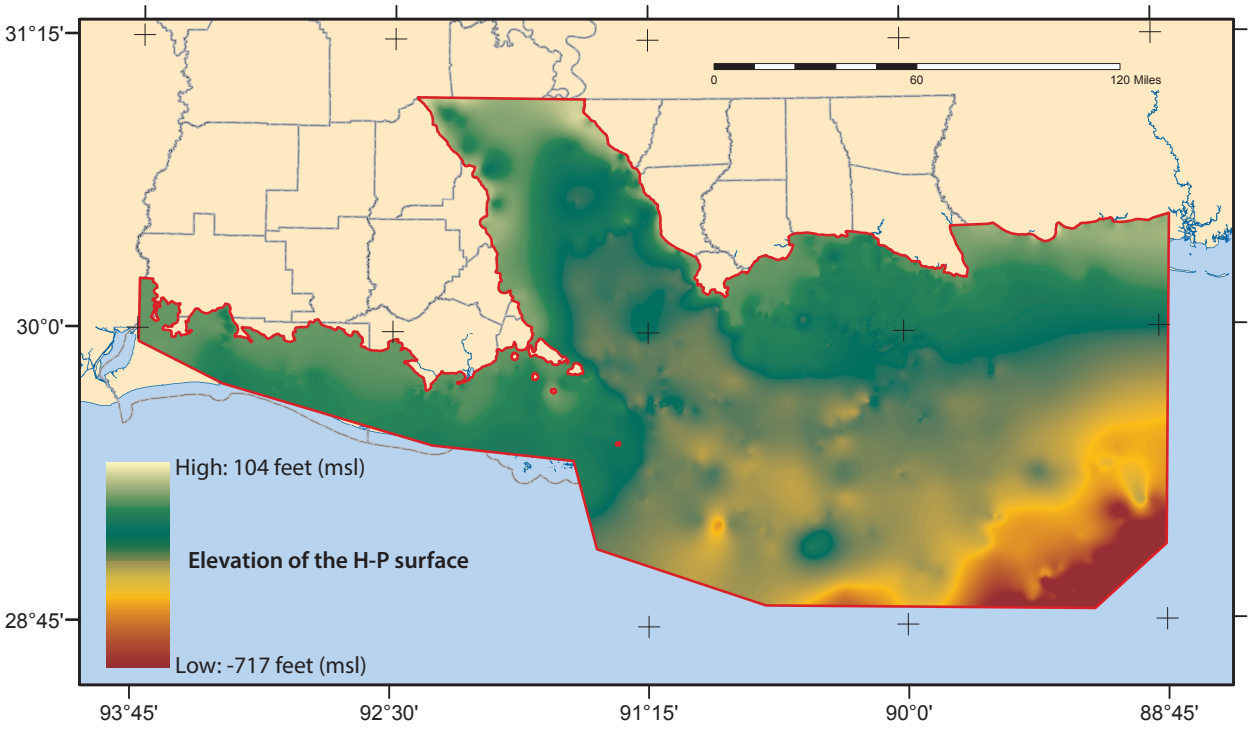

Figure 12 – The Holocene-Pleistocene surface structure map *is a predictive digital elevation model depicting the depth of the H-P surface relative to mean sea level. Cooler colors indicate higher elevations of the H-P surface. Hot colors indicate deeper elevations of the H-P surface.*

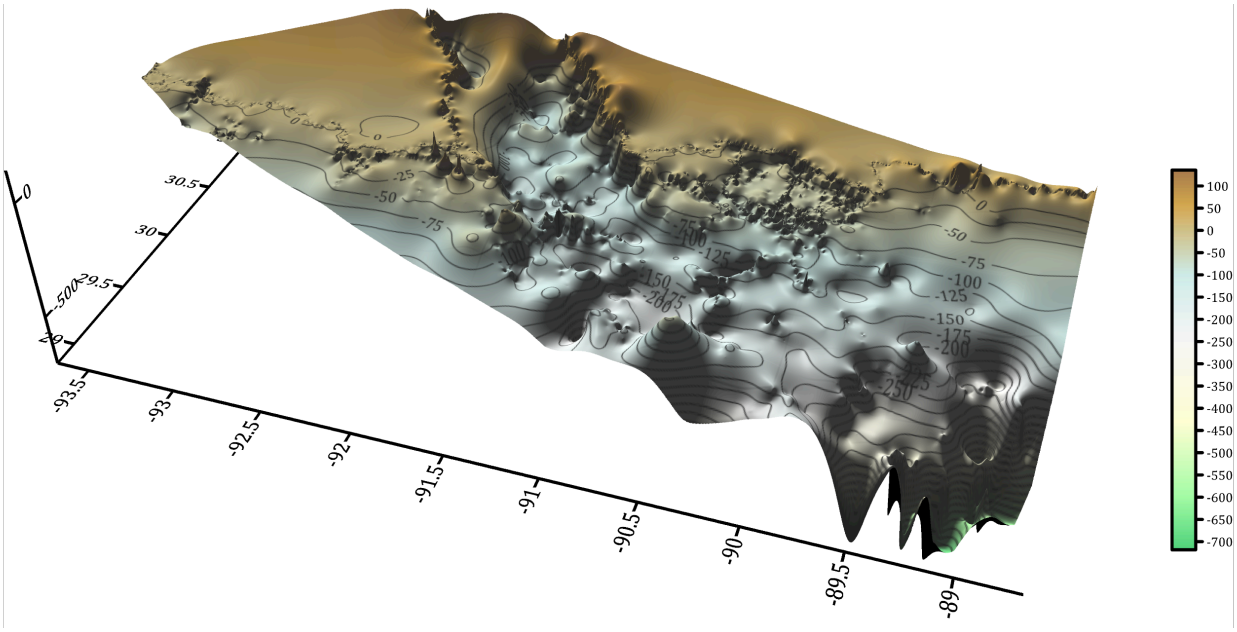

Figure 13 – The Holocene-Pleistocene surface 3-dimensional diagram.

Using the same finalized borings point dataset and the Empirical Bayesian Kriging function of ArcGIS 10.3, a predictive standard error map was generated for the Holocene-Pleistocene predictive surface (***Figure 14***). This map quantifies the potential for error in the interpolation based on the distribution of data points. It has the potential to help identify areas in need of further subsurface data to help increase the accuracy of the H-P surface model.

Clearly, H-P surface source data is almost entirely absent in the continental shelf area, the upper alluvial valley and in the Lake Borgne area as indicated by the uncolored areas of insufficient data. Darker areas represent zones of poorer confidence, while lighter shades indicate zones of higher confidence. Surface interpolations in areas of poorer confidence can display disappointing detail and sometimes include misleading artifacts of the algorithm due to inadequate data distribution.

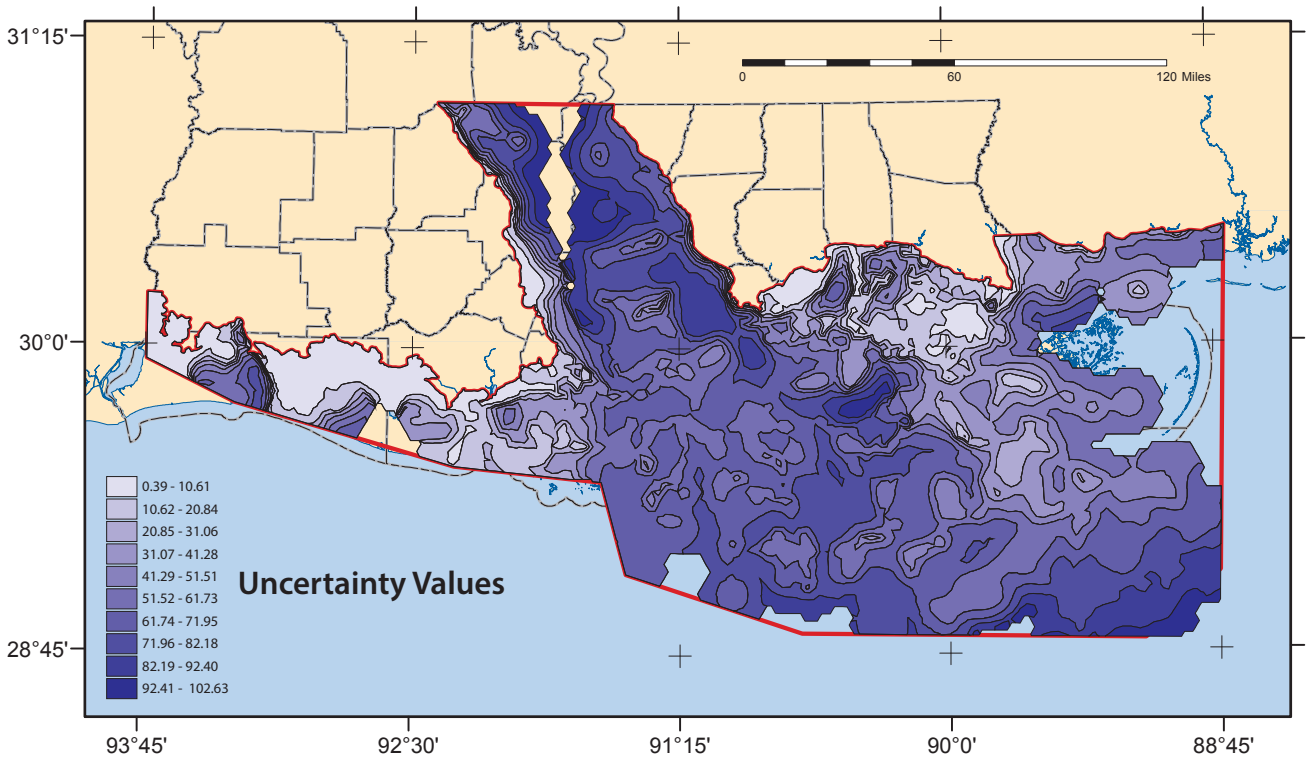

Figure 14 – Predictive Standard Error map *that depicts the measure of uncertainty of the predictive surface interpolated using De-trended Empirical Bayesian Kriging (ArcGIS 10.3.1). The predictive standard error is the square root of the variance of the difference between the mean of the many predicted semivariograms and the true semivariogram at corresponding locations on the surfaces. The larger the value, the greater the uncertainty. Darker purple shades indicate areas of higher uncertainty. Lighter shades indicate areas of lower uncertainty.*

A digital elevation model for the topography and bathymetry of the Louisiana Coastal Plain was created from US Geological Survey 30-meter DEM's. It depicts the topography of the exposed land surface and the adjacent coastal lake and seafloor bathymetry as a single surface that represents the top of the Holocene in the study area. *(**Figures 15 and 16**)*

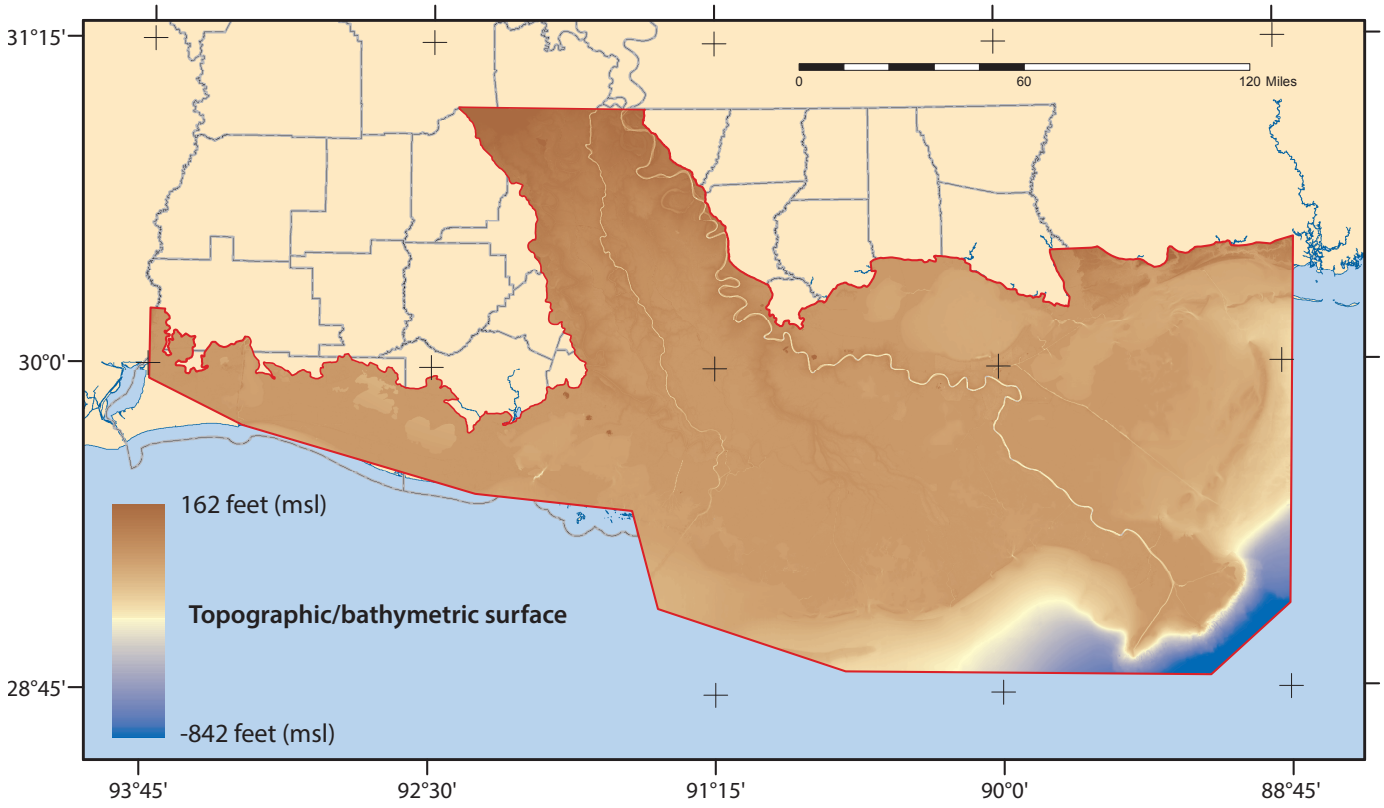

Figure 15 – Topographic/bathymetric surface map. *This digital elevation model depicts the exposed land surface topography and the bathymetry of coastal waters as a single surface that represents the top of the Holocene. (US Geological Survey, 2011)*

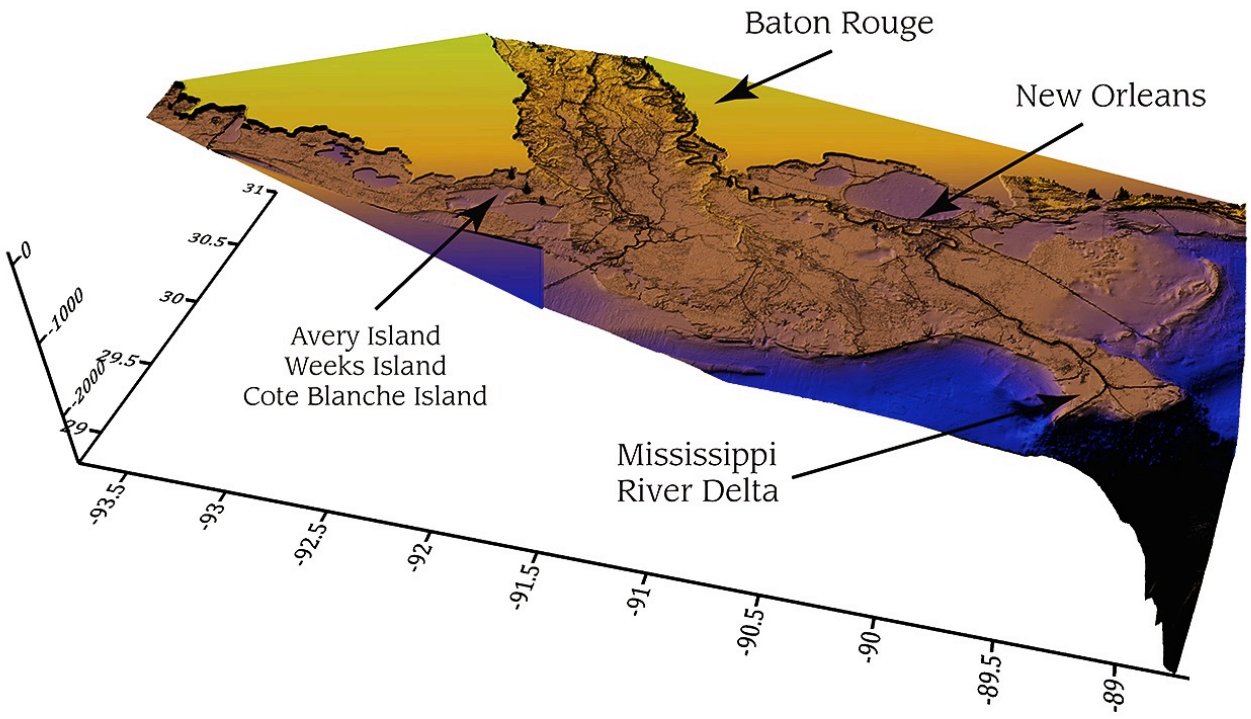

Figure 16 – Topographic/bathymetric surface 3-dimensional diagram. *A digital elevation model with elevations in feet.*

Using the Holocene-Pleistocene surface structure representing the base of the Holocene (***Figures 12 and 13***) and a digital topographic-bathymetric DEM (***Figures 15 and 16***) representing the top of the Holocene, an isopach of the Holocene interval was produced (***Figures 17 and 18***). An isopach map depicts the thickness of a geologic deposit. In this case, the isopach and the structure map are superficially similar since the topographic/bathymetric surface in much of coastal Louisiana is very close to mean sea level. The topographic/bathymetric surface is much more detailed than the developed H-P surface, so the isopach reflects that detail. Deep river channels reduce the thickness of the Holocene.

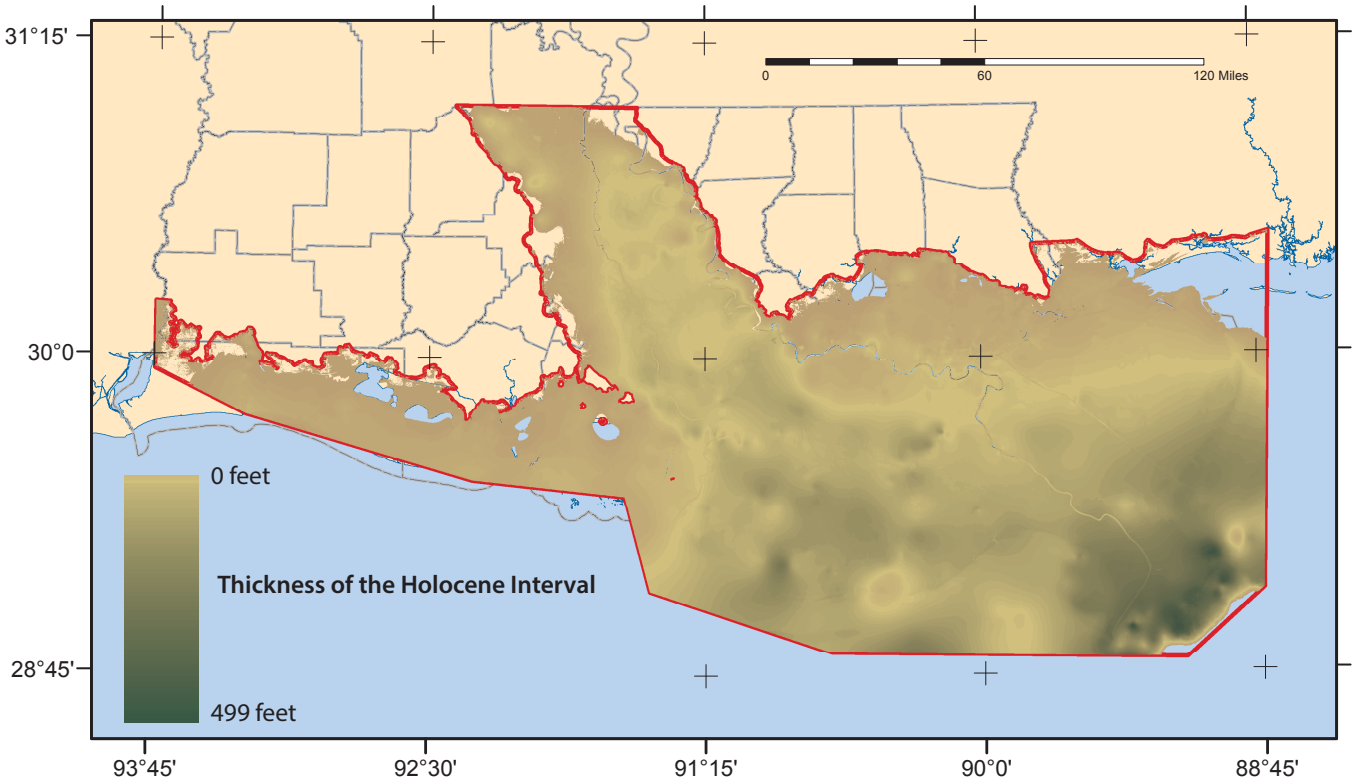

Figure 17 – Isopach map of the Holocene interval. *Light olive areas indicate zones of thin Holocene sediments. Darker olive indicates areas of thick Holocene sediments.*

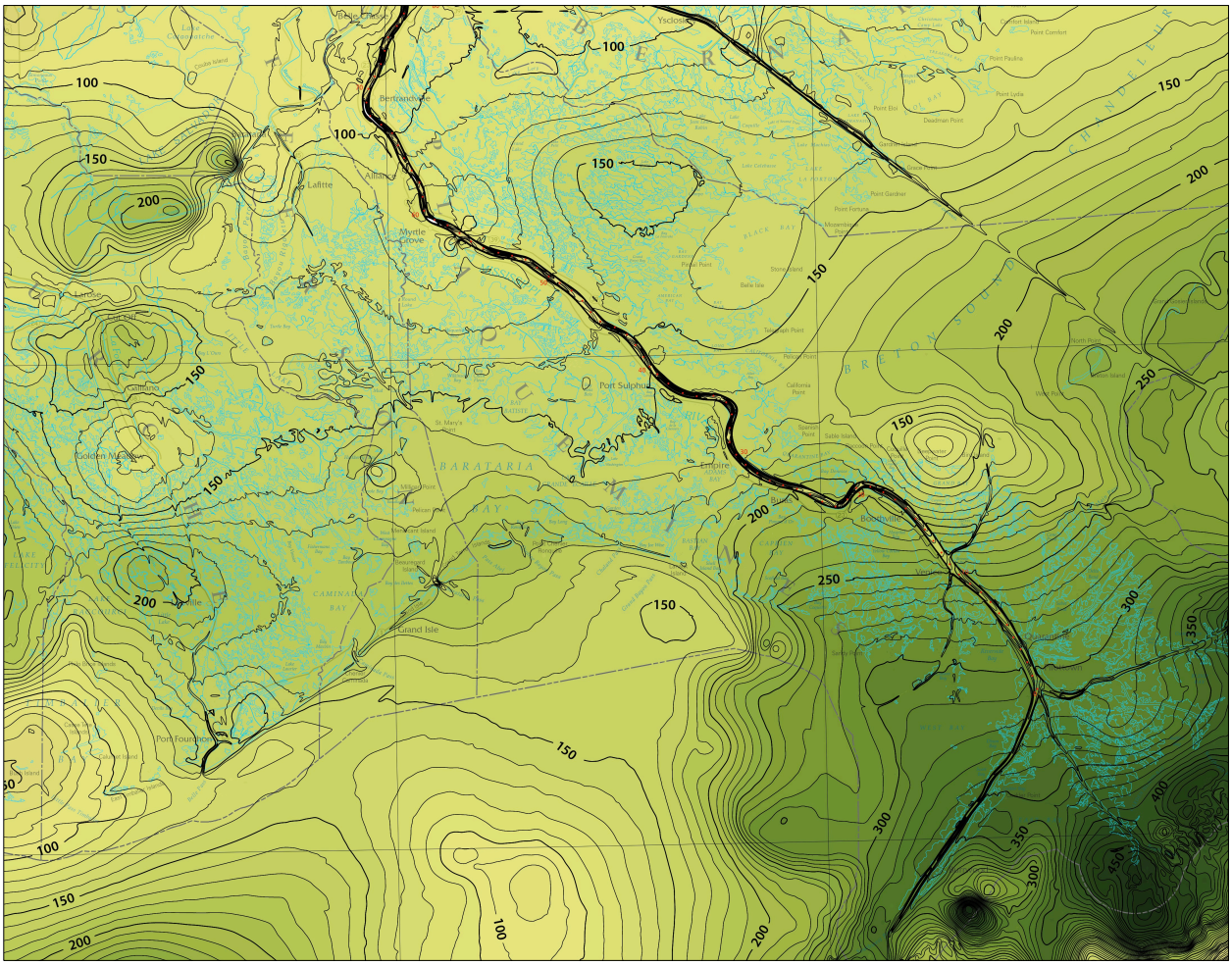

Figure 18 – Isopach detail of the Holocene Interval*. Contours represent the thickness of the Holocene. The interval is 10 feet. Note the effect of the deep channels of the Mississippi River and Mississippi River Gulf Outlet (MRGO) on the thickness.*

Task 5. Preparation of final report and digital deliverables

The team undertook a final technical review of the compiled data. Geologists reviewed draft plots of the GIS digital data and map products for interpretive issues, missing data, or other problems. Cartographers and GIS scientists reviewed the GIS dataset for duplication, data integration, juxtaposition issues, graphic flaws, and spatial accuracy.

CPRA personnel reviewed the datasets, maps and draft report and made several recommendations to refine the report and the maps to better accommodate non-geologist coastal researchers and planners.

This **final report** has been prepared describing the methodology, the data, and the deliverables. Figures, map plates, and data tables are included. An interpretation of the developed H-P surface was prepared at CPRA request to help clarify the surface for non-geologist coastal scientists and will be presented fully in the following sections.

GIS datasets of the Holocene-Pleistocene surface were created for use in GIS environments. ESRI shapefiles were created from the original boring data that was utilized. Digital elevation models were developed of the Holocene-Pleistocene surface. Metadata are provided to accompany the GIS datasets.

Cartographically developed **map plates** of the H-P surface structure, isopach, and topography-bathymetry are provided in PDF format and as large-format, hardcopy color prints.

Digital deliverables are provided on a DVD and also for FTP download.

Interpretation of the developed H-P surface

Pleistocene coastwise deposits are exposed at the surface and underlie the hill country and prairies of the Florida Parishes and of Southwestern Louisiana. These deposits have been carved away by the modern Mississippi River to form the central Holocene Mississippi River alluvial valley and they have been onlapped by Holocene coastal deposits to the east and west, becoming a buried surface gulfward ***(Figure 19)***.

The inland extent of the buried Holocene-Pleistocene surface is located where it is exposed at the surface as the terraces of the Pleistocene Prairie and Deweyville allogroups. Availability of subsurface boring data dropped off considerably in the offshore area so the developed H-P surface is truncated there.

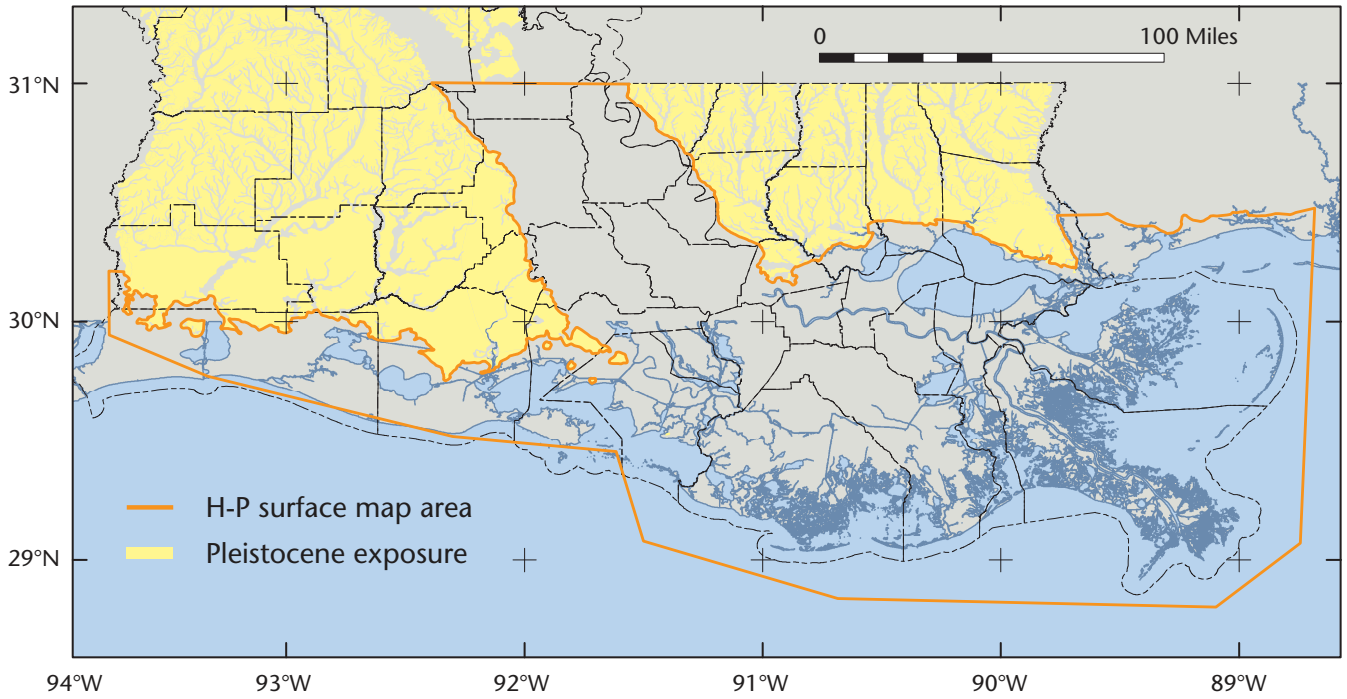

Figure 19 – Holocene-Pleistocene surface map area *in relation to the Pleistocene exposure.*

The Holocene-Pleistocene surface structure map ***(figure 12)*** exhibits the general features of the Louisiana coastal plain during the Last Glacial Maximum (Marine Isotope Stage 2). Even with the inconsistent data distribution in many areas and a resulting reduction in detail, geomorphological features are apparent.

The central feature of the H-P structure map is the ancestral Mississippi River Valley and its delta. Within the area of the modern Mississippi River alluvial valley, a narrow,

entrenched, and winding paleovalley, likely dating to the Last Glacial Maximum, can be discerned. Flanking these depressions are buried highs that may represent terraces of older braided river systems. Southwest of Houma, this paleovalley apparently breaks into two paleovalleys.

Broad, shallow platforms characterize the H-P surface in the Chenier plain and Pontchartrain basin. At the eastern end of the Chenier plain, the Holocene-Pleistocene surface is noticeably deformed by a series of salt dome outcrops that have created the "Five Islands" of south central Louisiana.

Tectonic activity is recognized to have helped shape the Louisiana coastal plain. The sediments and surface of the modern coastal plain are disrupted and deformed by faults that are the result of sediment loading, underground salt movement, and gravity tectonics of the thick Cenozoic sediments that underlie them *(**Figure 20**).*

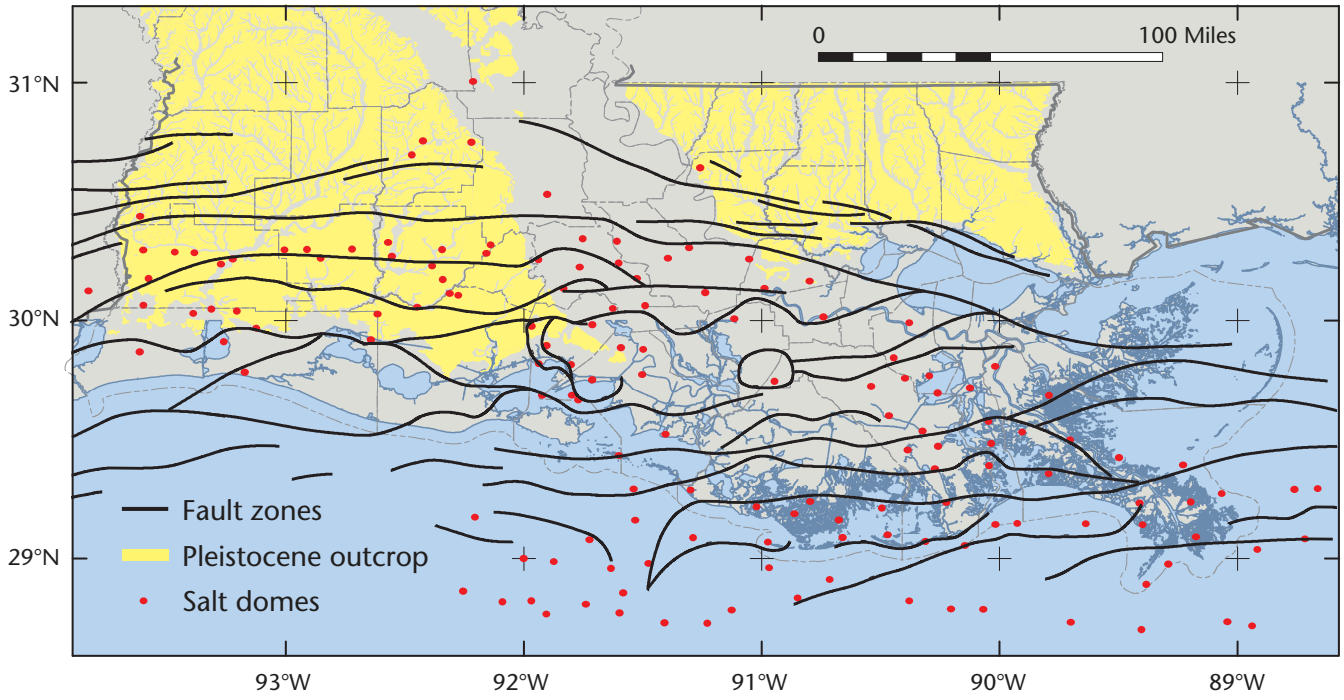

Figure 20 –Fault zones and salt domes in coastal Louisiana. *Adapted from GCAGS/GSA, 1972, Martin, 1978, and Reed, et al, 2005.*

Most coastal Louisiana faults are "normal faults", where hanging blocks have dropped down along the fault plane. Most are also "growth faults", where sediments on the down-dropped blocks are thicker than the beds on adjacent up-thrown blocks, evidence that they were active during the period of time that sediment accumulated. They form mainly by gravitational failure and slumping of unstable, rapidly deposited sediments. They occur

mainly as coast-parallel fault zones that represent the former locations of the older shelf-margins of major Cenozoic depositional episodes, which get younger basinward. They flatten out with depth to become the base of massive slide blocks *(Winker and Edwards 1983; Reed et al. 2009, Young et al. 2012).*

The maximum displacement (several hundred meters) of growth faults occurs deep beneath the surface and decreases upward to tens of meters in the shallow subsurface. The relief of active fault scarps is generally only a few meters on the Pleistocene terraces and is often unnoticeable in areas of active sedimentation on the delta and chenier plains.

The downward movement of the gulfward side of a growth fault in respect to a stable vertical datum would be observed as regional subsidence. The subsidence associated with growth faults is variable and can reach almost 40 mm/yr. Other faults are found around salt domes in a radial pattern. These faults are shorter, less than 5 km, and more localized than are the regional growth faults. Except for human-caused activity related to solution mining of salt caverns, they rarely cause subsidence over less than geologic periods of time *(Veerbeek 1979; O'Neill and Van Siclen 1984; Reed et al. 2009, Young et al. 2012).*

Surface Holocene faults have been previously mapped in the study area, related to salt dome intrusions or subsurface growth fault trends. Likewise deeper faults have been mapped during petroleum exploration. It is clear that the H-P surface and the Holocene interval are also affected by faulting. However source data limitations do not provide sufficient detail to reveal faulting in the developed Holecene-Pleistocene structure map.

Salt dome intrusions are quite a different matter. Salt diapirs not only intrude through the H-P surface but also up through the Holocene interval to stand above the modern surface in a few places. Other buried salt domes with no surface exposures may be associated with morphologic features mapped on the Holocene-Pleistocene structure and Holocene isopach maps ***(Figure 20, Table 2)***.

The origin of south Louisiana salt domes began with the emergence of a rift valley in the Mesozoic Era over 200 million years ago. The shallow inland sea that formed filled with the drainage from the surrounding high ground in the absence of an outlet to the ocean, analogous to today's Dead Sea. Drainage into the inland sea was not as great as evaporation causing the sea to desiccate, leaving behind the salts and other minerals that were in solution.

Over millions of years, about 5,000 feet of salt was deposited in the Gulf Coast Salt Dome Basin that was developed, forming what is today called the Louann Salt formation of Jurassic age. The bedded salt was then covered by the deposition of over 70,000 feet of mostly Cenozoic sediment in the ancestral Gulf of Mexico, burying the salt under enormous pressure. As this salt was buried, trapped above old hard rocks below and being more plastic and less dense than the overlying deposits, the salt layer became diapiric. A diapir is

a type of geologic intrusion in which a ductile and more mobile material is forced under pressure into brittle overlying rocks.

In the north Gulf of Mexico these diapirs come in the form of salt domes–tall pillars of intrusive salt rising upward from the deep salt bed. A few of these salt domes penetrate all the way to the land surface, exposing caprock "islands" standing above the plain and forming solution lakes, but most top out at various subsurface depths. Some of these domes intrude into the Pleistocene and Holocene sediments investigated in this study and can affect the H-P surface in various ways *(**Figure 20, Table 2**)*.

They can produce "windows" in the data where an intruding dome completely pierces the surface and overlying Holocene interval. Elsewhere they can produce high spots and low mounding on the structure map and thinner areas on the isopach where they intrude into the Pleistocene or Holocene deposits. Many other salt domes are too deep to affect the H-P surface at all.

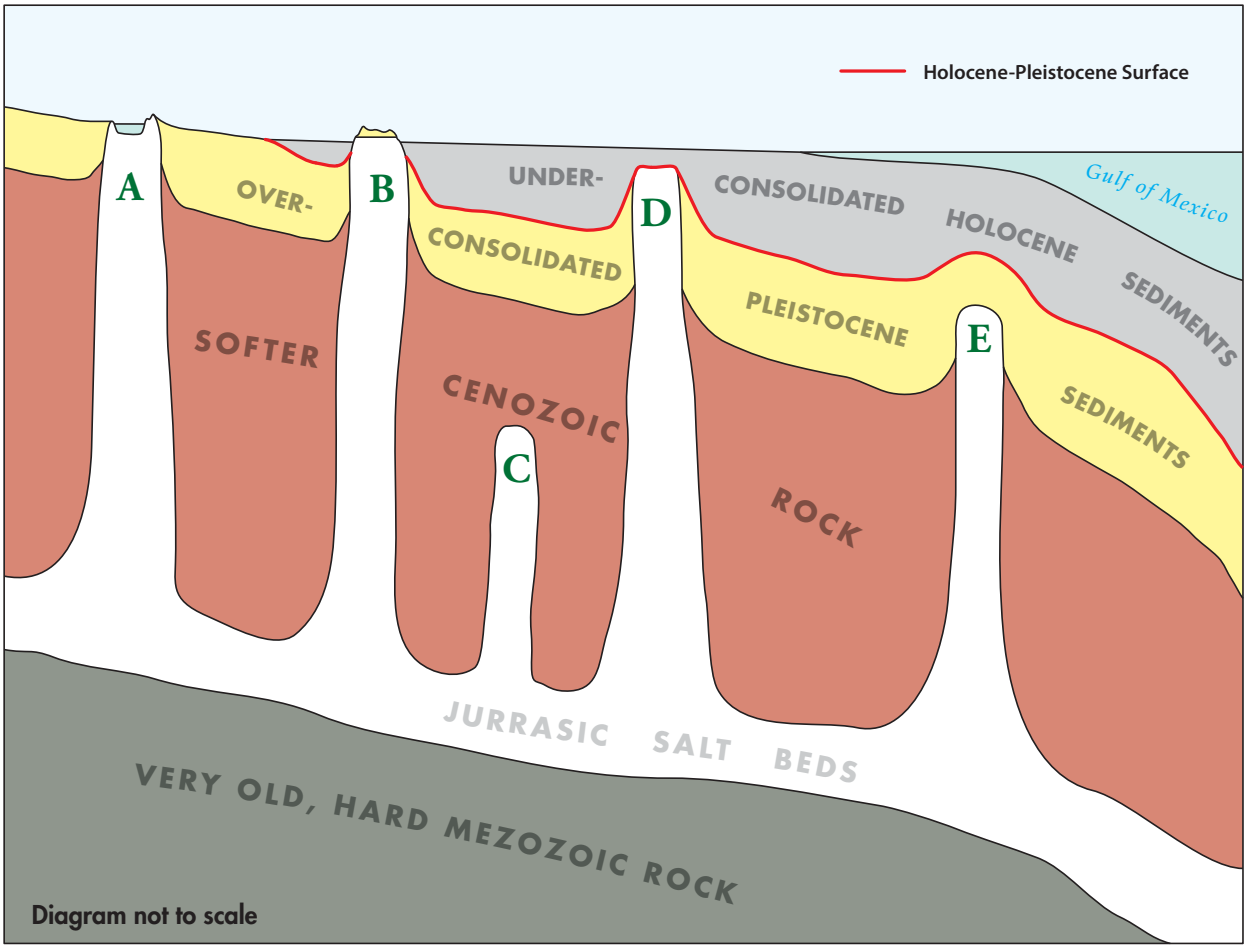

Figure 21 – Cross-section diagram of Gulf coast salt domes *and their possible effects on Holocene and Pleistocene strata. Features are exaggerated for clarity.*

In the diagrammatic cross-section *(**Figure 21**),* five typical salt domes are depicted in relation to the regional stratigraphy. Salt dome size is greatly exaggerated for clarity.

Dome A illustrates a salt dome that has intruded completely through the Pleistocene interval and its caprock outcrops at the surface of the Prairie terrace where a solution lake has formed. This is typical of Jefferson Island Dome. This dome outcrops outside the H-P surface map area and does not affect it.

Dome B has intruded through the Pleistocene and Holocene intervals and its eroded surface outcrop is capped with a consolidated remnant of the basal Pleistocene. This is typical of Avery Island Dome. This exposure, capped by Pleistocene sediment and surrounded by Holocene marshes, produces a window in the structure map where there is no mappable Holocene.

Dome C did not intrude high enough to affect the H-P surface at all. Many domes in the Gulf Coast Salt Dome Basin do not. Charenton Dome, deep beneath Bayou Teche, is typical of this type and is not thought to have impacted the H-P surface.

Dome D has intruded through the Pleistocene and into the Holocene, but does not outcrop at the surface. It can create a morphological peak in the structure map and a shallow spot in the isopach map. Rabbit Island Dome is an example of this type, almost an "island", intruding to only 15 feet from the surface.

Dome E never intruded into the Holocene but may possibly be correlated with features on the H-P surface. It may have uplifted Pleistocene or older sediments, mounding the H-P surface and creating a high spot. West Hackberry Dome is typical of this type. The source data were sometimes insufficient to differentiate dome types D and E so those have been listed provisionally as D/E ***(Table 2)***. Some deeper E domes are queried because their proximity to features on the H-P structure may be coincidental.

Caprock is a limestone/anhydrite carapace found atop many buried salt domes. It forms as a dissolution residue atop buried but still buoyant diapirs as the rising salt encounters groundwater. Caprock is most common and thickest on diapir crests that are currently close to the earth's surface but can be found atop structures as deep as 3,000 m. Most diapir capstones are 100 to 150 meters thick, but can be thicker than 300m *(Warren, 2006).*

An excellent, non-technical synthesis of the geologic history, tectonic activity, and delta development in the Louisiana coastal plain can be found in *Spearing, 2007*.

dome name	*parish*	*nature of the intrusion*	*type*	*longitude*	*latitude*	*diameter*
Anse la Butte	St. Martin	153’ depth to top of salt	D	-91.94	30.27	0.3 mi.
Avery Island	Iberia	outcrops in the Holocene	B	-91.91	29.90	0.5 mi.
Bayou Choctaw	Iberville	240’ depth to caprock	D/E	-91.31	30.21	2.0 mi.
Bay de Chene	Jefferson	7950’ depth to top of salt	E	-90.05	29.40	0.5 mi.
Belle Isle	St. Mary	outcrops in the Holocene	B	-91.40	29.53	0.5 mi.
Black Bayou	Cameron	879' depth to caprock	D/E	-93.62	30.03	1.0 mi.
Bully Camp	Lafourche	1253' depth to caprock	D/E	-90.38	29.46	0.75 mi.
Caillou Island	Terrebonne	2497' depth to caprock	E	-90.47	29.11	0.5 mi.
Chacahoula	Lafourche	878’ depth to caprock	D/E	-91.50	29.88	N/A
Clovelly	Lafourche	386' depth to caprock	D/E	-90.25	29.48	0.5 mi.
Cote Blanche Island	St. Mary	outcrops in the Holocene	B	-91.71	29.75	1.0 mi.
East Hackberry	Cameron	2931' depth to caprock	E	-93.33	30.02	1.0 mi.
Dog Lake	Terrebonne	1426' depth to caprock	D/E	-90.85	29.21	0.5 mi.
Fausse Pointe	Iberia	783' depth to caprock	D/E	-91.64	30.05	0.5 mi.
Four Isle Bay	Terrebonne	501' depth to caprock	D	-90.79	29.25	0.5 mi.
Garden Island Bay	Plaquemines	1353' depth to caprock	D/E	-89.16	29.10	1.0 mi.
Jefferson Island	Iberia	outcrops in the Pleistocene	A	-91.97	29.98	0.5 mi.
Iberia	Iberia	808' depth to caprock	D/E	-91.70	29.99	0.5 mi.
Lake Barre	Terrebonne	718' depth to caprock	D/E	-90.49	29.22	0.5 mi.
Lake Hermitage	Plaquemines	907' depth to caprock	D/E	-89.90	29.56	0.5 mi.
Lake Pelto	Terrebonne	1484' depth to caprock	D/E	-90.66	29.09	0.5 mi.
Napoleonville	Assumption	412' depth to caprock	D	-91.12	30.02	2.0 mi.
Potash	Plaquemines	521’ depth to caprock	D	-89.69	29.51	2.0 mi.
Rabbit Island	Iberia	12' depth to caprock	D	-91.60	29.43	N/A
Timbalier Bay	Lafourche	6427' depth to top of salt	E	-90.31	29.08	1.5 mi.
Valentine	Lafourche	268' depth to top of salt	D	-91.92	29.69	0.5 mi.
Vermilion Bay	Iberia	6575' depth to top of salt	D	-90.44	29.61	0.5 mi.
Weeks Island	Iberia	outcrops in the Holocene	B	-91.80	29.82	1.0 mi.
West Cote Blanche Bay	St. Mary	7545' depth to top of salt	E?	-91.80	29.69	0.2 mi.
West Hackberry	Cameron	1197’ depth to top of salt	E	-93.41	30.00	1.3 mi.

Table 2 – Salt domes known or suspected to have influenced the H-P surface. *Depths are below mean sea level. Caprock of significant thickness may overlie the top of salt depths, but insufficient borehole data is available to reveal a caprock depth if caprock exists. Diameters are approximate; domes can be very irregular in shape. Data from Beckman and Williamson (1990).*

1. Structure Map of the Holocene-Pleistocene Surface

Mississippi Alluvial Valley area – In this area, the structural map of the Holocene-Pleistocene surface depicts the general form of a paleovalley of the Mississippi River that likely dates to the Last Glacial Maximum, Marine Isotope Stage 2 ***(Figure 22)***. This paleovalley appears to be narrow, entrenched, and winding in form. What are in reality continuous buried paleochannels are depicted on the map by a series elongate, discontinuous depressions by the digital surface interpolation because of the sparse and clumped distribution of the available subsurface data.

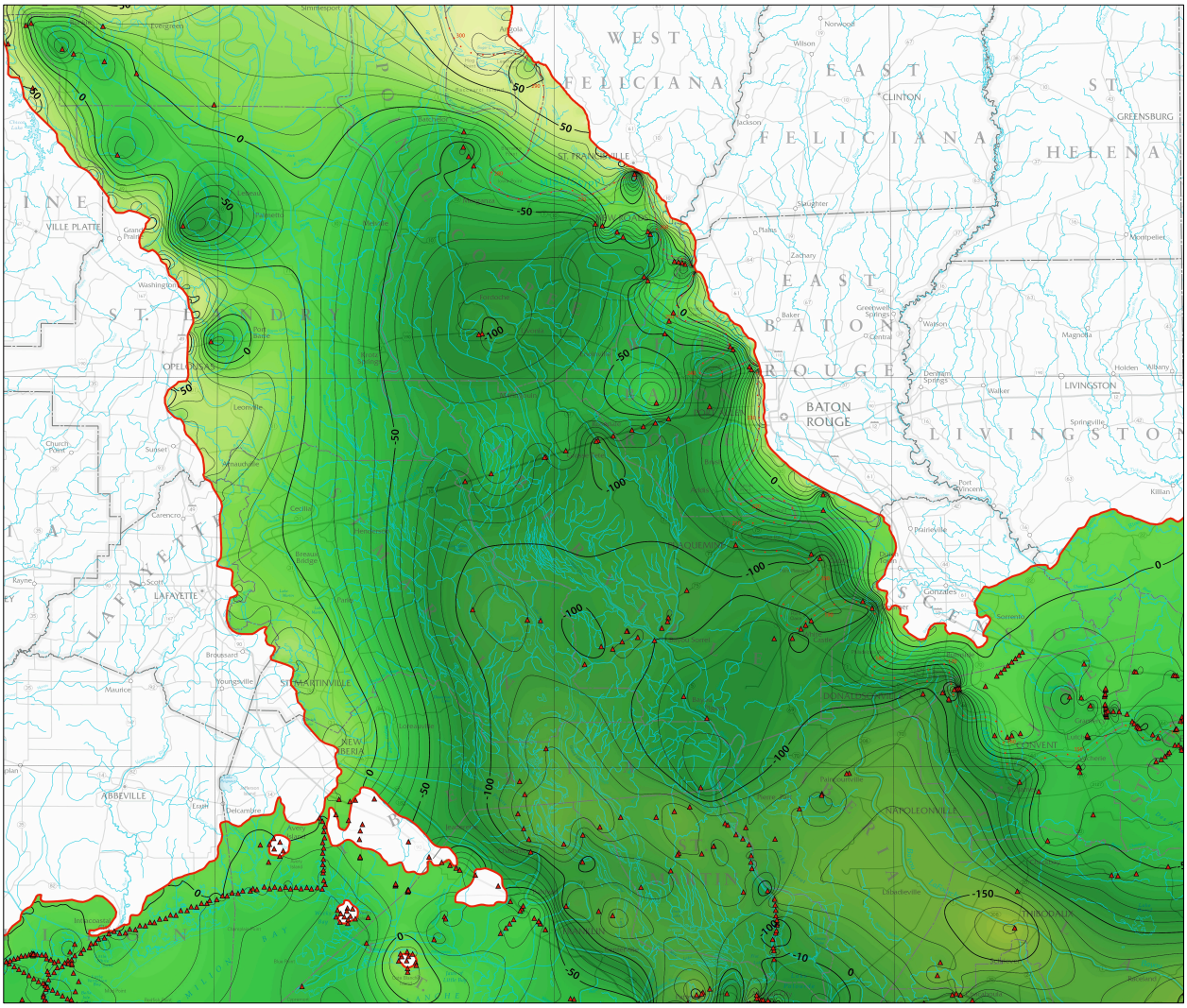

Figure 22 –Mississippi River Alluvial Valley area. *Structure map of the H-P surface. Detail from Plate 1.*

The shallow areas in the upper part of the paleovalley do not reflect the actual channeled and uneven nature of the H-P surface in that area due to inadequate subsurface data. The USACE has made numerous borings in this area but logs could not be located in Vicksburg and their DEM files lacked original boring log data. Hopefully the data exists and can be added when found. Sparse data also accounts for anomalously high H-P elevations along the western valley wall.

West of Donaldsonville, Louisiana, a large flat portion of the Holocene-Pleistocene Surface likely represents a terrace that is an erosional remnant of an older braided river system (Marine Isotope Stage 3 or 4). Other buried highs within the Mississippi Alluvial Valley might also be similar terraced braidbelt remnants that are poorly defined because of sparse subsurface data.

Better data on the eastern side of the paleovalley more accurately depicts the steep nature of the eastern valley wall. The apparent ridge across the river west of Baton Rouge is likely an interpolation artifact of the closely spaced, linear data points collected along Interstate 10. Older USACE geologic investigation maps reveal that paleochannels do continue north out of the study area.

Lake Pontchartrain Basin area – The structure map shows the Holocene-Pleistocene Surface to underlie Lake Pontchartrain Basin and New Orleans at a relatively shallow depth. In this area, the Holocene-Pleistocene surface represents the gulfward, gently sloping coast-parallel terrace surface of the Pleistocene Hammond alloformation, exposed to the north. This buried surface lies inland of the buried, gulfward extension of the ancestral Mississippi River paleovalley ***(Figure 23)***. At Des Allemandes and south of Belle Chase the terrace terminates at a distinct scarp that separates it from a much lower, broad surface that flanks the Mississippi paleovalleys

Despite a good density of data in this area, it is not possible to clearly define paleovalleys of the small coastal rivers due to their shallow depths, but isolated depressions indicate their presence. Likewise, the detail level is insufficient to depict the small displacements of fault-line scarps in the surface.

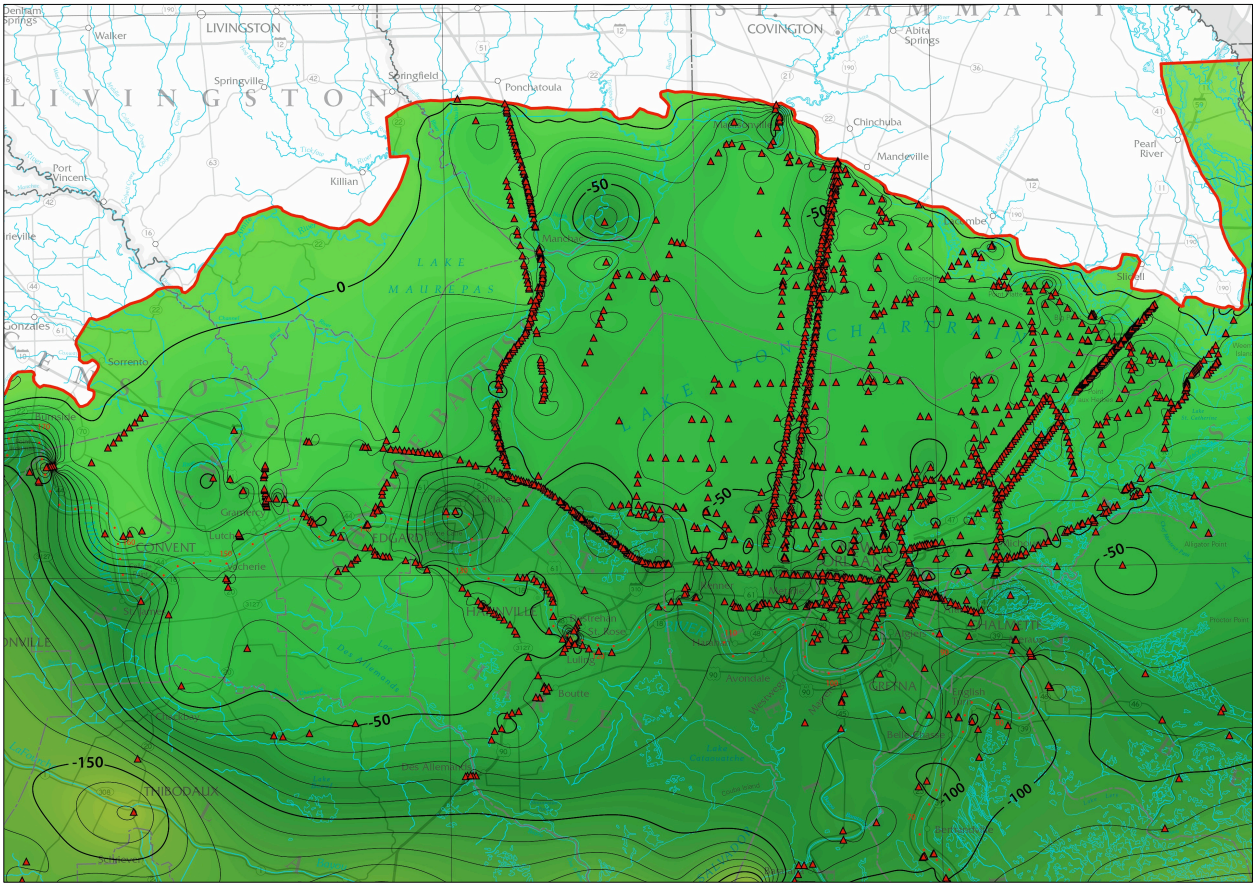

Figure 23 –Lake Pontchartrain Basin area. *Structure map of the H-P surface. Detail from Plate 1.*

Chenier Plain area – The Holocene-Pleistocene surface structure map shows a gently dipping, but poorly defined surface that underlies the Louisiana chenier plain in western Louisiana ***(Figure 24).*** This surface represents the deeply weathered surface of the buried Pleistocene Beaumont alloformation(Marine Isotope Stage 2), exposed to the north. During most of the last glacial epoch, the buried H-P surface was also the exposed surface of the ancient coastal plain, now covered by Holocene sediments of the Mermentau alloformation.

Unfortunately, the details of this former coastal plain are greatly obscured by the extremely poor density of data points in this area. As a result, it is currently impossible to define the paleovalleys and paleochannels of many of the streams that occupied this coastal plain and the paleovalleys and paleochannels of the larger Mermentau and Calcasieu Rivers. At best, they are represented by isolated depressions of which a few form linear associations to suggest their presence.

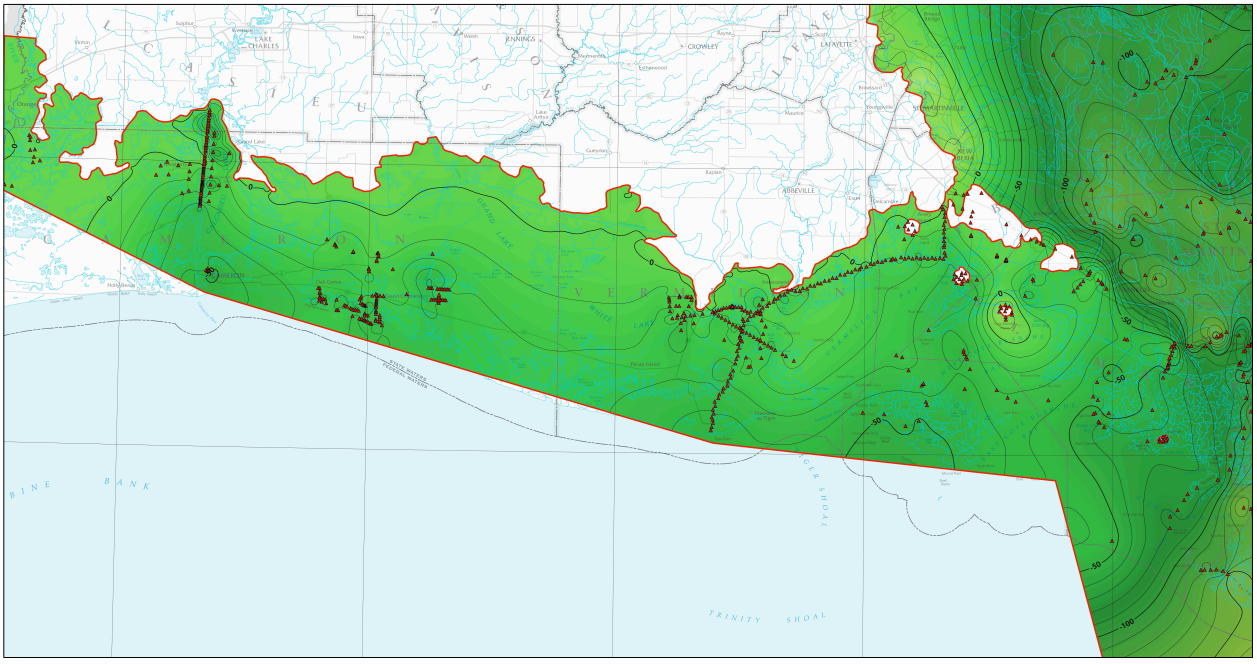

Figure 24 – Chenier Plain area. *Structure map of the H-P surface. Detail from Plate 1.*

St. Bernard/Balize area – The structural map of the Holocene-Pleistocene surface depicts a gulfward dipping trend surface in the St Bernard area ***(Figure 25)***. Under the Balize delta, the dip of this surface steepens abruptly along a distinct flexure. It does not flatten out near the boundary of the mapped area as suggested by the interpolation, but keeps dipping. This is an artifact of the absence of data points near the boundary.

The surface is in places deformed by isolated salt domes into mounded structures. In the southeast corner, the dip of this surface further steepens and grades into an area where it appears to be highly deformed by salt tectonics.

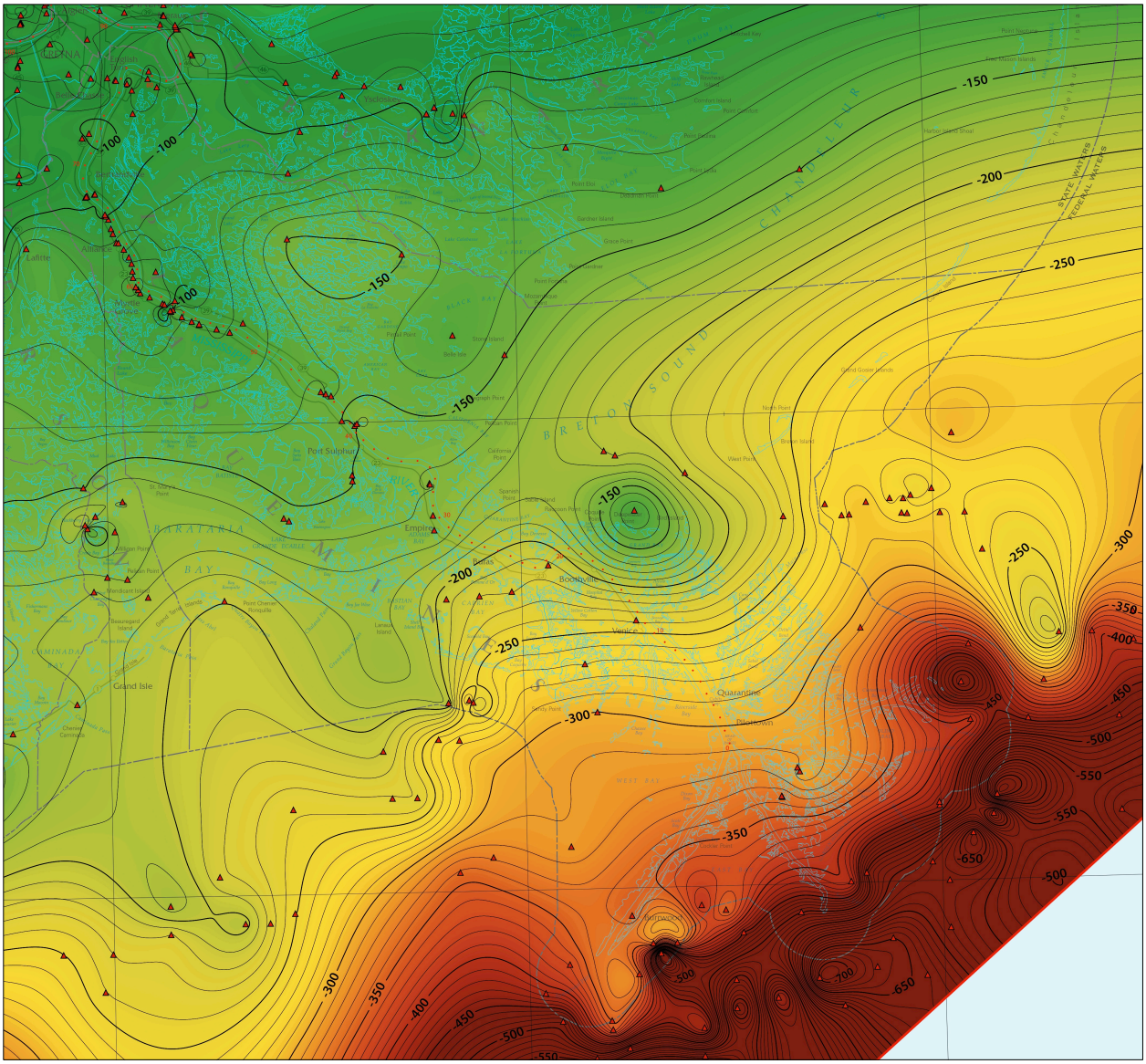

Figure 25 –St. Bernard/Balize area. *Structure map of the H-P surface. Detail from Plate 1.*

Five Islands Salt Domes area – In the Five Islands area, the structural map of the Holocene-Pleistocene surface shows two major features ***(Figure 26)***. One is a line of four diapiric structures where the Holocene-Pleistocene surface has been uplifted and intruded by salt domes to outcrop at the surface. Along with Jefferson Island, which outcrops nearby in the Pleistocene Prairie alloformation, the four intrusions create the famous “five islands” salt domes. This produces "windows" in the topstratum sediments overlying this surface.

The other major feature is an apparent scarp-like break between the gently sloping surface of the Beaumont alloformation and the lower, completely buried, and presumably younger surface that extends as isolated terrace fragments along the paleovalleys of the ancestral Mississippi River.

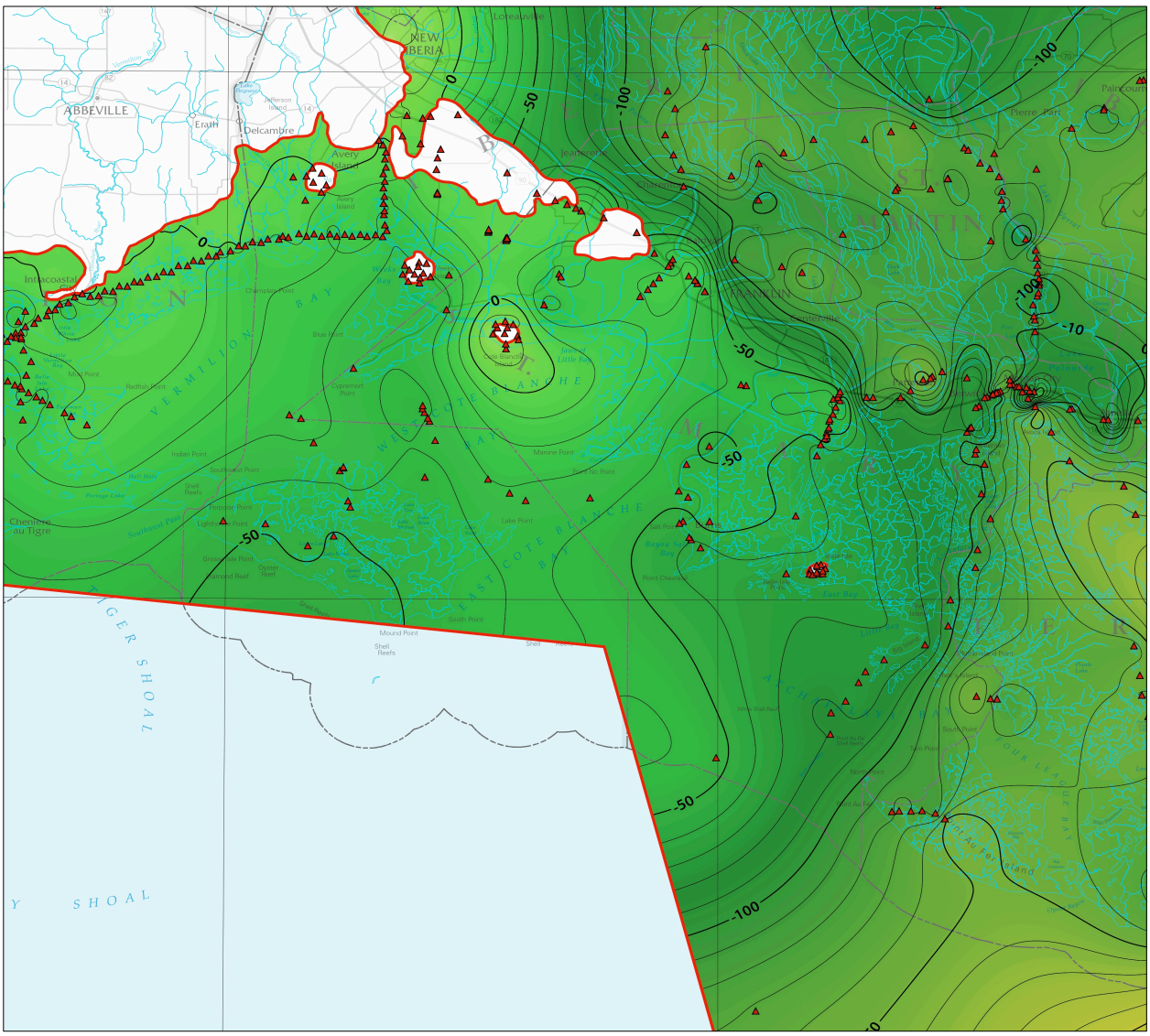

Figure 26 –Five Islands Salt Domes area. *Structure map of the H-P surface. Detail from Plate 1.*

Barataria/Terrebonne area – Within the Barataria/Terrebonne area, the lowstand paleovalley apparently breaks into two paleovalleys just northwest of Theriot ***(Figure 27)***. They likely represent two different Mississippi River paleovalleys that entrenched at different times. The shallowest of these paleovalleys extends southeast beneath Grand Isle. The deepest of these paleovalleys extends southwest beneath Calliou Lake. Of the two this is most likely the marine Isotope Stage 2 lowstand course of the Mississippi River.

The seemingly excessive thickness of sediment exhibited by the Caillou Lake paleovalley possibly reflects significant local subsidence associated with local sediment loading, salt tectonics, or both. It is possible that some of the paleovalley's depth might represent downcutting due to contemporaneous, Last Glacial Maximum uplift associated with glacial isostatic adjustment during the maximum advance of the Laurentide ice Sheet.

On either side of both paleovalleys a broad terrace-like surface can be seen, which has been deformed by salt dome intrusions and other tectonic processes. In addition, some of the irregularities may be artifacts resulting from the scattered nature of the data, contouring techniques, and unavoidable inconsistencies in interpretations of the contacts by different sources.

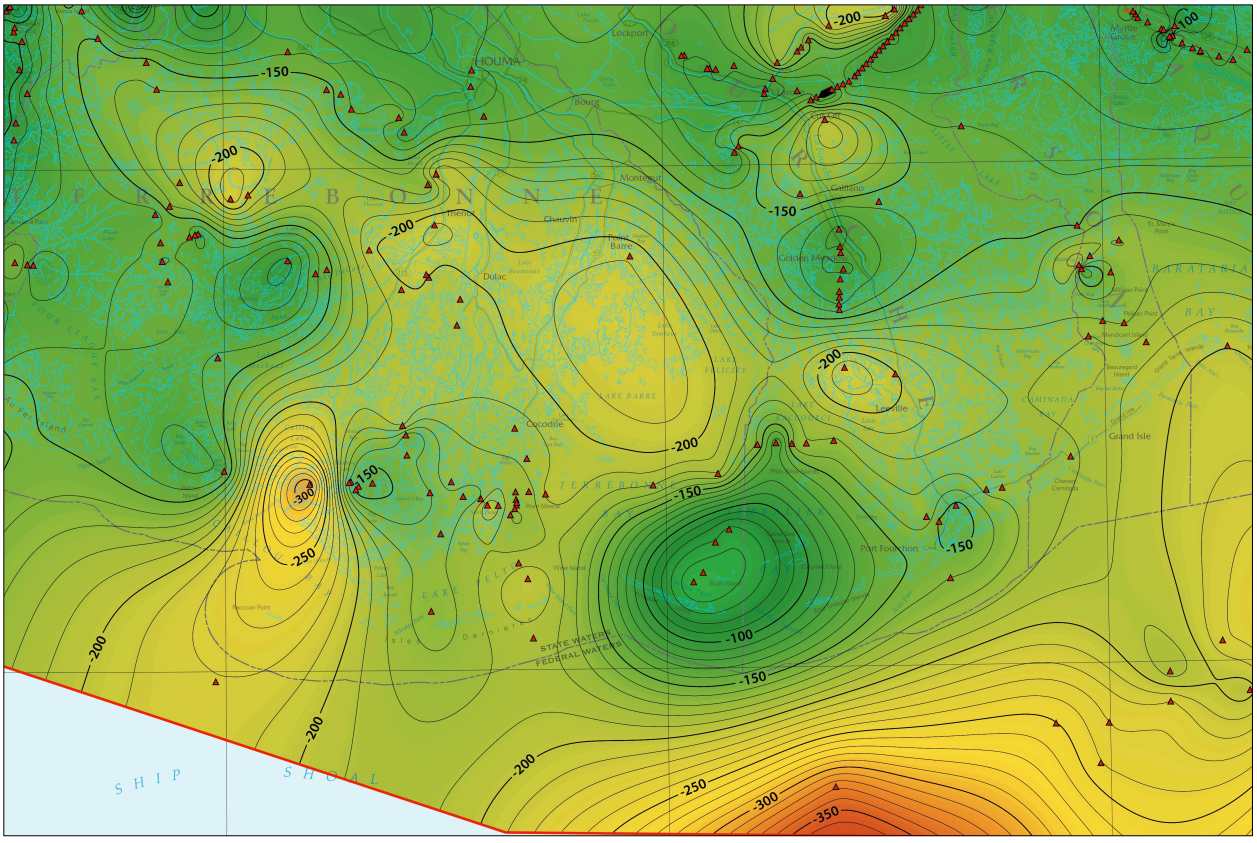

Figure 27 –Barataria/Terrebonne area. *Structure map of the H-P surface. Detail from Plate 1.*

2. Isopach map of the Holocene interval

An isopach map depicts the thickness of a geologic unit. In this case, the isopach of the Holocene interval is very similar in appearance to the structure map (elevation relative to mean sea level) because the topographic/bathymetric surface that represents the top of the Holocene, is within 3 feet of mean sea level over large portions of the mapped area.

Isopach map details of the chenier plain and delta plain ***(Figures 27 and 28)*** depict the thickness of terminal Pleistocene-to-Holocene fluvial, deltaic, and nearshore sediments comprising the topstratum. It shows the thickness of sediments lying between the former Last Glacial Maximum coastal plain (the Holocene-Pleistocene surface) and the surface of the modern coastal plain and coastal water bottoms. This is the thickness of sediments prone to consolidation. The amount of potential consolidation and resulting subsidence increases directly with thickness. The increase in potential settlement might be offset to an unknown extent within the older deltaic lobes as their sediments have had significant periods of time over which to dewater.

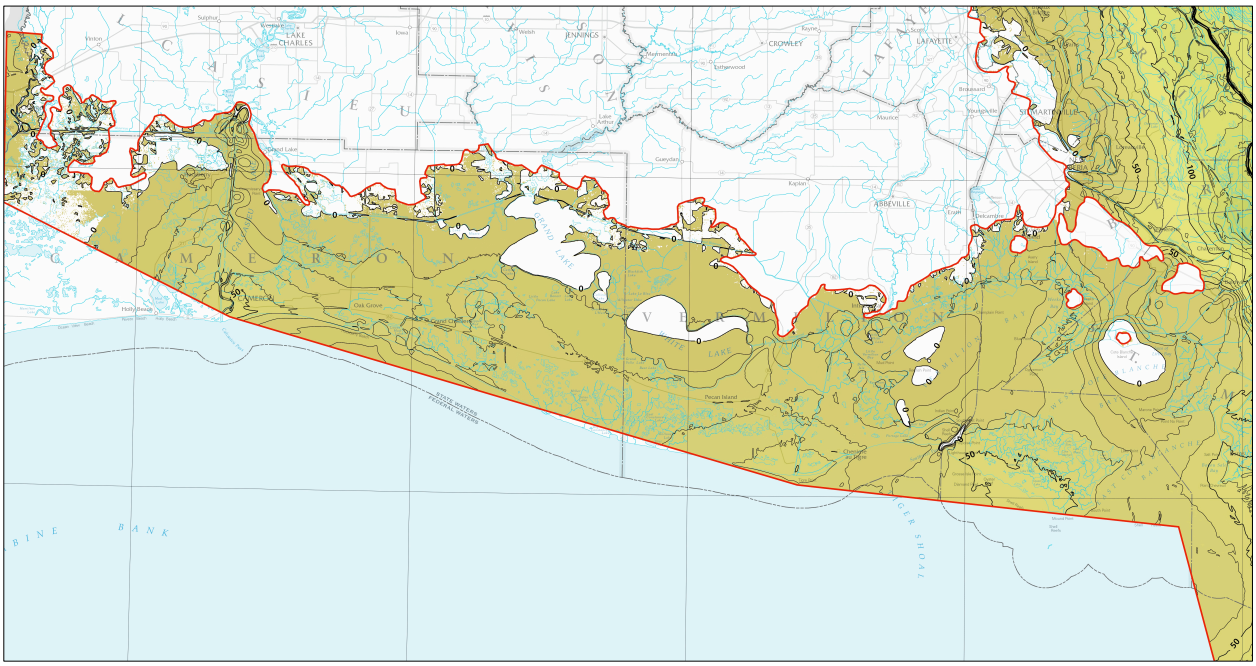

Figure 28 – Isopach of the Chenier Plain*, Southwestern Louisiana.*

Although the details are obscured by the sparse and unequal distribution of subsurface data, the isopach map of the topstratum in general illustrates the general trends in its thickness. The topstratum is thickest beneath the area of the modern Belize delta where the general accumulation of deltaic sediments has most recently occurred. The base of the topstratum in this area is highly irregular as the result of salt tectonics and possibly

because of significant inconsistencies and difficulties in the identification of Holocene-Pleistocene surface using a variety of subsurface data.

Beneath the Mississippi delta plain, thick accumulations of topstratum deposits are associated with two paleovalleys of the Mississippi River. The depth of the westernmost paleovalley is too deep to be explained by the Last glacial Maximum lowstand of sea level alone. As a result, other factors such as sediment loading; glacial isostatic adjustment to the formation of continental ice sheets and their melting; salt tectonics; or some combination of these and other factors are needed to explain the thickness of sediment within it.

In contrast to the delta plains, the topstratum underlying the New Orleans-Lake Pontchartrain area and chenier plain is relatively thin as it overlies the paleosurface of the Prairie allogroup. In numerous places the isopach map exhibits localized thinning of the topstratum over domal features. Some of these are localized areas that have been uplifted by salt domes. Other domes and depressions may be artifacts of misidentification of the Holocene-Pleistocene surface in surface borings or of the contouring software dealing the sparse and unevenly distributed data.

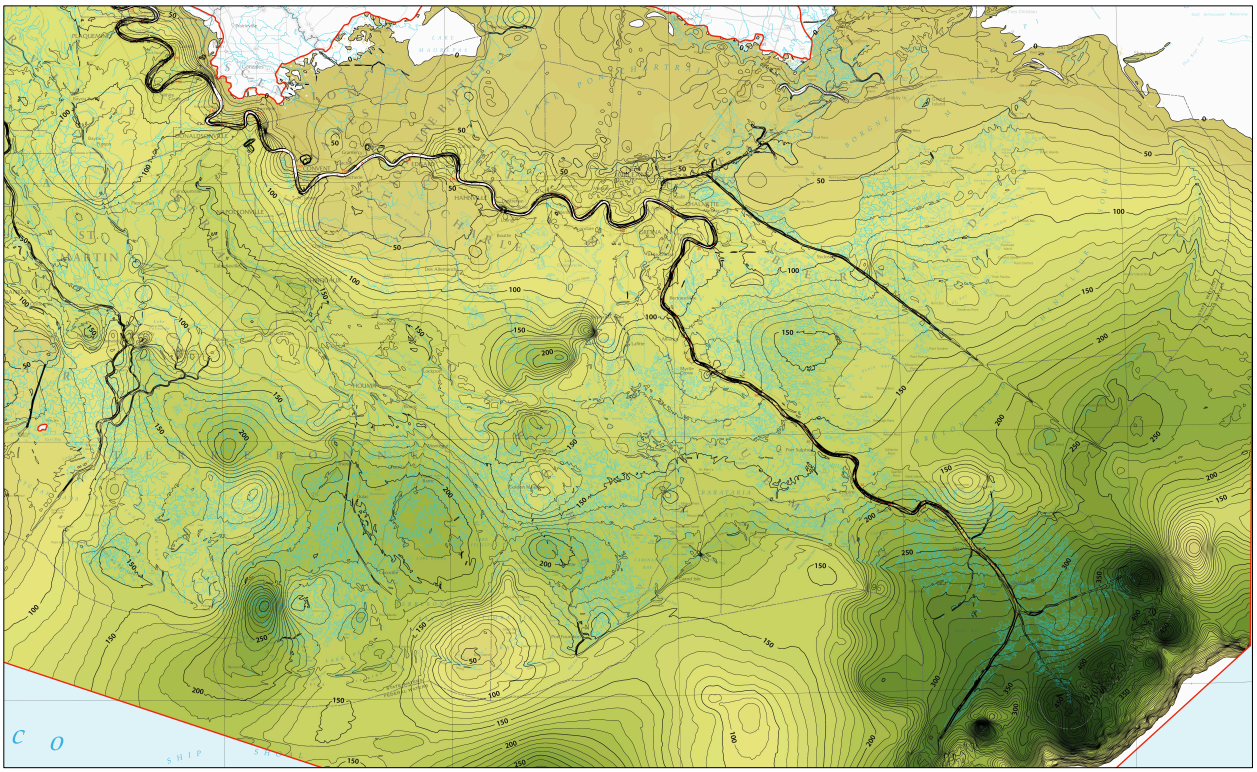

***Figure 29 – Isopach of the Delta Plain**, Southeastern Louisiana.*

3. Relation of the Holocene-Pleistocene surface to subsidence

One of the pressing questions that concern coastal scientists and engineers is how to predict the location, magnitude, and timing of subsidence in coastal Louisiana. The contemporaneous and voluminous literature about subsidence in coastal Louisiana agrees that six major processes contribute to subsidence:

1 – sediment loading
2 – basin tectonics
3 – glacial isostatic adjustment
4 – fluid withdrawal
5 – surface drainage, and most importantly for this study…
6 – topstratum sediment consolidation

Disagreement exists about the spatial and temporal scale of these processes and which is most influential within any one area. In part, this is the result of studies tending to look at one process at a time and the difficulty of examining how each of these processes might interact with each over time *(McCulloh et al. 2006; Dokka 2009; Reed and Yuill 2009)*.

Sediment loading – As initially recognized by *Fisk (1944)*, sediment loading is causing natural subsidence on a regional scale within the Louisiana coastal plain. Over the last 8,000 to 7,000 years ago, the deposition of thick accumulations of deltaic and coastal sediments by the Mississippi River has resulted in the downward depression of the underlying crust. The localized accumulation of the greatest thicknesses of sediment within a delta complex has caused the area covered by it to subside, whereas north of it, the crust and the fluvial and deltaic sediments overlying it have been tilted upward. The current rate of subsidence due to sediment loading, which reflects the mass and loading history of deltaic and coastal sediment accumulation, are estimated to be 1 to 8 mm/yr for the Mississippi River delta and adjacent lower Mississippi River valley. *(Fisk 1944; McCulloh et al. 2006; Reed and Yuill 2009)*.

Basin tectonics (growth faulting and halokinesis) – Natural subsidence also occurs along regional, generally east-west fault systems. These gulfward-sloping faults lie parallel to the modern coastline and perpendicular to the direction of delta growth. These are termed growth faults because the downward movement of their gulfward side occurs contemporaneously with and due to the accumulation of deltaic and coastal sediments. The movement on these faults results in gulfward sliding of the sediment blocks and subsidence of the delta plain *en echelon* between parallel fault zones. In addition, the gulfward flow of underlying salt deposits, loaded by coastal sediments, has contributed to fault movement. Recent studies have estimated that within the Louisiana Coastal Zone, rates of very low tectonic subsidence are an approximate order of magnitude about 0.1 mm/yr during the Holocene Age. *(McCulloh et al. 2006; Dokka 2009; Reed and Yuill 2009)*.

Glacial isostatic adjustment – Glacial isostatic adjustment (GIA) is the natural adjustments of the Earth's crust to the growth and disappearance of ice sheets and glaciers. These adjustments, as reflected in elevation changes of land and sea bottom, result from the addition or removal of ice from ice sheets and glaciers and the addition or removal of water from the world's oceans. During glacial stages, large ice sheets, some up to several kilometers thick, covered much of northern North America and other parts of the world.

The mass of the ice sheets upon the Earth's lithosphere caused the underlying crust to depress as material within the mantle flowed out from under the immense weight of the ice. Because the lithosphere partly supports the load of the ice sheet, the lithosphere will flex such that it is also depressed at some distance from the margin of the ice sheet. Upon melting of ice sheets and glaciers, mass is removed from the lithosphere and the continental shelves are loaded by water. Currently the residual effects of GIA appear to consist of a uniform and steady rate of subsidence in coastal Louisiana. Using models of lithospheric processes, regional subsidence due to GIA is currently estimated to be between 0.55 and 2.0 mm/yr. *(Ivens et al. 2007; Dokka 2009; Reed and Yuill 2009)*.

Fluid withdrawal –The human-induced pumping of groundwater or hydrocarbons results in the removal of pore fluids within a layer of porous sediment. This process is *consolidation*, in which the reduction of internal pore pressure causes the pores to collapse and volume of the layer of sediment to significantly decrease and the overlying land to subside. Although the pumping of groundwater has caused localized subsidence in parts of Louisiana north of the Louisiana Coastal Zone, fresh water wells are few in coastal Louisiana. Only local areas with high rates of fluid withdrawal associated with hydrocarbon production have been correlated with fault-reactivation high subsidence rates in southern Louisiana. Within or very near producing oil and gas fields, peak subsidence rates reached 23 mm/year and average between 8 to 12 mm/year. It is a regionally insignificant cause of subsidence *(Morton et al. 2002, McCulloh et al. 2006; Reed and Yuill 2009).*

Surface water drainage: localized dewatering and peat oxidation – Another very localized and human-made source of subsidence is the removal of surface water for drainage. Typically, the removal of surface water occurs in areas blocked from natural water flow by levees, roads, or agricultural dikes or in areas adjacent to canals. This causes the rapid removal of pore fluids from surface sediments with an associated consolidation and reduction in volume. Concurrent with consolidation, the drainage of water exposes organic matter within soils and sediments of marshes and swamps to an oxidizing environment. This results in the rapid destruction of the organic matter by oxidation and drastic reduction in the volume of sediment. The observed subsidence rates due to consolidation and oxidation of organics are highly variable and have been found to vary by two orders of magnitude between 0.1 to 10.0 mm/yr. These processes have severely affected large tracts of land drained for agricultural purposes and protected by levees for flood protection. (*Snowden et al. 1980; McCulloh et al. 2006; Reed and Yuill 2009).*

Topstratum sediment compression – The compression of sediment within the topstratum is a significant, but highly variable, contributor to subsidence in coastal Louisiana. It may account for 80% of subsidence as measured at the land surface *(Törnqvist, 2013)*. The rate and degree of accompanying subsidence that occurs is a function of the properties of the sediments and increases with thickness of the compacting sediment column and the load imposed above the compacting sediments (*McCulloh et al., 2006; Reed and Yuill, 2009).*

The coast-wide Holocene-Pleistocene surface dataset can play a role in assessing the important topstratum compression element of Louisiana coastal subsidence. The Holocene interval between the land surface/coastal water bottoms and the H-P surface comprises the pertinent topstratum. The structure map depicts the form of its base and the isopach map depicts its thickness, within the limitations of the source data.

Compression is the decrease in sediment volume due to a restructuring of the alignment of internal grains as a result of an applied stress, which results in the sediment becoming more tightly packed. Under the subsurface conditions found within the topstratum, the grains composing these sediments and their pores fluids can be regarded to be incompressible. As a result, the compression that occurs in these sediments is the result of time dependent expulsion of pore fluids, mainly water, in response to an applied stress, which is known as *consolidation*. The expulsion of pore fluids reduces the internal pore pressure causing pore collapse, realignment of the grains, and a corresponding decrease in the volume sediment and ultimately subsidence *(McClelland 1956; Kolb and Van Lopik, 1958; Kuecher et al. 1993; Reed and Yuill 2009).*

A significant control on the amount and rate of subsidence is the thickness of the topstratum alloformation overlying the H-P surface. Both the rate and total amount of potential subsidence increase with sediment thickness, as the volume of sediment within it shrinks because of consolidation. The present day compaction occurs in the sediments comprising the modern delta plain and valley fill of the Pleistocene entrenchment that overlies the H-P surface. The typical range of subsidence that has been attributed to compression, specifically by consolidation, of topstratum sediment ranges between 1.0 and 5.0 mm/year for the Mississippi River Delta and lower Mississippi River Alluvial Valley *(Roberts et al. 1994; Tornqvist et al. 2008; Kuecher et al. 1993; Reed and Yuill 2009).*

Another factor in rate of subsidence and potential for total future subsidence is the age of deposition of the topstratum, for which the delta lobes might serve as a useful proxy. Consolidation declines exponentially with time. As a result, the rates of subsidence and potential future total subsidence should decline as the age of the sedimentary deposit increases. Older delta deposits should subside at slower rates than younger delta deposits and have less potential for future subsidence, all else being equal (*Kuecher et al. 1993; Roberts et al. 1994; Tornqvist et al. 2008).*

The composition of the sediments also influences the rate and amount of compression resulting from consolidation and ultimately subsidence rates and the potential amount of subsidence. The higher the porosity within a sediment, the faster subsidence will occur and a greater amount of subsidence will occur. Thus, interchannel and interdistributary areas underlain by clayey, organically rich, and organic sediments can be expect to have higher subsidence rates than meander belts or natural levees underlain by thick, sandy point bar deposits.

The thickness of peat above the Holocene-Pleistocene surface will influence the potential amount of subsidence (*McCulloh et al., 2006; van Asselen et al., 2009*). Organically rich sediments can be expected to consolidate over a longer period of time and greater extent as the result of secondary consolidation that results from the compression of the organic material that they contain. Because of this, increasing the organic content (i.e. peat) of sediment increases subsidence rates and potential *(Kuecher et al. 1993; Roberts et al. 1994; McCulloh et al. 2006; Tornqvist et al. 2008).*

The local loading of the delta plain by fluvial and distributary sediments causes local increases in consolidation and accelerated subsidence within a strip of the delta plain adjacent to them. The channel, distributary mouth bar, and natural levee deposits of distributary channels and trunk delta channels that feed them, load the delta plain because they are denser than the sediment underlying surrounding delta plain. The natural levees are built up above the level of the delta plain. This localized loading of the delta plain causes accelerated consolidation that results in the delta plain adjacent to it to subside faster and to a greater degree than the delta plain in general.

A very small and undeterminable amount of subsidence can be currently attributed to the sediments beneath the Holocene-Pleistocene surface comprising the substratum and the Prairie and Deweyville allogroups. Because of their age, the exponential decrease in initial consolidation with time has decreased dewatering and resulting consolidation rates to values that are insignificant relative to the overlying topstratum. The Prairie allogroup has been deeply weathered over the long period of time it formed the surface of the Louisiana coastal plain during sea level lowstands. Its sediments have been deeply desiccated, altered, and cemented by the development of paleosols into characteristically very stiff and significantly overconsolidated sediments *(Fisk 1956; McClelland 1956).* Although specific data is lacking for the substratum and the Deweyville allogroups, they are likely to have also been similarly desiccated, altered, and cemented by weathering into stiff paleosols before their upper surfaces were buried by the Mermentau alloformation.

The maps

Cartographically developed map plates have been prepared to accompany the GIS datasets of the Holocene-Pleistocene surface. They were designed for use at a scale of 1:380,160 (one inch equals 8 miles), the same scale as the popular published maps **Official Map of Louisiana** *(Snead et al., 2000),* the **Louisiana Coastal Zone** *(Paulsell, Snead, and Pond, 2012)*, and **Louisiana Shoreline Loss 1937-2000** *(Snead, Peele, and Binselam, 2007)*. The H-P project maps are suitable for use as wall maps or conference-table exhibits.

The maps are published as georeferenced Adobe portable document format (PDF) files included in the document folder where this report resides and are hyperlinked below. They have been designed for full-scale color printing on large-format inkjet plotters with a sheet size of 26 by 60 inches. Page size reductions have been included below for illustrative purposes only ***(Figures 30, 31, 32)***, the original detail level being designed for full-scale reproduction.

The maps produced in this study are:

Plate 1 – Structure of the Holocene-Pleistocene Surface in Coastal Louisiana

Plate 2 – Isopach of the Holocene Interval in Coastal Louisiana

Plate 3 – Topography and Bathymetry in Coastal Louisiana

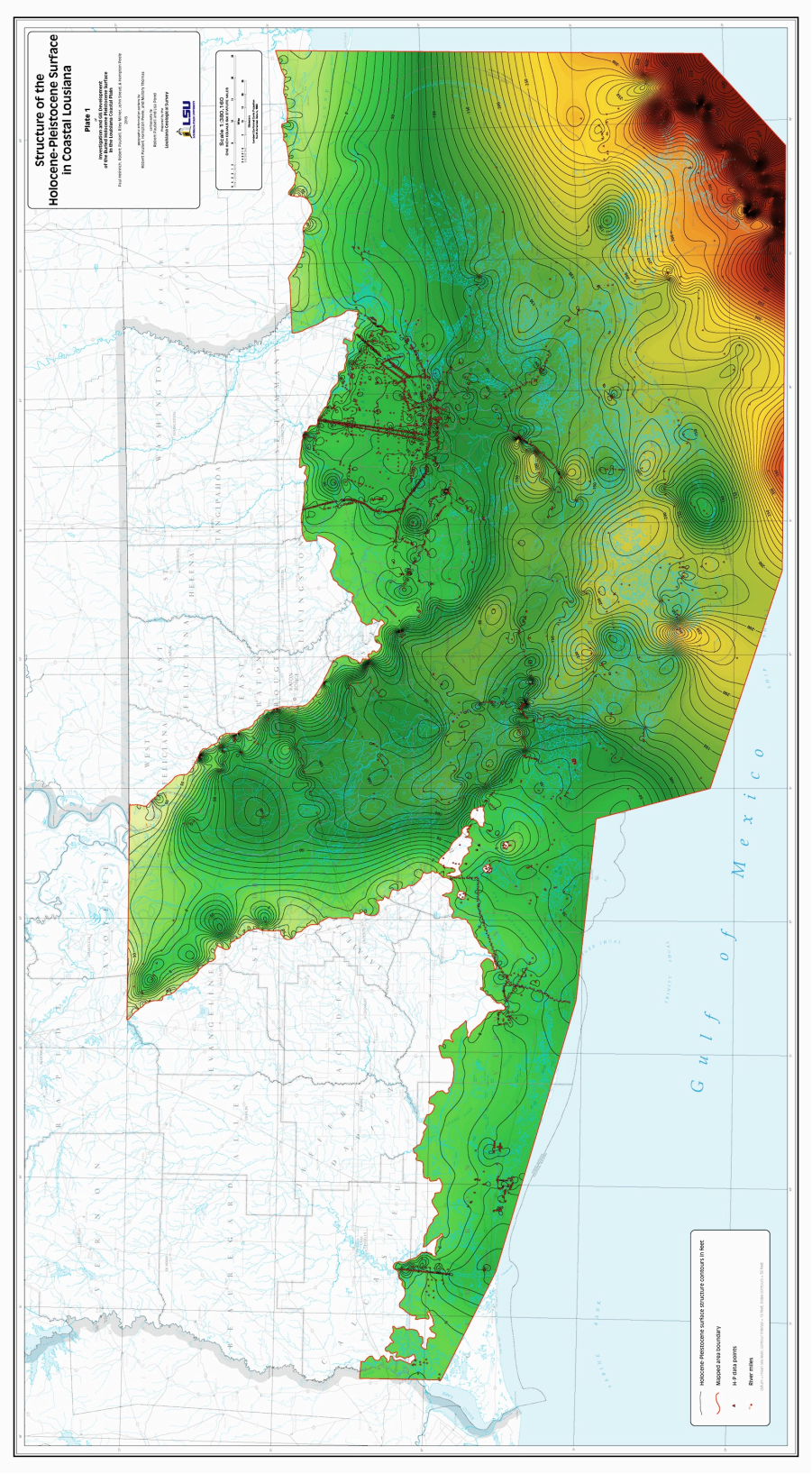

Figure 30 – Plate 1: Structure of the Holocene-Pleistocene Surface *in Coastal Louisiana. Small scale reduction of the 1:380,160 original.*

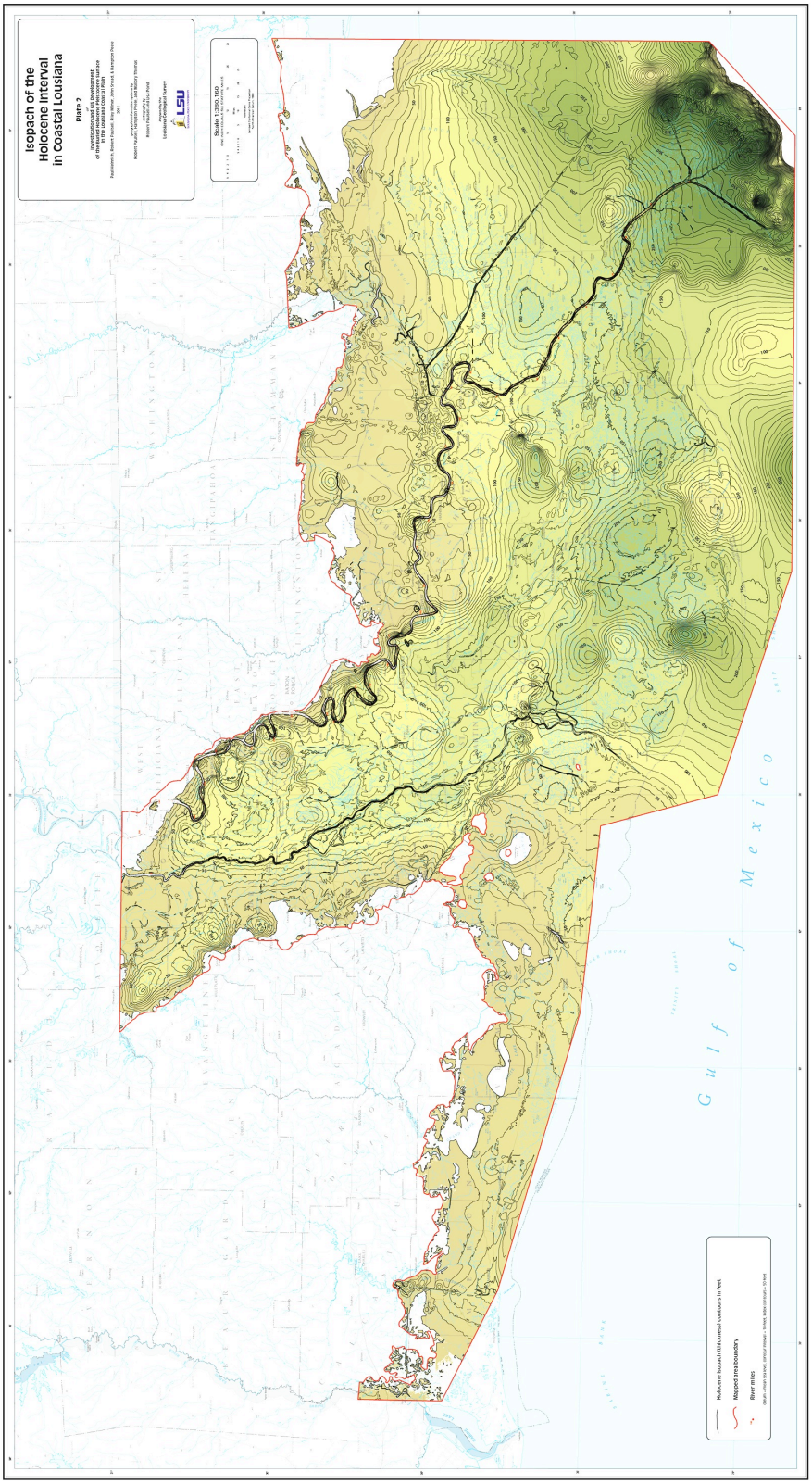

Figure 31 – Plate 2: Isopach of the Holocene Interval *in Coastal Louisiana. Small scale reduction of the 1:380,160 original.*

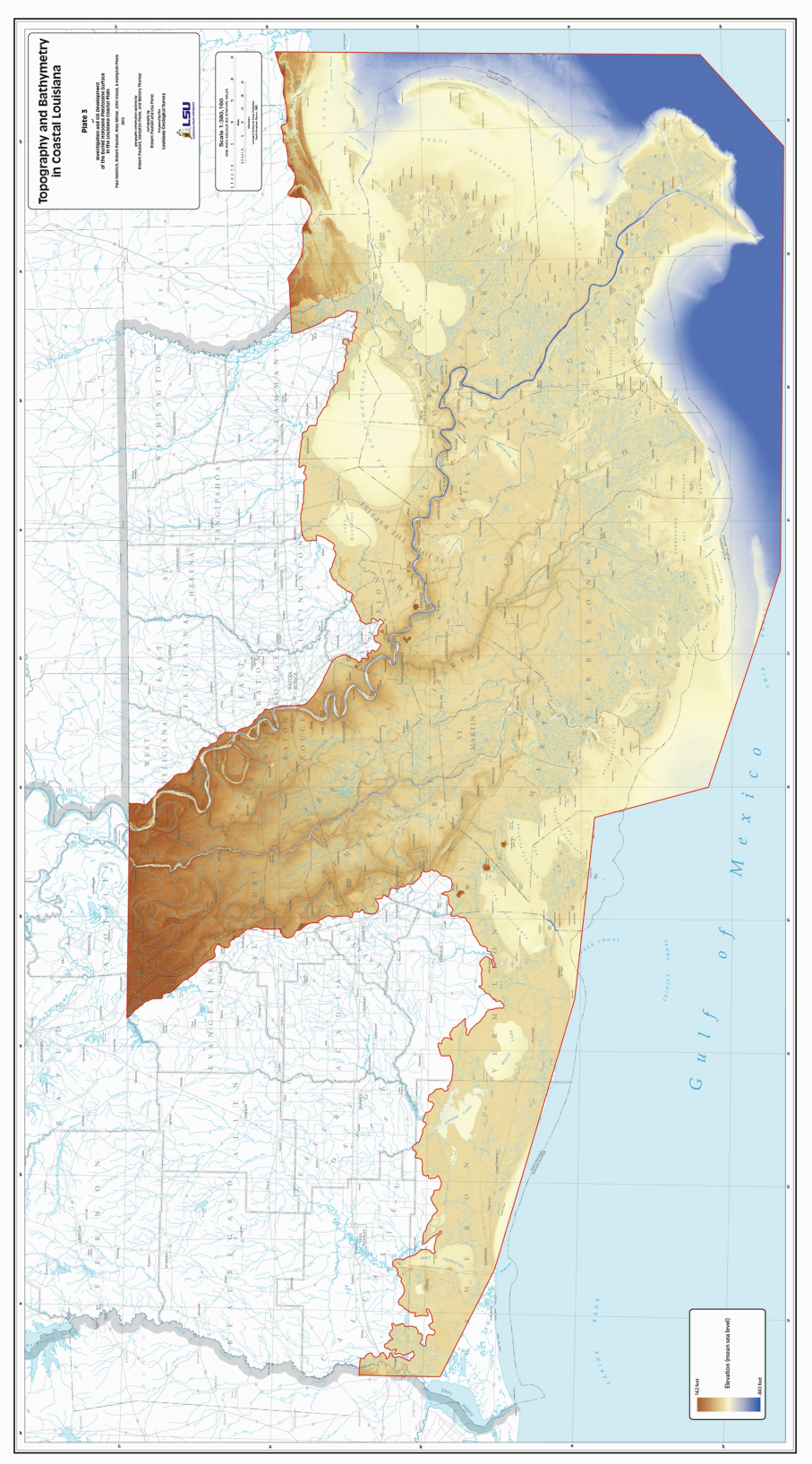

Figure 32 – Plate 3: Topography and Bathymetry in Coastal Louisiana. Small scale reduction of the 1:380,160 original.

Conclusions

1. Quality and accessibility of source data varies greatly.

Within the Louisiana coastal plain, there exists a seemingly paradoxical situation concerning subsurface data. On one hand, the Louisiana coastal plain and continental shelf is one of the most extensively drilled regions on the planet. Within it oil and gas wells have been drilled for over a century. Associated with the production of oil and gas, innumerable geotechnical studies involving the construction of needed infrastructure exist. Many thousands of soil borings have been commissioned and completed. Within this area many geotechnical studies have required the drilling of numerous borings for docks, refineries, highway bridges and causeways, and hundreds of miles of artificial levees. Judging from all of this work, the shallow subsurface of the Louisiana coastal plain should be one of the best documented in the world with logs from many thousands of borings that have been drilled, pounded, or cored into it over the last century.

However, after searching though the voluminous files from various organizations, it has been found that there exists a significant lack of high quality subsurface data that can be readily accessed for geological research. Despite the numerous logs of soil and other borings, only a small amount of these logs and other subsurface data can be located or, if located, accessed. Primarily, the databases that could be accessed were public records of the Louisiana DOTD, Louisiana Department of Natural Resources' SONRIS, Coastal Protection and Restoration Authority of Louisiana's LASARD, a part of CPRA's System Wide Assessment and Monitoring Program (SWAMP), and the US Army Corps of Engineers. Although a few private companies have large databases of boring logs and other data, they are quite reluctant to share this data or have lost or mislaid the subsurface data that they might have.

In a recent study, *Vine et al. (2014)* found that for most scientific papers published over the last twenty years, original raw data is unobtainable. They were unable to obtain this data because authors have changed their contact information since publication and can't be reached; because the data was stored using outdated technology; disposed of; or was not formally archived in a proper repository. In case of *Frazier (1967), Saucier (1994),* and Dr. Arnold Bouma's boring log collection, the researchers were deceased and could not be contacted. For *Frazier (1967),* where, if anywhere, any boring logs and other data were archived could not be determined. In case of *Saucier (1994)* and *Stanley et al. (1996),* a likely repository was found, but the data, i.e. cross-sections, maps, or boring logs could not be located in them.

2. Preservation of older boring data can be very poor.

The preservation of subsurface data was found to be poor. In academia, after research projects are finished and papers published, boring data and associated field notes get scattered in departmental and personal files that all too frequently become difficult to find and or worse, become hopelessly fragmented or simply disappear. Except for some engineering firms, the geotechnical reports and the subsurface data that they contain often are stored without indexing and eventually disposed of.

There are three recommendations to increase the amount of available geologic data for mapping and engineering studies.

- Continue to support the efforts of the Louisiana DOTD and DNR to search for legacy data in files and properly archive it within publically accessible databases such as LASARD and SONRIS.
- Undertake an effort to see that boring logs and other subsurface data generated in the future by consultants for Louisiana state agencies using public funds is archived in a central repository on a timely basis. Otherwise it eventually will become scattered and discarded or lost in un-inventoried, undocumented files and storage units.
- Require or encourage as a part of research permits that academic studies conducted on state lands archive a copy of their subsurface data, including precise location data, after a set period of time with an appropriate database such as LASARD and SONRIS and including appropriate metadata.

3. The available data is often ambiguous and not useful

Because most of the subsurface data was generated for engineering purposes, interpretation of this data often involves a significant amount of interpretation and ambiguity in terms of determining the depth of this contact. Although many soil boring contain detailed and useful descriptions of the sediment penetrated by a boring, others provide only bare-bone descriptions that lack information commonly used to differentiate Pleistocene from Holocene sediments. These boring descriptions lack important information such as the presence of carbonates or iron concretions, presence of shells, and the presence of slickensides and other structures. These features are not only important to differentiating different types of sediments, but evaluating their engineering and geohydrologic properties. In some cases, it appears the Holocene-Pleistocene contact was identified in the field based on criteria not recorded in the logs.

4. The sparseness of data in many areas may limit the dataset's usefulness in local assessments.

As shown in ***Figure 10***, the uneven distribution of adequate boring data within the Louisiana Coastal Zone creates areas where the confidence of the interpolated surface is less assured ***(Figure 14)***. This uneven distribution is the result of the development of bridges, artificial levees, and other public infrastructure mainly along the major waterways and within major urban areas. Fewer structures are built in the marshes and swamps of the Louisiana coastal zone and are often privately owned. As a result, any soil borings and other data associated with them typically remain inaccessible within proprietary corporate files.

In the areas of sparse data an applied effort to negotiate access to data held by private companies could be made with support from government. Detailed mapping of the H-P subsurface will ultimately require the collection of new subsurface data specifically for the purpose of better mapping the H-P surface for use in future determination of subsidence potential.

5. The mapped surface accurately depicts major structures but a higher detail level is needed to refine specific local features.

Despite issues with the quality, accessibility, preservation, distribution, sparseness, and usefulness of subsurface data within the Louisiana coastal zone, the compiled data does accurately depict the general geomorphology and structure of the Holocene-Pleistocene surface. Two entrenched Mississippi River paleovalleys, some scarp-like features, the sloping surface of the Prairie allogroup, and a lower surface bordering Mississippi River paleovalleys are recognized on the mapped H-P surface. These features have been deformed in places by salt tectonics and sediments. Quite prominent are local highs within the Holocene-Pleistocene surface where it has been uplifted by an underlying salt dome. The Holocene-Pleistocene surface is undoubtedly affected by faulting but cannot be currently resolved given the limitations of the available data. Similarly, limitations in the detail level of the available data prevented the definition of smaller features such as individual paleochannels and paleovalleys of smaller river stream systems.

6. **The structure of the Holocene-Pleistocene surface exerts a strong control on the potential for subsidence and associated land loss.**

All else being equal, the areas underlain by the thickest topstratum are the areas that have the most potential for subsidence. As a result, the areas of coastal Louisiana overlying the lower surfaces associated with Mississippi River paleovalleys should have the most potential for total and high rates of subsidence. Within these areas, the rates of and potential total subsidence will be further influenced by the age of the underlying topstratum. Older delta deposits should have a lesser potential for subsidence and high rates relative to younger deposits because they have had time since deposition to dewater.

For example, being thicker and younger, the Plaquemine delta lobe should have the greatest potential for total and high rates subsidence. Such younger deposits should be more unstable and prone to gravity slumping, subsidence, and land loss associated with faulting. In addition, variations in the overall lithology of the sediments comprising the topstratum can have significant effects on subsidence rates and total subsidence.

The New Orleans-Lake Pontchartrain area north of a scarp-like feature in the Holocene-Pleistocene surface and the chenier plain west of the "five islands" should be more stable and have a lesser potential for overall subsidence. However, local factors such as withdrawal of underground fluids and land drainage still can have drastic effects on subsidence and land loss. In both areas, the Holocene-Pleistocene surface will typically be close enough to the surface that it can serve as a base for foundations of major coastal engineering structures.

In addition to the depth of the Holocene-Pleistocene surface, variations in the lithology of the sediments comprising the various facies within the topstratum and the Mermentau alloformation can have significant effects on subsidence rates and total subsidence. It would be of great benefit to incorporate data on the internal facies of the Holocene interval into future Quaternary subsurface data collection efforts.

Suggestions for Future Research

The creation of a more comprehensive database of subsurface data for the shallow subsurface of the Louisiana coastal zone is needed. It will require more than just data concerning the depth of the Holocene-Pleistocene surface to fully understand the variation of subsidence rates. Eventually the variability in the stratigraphy, morphology, and lithology of the individual facies of the many fluvial, deltaic, and marine deposits that overlie it will have to be understood as thoroughly as the older geologic units underlying it, now revealed by deep oil and gas geophysical logs, micropaleontology, and 3D seismic technology.

This would involve collecting as much georeferenced subsurface data as possible into a comprehensive database. Part of this effort would involve a concerted effort to locate, access, and obtain copies of original data from *Gould and McFarlan (1959)*, *Fisk (1948a, 1948b)*, *LeBlanc (1949)*, and similar archives for this data if they still exist.

In addition, a formal effort should be made to locate much data that are currently hiding in the paper files of DOTD, USACE, and other agencies so that it can be entered into the database. Researchers currently conducting subsurface coastal research under CPRA funding could be required to provide copies of any collections of boring logs that they might have for this database, which should be properly assembled, indexed, and archived.

Similarly, rules and regulations might be amended to encourage or mandate that oil and gas companies drilling in Louisiana be required, as part of the future permitting processes, to provide representative logs of soil borings made of geotechnical investigations of marsh rigs and offshore platforms. While deep oil and gas data may be considered proprietary, the shallow Holocene and Pleistocene data most useful for coastal research into subsidence probably is not. As a part of this process, a more concerted effort could be made to obtain existing private shallow subsurface data from coastal engineering firms, perhaps with some official incentives. Access to proprietary 3D seismic data from oil companies would be valuable, if only the upper Quaternary units not considered in petroleum exploration, but this will involve costs for them.

A major envisioned project would be to utilize the surface, isopach, and standard error maps produced by this project to select areas totally lacking in H-P boring data and areas with a problematic sparseness of such data and undertake an effort to collect data from new borings strategically located to fill in areas of poor data coverage. This would require a detailed description of both cores and samples using either a geoprobe or a standard drilling rig depending on depth.

It is entirely possible, with the proper resources, to develop a much more detailed and useful structure map of the Holocene-Pleistocene surface and isopach map of the Holocene interval and perhaps to determine their more complex internal structures.

Digital deliverables

1. A geographic information system (GIS) dataset with ArcGIS shapefiles (.shp) of the original boring data and relevant base information, H-P surface structure, isopach, and DEM data, and associated metadata. This dataset includes a cartographically developed map document (.mxd) file.
2. Cartographically developed isopleth maps at 1:380,160 of the H-P surface structure, the isopach of the Holocene interval, and a DEM of the topographic-bathymetric elevation surface (plates 1, 2, and 3) suitable for use as wall maps. These map plates, the text maps, diagrams, and illustrations are also provided as PDF files for use in reports and presentations.
3. A final technical report on the project that describes the data, methodology, interpretations, and conclusions. A PDF file, it includes descriptions of all sources evaluated and an appendix of source borings used in the project.

Information dissemination

The results of the investigation will be disseminated through the CPRA website, technical papers, and presentations.

A preliminary presentation of the project was prepared and presented for a CPRA webinar in September 2014 after the first year of the project. A presentation of the ongoing project was prepared and presented at the 2015 Louisiana Remote Sensing and Geographic Information System Workshop. Further presentations will be made in 2016.

A paper discussing the final results and products of this investigation will be submitted to a region-appropriate professional journal such as the *Journal of Coastal Research*, *Southeastern Geology*, or the Gulf Coast Association of Geological Societies *Transactions*.

A 4 by 8-foot illustrated poster will be created after the project is completed and presented to inform and disseminate the results of the study to the intended audience of Louisiana coastal researchers, planners, GIS scientists and decision-makers involved in coastal research and planning efforts. The exhibit will be offered at the Louisiana RS/GIS workshop, the GCAGS conference, and at state coastal protection and restoration seminars and workshops. A detailed PDF file of the poster exhibit will be created and made available online for reference and ease of reproduction and distribution.

Metadata will be compiled and uploaded to appropriate state and federal indexes of geologic data to best enable Internet searches for the material.

Acknowledgements

A considerable number of people have given freely of their time, effort, and expertise to assist this research. For their advice about possible sources of data and mapping techniques, Dr. Michael Blum, (Department of Geology, University of Kansas); Dr. Zhixiong Shen (Department of Marine Sciences, Coastal Carolina University); Dr. Torbjörn E. Törnqvist (Department of Earth and Environmental Sciences, Tulane University); Dr. Mark Kulp (Department of Earth and Environmental Sciences, University of New Orleans); and Dr. David Weinstein (Coastal Environments, Inc., Baton Rouge, Louisiana) are heartily thanked.

Dr. James Flocks (St. Petersburg Coastal and Marine Science Center of the U.S. Geological Survey) provided invaluable GIS data sets. Dr. Gavin P. Gautreau, P.E., (Louisiana Transportation Research Center, Baton Rouge) arranged for invaluable and well appreciated access to the their soil boring database. Both Dr. Del Britsch (U.S. Army Corps of Engineers, New Orleans District) and Dr. Joseph B. Dunbar (U.S. Army Geotechnical and Structures Laboratory, Vicksburg) provided essential assistance in looking for and acquiring U.S. Army Corps of Engineers for this project. Dr. John Anderson (Cartographic Information Center, LSU) and Dr. Britsch searched their organization's archives for soil borings and other data of Dr. Roger Saucier.

The assistance of Dr. Juan Lorenzo (LSU Department of Geology and Geophysics) in the search for Dr. Arnold Bouma's well log archives is well appreciated. Dr. Harry H. Roberts of the LSU Coastal Studies Institute contributed valuable assistance and data. The staffs of Marsh Island and Roosevelt Wildlife Refuges were quite generous with their help and data. State Geologist Dr. Chacko John (Louisiana Geological Survey, LSU) offered broad institutional support and provided a technical edit of the report.

Syed Khalil and Ed Haywood of the Coastal Protection and Restoration Authority are thanked for their very helpful quarterly and final reviews of the project.

LGS graduate assistant Mallory N. Thomas is acknowledged for her diligent work with the georeferencing, digitizing and attributing effort in the GIS development tasks. Louisiana Geological Survey cartographer Lisa Pond made valuable map and technical diagram contributions that are appreciated.

Glossary

alloformation – the mappable, fundamental subdivision of sediments or sedimentary strata defined and identified on the basis of its bounding unconformities. These unconformities represent significant hiatuses in sediment deposition and/or periods of erosion of the underlying sediments prior to deposition of the overlying sediments. An alloformation may be lithologically, paleontologically and geochemically diverse.

allogroup – a grouping of alloformations related in time, origin, or both.

alluvium – loose, unconsolidated (not cemented together into a solid rock) soil, or sediments, which has been eroded, reshaped by water in some form, and re-deposited in a non-marine setting.

backswamp – the extensive, marshy or swampy, low-lying areas of a floodplain that lies between natural levees and valley walls or terraces.

braidbelt – the strip of land that the channel network of a braided river occupies, erodes underlying sediments and rock, and deposits sediments that the river carries.

braided river –a type of river that consists of multiple, interlaced channels that bifurcate and merge around mid-channel bars, resembling (in plan view) the strands of a complex braid. These bars may be vegetated and stable.

boring – A small-diameter, circular hole drilled or otherwise created in the surface of the ground to either determine the physical properties, retrieve samples, or both of the rock or sediment.

chenier – A long, narrow and commonly shoreline-parallel beach ridge that is separated by belts of marsh or swamp of variable width from adjacent cheniers. Typically, a chenier is 3 to 9 feet (1 to 6 m) high, 13 to 1,500 feet (45 to 457 m) wide, and tens of miles long. Cheniers are often well drained and frequently support trees on their higher segments.

chenier plain – a strip of coastal plain, typically adjacent to the shoreline, whose surface consists of narrow, discrete cheniers that are separated by belts of marsh or swamp of variable width.

coast-parallel terrace – a coast-parallel belt within a coastal plain that consists of a relatively level or gently plain, from which the surface descends on one side and ascends on the other. Also known in the published literature as “coast-parallel terraces."

coastal plain – a gently gulfward or seaward sloping plain bordering the shoreline of a gulf, sea or ocean and underlain by relatively horizontal or gently sloping layers of sediments.

compaction – the decrease in sediment volume resulting from either the expulsion or compression of pore air and consequent densification of sediment.

compression – the decrease in volume of sediment under stress as the result of either 1. compression of the solid grains; 2. compression of pore water or pore air; 3. expulsion of pore water or pore air from the voids; or combination of these, thus decreasing the void ratio and porosity of it.

consolidation – the typically gradual decrease in sediment volume that occurs as the direct result expulsion of pore water under steady pressure.

core – a cylinder of relatively undisturbed fill, sediment (soil), rock, or combination of these materials obtained by drilling into the Earth. In the case of unlithified sediments, cores can be obtained using either a Geoprobe, vibracore, or Shelby tube.

crevasse – a breach in a natural levee along the bank of a river through which floodwater flowed.

crevasse sediments – the sediments deposited by floodwaters issuing from a crevasse on the adjacent floodplain often as a fan-like landform, which is known as a "crevasse splay." Typically, they consist of thin sheet-like layers of sediment that thin away from the breach in the natural levee.

delta – a body of sediment, nearly flat and fan-shaped, deposited at or near the mouth of a river or stream where it enters a relatively large body of water, such as a gulf, sea, or lake.

deltaic plain – the level or nearly level surface of the landward part of a large delta; often characterized by multiple distributary channels and flat areas consisting of interdistributary marshes and swamps.

deltaic sediments – the sediments deposited to form a delta.

estuarine deposits – the sediments that accumulate within an estuary.

eustatic sea-level rise – An increase in the elevation of sea-level due to an increase in the volume of sea water. Eustatic sea-level rise is independent of and not part of subsidence.

fault – a discontinuity or fracture in the Earth's crust that is a result of differential movement along one side (fault block) of the discontinuity in respect to the other fault block.

flood basin – a relatively large area of land between valley walls and adjacent uplands that is almost entirely submerged during the highest known flood in a region. It includes small areas of natural leeves, terraces, and other landforms that rise above the flood level and lie within the overall area that can be flooded.

flood basin sediments – the sediments that accumulate within a flood basin.

fluvial sediments – The sediments deposited by rivers, streams, or creeks.

fluvial terrace – a long, narrow, nearly level or gently inclined planar surface that lies within a valley and bounded along the lower edge by a steeper descending slope and along the higher edge by a steeper ascending slope. The surface fluvial terrace lies exposed above the level of the floodplain and can sometimes be buried beneath younger sediments. An alluvial terrace is a fluvial terrace that is composed of unconsolidated to poorly consolidated fluvial sediments.

geologic contact – A geologic contact is the surface that separates different layers or types of sediment or rock.

geomorphic – of or relating to the form of the landscape and other natural features of the earth's surface.

georeference – the process of assigning real-world spatial coordinates to a physical map or raster image of a map.

glacial isostatic adjustment – the adjustment of the Earth's crust to an equilibrium state when loaded and unloaded by ice sheets and eustatic sea level changes during glacial-interglacial cycles

glacial meltwater – water released by the melting of ice sheets and glaciers. In case of the Pleistocene Mississippi River, the meltwater came from the melting of the Laurentide Ice Sheet that covered a large part of North America.

glacial stage – a long period of time, more than 10,000 years in length, characterized by climatic conditions associated with maximum extent of continental ice sheets during an ice age. The last glaciation was the Wisconsin Epoch.

halokinesis – the net upwards force that causes the salt to rise up through the overlaying lithosphere because of the buoyancy created by the relative low density of salt as compared to that of the surrounding sedimentary strata.

highstand – the period of time during which sea level is at it's highest.

Holocene Epoch – the geological epoch that began after the end of the Pleistocene Period at 11,700 years ago. The Holocene and Pleistocene epochs together form the Quaternary Period.

interglacial Stage – a long period of time, more than 10,000 years in length, characterized by climatic conditions associated with the minimum extent of continental ice sheets during an ice age. They separate consecutive glaciations within an ice age and have occurred at intervals of approximately 40,000 to 100,000 years. The previous interglaciation is the Sangamon Epoch.

interval – an informal term for a thickness of sediments that either have the same physical properties or accumulated during a specific interval of geologic time. For example, the *Holocene interval* is the thickness sediment that accumulated during the Holocene Stage.

isopach – map used to illustrate variations in thickness of a specific layer of rock or sediment. The lines on an isopach map connect points of equal thickness.

isopleth – a line drawn on a map through all points having the same numerical value of some measurable quantity. In case of the H-P surface, the isopleths consist of structural contours of the H-P surface

lacustrine – of, pertaining to, or growing in lakes and formed at the bottom or along the shore of lakes.

Lafayette meander belt – A relict, Late Pleistocene meander-belt, mantled with loess, which forms the upper surface of the Avoyelles alloformation.

landform – any topographic feature of the Earth's surface having a distinct shape and origin.

Last Glacial Maximum – an interval of time, between about 26,500 and 19,000 years ago, characterized by the maximum extent of continental ice sheets covering North America and other parts of the world and the corresponding lowest global sea levels during the last glaciation.

Late Pleistocene– a subdivision of the Pleistocene Epoch that consists of the previous interglacial and glacial stage between 126,000 and 11,700 years ago.

lateral migration – the lateral movement of a meandering river across its floodplain as the result of concurrent erosion of it banks and deposition on its bars.

Late Wisconsinan Substage – a subdivision of the last glaciation, Wisconsinan Stage, for North America between 26,500 and 19,000 years ago. It is the equivalent to the Last Glacial Maximum.

lithosphere – the solid outer section of Earth, which includes Earth's crust as well as the underlying cool, dense, and rigid upper part of the upper mantle.

loess – a clastic, predominantly silt-sized sediment that is formed by the accumulation of wind-blown silt, typically in the 20–50 micrometer size range. Loess is typically homogeneous, highly porous, and traversed by vertical capillaries. The vertical capillaries permit the sediment to fracture and form vertical bluffs.

log – a systematic and sequential record of geologic and engineering data obtained from a boring. Typically, a log contains statements as to the thickness and lithologic composition of the rocks and sediments in the order in which they were penetrated in a boring, together with all other pertinent data that was collected about their physical properties. A log may be recorded in either narrative, tabular, or a variety of graphic and symbolic formats.

longshore current – a current in a large body of water that moves parallel to shore. Longshore currents are created by swells hitting the shoreline at an angle and pushing water down the length of the beach in one direction.

lowstand – the period of time during which sea level is at it's lowest.

Marine Isotope Stage – a subdivision of the geologic record that represents an interval of time dominated by either a relatively warm or cool climate in the Earth's prehistory as deduced from oxygen isotope data from samples of deep-sea sediment.

Marine Isotope Stage 1 – a period of warming and relatively warm global climates and either rising or steady sea level between 11,700 years ago and present. Marine Isotope Stage 1 is equivalent to the Holocene Stage.

Marine Isotope Stage 2 – A period of relatively very cold global climates and sea level lowstand between 26,500 and 11,700 years ago at the maximum extent of continental ice sheets. Also known as *Late Wisconsinan Substage*.

Marine Isotope Stage 3 – A period of relatively cool global climates and sea levels were about 30 to 60 feet (9 to 18 meters) below present between 60,000 and 26,500 years ago. The extent of global continental ice sheets was intermediate in size between Marine Isotope Stage 2 and Marine Isotope Stage 1. Also known as *Middle Wisconsinan Substage*.

Marine Isotope Stage 4 – A period of relatively cold global climates and sea level lowstand between 75,000 and 60,000 years ago. The extent of continental ice sheets was intermediate in size between Marine Isotope Stage 3 and higher than Marine Isotope Stage 2. Overall sea level is higher than Marine Isotope Stage 2 and higher than Marine Isotope Stage 3. Also known as *Early Wisconsinan Substage*.

Marine Isotope Stage 5 – a period of relatively warm global climates and either rising or steady sea level between 126,000 and 75,000 years ago. This is the previous interglacial during which continental ice sheets were at their minimum extent and

sea levels were at their highest level. Marine Isotope Stage 5 is equivalent to the *Sangamonian Stage*.

meander-belt – the portion of a fluvial valley or floodplain in which a meandering river has migrated back and forth.

natural levee – a long, sinuous ridge, typically found on either side of river or stream course or channel, created by the deposition of sediment by overbank flooding from the river or stream.

onlap – the pinching out (termination) of shallowly dipping, younger strata against more steeply dipping, older strata,

overbank – The portion of a floodplain outside of a river or stream channel. This is the area of a floodplain, in which the deposition of fine-grained sediments (silt and clay) occurs from suspension by floodwaters that cannot be contained within the stream channel

paleovalley – an ancient valley that has been abandoned by the river, stream, or creek that created it. Paleovalleys can occur either at the surface or buried beneath younger sediments.

Pleistocene Epoch – an interval of geological time, which began 2.58 million years ago and ended 11,700 years ago and includes the most recent ice age. The Pleistocene and Holocene epochs together form the Quaternary Period.

point bar – A fluvial bar, often exhibiting a series of low, arcuate ridges of sand and silt developed on the inside of a migrating meander loop. A point bar grows by the episodic accretion of sediment on the concave side of the meander loop and erosion of the concave side, cutbank, of a migrating meandering river.

Quaternary Period – an interval of time between 2.58 million years ago and present that has been characterize by fluctuations between periods of glaciations and interglaciations. These fluctuations have resulted cyclic variations in the volume and extent of continental ice sheets, sea level, and global temperature and overall climate initially on 41,000- and more recently on 100,000-year time scales.

regional unconformity – an unconformity that can be recognized and mapped over a significant area, e.g. within multiple 1:100,000 quadrangles.

regression – an interval of geologic time during which shoreline migrates seaward, resulting in the emergence of former sea floor. The landward movement of the shoreline can be the result of a combination of uplift, increased sedimentation, a global drop in sea level, and other factors.

relict coastal plain – a coastal plain that exhibits landforms, *e.g.* beach ridges, deltas, fluvial courses, dunes, and so forth that are no longer being modified by the specific geomorphic processes that created them often in response to changes in sea level.

relict landforms – a landform that is no longer being modified by the geomorphic processes that created it.

sample – a specified amount of a sediment or rock collected for laboratory analysis or study.

Sangamonian age – in its broadest and typical usage (*sensu lato*), it is the term used in North America to designate the previous interglaciation during the period of time between 75,000 and 125,000 years ago.

secondary consolidation – the decrease in soil volume due to plastic deformation, readjustment, or combination of both processes of soil particles that occurs after excess pore water pressure dissipates.

strata – the layers of sediment, sedimentary rock, and volcanic rock, each of which has internally consistent characteristics that distinguish it from the other layers. A single layer of either sediment or rock is a stratum. It is the fundamental unit of and forms the basis of the study of stratigraphy.

stratigraphic unit – a stratigraphic unit is a volume of rock of identifiable origin and relative age range that is defined by the distinctive and dominant, easily mapped and recognized using either it physical characteristics or its fossil content. Although units must be mappable and distinct from one another, the contact need not be particularly distinct.

stratigraphy – a branch of geology which studies the interrelationship of layers (strata) of sediment, sedimentary rock, and volcanic rock; their internal layering (stratification); and their fossil content (biostratigraphy).

subaerial – a term (*subaerial*, literally "under the air") used in geology to describe events or features that are formed, located or taking place on the Earth's land surface and exposed to Earth's atmosphere in contrast to those located below water (subaqueous) and below glacial ice (subglacial).

subsidence – the downward displace of the Earth's surface in respect to an unchanging datum. Eustatic sea-level rise is independent of and not part of subsidence.

substratum – an informal term for sand, gravelly sand, and gravel fill of the Mississippi River that underlies the Holocene–Pleistocene surface and overlies the erosional base of the Mississippi Alluvial Valley. The topstratum consist of braid river sediment that accumulated episodically during Wisconsinan Stage (Marine Isotope Stages 2, 3, and 4). Older fluvial sediment might be present.

tectonic – relating to, causing, or resulting from structural deformation of the earth's crust.

time-transgressive – an individual layer or surface that was created at different times in different areas.

topstratum – an informal term for typically fine-grained, under consolidated sediments deposited over the Holocene-Pleistocene surface and accumulated during a period of sea level rise and regional transgression starting at the end of the Last Glacial Maximum about 19,000 year ago and continuing to modern times.

transgression (transgressive episode) – an interval of geologic time during which shoreline migrates inland, resulting in the submergence of formerly dry land. The landward movement of the shoreline can be the result of a combination of subsidence, reduced sedimentation, a global rise in sea level, and other factors.

unconformity – a surface separating younger strata on top of it from older strata below it along which there is evidence of either significant period of erosion, non-deposition, or a combination of both. In case of subaerial erosion or subaerial exposure the sediments underlying often show evidence of weathering and soil development during the period of erosion or non-deposition.

Wisconsinan age – an interval of geological time that consists of the last glaciation between 75,000 and 11,700 years ago.

References

Arabie Environmental Solutions, (2010), Logs from Legacy Lawsuit Files, Henry versus Apache 10995: Baton Rouge, LA, Department of Natural Resources.

Autin W.J., Burns S.F., Miller B.J., Saucier R.T., Snead J.I., 1991, Quaternary Geology of the Lower Mississippi Valley, *in* Quaternary Non-Glacial Geology of the Conterminous United States, ed. R.B. Morrison: Boulder, CO, Geological Society of America, Decade of North American Geology series, vol. K-2, p. 547–582.

Ayrer, J.E., 2010, Surface Stratigraphic Architecture of Pleistocene Sediments in The Greater New Orleans Area [MS thesis]: State College, PA, Dept. of Geology and Geophysics, Pennsylvania State University, 56 p.

Aronow, S., 1986, Surface Geology of Calcasieu Parish: Open-File Report no. 04-01, Baton Rouge, LA, Louisiana Geological Survey, 22 p.

Barrilleaux, J., 1986, The Geomorphology and Quaternary History of the Houston Barrier Segment of the Ingleside Strandplain, Calcasieu Parish, Louisiana. [M.S. thesis]: Lafayette, LA, University of Southwestern Louisiana, 92 p.

Beckman, J.D., and Williamson A.K., 1990, Salt-Dome Locations in the Gulf Coastal Plain, South-Central United States: Austin, TX, US Geological Survey, Water-Resources Investigations Report 90-4060, 44p.

Blum, M.D., Morton R.A., and Durbin J., 1995, "Deweyville" Terraces and Deposits of the Texas Gulf Coastal Plain: Transactions of the Gulf Coast Association of Geological Societies 45, p. 53-60.

Blum, M.D., Roberts H.H, 2012. The Mississippi Delta Region–Past, Present, and Future: *Annual Review of Earth and Planetary Sciences,* 40, p. 655–683.

Blum, M.D., Guccione M.J., Wysocki D.A., Robnett P.C., Rutledge E.M., 2000, Late Pleistocene Evolution of the Lower Mississippi Valley, Southern Missouri to Arkansas: Boulder, CO, Geological Society of America, Bull. 112, p. 221–35.

Breaux, J.J., and McDowell, C.S., 2014, Proposed headquarters boat house and airboat shed replacement for the Department of Wildlife and Fisheries Bird Island Bayou, Marsh Island, Louisiana: Broussard, LA, MBSB Group, Site Engineering, Inc., *for* State of Louisiana Facility Planning & Control, Report no. 13-G074-1. 25 p.

Byrne, J.V., Leroy D.O., and Riley C.M., 1959, The chenier plain and its stratigraphy, Southwestern Louisiana: Transactions of the Gulf Coast Association of Geological Societies 9, p. 227–260.

Coleman, J.M., 1988, Dynamic changes and processes in the Mississippi River delta: Boulder, CO, Geological Society of America, Bull. 100, p. 999–1015.

Cuomo, R.F., 1984, The Geologic and Morphologic Evolution of Ship Shoal, Northern Gulf of Mexico [MS Thesis]: Baton Rouge, Louisiana State University, 249 p.

Dokka, R.K., 2009, Comparison of Methods Used to Measure Modern Subsidence in Southeastern Louisiana: Gulf Coast Association of Geological Societies 59, p. 225-242.

Dunbar, J.B., Blaes M.R., Dueitt S.E., May J.R., and Stroud K.W., 1994, Geological investigation of the Mississippi River deltaic plain: Vicksburg, MS: US Army Corps of Engineers, Report 2, Technical Report GL-84-15, 2 p., 16 maps.

Dunbar, J.B., Blaes M.R., Dueitt S.E., and May J.R., 1995, Geological investigation of the Mississippi River deltaic plain: Vicksburg, MS: US Army Corps of Engineers, Report 3, Technical Report GL-84-15. 2 p., 7 maps.

Fisk, H.N., 1940, Geology of Avoyelles and Rapides Parishes: Baton Rouge, LA, Louisiana Geological Survey, Geological Bulletin 18, 240p., 2 pls.

Fisk, H.N., 1944, Geological Investigation of the Alluvial Valley of the Lower Mississippi River: Vicksburg, MS, US Army Corps of Engineers, 78 p. 61 pls.

Fisk, H.N., 1948a, Geological investigation of the lower Mermentau River Basin and adjacent areas in coastal Louisiana: Vicksburg, MS, Mississippi River Commission. 40 p.

Fisk, H.N., 1948b, Geological investigation of the Calcasieu lock site: Vicksburg, MS, Mississippi River Commission. 14 p.

Fisk, NH., 1956, Near-surface sediments of the continental shelf off Louisiana, *in* Proceedings of the Eighth Texas Conference on Soil Mechanics and Foundation Engineering, Austin, Texas, September 14 and 15, 1956: The University of Texas. Bureau of Engineering Research Special publications 29, p. 1-36 p.

Flocks, J., 2013, personal communication, July 22, 2013.

Frazier, D.E., 1967, Recent Deltaic Deposits of the Mississippi River – Their Development and Chronology: Transactions of the Gulf Coast Association of Geological Societies, 17, p. 287-315.

Frazier, D.E., 1974, Depositional episodes – their relationship to the Quaternary stratigraphic framework in the northwestern portion of the Gulf Basin: Austin, TX, Bureau of Economic Geology, Geological Circular 74-1. 28 p.

González, J.L., and Törnqvist T.E., 2009, A new Late Holocene sea-level record from the Mississippi Delta–evidence for a climate/sea level connection?: Quaternary Science Review 28, p. 1737–1749.

Gould, H.R., and McFarlan E. Jr., 1959, Geologic history of the chenier plain, southwestern Louisiana: Transactions of the Gulf Coast Association of Geological Societies, 9, p. 261–270.

Gulf Coast Association of Geological Societies and American Association of Petroleum Geologists, 1972, Tectonic map of Gulf Coast region USA: Tulsa, OK, American Association of Petroleum Geologists, 1:1,000,000.

Heinrich, P.V., Snead J., and McCulloh R.P., 2003, Crowley 30 x 60 minute Geologic Quadrangle: Baton Rouge, LA, Louisiana Geological Survey, 1:100,000.

Heinrich, P.V., 2005a, Surface Faulting Within the New Iberia, Louisiana Region: Louisiana Geological Survey*, NewsInsights* 15, p. 1-3.

Heinrich, P.V., 2005b, Port Arthur 30 x 60 minute geologic quadrangle: Baton Rouge, LA, Louisiana Geological Survey, 1:100,000.

Heinrich, P.V., 2006a, Pleistocene and Holocene Fluvial Systems of the Lower Pearl River, Mississippi and Louisiana, USA: Transactions of the Gulf Coast Association of Geological Societies, 56, p. 267-278.

Heinrich, P.V., 2006b, White Lake 30 x 60 minute geologic quadrangle: Baton Rouge, LA, Louisiana Geological Survey, 1:100,000.

Heinrich, P.V., and Autin W.J., 2000, Baton Rouge 30 x 60 minute geologic quadrangle: Baton Rouge, LA, Louisiana Geological Survey, 1:100,000.

Heinrich, P.V., and McCulloh R.P., 2004, Gulfport 30 x 60 minute geologic quadrangle: Baton Rouge, LA, Louisiana Geological Survey, 1:100,000.

Heinrich, P.V., Milner R., Snead J., Peele H., and Paulsell R., 2011a, Quaternary Geology of the Louisiana Coastal Plain & Continental Shelf: Baton Rouge, LA, Louisiana Geological Survey, *for* Office of Coastal Protection and Restoration. 48 p.

Heinrich, P.V., Milner R., Snead J., Peele H., and Paulsell R., 2011b, Bibliography of Louisiana Coastal Plain and Continental Shelf Geology: Baton Rouge, LA, Louisiana Geological Survey, *for* Office of Coastal Protection and Restoration. 33 p.

Ivins, E.R., Dokka, R.K., and Blom, R.G., 2007, Post-glacial sediment load and subsidence in coastal Louisiana: Geophysical Research Letters, 29, p. 3733-3736.

Kesel, R.H., 2008, A revised Holocene geochronology for the lower Mississippi valley: Geomorphology 101, p. 78–89.

Kolb, C.R., 1962, Distribution of soils bordering the Mississippi River from Donaldsonville to the Head of Passes: Vicksburg, MS: US Army Corps of Engineers, Technical Report 3-601. 116 p.

Kolb, C.R., Van Lopik J.R., 1958, Geological investigation of the Mississippi River Gulf Outlet channel: Vicksburg, MS: US Army Corps of Engineers, Waterways Experiment Station, Misc. Paper No. 3-259.

Kolb, C.R., Smith L., Silva R.C., 1975, Pleistocene sediments of the New Orleans-Lake Pontchartrain area: Vicksburg, MS: US Army Corps of Engineers, Technical Report S-76-6.

Kuecher, G.J., 1994, Geologic framework and consolidation settlement potential of the Lafourche Delta, topstratum valley fill – implications for wetland loss in Terrebonne and Lafourche parishes, Louisiana: [PhD thesis]: Baton Rouge, LA: Louisiana State University, 375 p.

Kuecher, G.J., Chandra, N., Roberts, H.H., Suhayda, J.N., Williams, S.J., Penland, S., and Autin, W,J., 1993, Consolidation settlement potential in south Louisiana: Proceedings, Coastal Zone 1993, 8th symposium on coastal and ocean management, p. 1197-1214.

Kuecher, G.J., Roberts H.H, Thompson M.D., and Matthews I., 2001, Evidence for active growth faulting in the Terrebonne delta plain, south Louisiana–Implications for wetland loss and the vertical migration of petroleum: *Environmental Geosciences* 8-2, p. 77-94.

Kulp, M.A., 2000, Holocene stratigraphy, history, and subsidence – Mississippi River Delta region, north central Gulf of Mexico [PhD thesis]: Lexington, KY: University of Kentucky, 336 p.

Kulp, M., FitzGerald D., Penland S., 2005, Sand-rich lithosomes of the Holocene Mississippi River delta plain, *in* River Deltas-Concepts, Model, and Examples, eds. Bhattacharya J.P., Giosan L.: Tulsa, OK, Soc. Sedimentary Geology, Spec. Pub. 83, p. 279–94.

Kulp, M.A., Howell P., Adiau S., Penland S., Kindinger J., Williams S.J, 2002, Latest Quaternary stratigraphic framework of the Mississippi delta region: Transactions of the Gulf Coast Association of Geological Societies, 52, p. 572–82.

LeBlanc, R.J., 1949, Recent and Pleistocene Geology of the Calcasieu Entrenched Valley System of Southwest Louisiana: Houston, TX: Shell Oil Company, Exploration and Production Research Division, Report 128.

Martin, R. G., 1978, Northern and eastern Gulf of Mexico continental margin–stratigraphic and structural framework, *in* Framework, facies, and oil-trapping characteristics of the upper continental margin, Bouma, A. H., G. T. Moore, and J. M. Coleman, eds.: American Association of Petroleum Geologists Studies in Geology, no. 7, p. 21–42.

May, J.R., Britsch L.D., Dunbar J.B., Rodriquez J.P., Wlosinski L.B., 1984, Geological investigation of the Mississippi River deltaic plain: Vicksburg, MS: US Army Corps of Engineers, Technical Report GL–84–15, 2 p., 26 maps.

McCulloh, R.P., Heinrich P.V., and Good B., 2006, Geology and Hurricane-Protection Strategies in the Greater New Orleans Area: Baton Rouge, LA: Louisiana Geological Survey, Public Information Series No. 11, 32 p.

McCulloh, R.P., Heinrich P.V., Snead J., 2003, Ponchatoula 30 x 60 minute Geologic Quadrangle: Baton Rouge, LA: Louisiana Geological Survey, 1:100,000.

McFarlan, E. Jr., and LeRoy D.O., 1988a, Subsurface geology of the late Tertiary and Quaternary deposits, coastal Louisiana and the adjacent continental shelf: Transactions of the Gulf Coast Association of Geological Societies 38, p. 421-433.

McFarlan, E. Jr., and LeRoy D.O., 1988b, Subsurface geology of the late Tertiary and Quaternary deposits, coastal Louisiana and the adjacent continental shelf – unpublished supplement of cross-sections: Houston, TX: McFarlan Geological Consultants.

Miller, W. III., 1983, Stratigraphy of Newly Exposed Quaternary Sediments, Eastern Orleans Parish, Louisiana: New Orleans, LA, Tulane Studies in Geology and Paleontology 17, p. 85-104.

Milliken, K., Anderson J.B., Rodriguez A.B., 2008, Record of dramatic Holocene environmental changes linked to eustasy and climate change in Calcasieu Lake, Louisiana, USA, *in* Response of Gulf Coast Estuaries to Sea-Level Rise and Climate Change, eds. J.B. Anderson and A.B. Rodriguez: Boulder, CO, Geological Society of America, Special Paper 443, p.43-63.

Morgan, J.P, 1963, Mudlumps at the mouths of the Mississippi River: Baton Rouge, LA, Louisiana State University Press, Coastal studies series 10, 190 p.

Morton, R.A., Buster, N.A., and Krohn, M.D., 2002, Subsurface controls on historical subsidence rates and associated wetland loss in south-central Louisiana: Gulf Coast Association of Geological Societies Transactions, 52p. 767-778.

Mossa, J., Autin W.J., 1989, Quaternary Geomorphology and Stratigraphy of the Florida Parishes, Southeastern Louisiana–A Field Trip: Baton Rouge, LA: Louisiana Geological Survey, Guidebook Series 5, 98 p.

O'Neill, M.W., and Van Siclen, D.C., 1984, Activation of Gulf Coast faults by depressuring of aquifers and an engineering approach to siting structures along their traces: Association of Engineering Geologists Bulletin 21, p. 73–87.

Orten, E.W., 1959, A Geological Study of Marsh Island Iberia Parish, Louisiana: New Orleans, LA, Louisiana Wildlife and Fisheries Commission, Refuge Division, Technical Bulletin, 28 pp.

Paulsell, R.L., Snead J., and Pond L.G., 2012, Louisiana Coastal Zone 2012: Baton Rouge, LA, Department of Natural Resources, Coastal Management Division, 1:380,160.

Poche, C. M., and Ventura b., 2014, Marsh Island Wildlife Refuge Levee/Bulkhead Repairs: Lafayette, LA, Royal Engineers and Consultants, LLC, *for* Department of Natural Resources, Gulf South Engineering & Testing File No. 14-013.

Reed, D.J., and Yuill B., 2009, Understanding Subsidence in Coastal Louisiana: New Orleans, LA, Pontchartrain Institute for Environmental Sciences, University of New Orleans.

Reed, J.C., Jr., J.O. Wheeler, and B.E. Tucholke (compilers), 2005, Geologic Map of North America, *in* Decade of North American Geology: Boulder, CO, Geological Society of America, Continent-Scale Map 001, 1:5,000,000.

Rittenour, T.M., Blum M.D., Goble R.J., 2007, Fluvial evolution of the lower Mississippi River valley during the last 100 kyr glacial cycle–response to glaciation and sea-level change: Boulder, CO, Geological Society of America, Bull. 119, p. 586–608

Roth, M., 1999, Late Pleistocene to Recent subsurface geology of Lake Pontchartrain, Louisiana–an integration of geophysical and geological techniques [M.S. thesis]: New Orleans, LA, University of New Orleans, 352 p.

Roberts, H.H., Coleman J.M., 1996, Holocene evolution of the deltaic plain–A perspective-from Fisk to present: *Engineering Geology* 45, p. 113–38.

Roberts, H.H., Bailey, A., and Kuecher, G.J., 1994, Subsidence is the Mississippi River delta: Important influences of valley filling by cyclic deposition, primary consolidation phenomena, and early diagenesis: Transactions of the Gulf Coast Association of Geological Societies 44, p. 619-629.

Saucier, R.T., 1994, Geomorphology and Quaternary Geologic History of the Lower Mississippi Valley: Vicksburg, MS, US Army Corps of Engineers.

Saucier, R.T., and Snead J., 1989, Quaternary geology of the Lower Mississippi Valley, *in* Quaternary non-glacial geology of the conterminous United States, 1991, ed. R.B. Morrison: Boulder, CO, Geological Society of America, Decade of North American Geology series, vol K-2, plate 6, 1:1,100,000.

Saucier, R.T., and Snowden J.O., 1995, Engineering geology of the New Orleans area, *in* Guidebook of geological excursions: New Orleans, LA, Geological Society of America annual meeting, November 6–9, 1995, eds. C.J. John and W.J. Autin, p. 131-154.

Shen, Z., Törnqvist T.E., Autin W.J., Mateo Z.R.P., Straub K.M., and Mauz B., 2012, Rapid and widespread response of the Lower Mississippi River to eustatic forcing during the last glacial-interglacial cycle: Geological Society of America, Bull. 124, p. 690-704.

Siringan, F.P. 1993, Coastal lithosome evolution and preservation during an overall rising sea level–East Texas Gulf Coast and continental shelf [Ph.D. thesis]: Houston, TX, Rice University, 226 p.

Snead, J., and Heinrich P.V., 2012. Morgan City 30 x 60 minute geologic quadrangle: Baton Rouge, LA, Louisiana Geological Survey, 1:100,000.

Snead, J., Heinrich P.V., and McCulloh R.P., 2002, Lake Charles 30 x 60 minute geologic quadrangle: Baton Rouge, LA, Louisiana Geological Survey, 1:100,000.

Snead, J., and McCulloh R.P., 1984, Geologic Map of Louisiana 1984: Baton Rouge, LA, Louisiana Geological Survey, 1:500,000.

Snead J., Millet E.B., Paulsell R.L., Pond L.G., Peele R.H., Koch E., 2000, Official Map of Louisiana 2000: Baton Rouge, LA, Louisiana Department of Transportation and Development, 1:380,160.

Snead, J., Peele R.H., and Binselam S.A., 2007, Louisiana Shoreline Change 1937–2000: Baton Rouge, LA, Center for the Health Impacts of Hurricanes, Louisiana State University, 1:380,160.

Snowden, J.O., Ward, W.C., and Studlick, J.R.J., 1980, Geology of Greater New Orleans–its relationship to land subsidence and flooding: New Orleans, LA, New Orleans Geological Society, 32 p.

Soil Testing Engineers, Inc., 2006, Report of Geological Investigations Gentilly Landfill Slope Stability Analysis, New Orleans (Orleans Parish), Louisiana: Baton Rouge, Louisiana Department of Environmental Quality.

Spearing, D., 2007, Roadside Geology of Louisiana (revised edition): Missoula MT, Mountain Press Publishing Co., 240 p.

Stanley, J.D., Warne A.G., and Dunbar J.B., 1996, Eastern Mississippi delta–late Wisconsin unconformity, overlying transgressive facies, sea level and subsidence: *Engineering Geology* 45, p. 359-381.

Törnqvist, T.E., González J.L., Newsom L.A., van der Borg K., de Jong A.F.M., and Kurnik W.K., 2004, Deciphering Holocene sea-level history on the U.S. Gulf Coast–a high-resolution record from the Mississippi Delta: Boulder, CO, Geological Society of America Bull. 116, p. 1026–1039.

Törnqvist, T.E., Wallace, D.J., Storms, J.E.A., Wallinga, J., Van Dam, R.L. , Blaaum, M., Derksen, M.S., Klerks, C.J.W. , Meijneken, C., and Snijders, E.M.A., 2008, Mississippi delta subsidence primarily caused by compaction of Holocene strata: Nature Geoscience 1, p. 173-176.

Törnqvist, T.E., 2013, Subsidence mechanisms and rates within and beyond coastal Louisiana–An overview of recent progress: Special lecture, January 17, 2013, Baton Rouge, LA, Department of Geology and Geophysics, Louisiana State University.

United States Geological Survey, 2014, Topographic-bathymetric 3-meter digital elevation model: Reston, VA, US Geological Survey National Geospatial Program, The National Map.

van Asselen, S., Stouthamer E., and van Asch T.W.J., 2009, Effects of peat compaction on delta evolution–A review on processes, responses, measuring and modeling: *Earth Science Review* 92, p. 35–51.

Verbeek, E.R., 1979, Surface Faults in the Gulf Coastal Plain between Victoria and Beaumont, Texas: *Tectonophysics* 52, p. 373–375.

Vines, T.H., Albert A.Y.K., Andrew R.L., Débarre F., Bock D.G., Franklin M.T., Gilbert K.J., Moore J.S., Renaut S., Rennison D.J., 2104, The Availability of Research Data Declines Rapidly with Article Age: *Current Biology* 24(1), p. 94–97

Warren, J.K., 2006, Evaporites – Sediments, Resources and Hydrocarbons: Berlin, Germany, Springer-Verlag Science Media, 1035 p.

Wellner, J., Sarzalejo S.S., Logoe M., and Janderson J.B., 2004, Late Quaternary stratigraphic evolution of the west Louisiana/east Texas continental shelf, *in* Late Quaternary Stratigraphic Evolution of the Northern Gulf of Mexico Margin, eds. J.B Anderson and RH Fillon: Tulsa OK, Society of Sedimentary Geology, Spec. Pub. 79, p. 217-36.

Wessel, S., 2010, Late Quaternary Mississippi River Incised Valley Fill–Transgressive Depositional Packages [MS thesis]: New Orleans, LA, University of New Orleans, 157 p.

Winker, C.D., 1991, Quaternary Geology, Northwestern Gulf Coast, *in* Quaternary Non-Glacial Geology of the Conterminous United States, ed. R.B. Morrison: Boulder, CO, Geological Society of America, Decade of North American Geology series, vol. K-2, plate 8, 1:2,000,000.

Winker, C.D., and Edwards, M.B., 1983, Unstable Progradational Clastic Shelf Margins, *in* The Shelfbreak–Critical Interface on Continental Margins, eds. Stanley, D. J., and G.T. Moore: Tulsa, OK, Society for Sedimentary Geology, Spec. Pub. 33, p. 139-157.

Woudloper, 2009. Two diagrams illustrating the shift of sedimentary facies during regression: Creative Commons free license, ©Woudloper 2009, https://commons.wikimedia.org/wiki/File:Offlap_%26_onlap_EN.svg

Young, S.C, Ewing T., Hamlin S., Baker E., and Lupin D., 2012, Updating the Hydrogeologic Framework for the Northern Portion of the Gulf Coast Aquifer (Final Report): Austin, TX, Texas Water Development Board, 283 p.

Yu, S.Y., Törnqvist T.E., and Hu P., 2012, Quantifying Holocene lithospheric subsidence rates underneath the Mississippi Delta: *Earth and Planetary Science Letters* 331–332, p. 21-30.

Appendix

As a result of the literature review and data assessment, it is clear that geotechnical reports and their associated digital data often become separated. Original boring data is commonly not archived and is sometimes lost or misplaced if not incorporated into the report.

A complete table of the boring data used in this study is included below.

H-P ID	Source	Source ID	North Latitude	West Longitude	H-P depth (msl)
1	USACE	NOB-15/16	29.96023948	-90.09235282	-70
2	USACE	W-67.6-U	29.74408257	-90.01793244	-90
3	USACE	R-67.6-R	29.74476402	-90.0168122	-105
4	USACE	R-67.3-L	29.74681597	-90.00733923	-90
5	USACE	QP1	29.28980209	-90.2362569	-200
6	USACE	BDA-8	29.821702	-90.47779578	-90
7	USACE	BDA-13	29.8214641	-90.47541746	-85
8	USACE	SC-28	29.87679415	-90.43493587	-58
9	USACE	22-D	29.89679168	-90.39936155	-58
10	USACE	16-D	29.89584684	-90.39911784	-60
11	USACE	U-14	29.94914851	-90.3708226	-65
12	USACE	U-15	29.95115213	-90.36968418	-58
13	USACE	U-16	29.95190048	-90.36884666	-58
14	USACE	U-7	29.93362417	-90.38021223	-60
15	USACE	WL-1	29.93831213	-90.37641357	-50
16	USACE	WL-5	29.94137959	-90.37457935	-163
17	USACE	CA-9	29.97338439	-90.46546149	-50
18	USACE	KU-1	29.97303217	-90.46448966	-45
19	USACE	KU-4	29.97022463	-90.46065073	-44
20	USACE	KU-24	29.94952824	-90.43105014	-46
21	USACE	53942	29.60949898	-90.47528807	-120
22	USACE	PP-1	29.74864684	-90.93084906	-135
23	USACE	73UW	29.81025605	-91.41247919	-135
24	USACE	SMN-96	29.89918784	-91.26376494	-118
25	USACE	LO-5	29.6711445	-91.38425404	-50
26	USACE	LO-4	29.66921849	-91.38496648	-50
27	USACE	OSB-32	29.66293139	-91.38528754	-38
28	USACE	LO-3	29.65531248	-91.38755326	-55
29	USACE	OSB-36	29.65276298	-91.38930271	-41
30	USACE	LO-1	29.64687055	-91.39370864	-60
31	USACE	LO-9	29.63630546	-91.39759239	-62
32	USACE	LO-8	29.69713023	-91.37380217	-52
33	USACE	LO-7	29.69500132	-91.37510311	-52
34	USACE	LO-6	29.69171523	-91.3761195	-52
35	USACE	CC-98	29.78740683	-91.577441	-22
36	USACE	FEB-13	29.82267084	-91.54411078	-22
37	USACE	FEB-7	29.79217989	-91.51163365	-37
38	USACE	FEB-9	29.80290144	-91.52151531	-26
39	USACE	FEB-1	29.79997095	-91.5191398	-26
40	USACE	F8	30.25448951	-90.40070831	-36
41	USACE	MAB-2	30.13041756	-90.71568552	-22
42	USACE	MAB-6	30.11950295	-90.63919324	-10
43	USACE	MAB-4	30.11989931	-90.64172413	-16
44	USACE	MAB-8	30.11459054	-90.58161737	-16
45	USACE	MAA-3	30.08709293	-90.72023476	-12
46	USACE	MAA-5	30.06952284	-90.68095344	-23
47	USACE	MAA-7	30.06865044	-90.66452643	-19

48	USACE	2U	30.04666137	-90.63478765	-50
49	USACE	1U	30.04817969	-90.63667589	-50
50	USACE	MAA-9A	30.05302266	-90.64250411	-45
51	USACE	MAA-11	30.03865618	-90.61536143	-41
52	USACE	R141.4R	30.03480707	-90.60762953	-39
53	USACE	R134.4L	30.05640098	-90.49986876	-95
54	USACE	R133.8L	30.05661798	-90.49038038	-102
55	USACE	PLB-4B	30.05686741	-90.25799453	-44
56	USACE	AN-15	30.0934457	-90.95389275	-108
57	USACE	SJ-66	30.03946159	-90.84850017	-15
58	USACE	US-7	30.03912222	-90.82315079	-16
59	USACE	US-5	30.03713685	-90.82974367	-3
60	USACE	US-9	30.0417543	-90.81067157	-4
61	USACE	P-6	30.09859844	-90.90786241	-130
62	USACE	P-7	30.09883237	-90.90663018	-127
63	USACE	B-28	30.09927747	-90.90449414	-128
64	USACE	B-35	30.09960385	-90.90244067	-100
65	USACE	B-45	30.09997751	-90.9003049	-30
66	USACE	AT-58	30.10264049	-90.86167227	-4
67	USACE	SP-17	30.11568803	-90.84483564	-3
68	USACE	SP-15	30.12018671	-90.83903926	-5
69	USACE	SP-13	30.12457947	-90.83361235	-4
70	USACE	SP-11	30.12898386	-90.82817122	-5
71	USACE	SP-9	30.13348253	-90.8225649	-5
72	USACE	SP-7	30.13783897	-90.81715041	-4
73	USACE	SP-5	30.14208857	-90.8118455	-6
74	USACE	SP-3	30.14620797	-90.8067598	-2
75	USACE	AT-50	30.09475161	-90.92493289	-97
76	USACE	DM-1	30.08687353	-90.91605302	-100
77	USACE	DM-3	30.08552113	-90.91531122	-100
78	USACE	IB-12	30.16531649	-91.17339037	-85
79	USACE	IB-196	30.16562525	-91.14652147	-105
80	USACE	WC-1	30.17759961	-91.13379872	-95
81	USACE	WC-8G	30.18245489	-91.12683036	-95
82	USACE	WC-9G	30.18814326	-91.11855824	-101
83	USACE	NR-5	30.2037679	-91.02841012	-85
84	USACE	NR-9	30.21269535	-91.04216299	-83
85	USACE	IR-14	30.40716711	-91.48123961	-58
86	USACE	IR-10	30.41953413	-91.43617659	-105
87	USACE	IR-5	30.43818411	-91.36634808	-71
88	USACE	IR-4	30.44276416	-91.34837783	-84
89	USACE	WBR-92	30.46366391	-91.26800766	-88
90	USACE	IR-9	30.42037999	-91.43346312	-106
91	USACE	IR-8	30.42607145	-91.4108677	-73
92	USACE	IR-6	30.43365318	-91.38313642	-77
93	USACE	IR-3	30.4481855	-91.32884177	-70
94	USACE	CB-2G	30.46856612	-91.34692496	-13
95	USACE	PL-1	30.28565444	-91.22985451	-88
96	USACE	IB-87	30.27370833	-91.11806101	-85
97	USACE	IB-50	30.26810926	-91.10515094	-109
98	USACE	TP-1	30.54049532	-91.23704041	-30
99	USACE	3-U	30.51464133	-91.20852674	-17
100	USACE	FN-2	30.51122715	-91.20577294	-19
101	USACE	TP-2	30.53688574	-91.2328494	-42
102	USACE	PC-38	30.69888082	-91.43723993	-48
103	USACE	PC-65	30.69635258	-91.42685353	-1
104	USACE	NR-1	30.68836821	-91.40487634	-38
105	USACE	NR-5	30.68206528	-91.39606941	-48
106	USACE	255.0	30.65050938	-91.31971184	-12
107	USACE	254.65	30.64966326	-91.31369528	-19
108	USACE	254.25	30.64862187	-91.30813012	-40
109	USACE	253.5	30.64667015	-91.30369345	-40
110	USACE	WBR-84	30.55740774	-91.3341714	-50

111	USACE	2-4	30.57373109	-91.3278086	-20
112	USACE	AR-2	30.58454813	-91.32136943	-7
113	USACE	NR-17	30.62564627	-91.3592638	-18
114	USACE	NR-14	30.63076228	-91.36488294	-62
115	USACE	UFR-2	30.68885744	-91.35900933	-20
116	USACE	UFR-5	30.68537651	-91.35544851	-60
117	USACE	PC-36	30.5564327	-91.61031376	-88
118	USACE	PC-76	30.55763262	-91.60554051	-103
119	USACE	BS-2	30.76275667	-91.37872735	-42
120	USACE	PC-106	30.81707659	-91.63309595	-25
121	USACE	TP-10	30.77339416	-91.6182726	-38
122	USACE	TP-15	30.78545208	-91.62596803	-55
123	USACE	TP-20	30.79753487	-91.63378421	-59
124	USACE	C56	30.24371357	-90.40571654	-27
125	USACE	C54	30.23877097	-90.40737279	-30
126	USACE	C48	30.22218781	-90.41344174	-31
127	USACE	C52	30.22725183	-90.41174995	-30
128	USACE	C-38	30.20154811	-90.42853874	-38
129	USACE	C30	30.18023833	-90.44368793	-38
130	USACE	C18	30.15029706	-90.44780221	-42
131	USACE	C10	30.12246255	-90.44658089	-42
132	USACE	C12	30.1305628	-90.44885163	-43
133	USACE	C8	30.11688864	-90.44484739	-46
134	USACE	C6	30.11251876	-90.44362775	-49
135	USACE	C2	30.10121244	-90.43921922	-59
136	USACE	C4	30.10441816	-90.44132289	-50
137	USACE	C26	30.16934149	-90.44503136	-51
138	USACE	C28	30.174291	-90.44432259	-46
139	USACE	73652	30.16336614	-91.35030605	-100
140	USACE	253UE	30.09137434	-91.30718663	-84
141	USACE	65081	30.06333423	-91.27308036	-85
142	USACE	53408	30.13260644	-91.45346134	-103
143	USACE	58973	30.15556438	-91.42902748	-98
144	USACE	55186	30.1524708	-91.41200286	-110
145	USACE	52821	30.16175576	-91.39805535	-110
146	USACE	SOC-1	30.17520021	-91.39133798	-108
147	USACE	SOC-2	30.17541982	-91.39024511	-107
148	USACE	54406	30.16738979	-91.37493976	-112
149	USACE	49579	30.17919359	-91.3393789	-105
150	USACE	52357	30.18759445	-91.33097076	-110
151	USACE	53676	30.19285405	-91.32979338	-110
152	USACE	111223	30.22762208	-91.30236902	-107
153	USACE	58638	30.20286586	-91.6190689	-110
154	USACE	77101	30.18981234	-91.53810065	-110
155	USACE	37589	30.18900006	-91.51864089	-104
156	USACE	58559	30.02460113	-91.5104595	-130
157	USACE	S-4	30.37772928	-91.59176713	-53
158	USACE	S-6	30.39873319	-91.51276915	-83
159	USACE	156	30.39917859	-91.51090893	-76
160	USACE	102	30.36767167	-91.6304877	-85
161	USACE	76MHUT	29.70453704	-89.98626324	-105
162	USACE	67MHUT	29.64766663	-89.9594945	-124
163	USACE	62MHU	29.62856588	-89.9249694	-118
164	USACE	PC-1	29.6218238	-89.91829317	-64
165	USACE	R54.5RU	29.60699961	-89.88335772	-120
166	USACE	R-76.8-UR	29.86696997	-89.97954174	-90
167	USACE	R-79.7-R	29.87647408	-89.93942311	-88
168	USACE	MRGO-40D	29.83224861	-89.59239826	-90
169	USACE	MRGO-1B	29.82556546	-89.60200979	-97
170	USACE	R32.4UR	29.43228015	-89.60685771	-160
171	USACE	4-USP	30.08842276	-89.85876858	-25
172	USACE	BL-8E	30.02235918	-89.88556469	-50
173	USACE	BL-5E	30.01615249	-89.90133964	-55

174	USACE	1406	30.00947926	-89.93506663	-70
175	USACE	PCS-1(PROJ)	30.01290089	-89.96606387	-55
176	USACE	CMB-8	30.0673261	-89.80562465	-50
177	USACE	B15	30.02703936	-89.72164545	-54
178	USACE	B7	30.06035104	-89.73555892	-50
179	USACE	B-18U	30.16753856	-89.72011562	-12
180	USACE	2A-1	30.1692584	-89.71854378	-16
181	USACE	2A-U2	30.17721286	-89.71080867	-12
182	USACE	2A-6	30.17920369	-89.70906053	-11
183	USACE	2A-7	30.17969483	-89.70859499	-12
184	USACE	RPH-5	30.20428277	-89.69995631	-8
185	USACE	RPH-4	30.20383779	-89.70013522	-8
186	USACE	RP-2	30.16864822	-89.73576609	-29
187	USACE	RP-3	30.16977903	-89.73477581	-30
188	USACE	RP-4	30.17076219	-89.73390226	-27
189	USACE	RP-5	30.17184262	-89.73285556	-24
190	USACE	RP-6	30.17277331	-89.73175407	-20
191	USACE	RP-7	30.1736571	-89.73088205	-18
192	USACE	RP-10	30.17468713	-89.72977892	-17
193	USACE	RP-8	30.17576891	-89.72884649	-16
194	USACE	G-11	30.18076636	-89.72304687	-10
195	Roth Geotech	25	30.36149333	-90.41822988	-8
196	USACE	B-1	30.30927307	-90.40524489	-25
197	Flock-Stanley	R43.7L	29.53032226	-89.73119146	-138
198	Flock-Stanley	BBA-3	29.58979167	-89.57599947	-131
199	Flock-Stanley	R44.2L	29.53278006	-89.73706913	-142
200	Flock USACE	R43.2L	29.52813747	-89.72480338	-139
201	Flock USACE	BIB-4	29.38991969	-89.02978595	-275
202	Flock USACE	BIBC-5	29.40913445	-89.0251592	-256
203	Flock USACE	BIC-2	29.38943886	-89.10914336	-273
204	Flock USACE	BIC-3	29.40294985	-89.07935944	-287
205	Flock-Stanley	BIC-4	29.40634988	-89.05056351	-266
206	Flock USACE	BIC-5	29.40587973	-89.03406639	-273
207	Flock-Stanley	BIC-6	29.41581128	-88.99955725	-262
208	Flock USACE	15	30.22956119	-89.77448822	-3
209	Flock USACE	40	30.18833744	-89.81869692	-19
210	Flock USACE	10	30.16396686	-89.84461156	-17
211	Flock USACE	60	30.12248517	-89.87812002	-31
212	Flock USACE	50	30.10079212	-89.89771331	-29
213	Flock USACE	EDAB-4	29.09331683	-89.19027172	-336
214	Flock-Stanley	EDB-5	29.09252771	-89.18948449	-336
215	Flock-Stanley	EDB-1	29.00111925	-89.10882406	-415
216	Flock-Stanley	EDC-2	29.0830571	-89.00010718	-440
217	Flock-Stanley	EDC-1	29.07959933	-88.99982752	-440
218	Flock USACE	FTLA-10	29.31260808	-89.85858382	-199
219	Flock USACE	FTBL-7	29.39920044	-89.78500959	-153
220	Flock USACE	LA-3	29.14243517	-90.18907683	-148
221	Flock USACE	LA-8	29.15821211	-90.16955168	-148
222	Flock USACE	LA-11	29.17359332	-90.13497746	-173
223	Flock USACE	LA-13	29.17537115	-90.11699133	-173
224	Flock USACE	LA-24	29.20533715	-90.03871823	-179
225	Flock USACE	LB-13	29.14749707	-90.20327378	-164
226	Flock USACE	LB-4	29.08622896	-90.177	-160
227	Flock USACE	MAA-1	30.08817719	-90.73741224	-49
228	Flock USACE	MAA-4	30.07678141	-90.70694723	-45
229	Flock USACE	MAA-6	30.06919382	-90.67318161	-63
230	Flock USACE	MAA-8	30.06544299	-90.65294865	-22
231	Flock USACE	MAA-9	30.05602281	-90.64543961	-30
232	Flock USACE	MAA-10	30.04995267	-90.63850821	-32
233	Flock USACE	MAA-14	30.01854267	-90.57302318	-31
234	Flock USACE	NOB-2	29.88252096	-90.09896096	-71
235	Flock USACE	NOB-1	29.85903924	-90.09988502	-88
236	Flock USACE	HDU-45	29.7683314	-90.09947258	-97

237	Flock-Stanley	HDU-37	29.76008262	-90.09922933	-90
238	Flock USACE	2A-10	30.18616399	-89.70814516	-16
239	Flock USACE	2A-5	30.178327	-89.70977832	-12
240	Flock USACE	2A-4	30.17626009	-89.71171182	-14
241	Flock USACE	2A-3	30.17412141	-89.71369488	-11
242	Flock USACE	2A-2	30.17156648	-89.71632257	-12
243	Flock USACE	B-14	30.06975738	-89.72348334	-46
244	Flock USACE	B-7	30.06018354	-89.73551552	-50
245	Flock USACE	B8	30.03453391	-89.73687573	-51
246	Flock USACE	B-15	30.02688363	-89.72154518	-55
247	Flock USACE	4-R	30.14907444	-89.74273318	-23
248	Flock USACE	G-7	30.17748003	-89.72700628	-13
249	Flock USACE	G-9	30.18577638	-89.71775119	-3
250	Flock USACE	G-10	30.18932171	-89.71423114	-1
251	Flock USACE	G-8	30.19341247	-89.7105956	-5
252	Flock USACE	G-14	30.21571785	-89.69167477	-3
253	Flock USACE	RPH-6	30.23140631	-89.66987392	-3
254	Flock USACE	RPH-7	30.23144938	-89.66903071	-2
255	Flock USACE	RPH 11	30.23456422	-89.64686018	-20
256	Flock USACE	RPH 1	30.23944458	-89.61543148	-20
257	Flock-Stanley	SWPA-1	28.92000815	-89.45030619	-368
258	Flock-Stanley	SWPA-8	28.94075809	-89.34927997	-344
259	Flock-Stanley	SWPA-9	28.94084644	-89.32033297	-343
260	Flock-Stanley	SWPA-11	28.9744351	-89.26078329	-348
261	Flock-Stanley	BUR-1	28.97044025	-89.37409418	-347
262	Flock-Stanley	SWPB-3	28.90841768	-89.36703269	-350
263	Flock-Stanley	SWPB-2	28.85969424	-89.40102157	-350
264	Flock-Stanley	SWPB-1	28.85016783	-89.40001717	-358
265	Flock USACE	SBA-2	29.86360267	-89.9661836	-103
266	Flock-Stanley	CE-18CU	29.86186902	-89.77255376	-87
267	Flock USACE	R-79.9-L	29.86843911	-89.94078572	-87
268	Flock-Stanley	SBB-4	29.83169574	-89.95971075	-91
269	Flock-Stanley	VA-11	29.43855686	-89.2976197	-203
270	Flock USACE	VB-13	29.45882251	-89.38194268	-191
271	Flock-Stanley	VB-8	29.28339758	-89.3609654	-238
272	Flock-Stanley	WDC-1 (proj)	29.04496	-89.44547988	-313
273	Flock USACE	98	30.35612535	-90.09577517	-26
274	Flock USACE	LBB-1	30.37826296	-90.16276856	-41
275	Flock USACE	PF-12	30.33244961	-90.43036747	-13
276	Flock USACE	3P	30.26530306	-90.41501092	-5
277	Flock USACE	7P	30.25856082	-90.41335715	-4
278	Flock USACE	9P	30.25456572	-90.41243813	-7
279	Flock USACE	F-1	30.16802938	-90.39784223	-25
280	Flock USACE	F-2	30.16422481	-90.39768845	-25
281	Flock USACE	F-4	30.16028528	-90.39791705	-25
282	Flock USACE	F-6	30.15636425	-90.39912694	-25
283	Flock USACE	DEC-1	30.01940374	-90.24673173	-44
284	Flock USACE	WW-5047Z	29.48345596	-90.76556569	-167
285	Flock USACE	WW-5056Z	29.4939116	-90.75595814	-195
286	Flock USACE	26934	29.59712634	-91.52847743	-46
287	Flock USACE	230	29.68251527	-91.37823308	-32
288	Flock USACE	260	29.67571015	-91.38115104	-30
289	Flock USACE	310	29.66179777	-91.38610082	-35
290	Flock USACE	34	29.65824414	-91.3876746	-43
291	Flock USACE	620	29.57933055	-91.41903222	-53
292	Flock USACE	WL-3	29.5244866	-91.42880643	-67
293	Flock USACE	113021	29.18658194	-90.83103566	-148
294	Flock USACE	86UW	29.87894956	-91.45674333	-97
295	Flock USACE	5143Z	29.60978606	-90.47190259	-121
296	Flock USACE	WW-5041Z	29.36894616	-90.72986068	-197
297	Flock USACE	62176	29.73196144	-90.93523362	-148
298	Flock USACE	73471	29.67772661	-90.9322473	-129
299	Flock USACE	82120	29.67189879	-90.9297787	-135

300	Flock USACE	48462	29.61677181	-90.92409808	-139
301	Flock USACE	62950	29.57871138	-90.88016415	-153
302	Flock USACE	69819	29.57407802	-90.8639497	-143
303	Flock USACE	66219	29.55918475	-90.85188175	-139
304	Flock USACE	CH-43	29.68788657	-90.85549009	-107
305	Flock USACE	BDA-2	29.82087692	-90.4829231	-72
306	Flock USACE	BDA-5	29.82148139	-90.4809987	-79
307	Flock USACE	BDA-19	29.82148439	-90.47229779	-83
308	Flock USACE	SC-106	29.85316138	-90.45616248	-59
309	Flock USACE	PGP-1X	29.86076772	-90.45277422	-55
310	Flock USACE	DAB-1	29.8631423	-90.4456523	-48
311	Flock USACE	DAB-2	29.87450172	-90.43989556	-49
312	Flock USACE	PSP-1	29.87805679	-90.42803666	-57
313	Flock USACE	SBT-1	29.89029722	-90.41053614	-62
314	Flock USACE	HH-5	29.88991045	-90.40647352	-63
315	Flock USACE	KU-71	29.89837969	-90.40218062	-62
316	Flock USACE	OL-15-D	29.89848095	-90.40037136	-60
317	Flock USACE	STC-2	29.89927275	-90.39721337	-61
318	Flock USACE	U-6	29.93037429	-90.38219646	-59
319	Flock USACE	U-8	29.93609789	-90.37711407	-61
320	Flock USACE	U-17	29.95376976	-90.36796904	-60
321	Flock USACE	U-19	29.95691884	-90.36615977	-57
322	Flock USACE	PO-7	29.98486906	-90.35949836	-61
323	Flock USACE	KMS-25	29.98837718	-90.48415683	-49
324	Flock USACE	WS-9	29.9835342	-90.47863033	-41
325	Flock USACE	CA-10	29.97643582	-90.46812014	-37
326	Flock USACE	KU-3	29.97199546	-90.46236338	-39
327	Flock USACE	LP-4	29.97031449	-90.45920539	-45
328	Flock USACE	KU-6	29.96824533	-90.45614608	-42
329	Flock USACE	8	29.96587444	-90.452544	-41
330	Flock USACE	9	29.96449515	-90.45006037	-42
331	Flock USACE	12	29.96213869	-90.4463267	-43
332	Flock USACE	14	29.95956673	-90.44214894	-42
333	Flock USACE	19	29.95522716	-90.43594809	-49
334	Flock USACE	KU-26	29.94693421	-90.4292867	-48
335	Flock USACE	44	29.92612099	-90.41777319	-51
336	Flock USACE	61	29.90973519	-90.40783869	-60
337	Flock USACE	OL-14-D	29.90007627	-90.40173653	-63
338	Flock USACE	PS-5	29.55103143	-90.70114681	-135
339	Flock USACE	SP-2	29.58083422	-90.7157371	-123
340	Flock USACE	TH-5	29.5970893	-90.71460938	-129
341	Flock USACE	C-123	29.70736043	-90.57213528	-150
342	Flock USACE	CC-86	29.79973315	-91.56402246	-17
343	Flock USACE	117149	29.43467841	-91.03105667	-125
344	Flock USACE	19	29.69438697	-91.21835989	-85
345	Flock USACE	4	29.69574881	-91.21475662	-135
346	Flock USACE	51	29.70172202	-91.19172208	-96
347	Flock USACE	DB-59	29.66883531	-91.07084027	-128
348	Flock USACE	64468	29.62818288	-91.22712984	-99
349	Flock USACE	109A-UE	29.92601908	-91.24275099	-128
350	Flock USACE	233-UE	29.79770045	-91.17097708	-94
351	Flock USACE	65.9R	29.72494782	-89.99557393	-97
352	Flock USACE	63.5R	29.69456019	-89.97978544	-120
353	Flock USACE	35298	29.16615559	-90.66769067	-170
354	Flock USACE	BG-1	29.73817735	-90.14509147	-88
355	Kulp Offshore SA	EI18	29.35	-91.5	-47
356	Kulp Offshore SA	MP49	29.4	-89.36	-122
357	Kulp Offshore SA	EI83	29.11	-91.46	-132
358	Kulp Offshore SA	GI42	28.99	-89.93	-186
359	Kulp Offshore SA	WD22	29.2	-89.59	-197
360	Kulp Offshore SA	Wd69	28.97	-89.84	-198
361	Kulp Offshore SA	WD29	29.31	-89.59	-207
362	Kulp Offshore SA	WD31	29.15	-89.67	-211

363	Kulp Offshore SA	GI32	29.02	-89.87	-217
364	Kulp Offshore SA	GI40	28.99	-91.01	-219
365	Kulp Offshore SA	GI45	28.96	-89.93	-220
366	Kulp Offshore SA	WD70	28.97	-89.81	-226
367	Kulp Offshore SA	GI47	28.94	-90	-230
368	Kulp Offshore SA	MP127	29.26	-88.85	-230
369	Kulp Offshore SA	MP45	29.39	-89.18	-231
370	Kulp Offshore SA	WD44	29.1	-89.66	-231
371	Kulp Offshore SA	WD45	29.1	-89.63	-232
372	Kulp Offshore SA	WD23	29.2	-89.56	-234
373	Kulp Offshore SA	WD40	29.09	-89.78	-238
374	Kulp Offshore SA	GI52	28.9	-90.01	-240
375	Kulp Offshore SA	GI48	28.94	-90.06	-250
376	Kulp Offshore SA	WD71	28.98	-89.78	-250
377	Kulp Offshore SA	MP59	29.35	-88.94	-263
378	Kulp Offshore SA	MP40	29.39	-88.96	-269
379	Kulp Offshore SA	MP41	29.39	-88.99	-282
380	Kulp Offshore SA	MP43	29.39	-89.1	-286
381	Kulp Offshore SA	MP67	29.27	-89.09	-310
382	Kulp Offshore SA	MP148	29.21	-88.87	-325
383	Kulp Offshore SA	ST47	28.88	-90.31	-328
384	Kulp Offshore SA	WD60	29.02	-89.58	-342
385	Kulp Offshore SA	MP142	29.28	-88.76	-348
386	Kulp Offshore SA	MP300	29.26	-88.81	-389
387	Kulp Offshore SA	SP27	28.98	-89.29	-390
388	Kulp Offshore SA	MP299	29.25	-88.76	-394
389	Kulp Offshore SA	MP76	29.17	-88.96	-400
390	Kulp Offshore SA	MP71	29.25	-88.96	-413
391	Kulp Offshore SA	WD85	28.89	-89.48	-413
392	Kulp Offshore SA	SP55	28.85	-89.29	-426
393	Kulp Offshore SA	SP46	28.88	-89.2	-430
394	Kulp Offshore SA	MP151	29.17	-88.89	-442
395	Kulp Offshore SA	SP37	28.95	-89.24	-452
396	Kulp Offshore SA	MP312	29.17	-88.78	-473
397	Kulp Offshore SA	MP311	29.18	-88.74	-482
398	Kulp Offshore SA	WD109	28.86	-89.46	-483
399	Kulp Offshore SA	SP52	28.97	-89.17	-500
400	Kulp Offshore SA	SP20	29.01	-89.09	-507
401	Kulp Offshore SA	MP75	29.21	-88.97	-519
402	Kulp Offshore SA	SP77	28.83	-89.38	-525
403	Kulp Offshore SA	SP78	28.82	-89.42	-526
404	Kulp Offshore SA	SP45	28.9	-89.25	-559
405	Kulp Offshore SA	SP39	28.93	-89.34	-563
406	Kulp Offshore SA	SP18	29.02	-89.01	-570
407	Kulp Offshore SA	SP70	29	-88.99	-574
408	Kulp Offshore SA	MC20	28.95	-88.99	-579
409	Kulp Offshore SA	SP63	29.07	-88.78	-590
410	Kulp Offshore SA	SP75	28.82	-89.29	-591
411	Kulp Offshore SA	SP51	28.87	-89.12	-600
412	Kulp Offshore SA	SP60	29.05	-88.96	-616
413	Kulp Offshore SA	SP54	28.87	-89.25	-620
414	Kulp Offshore SA	MC63	28.9	-89.02	-640
415	Kulp Offshore SA	SP33	28.94	-89.06	-649
416	Kulp Offshore SA	SP66	29.09	-88.93	-662
417	Kulp Offshore SA	SP49	28.91	-89.08	-664
418	Kulp Offshore SA	SP47	28.9	-89.15	-707
419	Kulp Onshore	MAB-1	30.13	-90.55	-17
420	Kulp Onshore	MAB-3	30.13	-90.55	-23
421	Kulp Onshore	MAB-5	30.12	-90.56	-12
422	Kulp Onshore	VB-8	29.87	-89.99	-91
423	Kulp Onshore	C-12	29.16	-90.67	-171
424	Kulp Onshore	AS-6	29.84	-91.22	-121
425	Kulp Onshore	DB-26	29.68	-91.14	-105

426	Kulp Onshore	773323	29.69	-90.092	-125
427	Kulp Onshore	DL-1	29.18	-90.85	-148
428	Kulp Onshore	40-U-W	29.72	-90.27	-125
429	Kulp Onshore	96	30.35	-91.1	-29
430	Kulp Onshore	90	30.33	-91.1	-28
431	LaDOTD	L-1	29.73012558	-90.14580999	-94
432	LaDOTD	L-2	29.72454025	-90.14947167	-90
433	LaDOTD	L-3	29.71915218	-90.15293807	-88
434	LaDOTD	L-4	29.71377312	-90.15644067	-86
435	LaDOTD	L-5	29.70842415	-90.16000362	-91
436	LaDOTD	L-6	29.70302171	-90.16345887	-86
437	LaDOTD	L-7	29.69839555	-90.16834896	-89
438	LaDOTD	L-8	29.6947246	-90.17415656	-102
439	LaDOTD	L-10	29.68862222	-90.18040594	-112
440	LaDOTD	L-9	29.68948146	-90.1798454	-110
441	LaDOTD	L-11	29.68781681	-90.18104401	-112
442	LaDOTD	L-12	29.68704471	-90.18171811	-112
443	LaDOTD	L-13	29.68650556	-90.18265972	-112
444	LaDOTD	L-14	29.68578057	-90.18338853	-112
445	LaDOTD	L-16	29.6842419	-90.18474229	-112
446	LaDOTD	L-17	29.68306303	-90.18584787	-97
447	LaDOTD	L-18	29.68241537	-90.18643998	-115
448	LaDOTD	L-19	29.68195752	-90.18688523	-116
449	LaDOTD	L-20	29.68084129	-90.18780347	-114
450	LaDOTD	L-21	29.67970056	-90.18895032	-112
451	LaDOTD	L-22	29.67897266	-90.18967144	-114
452	LaDOTD	L-23	29.67821532	-90.19035336	-116
453	LaDOTD	L-24	29.67747616	-90.19105932	-114
454	LaDOTD	L-25	29.6767368	-90.191765	-115
455	LaDOTD	L-26	29.67598922	-90.19245945	-118
456	LaDOTD	L-27	29.67526186	-90.19318142	-115
457	LaDOTD	L-28	29.67457523	-90.1939581	-122
458	LaDOTD	L-29	29.66942939	-90.19794097	-123
459	LaDOTD	L-30	29.66278676	-90.1992517	-117
460	LaDOTD	L-31	29.65703541	-90.20126019	-113
461	LaDOTD	L-32	29.65190308	-90.20516468	-119
462	LaDOTD	L-33	29.64785846	-90.21016003	-121
463	LaDOTD	L-34	29.64343141	-90.2151306	-122
464	LaDOTD	L-35	29.63899697	-90.22007956	-121
465	LaDOTD	L-36	29.63435139	-90.2252988	-120
466	LaDOTD	L-37	29.62998189	-90.23031311	-120
467	LaDOTD	L-38	29.62555589	-90.23526211	-132
468	LaDOTD	L-39	29.62111323	-90.24019132	-124
469	LaDOTD	L-40	29.61668281	-90.24513443	-120
470	LaDOTD	L-41	29.61250567	-90.24984418	-121
471	LaDOTD	L-42	29.60803654	-90.25474141	-120
472	LaDOTD	L-43	29.60358549	-90.25965949	-121
473	LaDOTD	L-44	29.59916381	-90.264612	-121
474	LaDOTD	L-45	29.59491499	-90.26924963	-122
475	LaDOTD	L-46	29.59053704	-90.2742524	-122
476	LaDOTD	L-47	29.58704895	-90.27804685	-127
477	LaDOTD	L-48	29.58208447	-90.28459879	-124
478	LaDOTD	L-49	29.57929812	-90.29139627	-137
479	LaDOTD	L-50	29.57668252	-90.29781172	-142
480	LaDOTD	L-51	29.57402054	-90.30420154	-124
481	LaDOTD	L-52	29.57349695	-90.30548419	-122
482	LaDOTD	L-53	29.57308141	-90.30647735	-121
483	LaDOTD	L-54	29.57242715	-90.30803731	-123
484	LaDOTD	L-55	29.57218392	-90.30874072	-121
485	LaDOTD	L-56	29.57157347	-90.31001135	-123
486	LaDOTD	L-57	29.57119585	-90.31102495	-123
487	LaDOTD	L-58	29.5707608	-90.31200754	-121
488	LaDOTD	L-59	29.57039193	-90.31302581	-123

489	LaDOTD	L-60	29.56986946	-90.31423949	-123
490	LaDOTD	L-61	29.56957371	-90.31501896	-129
491	LaDOTD	L-62	29.56915257	-90.31600906	-129
492	LaDOTD	L-63	29.56651263	-90.32213519	-120
493	LaDOTD	L-64	29.56379342	-90.32849296	-142
494	LaDOTD	L-15	29.68520616	-90.18390638	-112
495	Flock USACE	47356	29.64686	-90.24207	-196
496	Flock USACE	WAJ-5	29.65327	-90.23169	-193
497	Flock USACE	35540	29.6634	-90.18757	-127
498	Flock USACE	B-100	29.67982	-90.19013	-115
499	Flock USACE	63236	29.70277	-90.17898	-195
500	Flock USACE	70282	29.70911	-90.17284	-107
501	Flock-Stanley	B-102	29.73809	-90.13963	-88
502	Flock USACE	JB-2	29.73912	-90.13078	-88
503	Flock USACE	IRP-2	29.67772	-90.2213	-143
504	Flock-Stanley	B-101	29.68413	-90.18642	-109
505	Flock-Stanley	W-67.6 -U	29.74356	-90.01905	-92
506	Flock USACE	R-67.6- R	29.74433	-90.01777	-103
507	Flock USACE	R-67.3- L	29.74651	-90.00815	-93
508	Flock USACE	WW-50 32Z	29.37902	-90.79655	-198
509	Flock USACE	35272	29.4432	-90.75845	-211
510	Flock USACE	WW-50 47Z	29.48324	-90.76547	-167
511	Flock USACE	WW-50 56Z	29.49369	-90.75587	-194
512	Flock USACE	65852	29.47054	-90.99025	-215
513	Flock USACE	60175	29.47417	-90.97045	-200
514	Flock USACE	92812	29.4085	-90.92574	-109
515	Flock USACE	175617	29.39542	-90.89395	-139
516	Flock USACE	145452	29.39936	-90.88128	-147
517	Flock USACE	971055	29.41867	-90.83288	-198
518	Flock USACE	78733	29.39371	-90.76817	-205
519	Flock USACE	37406	29.39104	-90.76534	-194
520	Flock USACE	69200	29.59631	-91.6281	-37
521	Flock USACE	MT-1	29.5723	-91.53719	-52
522	Flock USACE	SWD-1	29.57417	-91.53358	-54
523	Flock USACE	P-1	29.57407	-91.50651	-44
524	Flock USACE	CE-2	29.64537	-91.50696	-53
525	Flock USACE	27165	29.62825	-91.53011	-46
526	Flock USACE	CE-1	29.60304	-91.53795	-45
527	Flock USACE	34120	29.55903	-91.5273	-58
528	Flock USACE	HB-1	29.55685	-91.52528	-59
529	Flock USACE	38458	29.54914	-91.51582	-62
530	Flock USACE	CE-30	29.70373	-91.47466	-41
531	Flock USACE	CE-32	29.70294	-91.46938	-42
532	Flock USACE	BI-35	29.69012	-91.38071	-35
533	Flock USACE	BI-36	29.68864	-91.37385	-38
534	Flock USACE	BI-4	29.69169	-91.34695	-114
535	Flock USACE	BI-48	29.6916	-91.34031	-117
536	Flock USACE	BI-1	29.6915	-91.3123	-100
537	Flock USACE	BI-69	29.698	-91.30218	-134
538	Flock USACE	45-UW	29.70836	-91.28924	-155
539	Flock USACE	22259	29.70964	-91.28181	-146
540	Flock USACE	29851	29.71143	-91.27991	-143
541	Flock USACE	40-UW	29.71596	-91.2699	-125
542	Flock USACE	FI-7	29.24379	-90.79646	-188
543	Flock USACE	34475	29.23422	-90.79277	-155
544	Flock USACE	159026	29.21418	-90.79175	-159
545	Flock USACE	78097	29.17657	-90.76594	-161
546	Flock USACE	77181	29.13562	-90.75407	-167
547	Flock USACE	59894	29.05863	-90.76554	-165
548	Flock USACE	BJ-1	29.19936	-90.9992	-140
549	Flock USACE	130615	29.18576	-90.90234	-302
550	Flock USACE	120012	29.18724	-90.85742	-157
551	Flock USACE	119774	29.18793	-90.85552	-156

552	Flock USACE	DL-3	29.18359	-90.84692	-147
553	Flock USACE	HC-199	30.22303	-89.11095	-12
554	Flock USACE	HC-200	30.21384	-89.08541	-30
555	Flock USACE	ADB-1	29.90204	-91.48434	-136
556	Flock USACE	ADB-4	29.91369	-91.45627	-109
557	Flock USACE	ADB-7	29.92388	-91.43118	-136
558	Flock USACE	ADB-1 0	29.93655	-91.40053	-124
559	Flock USACE	33146	29.93648	-91.34825	-126
560	Flock USACE	48784	29.94381	-91.32146	-138
561	Flock USACE	BL-1	29.94949	-91.29866	-125
562	Flock USACE	PT-1	29.97443	-91.28239	-77
563	Flock USACE	W-W	29.82248	-91.48104	-110
564	Flock USACE	DF-14	29.81582	-91.43304	-117
565	Flock USACE	DF-12	29.84652	-91.37086	-103
566	Flock USACE	DF-11	29.86775	-91.3269	-112
567	Flock USACE	42441	29.88819	-91.31689	-126
568	Flock USACE	MB-1	29.89043	-91.31501	-130
569	Flock USACE	69220	29.88936	-91.28116	-129
570	Flock USACE	SMN-9 6	29.89892	-91.26311	-116
571	Flock USACE	68	30.2503	-90.12086	-45
572	Flock USACE	RCP-5	30.41411	-90.15652	-28
573	Flock USACE	NB-8	30.4102	-90.15737	-34
574	Flock USACE	MR-1	30.40339	-90.15345	-55
575	Flock USACE	MR-7	30.39998	-90.15308	-53
576	Flock USACE	MR-11	30.39889	-90.1535	-37
577	Flock USACE	RCP-1	30.39426	-90.15605	-47
578	Flock USACE	RCP-2	30.38177	-90.16032	-48
579	Flock USACE	3LUW	29.57072	-90.38139	-117
580	Flock USACE	SH-6	29.57545	-90.38004	-116
581	Flock USACE	57354	29.60152	-90.36611	-168
582	Flock USACE	54154	29.61259	-90.34324	-158
583	Flock USACE	55306	29.61642	-90.33872	-161
584	Flock USACE	5127Z	29.62363	-90.33023	-149
585	Flock USACE	WAJ-3	29.63796	-90.30669	-198
586	Flock USACE	5142Z	29.59644	-90.44611	-118
587	Flock USACE	5085Z	29.59537	-90.43627	-124
588	Flock USACE	3E	29.58563	-90.37143	-122
589	Flock USACE	8DE	29.57319	-90.34382	-124
590	Flock USACE	16UE	29.54399	-90.31268	-188
591	Flock USACE	5166Z	29.59636	-90.4433	-120
592	Flock USACE	5147Z	29.59893	-90.41545	-122
593	Flock USACE	OS-1	29.34318	-90.73383	-195
594	Flock USACE	32202	29.41038	-90.53642	-208
595	Flock-Stanley	R32.4U R	29.43336	-89.60757	-163
596	Flock-Stanley	R30.3R	29.39921	-89.6041	-164
597	Flock USACE	M-5	29.38362	-89.60297	-163
598	Flock USACE	DB-75	29.68914	-90.99812	-116
599	Flock USACE	DB-4	29.6916	-90.9808	-120
600	Flock USACE	DB-23	29.69634	-90.95525	-117
601	Flock USACE	CH-1	29.70709	-90.91339	-117
602	Flock USACE	CH-5	29.70859	-90.90775	-141
603	Flock USACE	CH-11	29.70661	-90.90121	-132
604	Flock USACE	CH-23	29.69961	-90.88423	-112
605	Flock USACE	CH-33	29.69359	-90.87003	-102
606	Flock USACE	CH-35	29.6926	-90.867	-113
607	Flock USACE	CH-47	29.6855	-90.84976	-119
608	Flock USACE	CH-59	29.68264	-90.83153	-112
609	Flock USACE	CH-61	29.68254	-90.82849	-118
610	Flock USACE	C-210	29.68097	-90.75014	-124
611	Flock USACE	LA-41	29.86861	-91.63754	-10
612	Flock USACE	DF-16	29.82847	-91.56292	-33
613	Flock USACE	CC-4	29.81619	-91.54857	-34
614	Flock USACE	DF-15	29.80686	-91.52788	-10

615	Flock USACE	8-Feb	29.80263	-91.52097	-25
616	Flock USACE	31-Jan	29.79973	-91.51859	-26
617	Flock USACE	6-Feb	29.79222	-91.51122	-36
618	Flock USACE	24-UW	29.98259	-91.54944	-116
619	Flock USACE	26-UW	29.96587	-91.54183	-129
620	Flock USACE	WAB-75	29.94102	-91.55196	-124
621	Flock USACE	WAB-77	29.92184	-91.54351	-122
622	Flock USACE	WAB-79	29.90822	-91.5358	-126
623	Flock USACE	P-42	29.89191	-91.53307	-98
624	Flock USACE	CC-12	29.8191	-91.54653	-31
625	Flock USACE	CC-80	29.80519	-91.55803	-12
626	Flock USACE	CC-92	29.7941	-91.56951	-13
627	Flock USACE	VF-1	29.99871	-90.7254	-33
628	Flock USACE	VF-11	29.99737	-90.7237	-28
629	Flock USACE	VF-10	29.9912	-90.72314	-33
630	Flock USACE	A-6	29.93662	-90.70417	-45
631	Flock USACE	A-7	29.85779	-90.66858	-59
632	Flock USACE	BR-5	29.85888	-90.67784	-69
633	Flock USACE	ET-8	29.86049	-90.64155	-56
634	Flock USACE	BB-6	29.86901	-90.59452	-49
635	Flock USACE	31754	29.487	-91.04802	-174
636	Flock USACE	161242	29.46335	-91.05968	-159
637	Flock USACE	30695	29.45521	-91.07604	-138
638	Flock USACE	65527	29.42716	-91.0702	-145
639	Flock USACE	57059	29.40841	-91.06828	-139
640	Flock USACE	89012	29.38811	-91.06202	-149
641	Flock USACE	66480	29.31225	-91.00574	-142
642	Flock USACE	49251	29.40796	-91.23602	-151
643	Flock USACE	53404	29.40571	-91.22179	-129
644	Flock USACE	50065	29.40527	-91.21502	-126
645	Flock USACE	64111	29.43274	-91.03722	-140
646	Flock USACE	59090	29.43554	-91.0273	-129
647	Flock USACE	LR-10	29.43471	-90.2981	-118
648	Flock USACE	55637	29.41739	-90.29732	-120
649	Flock USACE	50561	29.41128	-90.29658	-128
650	Flock USACE	78814	29.39488	-90.29381	-115
651	Flock USACE	108511	29.38511	-90.29743	-126
652	Flock USACE	75020	29.37268	-90.29872	-123
653	Flock USACE	75021	29.36696	-90.29872	-125
654	Flock USACE	106791	29.36006	-90.29935	-130
655	Flock USACE	53763	29.35453	-90.299	-137
656	Flock USACE	49501	29.29699	-90.29399	-215
657	Flock USACE	53323	29.4617	-90.25232	-144
658	Flock USACE	MP-2	29.68171	-91.23581	-73
659	Flock USACE	SPC-1	29.68322	-91.23252	-78
660	Flock USACE	LA-2	29.69118	-91.22681	-96
661	Flock USACE	6	29.69184	-91.2241	-109
662	Flock USACE	10	29.69363	-91.21951	-82
663	Flock USACE	2A	29.69497	-91.2162	-82
664	Flock USACE	5	29.69629	-91.21304	-135
665	Flock USACE	7	29.69717	-91.21072	-127
666	Flock USACE	49	29.70133	-91.19411	-94
667	Flock USACE	57	29.70082	-91.18421	-77
668	Flock USACE	64	29.69752	-91.18082	-117
669	Flock USACE	74	29.69669	-91.17654	-44
670	Flock USACE	25	29.68033	-91.13776	-105
671	Flock USACE	DB-37	29.67017	-91.106	-87
672	Flock USACE	42	29.66985	-91.10128	-46
673	Flock USACE	DB-71	29.67181	-91.02304	-87
674	Flock USACE	LW-1	29.70805	-91.2011	-125
675	Flock USACE	CNB-2	29.70375	-91.201	-117
676	Flock USACE	GTB-2	29.7034	-91.19771	-84
677	Flock USACE	CH-1	29.6965	-91.18828	-78

678	Flock USACE	TP-3	29.69042	-91.18249	-42
679	Flock USACE	BB-A	29.68249	-91.17526	-136
680	Flock USACE	74918	29.65843	-91.15904	-138
681	Flock USACE	48134	29.63103	-91.14065	-149
682	Flock USACE	40354	29.6068	-91.08553	-153
683	Flock USACE	67924	29.57997	-91.07374	-160
684	Flock USACE	MCL-1	29.71002	-91.24468	-69
685	Flock USACE	MI-2	29.66318	-91.24052	-76
686	Flock USACE	127.8- UW	29.66209	-91.24213	-71
687	Flock USACE	LA-1	29.65851	-91.2449	-94
688	Flock USACE	45297	29.64206	-91.23545	-106
689	Flock USACE	BLF-1	29.63763	-91.23642	-111
690	Flock USACE	64468	29.62797	-91.22703	-112
691	Flock USACE	39608	29.59999	-91.23033	-99
692	Flock USACE	11-B	29.57635	-91.2212	-120
693	Flock USACE	LA-2	29.54703	-91.23446	-103
694	Flock USACE	7-U	29.53009	-91.23669	-108
695	Flock USACE	53D	29.7867	-89.43327	-121
696	Flock USACE	71.9-U ET	29.92828	-91.24678	-127
697	Flock USACE	112A-UE	29.91382	-91.23066	-129
698	Flock USACE	113A-UE	29.90849	-91.22066	-128
699	Flock USACE	146-UE	29.90085	-91.21146	-128
700	Flock USACE	148-UE	29.88693	-91.20844	-115
701	Flock USACE	149-UE	29.87845	-91.20895	-123
702	Flock USACE	151-UE	29.87031	-91.20746	-121
703	Flock USACE	97-UE	29.8415	-91.18435	-93
704	Flock USACE	100-UE	29.8309	-91.17406	-142
705	Flock USACE	102-UE	29.82355	-91.17333	-122
706	Flock USACE	104-UE	29.81669	-91.17258	-118
707	Flock USACE	106-UE	29.80959	-91.1723	-119
708	Flock USACE	A1-UE	29.80405	-91.171	-97
709	Flock USACE	261-UE	29.79987	-91.17055	-94
710	Flock USACE	A2-UE	29.79059	-91.17173	-93
711	Flock USACE	A3-UE	29.78739	-91.17286	-93
712	Flock USACE	140	29.77921	-91.17717	-93
713	Flock USACE	144-UE	29.76854	-91.17632	-101
714	Flock USACE	161-UE	29.7647	-91.17535	-121
715	Flock USACE	164-UE	29.75364	-91.17524	-91
716	Flock USACE	AS-6	29.9229	-91.21619	-121
717	Flock USACE	28845	29.90794	-91.17316	-121
718	Flock USACE	AS-8	29.94672	-91.13707	-130
719	Flock USACE	AS-69	29.96394	-91.1041	-110
720	Flock USACE	P-4	29.96596	-91.10376	-129
721	Flock USACE	AS-11	29.99172	-91.06727	-132
722	Flock USACE	P-3	29.99206	-91.0634	-131
723	Flock USACE	65.6R	29.72323	-89.99448	-102
724	Flock USACE	64.5R	29.70985	-89.98853	-101
725	Flock-Stanley	76MH UT	29.70444	-89.98624	-101
726	Flock USACE	TAL-6	29.69464	-89.9823	-114
727	Flock USACE	62.9R	29.68763	-89.97336	-112
728	Flock USACE	1	29.67919	-89.96728	-102
729	Flock USACE	61.6R	29.67247	-89.96408	-114
730	Flock USACE	60.9R	29.6643	-89.96333	-120
731	Flock USACE	60.4R	29.65755	-89.96265	-119
732	Flock USACE	67MH UT	29.64741	-89.95959	-126
733	Flock USACE	R59.7R	29.64472	-89.95674	-123
734	Flock USACE	8	29.64101	-89.95425	-112
735	Flock-Stanley	R58.8R U	29.63643	-89.94294	-113
736	Flock USACE	R57.7R	29.62943	-89.92739	-117
737	Flock USACE	WP-2	29.62081	-89.91718	-115
738	Flock USACE	R55.9R	29.61486	-89.90418	-119
739	Flock USACE	57MHU	29.60988	-89.89229	-121
740	Flock USACE	R54.5R U	29.60625	-89.88342	-122

741	Flock USACE	R53.3R	29.6012	-89.86224	-118
742	Flock USACE	MS-31	29.5976	-89.8464	-121
743	Flock-Stanley	WP-10	29.62256	-89.91483	-116
744	Flock USACE	IS-1	29.63235	-89.91228	-97
745	Flock USACE	LA-4	29.3722	-91.38419	-81
746	Flock USACE	386	29.39263	-91.38348	-84
747	Flock USACE	304	29.40369	-91.36862	-74
748	Flock USACE	277	29.42126	-91.35548	-75
749	Flock USACE	274	29.43158	-91.3485	-75
750	Flock USACE	270	29.44295	-91.32955	-75
751	Flock USACE	329	29.45687	-91.28805	-78
752	Flock USACE	LA-3	29.47474	-91.26441	-97
753	Flock USACE	72	29.4994	-91.2621	-96
754	Flock USACE	91171	29.29875	-91.32195	-118
755	Flock USACE	8558	29.29944	-91.31474	-130
756	Flock USACE	77494	29.29924	-91.3027	-119
757	Flock USACE	82447	29.29963	-91.29143	-120
758	Flock USACE	143542	29.29717	-91.27791	-120
759	Flock USACE	72020	29.29194	-91.26835	-150
760	Flock USACE	PF-7	30.34985	-90.43449	-10
761	Flock USACE	PF-9	30.3447	-90.43327	-14
762	Flock USACE	PMH-1	30.3361	-90.43125	-19
763	Flock USACE	1	30.32833	-90.4297	-14
764	Flock USACE	7	30.31603	-90.42664	-15
765	Flock USACE	13	30.30488	-90.42408	-9
766	Flock USACE	PMH-1 2	30.3016	-90.42322	-17
767	Flock USACE	PF-14	30.29219	-90.42097	-14
768	Flock USACE	23	30.28301	-90.41875	-10
769	Flock USACE	27	30.27589	-90.41735	-5
770	Flock USACE	PF-15	30.27416	-90.41686	-15
771	Flock USACE	1P	30.26863	-90.41566	-8
772	Flock USACE	5P	30.26143	-90.41396	-7
773	Flock USACE	10P	30.25335	-90.41225	-6
774	Flock USACE	3F	30.24299	-90.41056	-9
775	Flock USACE	20P	30.23671	-90.40891	-20
776	Flock USACE	25P	30.22829	-90.40765	-18
777	Flock USACE	PMH-5	30.21639	-90.40543	-25
778	Flock USACE	B1	30.21379	-90.40479	-45
779	Flock USACE	B-1	30.19054	-90.40149	-26
780	Flock USACE	B-3	30.18802	-90.40105	-24
781	Flock USACE	B-6	30.1855	-90.40067	-40
782	Flock USACE	B-9	30.18274	-90.40024	-30
783	Flock USACE	B-11	30.18025	-90.3997	-27
784	Flock USACE	PMH-7	30.17305	-90.39838	-25
785	Flock USACE	C-64	30.16562	-90.39779	-24
786	Flock USACE	PF-593	30.15872	-90.39826	-42
787	Flock USACE	F-8	30.1543	-90.40039	-27
788	Flock USACE	LPL-B 1	30.40358	-90.46494	-17
789	Flock USACE	POM-1	30.27651	-90.33303	-14
790	Flock USACE	58	30.22655	-90.12686	-29
791	Flock USACE	53-8	30.04813	-90.16769	-82
792	Flock USACE	JLD-7	30.04923	-90.14385	-51
793	Flock USACE	9G	30.07641	-90.01539	-61
794	Flock USACE	10G	30.07934	-90.0096	-53
795	Flock USACE	30-Nov	30.0192	-90.24666	-48
796	Flock USACE	7270	29.24013	-90.66914	-185
797	Flock USACE	80606	29.20992	-90.65573	-183
798	Flock USACE	128322	29.17677	-90.66891	-173
799	Flock USACE	35960	29.16927	-90.66839	-169
800	Flock USACE	35909	29.16356	-90.66799	-179
801	Flock USACE	40590	29.1539	-90.67486	-169
802	Flock USACE	41076	29.10597	-90.66615	-187
803	Flock USACE	95201	29.09015	-90.65584	-199

804	Flock USACE	CAL-1	29.03117	-90.6501	-186
805	Flock USACE	55709	29.18723	-90.74167	-175
806	Flock USACE	62945	29.17263	-90.72833	-165
807	Flock USACE	38941	29.17022	-90.70833	-174
808	Flock USACE	52443	29.16381	-90.70083	-199
809	Flock USACE	54977	29.16346	-90.68863	-188
810	Flock USACE	71279	29.17687	-90.65388	-177
811	Flock USACE	89716	29.17426	-90.63488	-192
812	Flock USACE	101204	29.18214	-90.51279	-179
813	Flock USACE	155.9	29.97927	-90.81219	-78
814	Flock USACE	B-2	29.9671	-90.7842	-40
815	Flock USACE	MT-2	29.9038	-90.77168	-37
816	Flock USACE	5256	29.83922	-90.8168	-132
817	Flock USACE	LR-2	29.79208	-90.82121	-170
818	Flock USACE	ED-16	30.20657	-89.48825	-24
819	Flock USACE	ED-15	30.20631	-89.48209	-30
820	Flock USACE	ED-14	30.21004	-89.46648	-32
821	Flock USACE	ED-10	30.21003	-89.46005	-35
822	Flock USACE	ED-9	30.21832	-89.44433	-34
823	Flock USACE	ED-7	30.22067	-89.43928	-33
824	Flock USACE	ED-4	30.23922	-89.43735	-27
825	Flock USACE	ED-5	30.23425	-89.4417	-31
826	Flock USACE	ED-11	30.20166	-89.45705	-39
827	Flock USACE	ED-1	30.1865	-89.45648	-42
828	Flock USACE	88451	29.1374	-90.42719	-68
829	Flock USACE	62664	29.12468	-90.44283	-68
830	Flock USACE	57037	29.09471	-90.45707	-54
831	Flock USACE	26320	29.08538	-90.46799	-50
832	Flock USACE	76187	29.19293	-90.43911	-177
833	Flock USACE	76629	29.2213	-90.39392	-156
834	Flock USACE	49052	29.22283	-90.37292	-125
835	Flock USACE	51926	29.22188	-90.35493	-159
836	Flock USACE	69486	29.22208	-90.33845	-169
837	Flock USACE	69814	29.22444	-90.30733	-169
838	Flock USACE	29D	29.86805	-89.71249	-83
839	Flock USACE	7U	29.85661	-89.67701	-89
840	Flock USACE	6U	29.82558	-89.57002	-68
841	Flock USACE	MRGO -1B	29.8252	-89.60162	-98
842	Flock USACE	MRGO -40D	29.83181	-89.592	-91
843	Roth Vibracore	PON98-3	30.03767	-90.0389	-63
844	Roth Vibracore	LP-95-1	30.16735	-90.0668	-31
845	Roth Vibracore	PON97-3	30.2214	-90.3415	-30
846	Roth Vibracore	PON97-2	30.22755	-90.339	-29
847	Roth Vibracore	PON98-7	30.20687	-90.1202	-29
848	Roth Vibracore	PON96-13	30.189	-89.9422	-29
849	Roth Vibracore	PON98-10	30.24158	-89.959	-29
850	Roth Vibracore	PON97-1a	30.25312	-90.1526	-28
851	Roth Vibracore	BL98-13	30.28543	-89.9382	-27
852	Roth Vibracore	PON96-1	30.2205	-89.9562	-27
853	Roth Vibracore	PON96-12	30.16392	-89.9034	-27
854	Roth Vibracore	PON96-3	30.24068	-90.0228	-27
855	Roth Vibracore	PON96-4	30.22695	-90.0538	-26
856	Roth Vibracore	R96-3	30.18163	-89.7785	-26
857	Roth Vibracore	PON98-26	30.24707	-90.1199	-26
858	Roth Vibracore	R96-7	30.14393	-89.7574	-25
859	Roth Vibracore	PON96-8	30.2625	-90.1133	-25
860	Roth Vibracore	PON97-13	30.19947	-89.8141	-25
861	Roth Vibracore	LP-95-6	30.16665	-89.9581	-25
862	Roth Vibracore	PON98-19	30.21253	-89.8978	-24
863	Roth Vibracore	R96-5	30.15013	-89.7689	-24
864	Roth Vibracore	LP-95-13	30.2505	-90.0622	-24
865	Roth Vibracore	PON98-17	30.16733	-89.8669	-23
866	Roth Vibracore	PON96-9	30.2851	-90.1466	-22

867	Roth Vibracore	PON97-49	30.24833	-89.9214	-22
868	Roth Vibracore	PON98-18	30.20055	-89.8412	-22
869	Roth Vibracore	PON96-14	30.33787	-90.1739	-22
870	Roth Vibracore	PON96-10	30.3	-90.1768	-21
871	Roth Vibracore	PON98-9	30.30053	-90.1026	-21
872	Roth Vibracore	PON97-43	30.2432	-89.8736	-21
873	Roth Vibracore	PON96-15	30.37117	-90.1721	-19
874	Roth Vibracore	PON97-12	30.19437	-89.7995	-18
875	Roth Vibracore	PON97-40	30.28652	-89.9376	-18
876	Roth Vibracore	PON97-4	30.3441	-90.0948	-17
877	Roth Vibracore	LP-95-4	30.26447	-90.0902	-17
878	Roth Vibracore	PON98-13	30.25017	-89.9366	-16
879	Roth Vibracore	PON98-20	30.247	-89.9012	-16
880	Roth Vibracore	PON96-16	30.36328	-90.1437	-14
881	Roth Vibracore	BL98-14	30.27935	-89.955	-13
882	Roth Vibracore	PON97-46	30.28613	-90.0233	-11
883	Roth Vibracore	PON97-11	30.22173	-89.8372	-10
884	Roth Vibracore	PON97-8	30.22233	-89.8368	-10
885	Roth Vibracore	PON97-6	30.2231	-89.8359	-10
886	Roth Vibracore	LP-95-5	30.3172	-90.05	-10
887	Roth Vibracore	PON97-45	30.30528	-90.058	-10
888	Roth Vibracore	PON97-10	30.22175	-89.8353	-10
889	Roth Vibracore	PON97-47	30.30635	-90.0005	-9
890	Roth Vibracore	PON97-9	30.22357	-89.8347	-9
891	Roth Vibracore	PON98-11	30.25673	-89.9586	-8
892	Roth Vibracore	BL98-5	30.27895	-89.9543	-8
893	Roth Vibracore	BL98-16	30.25978	-89.9835	-8
894	Roth Vibracore	BL98-17	30.2496	-89.932	-7
895	Roth Vibracore	BL98-12	30.25422	-89.931	-7
896	Roth Vibracore	BL98-19	30.26812	-89.9792	-7
897	Roth Vibracore	BL98-22	30.26997	-89.9633	-6
898	Roth Vibracore	BL98-21	30.27217	-89.97228	-6
899	Roth Vibracore	PON97-44	30.311995	-90.0456	-6
900	Roth Vibracore	PON97-7	30.2237	-89.837	-6
901	Roth Vibracore	BL98-10	30.2626	-89.9212	-5
902	Roth Vibracore	BL98-9	30.25078	-89.9256	-5
903	Roth Vibracore	BL98-20	30.28091	-89.9676	-5
904	Roth Vibracore	BL98-15a	30.27547	-89.949	-4
905	Roth Vibracore	BL98-11	30.25832	-89.9256	-3
906	Roth Vibracore	BL98-15b	30.27547	-89.949	-2
907	Roth Seismic	162843	30.16487	-90.39832	-57
908	Roth Seismic	190500	30.18714	-90.356078	-48
909	Roth Seismic	191322	30.1970833	-90.350945	-47
910	Roth Seismic	192327	30.20904	-90.346885	-48
911	Roth Seismic	193332	30.2213367	-90.341533	-46
912	Roth Seismic	194335	30.2333917	-90.336362	-44
913	Roth Seismic	195336	30.24563	-90.331037	-44
914	Roth Seismic	200150	30.2557767	-90.326568	-43
915	Roth Seismic	200853	30.2643383	-90.32306	-41
916	Roth Seismic	257	30.1352625	-90.321896	-44
917	Roth Seismic	201053	30.2662417	-90.321643	-44
918	Roth Seismic	201955	30.2648483	-90.309713	-42
919	Roth Seismic	232802	30.0680833	-90.305145	-47
920	Roth Seismic	231857	30.0797483	-90.303987	-42
921	Roth Seismic	230753	30.087185	-90.303447	-41
922	Roth Seismic	203000	30.2632967	-90.296255	-41
923	Roth Seismic	220337	30.161735	-90.296153	-45
924	Roth Seismic	164705	30.102033	-90.290468	-38
925	Roth Seismic	203842	30.2621433	-90.28473	-41
926	Roth Seismic	205024	30.2520183	-90.284083	-39
927	Roth Seismic	204118	30.2629383	-90.282617	-43
928	Roth Seismic	203918	30.2650567	-90.281555	-33
929	Roth Seismic	21	30.3131719	-90.281352	-38

930	Roth Seismic	163701	30.1015067	-90.274843	-37
931	Roth Seismic	204847	30.261135	-90.271425	-41
932	Roth Seismic	202313	30.28235	-90.268448	-32
933	Roth Seismic	131	30.2942625	-90.265772	-30
934	Roth Seismic	201311	30.29292	-90.260185	-33
935	Roth Seismic	162657	30.1010067	-90.259492	-37
936	Roth Seismic	121	30.2921656	-90.254318	-30
937	Roth Seismic	197	30.1355801	-90.247638	-35
938	Roth Seismic	161655	30.1005733	-90.244118	-36
939	Roth Seismic	187	30.1354708	-90.235152	-37
940	Roth Seismic	548	30.0535632	-90.23449	-52
941	Roth Seismic	143029	30.0529367	-90.233143	-50
942	Roth Seismic	144035	30.0657933	-90.232278	-47
943	Roth Seismic	145036	30.07885	-90.231083	-43
944	Roth Seismic	150039	30.09207	-90.230082	-38
945	Roth Seismic	152045	30.11839	-90.228213	-41
946	Roth Seismic	155254	30.160805	-90.2249	-47
947	Roth Seismic	91	30.36464047	-90.224572	-34
948	Roth Seismic	160057	30.1711767	-90.22389	-42
949	Roth Seismic	558	30.0518693	-90.223719	-55
950	Roth Seismic	183258	30.1666283	-90.219238	-44
951	Roth Seismic	101	30.3721266	-90.216492	-34
952	Roth Seismic	155747	30.0997667	-90.215195	-46
953	Roth Seismic	167	30.1355801	-90.210072	-44
954	Roth Seismic	111	30.3797457	-90.2082	-28
955	Roth Seismic	184259	30.1666283	-90.205317	-42
956	Roth Seismic	2	30.3803331	-90.202654	-30
957	Roth Seismic	154742	30.3993033	-90.199998	-45
958	Roth Seismic	11	30.3776557	-90.19217	-25
959	Roth Seismic	153739	30.0987883	-90.18446	-46
960	Roth Seismic	190121	30.166525	-90.17999	-42
961	Roth Seismic	152735	30.0982783	-90.16911	-48
962	Roth Seismic	191123	30.1666567	-90.166777	-42
963	Roth Seismic	127	30.1355357	-90.160348	-43
964	Roth Seismic	41	30.2697361	-90.157992	-23
965	Roth Seismic	192	30.2172145	-90.156011	-35
966	Roth Seismic	182	30.2278184	-90.154754	-33
967	Roth Seismic	170	30.2397132	-90.153894	-33
968	Roth Seismic	151733	30.0979267	-90.153875	-49
969	Roth Seismic	192128	30.16673	-90.15356	-40
970	Roth Seismic	162	30.2476259	-90.15317	-33
971	Roth Seismic	144037	30.2545283	-90.152638	-32
972	Roth Seismic	152	30.2572804	-90.152186	-30
973	Roth Seismic	142	30.2661665	-90.151155	-28
974	Roth Seismic	132	30.2751482	-90.150554	-26
975	Roth Seismic	92	30.3196469	-90.150464	-27
976	Roth Seismic	117	30.1356074	-90.148238	-41
977	Roth Seismic	92	30.3088723	-90.147664	-31
978	Roth Seismic	82	30.3154805	-90.146975	-31
979	Roth Seismic	31	30.2725766	-90.14638	-29
980	Roth Seismic	51	30.3672157	-90.145916	-24
981	Roth Seismic	12	30.3626327	-90.143887	-27
982	Roth Seismic	3	30.3691009	-90.143238	-22
983	Roth Seismic	150833	30.0989217	-90.14118	-50
984	Roth Seismic	193132	30.1666117	-90.140053	-40
985	Roth Seismic	143033	30.2533567	-90.138798	-34
986	Roth Seismic	108	30.1355494	-90.137563	-42
987	Roth Seismic	21	30.2708896	-90.134277	-27
988	Roth Seismic	61	30.3640841	-90.133977	-24
989	Roth Seismic	231106	30.1348083	-90.132595	-48
990	Roth Seismic	231606	30.14085	-90.131867	-45
991	Roth Seismic	193832	30.1667283	-90.130697	-40
992	Roth Seismic	232106	30.1469867	-90.13045	-45

993	Roth Seismic	232604	30.153	-90.12992	-42
994	Roth Seismic	233105	30.15904	-90.128755	-45
995	Roth Seismic	233604	30.1651233	-90.1276	-45
996	Roth Seismic	142146	30.2519017	-90.126685	-37
997	Roth Seismic	234105	30.17123	-90.126497	-47
998	Roth Seismic	195945	30.1663233	-90.126235	-45
999	Roth Seismic	234604	30.1772	-90.125425	-43
1000	Roth Seismic	152556	30.0928533	-90.124852	-51
1001	Roth Seismic	235105	30.1831333	-90.124445	-39
1002	Roth Seismic	235605	30.1890767	-90.12342	-37
1003	Roth Seismic	11	30.2695611	-90.123014	-29
1004	Roth Seismic	103	30.1949067	-90.122382	-37
1005	Roth Seismic	71	30.361294	-90.121846	-33
1006	Roth Seismic	603	30.2008317	-90.121203	-36
1007	Roth Seismic	1103	30.206725	-90.120203	-36
1008	Roth Seismic	153058	30.0921983	-90.11983	-43
1009	Roth Seismic	1604	30.212695	-90.119178	-35
1010	Roth Seismic	2103	30.2186367	-90.118117	-36
1011	Roth Seismic	2604	30.2246983	-90.117112	-36
1012	Roth Seismic	3104	30.23067	-90.116182	-37
1013	Roth Seismic	2	30.2666275	-90.115494	-29
1014	Roth Seismic	141242	30.2492867	-90.115407	-28
1015	Roth Seismic	3604	30.2366467	-90.115318	-34
1016	Roth Seismic	153600	30.0914767	-90.114485	-44
1017	Roth Seismic	4104	30.24271	-90.11414	-32
1018	Roth Seismic	200950	30.1667033	-90.112937	-41
1019	Roth Seismic	165628	30.2513183	-90.111813	-30
1020	Roth Seismic	170530	30.26151	-90.110983	-29
1021	Roth Seismic	164525	30.2498033	-90.110717	-30
1022	Roth Seismic	81	30.3583604	-90.109593	-35
1023	Roth Seismic	171531	30.2729333	-90.107687	-28
1024	Roth Seismic	175336	30.2848667	-90.105423	-28
1025	Roth Seismic	173541	30.29689	-90.103282	-30
1026	Roth Seismic	164821	30.24966	-90.102367	-31
1027	Roth Seismic	174545	30.3088617	-90.101003	-28
1028	Roth Seismic	201955	30.166635	-90.099505	-42
1029	Roth Seismic	175546	30.3209233	-90.098888	-26
1030	Roth Seismic	90	30.3558776	-90.098753	-32
1031	Roth Seismic	155106	30.0893317	-90.098052	-42
1032	Roth Seismic	180549	30.3329	-90.096777	-25
1033	Roth Seismic	181551	30.344865	-90.092482	-25
1034	Roth Seismic	182456	30.35551	-90.092482	-25
1035	Roth Seismic	182656	30.0578	-90.091993	-23
1036	Roth Seismic	2	30.2764391	-90.091274	-30
1037	Roth Seismic	11	30.2679048	-90.090605	-25
1038	Roth Seismic	21	30.2583152	-90.090127	-27
1039	Roth Seismic	31	30.2487119	-90.089977	-30
1040	Roth Seismic	163817	30.24907	-90.088532	-35
1041	Roth Seismic	160106	30.08787	-90.086083	-41
1042	Roth Seismic	183601	30.351295	-90.084908	-25
1043	Roth Seismic	145947	30.0596167	-90.080883	-52
1044	Roth Seismic	205712	30.0582333	-90.078787	-44
1045	Roth Seismic	210414	30.067205	-90.07799	-42
1046	Roth Seismic	184602	30.3431767	-90.076665	-24
1047	Roth Seismic	203857	30.1664533	-90.074493	-41
1048	Roth Seismic	151110	30.086125	-90.073435	-40
1049	Roth Seismic	17	30.041122	-90.073031	-48
1050	Roth Seismic	141903	30.1134133	-90.072503	-41
1051	Roth Seismic	142906	30.1250683	-90.071005	-42
1052	Roth Seismic	185609	30.33507	-90.0689293	-24
1053	Roth Seismic	145739	30.1581667	-90.0667	-40
1054	Roth Seismic	4	30.0439838	-90.066283	-48
1055	Roth Seismic	150743	30.169785	-90.065268	-38

1056	Roth Seismic	151749	30.18141	-90.063895	-39
1057	Roth Seismic	162518	30.084555	-90.063728	-41
1058	Roth Seismic	152750	30.192735	-90.062615	-36
1059	Roth Seismic	153751	30.204085	-90.061353	-34
1060	Roth Seismic	204904	30.1664633	-90.061257	-39
1061	Roth Seismic	190613	30.3274217	-90.06028	-25
1062	Roth Seismic	3	30.2265036	-90.060238	-32
1063	Roth Seismic	155800	30.22707	-90.05884	-42
1064	Roth Seismic	69	30.225199	-90.058373	-36
1065	Roth Seismic	12	30.2356116	-90.057636	-30
1066	Roth Seismic	14	30.0481844	-90.056379	-47
1067	Roth Seismic	42	30.2674335	-90.054733	-32
1068	Roth Seismic	143934	30.0655	-90.053917	-46
1069	Roth Seismic	52	30.2779383	-90.053831	-32
1070	Roth Seismic	191616	30.319265	-90.052062	-23
1071	Roth Seismic	82	30.3092923	-90.051393	-30
1072	Roth Seismic	163122	30.0828017	-90.051147	-43
1073	Roth Seismic	101	30.3291511	-90.049528	-26
1074	Roth Seismic	61	30.2290991	-90.049515	-37
1075	Roth Seismic	205910	30.1686333	-90.04796	-39
1076	Roth Seismic	24	30.0526957	-90.046762	-48
1077	Roth Seismic	143133	30.0677833	-90.0433	-48
1078	Roth Seismic	193102	30.3078933	-90.040182	-24
1079	Roth Seismic	51	30.2340783	-90.038586	-38
1080	Roth Seismic	164127	30.0810183	-90.037095	-44
1081	Roth Seismic	152533	30.239685	-90.036513	-37
1082	Roth Seismic	210953	30.1672167	-90.034127	-40
1083	Roth Seismic	41	30.2392385	-90.02761	-34
1084	Roth Seismic	153536	30.236345	-90.022777	-34
1085	Roth Seismic	31	30.243883	-90.016477	-36
1086	Roth Seismic	54	30.0642388	-90.015145	-45
1087	Roth Seismic	140922	30.0746333	-90.015017	-50
1088	Roth Seismic	2	30.1351361	-90.01408	-42
1089	Roth Seismic	11	30.1347844	-90.005487	-42
1090	Roth Seismic	64	30.0666327	-90.004565	-42
1091	Roth Seismic	170455	30.0785817	-90.004477	-48
1092	Roth Seismic	135901	30.07815	-90.00265	-49
1093	Roth Seismic	155538	30.2299417	-89.995335	-41
1094	Roth Seismic	135026	30.0802167	-89.993633	-44
1095	Roth Seismic	2	30.0724862	-89.9918	-42
1096	Roth Seismic	171459	30.0775733	-89.990858	-43
1097	Roth Seismic	2	30.2566486	-89.988986	-20
1098	Roth Seismic	10	30.0779132	-89.986035	-41
1099	Roth Seismic	12	30.0792959	-89.984553	-41
1100	Roth Seismic	160541	30.2271983	-89.981495	-34
1101	Roth Seismic	172500	30.0765583	-89.977963	-44
1102	Roth Seismic	21	30.0855626	-89.977886	-41
1103	Roth Seismic	41	30.1387493	-89.971965	-39
1104	Roth Seismic	31	30.0923552	-89.970243	-41
1105	Roth Seismic	173504	30.07515	-89.965152	-49
1106	Roth Seismic	41	30.0993118	-89.962546	-40
1107	Roth Seismic	161943	30.22355	-89.961882	-36
1108	Roth Seismic	51	30.1397226	-89.959786	-36
1109	Roth Seismic	225159	30.1150533	-89.959427	-41
1110	Roth Seismic	2241557	30.1267917	-89.958742	-41
1111	Roth Seismic	230308	30.1022033	-89.95783	-41
1112	Roth Seismic	223157	30.13855	-89.957767	-40
1113	Roth Seismic	222155	30.150495	-89.957	-39
1114	Roth Seismic	221154	30.1623433	-89.956593	-40
1115	Roth Seismic	231411	30.0917967	-89.956487	-41
1116	Roth Seismic	220854	30.1659017	-89.956405	-36
1117	Roth Seismic	232216	30.0818817	-89.955527	-45
1118	Roth Seismic	213444	30.206305	-89.955283	-37

1119	Roth Seismic	232917	30.073125	-89.954218	-44
1120	Roth Seismic	174406	30.0740567	-89.953298	-43
1121	Roth Seismic	221204	30.16669	-89.953158	-39
1122	Roth Seismic	162544	30.2220133	-89.953092	-35
1123	Roth Seismic	54	30.1085701	-89.952464	-42
1124	Roth Seismic	61	30.1405627	-89.947663	-34
1125	Roth Seismic	61	30.1136415	-89.946911	-35
1126	Roth Seismic	222111	30.1665517	-89.940618	-42
1127	Roth Seismic	71	30.1207552	-89.939043	-35
1128	Roth Seismic	163548	30.21919	-89.938952	-35
1129	Roth Seismic	71	30.1418777	-89.935655	-32
1130	Roth Seismic	81	30.1281284	-89.931277	-34
1131	Roth Seismic	164550	30.2164733	-89.924915	-34
1132	Roth Seismic	81	30.1430557	-89.923744	-31
1133	Roth Seismic	91	30.1354776	-89.923429	-35
1134	Roth Seismic	42	30.1790816	-89.917357	-32
1135	Roth Seismic	101	30.1429738	-89.915219	-30
1136	Roth Seismic	165554	30.21453	-89.911083	-36
1137	Roth Seismic	91	30.1445242	-89.910875	-30
1138	Roth Seismic	111	30.1504904	-89.90688	-25
1139	Roth Seismic	2	30.2504195	-89.903854	-30
1140	Roth Seismic	119	30.1578363	-89.90354	-26
1141	Roth Seismic	97	30.2476635	-89.90285	-21
1142	Roth Seismic	22	30.1630306	-89.90285	-30
1143	Roth Seismic	11	30.1713601	-89.900494	-29
1144	Roth Seismic	225159	30.167295	-89.900262	-40
1145	Roth Seismic	91	30.244357	-89.900179	-24
1146	Roth Seismic	101	30.1456614	-89.900084	-29
1147	Roth Seismic	71	30.2272003	-89.898909	-21
1148	Roth Seismic	81	30.236421	-89.898847	-25
1149	Roth Seismic	21	30.1807072	-89.898574	-24
1150	Roth Seismic	61	30.21786	-89.898253	-25
1151	Roth Seismic	170555	30.2115017	-89.898185	-37
1152	Roth Seismic	51	30.2086597	-89.897345	-28
1153	Roth Seismic	31	30.190085	-89.897338	-25
1154	Roth Seismic	41	30.1994185	-89.896942	-26
1155	Roth Seismic	12	30.155179	-89.895555	-34
1156	Roth Seismic	11	30.249412	-89.895159	-30
1157	Roth Seismic	3	30.1490321	-89.887926	-34
1158	Roth Seismic	230206	30.167155	-89.886147	-40
1159	Roth Seismic	21	30.2457408	-89.886102	-27
1160	Roth Seismic	171601	30.2089883	-89.884928	-37
1161	Roth Seismic	191142	30.1495367	-89.881065	-38
1162	Roth Seismic	31	30.2402186	-89.878077	-30
1163	Roth Seismic	190442	30.15719	-89.8751	-37
1164	Roth Seismic	231208	30.166795	-89.871992	-39
1165	Roth Seismic	172603	30.2065183	-89.871925	-38
1166	Roth Seismic	41	30.2352121	-89.869443	-30
1167	Roth Seismic	185439	30.1681733	-89.866723	-38
1168	Roth Seismic	51	30.2290888	-89.861486	-32
1169	Roth Seismic	173606	30.2038467	-89.859338	-36
1170	Roth Seismic	184436	30.1789883	-89.858212	-36
1171	Roth Seismic	61	30.2223918	-89.854096	-30
1172	Roth Seismic	183432	30.189525	-89.849963	-35
1173	Roth Seismic	71	30.2153499	-89.846945	-33
1174	Roth Seismic	174609	30.200855	-89.846713	-36
1175	Roth Seismic	182431	30.1997833	-89.841313	-35
1176	Roth Seismic	175110	30.1994383	-89.840333	-35
1177	Roth Seismic	80	30.2091856	-89.840244	-34
1178	Roth Seismic	2254	30.1253667	-89.8339	-31
1179	Roth Seismic	181425	30.210085	-89.833183	-37
1180	Roth Seismic	193747	30.20282	-89.830302	-41
1181	Roth Seismic	2039	30.1250667	-89.830267	-41

1182	Roth Seismic	2049	30.11615	-89.829517	-33
1183	Roth Seismic	2059	30.1077	-89.828033	-44
1184	Roth Seismic	180519	30.217405	-89.826375	-30
1185	Roth Seismic	2303	30.1275167	-89.823983	-33
1186	Roth Seismic	2029	30.1321833	-89.823	-41
1187	Roth Seismic	194550	30.2006017	-89.819517	-38
1188	Roth Seismic	2313	30.1314333	-89.81255	-42
1189	Roth Seismic	2009	30.1479833	-89.810033	-36
1190	Roth Seismic	195553	30.19646	-89.807332	-27
1191	Roth Seismic	1959	30.1562833	-89.804083	-39
1192	Roth Seismic	2323	30.1345667	-89.801233	-44
1193	Roth Seismic	99	30.1776	-89.799667	-54
1194	Roth Seismic	2	30.1954843	-89.797897	-25
1195	Roth Seismic	1949	30.1643333	-89.7978	-42
1196	Roth Seismic	11	30.1883604	-89.797494	-35
1197	Roth Seismic	41	30.164523	-89.797303	-35
1198	Roth Seismic	31	30.1734125	-89.797146	-39
1199	Roth Seismic	21	30.180574	-89.797119	-27
1200	Roth Seismic	200534	30.19283	-89.796377	-36
1201	Roth Seismic	1782	30.17525	-89.793883	-53
1202	Roth Seismic	2333	30.1373833	-89.790333	-50
1203	Roth Seismic	201539	30.18991583	-89.78411	-38
1204	Roth Seismic	2343	30.1434667	-89.781283	-38
1205	Roth Seismic	202040	30.1869817	-89.777748	-39
1206	Roth Seismic	9702	30.1527667	-89.772833	-42
1207	Roth Seismic	202442	30.1850817	-89.772802	-33
1208	Roth Seismic	2353	30.1483833	-89.771683	-32
1209	Roth Seismic	11385	30.1480167	-89.767767	-33
1210	Roth Seismic	203043	30.1822033	-89.765567	-39
1211	Roth Seismic	12870	30.1475667	-89.762033	-37
1212	Roth Seismic	203646	30.17875	-89.758723	-26
1213	Roth Seismic	14157	30.14335	-89.757	-41
1214	Roth Geotech	51	30.0555	-90.37	-72
1215	Roth Geotech	117-3	29.96	-90.0267	-66
1216	Roth Geotech	13-52	30.1092	-89.9212	-35
1217	Roth Geotech	7	30.2172	-89.7855	-4
1218	Roth Geotech	6	30.2158	-89.7892	-4
1219	Roth Geotech	5	30.215	-89.7895	-4
1220	Roth Geotech	4	30.2142	-89.7905	-4
1221	Roth Geotech	27	30.3583	-90.4167	-4
1222	Roth Geotech	4P	30.3492	-90.4143	-4
1223	Roth Geotech	19	30.2312	-89.7722	-5
1224	Roth Geotech	17	30.2305	-89.7728	-5
1225	Roth Geotech	18	30.23	-89.7733	-5
1226	Roth Geotech	3	30.2128	-89.7917	-5
1227	Roth Geotech	7P	30.345	-90.413	-5
1228	Roth Geotech	10P	30.3412	-90.412	-5
1229	Roth Geotech	11P	30.34	-90.4117	-5
1230	Roth Geotech	8	30.22	-89.7833	-6
1231	Roth Geotech	3P	30.35	-90.4147	-6
1232	Roth Geotech	5P	30.3477	-90.4138	-6
1233	Roth Geotech	1F	30.3358	-90.4112	-6
1234	Roth Geotech	15	30.2288	-89.7742	-7
1235	Roth Geotech	13	30.2272	-89.7762	-7
1236	Roth Geotech	2	30.2117	-89.7925	-7
1237	Roth Geotech	2P	30.3517	-90.415	-7
1238	Roth Geotech	6P	30.3465	-90.4133	-7
1239	Roth Geotech	9P	30.3423	-90.4122	-7
1240	Roth Geotech	12P	30.3382	-90.4108	-7
1241	Roth Geotech	13P	30.3372	-90.4107	-7
1242	Roth Geotech	15P	30.3342	-90.41	-7
1243	Roth Geotech	14	30.2278	-89.775	-8
1244	Roth Geotech	9	30.2212	-89.7833	-8

1245	Roth Geotech	3	30.395	-90.4283	-8
1246	Roth Geotech	21	30.3683	-90.42	-8
1247	Roth Geotech	29	30.3555	-90.4158	-8
1248	Roth Geotech	1P	30.3555	-90.4155	-8
1249	Roth Geotech	12	30.225	-89.7783	-9
1250	Roth Geotech	11	30.2242	-89.78	-9
1251	Roth Geotech	13	30.3805	-90.4242	-9
1252	Roth Geotech	23	30.3642	-90.4183	-9
1253	Roth Geotech	14P	30.335	-90.41	-9
1254	Roth Geotech	3F	30.3325	-90.4105	-9
1255	Roth Geotech	PF-7	30.415	-90.4333	-10
1256	Roth Geotech	10	30.2222	-89.7817	-11
1257	Roth Geotech	17	30.3738	-90.4225	-11
1258	Roth Geotech	21P	30.3263	-90.4087	-11
1259	Roth Geotech	5	30.3925	-90.4275	-12
1260	Roth Geotech	PF-16	30.3435	-90.4125	-12
1261	Roth Geotech	PMH-3	30.3392	-90.4112	-12
1262	Roth Geotech	70	30.2113	-89.7933	-13
1263	Roth Geotech	67	30.2092	-89.7962	-13
1264	Roth Geotech	PF-8	30.4125	-90.4333	-13
1265	Roth Geotech	23P	30.3232	-90.4083	-13
1266	Roth Geotech	112-45	30.3617	-90.0945	-13
1267	Roth Geotech	66	30.2083	-89.7972	-14
1268	Roth Geotech	MAB-9	30.1142	-90.5788	-14
1269	Roth Geotech	PF-9	30.4112	-90.433	-14
1270	Roth Geotech	PF-10	30.41	-90.4325	-14
1271	Roth Geotech	PF-12	30.4017	-90.43	-14
1272	Roth Geotech	7	30.3895	-90.4267	-14
1273	Roth Geotech	9	30.3867	-90.4258	-14
1274	Roth Geotech	11	30.3833	-90.425	-14
1275	Roth Geotech	PF-14	30.3712	-90.4212	-14
1276	Roth Geotech	PF-15	30.3575	-90.4167	-14
1277	Roth Geotech	65	30.2075	-89.7983	-15
1278	Roth Geotech	64	30.2067	-89.7988	-15
1279	Roth Geotech	63	30.2058	-89.7995	-15
1280	Roth Geotech	1	30.3983	-90.4295	-15
1281	Roth Geotech	PF-13	30.385	-90.425	-15
1282	Roth Geotech	22P	30.3247	-90.4085	-15
1283	Roth Geotech	RP-1	30.1675	-89.7367	-15
1284	Roth Geotech	69	30.2112	-89.7938	-16
1285	Roth Geotech	57	30.2017	-89.8038	-16
1286	Roth Geotech	34	30.1833	-89.8233	-16
1287	Roth Geotech	MB-8	30.1145	-90.5817	-16
1288	Roth Geotech	15	30.3767	-90.4228	-16
1289	Roth Geotech	25P	30.3208	-90.4077	-16
1290	Roth Geotech	26P	30.32	-90.4075	-16
1291	Roth Geotech	5R2	30.1567	-89.7412	-16
1292	Roth Geotech	B-10U	30.1592	-89.7408	-16
1293	Roth Geotech	6R	30.1608	-89.7408	-16
1294	Roth Geotech	110-18	30.28	-90.1067	-16
1295	Roth Geotech	68	30.21	-89.795	-17
1296	Roth Geotech	62	30.205	-89.8	-17
1297	Roth Geotech	58	30.2022	-89.803	-17
1298	Roth Geotech	36	30.1845	-89.8222	-17
1299	Roth Geotech	31	30.1805	-89.8262	-17
1300	Roth Geotech	30	30.18	-89.8267	-17
1301	Roth Geotech	10	30.1633	-89.8445	-17
1302	Roth Geotech	9	30.1625	-89.8458	-17
1303	Roth Geotech	98	30.3558	-90.0865	-17
1304	Roth Geotech	B-9U	30.1562	-89.7417	-17
1305	Roth Geotech	111-19	30.325	-90.1005	-17
1306	Roth Geotech	112-44	30.3567	-90.095	-17
1307	Roth Geotech	32	30.1815	-89.825	-18

1308	Roth Geotech	20	30.1717	-89.8358	-18
1309	Roth Geotech	61	30.2045	-89.8005	-18
1310	Roth Geotech	38	30.1867	-89.82	-18
1311	Roth Geotech	29	30.1788	-89.8278	-18
1312	Roth Geotech	28	30.1782	-89.8288	-18
1313	Roth Geotech	19	30.1708	-89.8367	-18
1314	Roth Geotech	17	30.1695	-89.8383	-18
1315	Roth Geotech	PMH-2	30.3783	-90.4233	-18
1316	Roth Geotech	20P	30.3278	-90.4092	-18
1317	Roth Geotech	B-7U	30.1545	-89.7425	-18
1318	Roth Geotech	B-12U	30.1625	-89.7408	-18
1319	Roth Geotech	112-40	30.3342	-90.0975	-18
1320	Roth Geotech	112-42	30.3458	-90.0962	-18
1321	Roth Geotech	60	30.2038	-89.8012	-19
1322	Roth Geotech	59	30.2033	-89.8017	-19
1323	Roth Geotech	56	30.2008	-89.8045	-19
1324	Roth Geotech	55	30.2	-89.805	-19
1325	Roth Geotech	42	30.19	-89.8167	-19
1326	Roth Geotech	41	30.1888	-89.8175	-19
1327	Roth Geotech	40	30.1882	-89.8183	-19
1328	Roth Geotech	37	30.1858	-89.8205	-19
1329	Roth Geotech	33	30.1822	-89.8245	-19
1330	Roth Geotech	23	30.1745	-89.8333	-19
1331	Roth Geotech	22	30.1738	-89.8342	-19
1332	Roth Geotech	21	30.1728	-89.835	-19
1333	Roth Geotech	18	30.1705	-89.8375	-19
1334	Roth Geotech	65	30.1392	-89.865	-19
1335	Roth Geotech	MAC-4	30.0825	-90.56	-19
1336	Roth Geotech	PMH-1	30.4047	-90.4308	-19
1337	Roth Geotech	18P	30.3303	-90.4097	-19
1338	Roth Geotech	24P	30.322	-90.4078	-19
1339	Roth Geotech	B-6U	30.1525	-89.7417	-19
1340	Roth Geotech	111-15	30.3362	-90.0972	-19
1341	Roth Geotech	54	30.1992	-89.8067	-20
1342	Roth Geotech	52	30.1973	-89.8078	-20
1343	Roth Geotech	49	30.1947	-89.8108	-20
1344	Roth Geotech	48	30.1942	-89.8117	-20
1345	Roth Geotech	35	30.1838	-89.8228	-20
1346	Roth Geotech	27	30.1772	-89.83	-20
1347	Roth Geotech	26	30.1767	-89.8305	-20
1348	Roth Geotech	25	30.1758	-89.8317	-20
1349	Roth Geotech	16	30.1683	-89.8388	-20
1350	Roth Geotech	14	30.1667	-89.8408	-20
1351	Roth Geotech	13	30.1662	-89.8415	-20
1352	Roth Geotech	11	30.165	-89.8433	-20
1353	Roth Geotech	8	30.1617	-89.8475	-20
1354	Roth Geotech	7	30.1608	-89.8483	-20
1355	Roth Geotech	5	30.1583	-89.8508	-20
1356	Roth Geotech	PF-17	30.3293	-90.4092	-20
1357	Roth Geotech	112-41	30.3392	-90.0972	-20
1358	Roth Geotech	111-13	30.3408	-90.0968	-20
1359	Roth Geotech	53	30.1983	-89.8075	-21
1360	Roth Geotech	43	30.1905	-89.8158	-21
1361	Roth Geotech	39	30.1872	-89.8195	-21
1362	Roth Geotech	24	30.175	-89.8325	-21
1363	Roth Geotech	6	30.16	-89.85	-21
1364	Roth Geotech	19-R	30.1383	-89.755	-21
1365	Roth Geotech	112-34	30.2817	-90.1075	-21
1366	Roth Geotech	111-29	30.2892	-90.1065	-21
1367	Roth Geotech	112-39	30.267	-90.1	-21
1368	Roth Geotech	13-39	30.1378	-89.8962	-21
1369	Roth Geotech	50	30.1955	-89.81	-22
1370	Roth Geotech	45	30.1917	-89.815	-22

1371	Roth Geotech	44	30.1912	-89.8155	-22
1372	Roth Geotech	15	30.1675	-89.84	-22
1373	Roth Geotech	12	30.1657	-89.8425	-22
1374	Roth Geotech	2	30.1558	-89.8538	-22
1375	Roth Geotech	1	30.1545	-89.855	-22
1376	Roth Geotech	92	30.3353	-90.1012	-22
1377	Roth Geotech	MAC-5	30.0783	-90.5628	-22
1378	Roth Geotech	B-4U	30.1458	-89.7462	-22
1379	Roth Geotech	4-R	30.1483	-89.7433	-22
1380	Roth Geotech	111-30	30.2853	-90.1067	-22
1381	Roth Geotech	112-35	30.2917	-90.1058	-22
1382	Roth Geotech	112-37	30.3147	-90.1017	-22
1383	Roth Geotech	111-20	30.3233	-90.012	-22
1384	Roth Geotech	111-14	30.3375	-90.0967	-22
1385	Roth Geotech	111-12	30.3433	-90.0965	-22
1386	Roth Geotech	112-43	30.3508	-90.0955	-22
1387	Roth Geotech	51	30.1965	-89.8092	-23
1388	Roth Geotech	46	30.1925	-89.8138	-23
1389	Roth Geotech	3	30.1567	-89.8528	-23
1390	Roth Geotech	91	30.3317	-90.1017	-23
1391	Roth Geotech	MAB-10	30.1133	-90.5633	-23
1392	Roth Geotech	17P	30.3317	-90.41	-23
1393	Roth Geotech	PF-19	30.3158	-90.4067	-23
1394	Roth Geotech	110-19	30.295	-90.105	-23
1395	Roth Geotech	111-28	30.2983	-90.1048	-23
1396	Roth Geotech	111-27	30.3017	-90.1042	-23
1397	Roth Geotech	112-38	30.3217	-90.1015	-23
1398	Roth Geotech	111-16	30.3325	-90.0988	-23
1399	Roth Geotech	4	30.1575	-89.8517	-24
1400	Roth Geotech	62	30.1275	-89.8733	-24
1401	Roth Geotech	B-3U	30.1408	-89.7508	-24
1402	Roth Geotech	20-SP	30.1383	-89.875	-24
1403	Roth Geotech	95	30.345	-90.0987	-24
1404	Roth Geotech	94	30.3417	-90.1	-24
1405	Roth Geotech	MAC-11	30.0578	-90.57	-24
1406	Roth Geotech	MAC-12	30.0458	-90.58	-24
1407	Roth Geotech	PMH-5	30.3108	-90.4058	-24
1408	Roth Geotech	B-3	30.2872	-90.4012	-24
1409	Roth Geotech	B-4	30.2862	-90.4008	-24
1410	Roth Geotech	PMH-7	30.275	-90.3983	-24
1411	Roth Geotech	C-64	30.2683	-90.3982	-24
1412	Roth Geotech	55	30.1245	-90.1292	-24
1413	Roth Geotech	54	30.2113	-90.13	-24
1414	Roth Geotech	112-31	30.2495	-90.1138	-24
1415	Roth Geotech	111-18	30.3283	-90.0995	-24
1416	Roth Geotech	13-38	30.14	-89.8945	-24
1417	Roth Geotech	F-11	30.2467	-90.4025	-25
1418	Roth Geotech	47	30.1933	-89.8125	-25
1419	Roth Geotech	64	30.1325	-89.87	-25
1420	Roth Geotech	63	30.13	-89.8717	-25
1421	Roth Geotech	18-R	30.1342	-89.7608	-25
1422	Roth Geotech	8-SP	30.1362	-89.8725	-25
1423	Roth Geotech	19-SP	30.1333	-89.8733	-25
1424	Roth Geotech	18-SP	30.1292	-89.8708	-25
1425	Roth Geotech	14-SP	30.11	-89.8625	-25
1426	Roth Geotech	MAB-7	30.1145	-90.5842	-25
1427	Roth Geotech	MAC-6	30.075	-90.565	-25
1428	Roth Geotech	0	30.0558	-90.5742	-25
1429	Roth Geotech	B-1	30.2895	-90.4015	-25
1430	Roth Geotech	B-12	30.2797	-90.3997	-25
1431	Roth Geotech	F-1	30.2703	-90.3978	-25
1432	Roth Geotech	F-2	30.2667	-90.3978	-25
1433	Roth Geotech	F-4	30.2628	-90.3983	-25

1434	Roth Geotech	C-62	30.2595	-90.3992	-25
1435	Roth Geotech	F-6	30.2583	-90.3997	-25
1436	Roth Geotech	C-60	30.2533	-90.4012	-25
1437	Roth Geotech	56	30.2183	-90.1283	-25
1438	Roth Geotech	110-20	30.31	-90.1032	-25
1439	Roth Geotech	13-41	30.1333	-89.9	-25
1440	Roth Geotech	13-40	30.1358	-89.8983	-25
1441	Roth Geotech	13-37	30.1422	-89.8925	-25
1442	Roth Geotech	13-36	30.1445	-89.8905	-25
1443	Roth Geotech	13-35	30.1467	-89.8883	-25
1444	Roth Geotech	F-10	30.2495	-90.4017	-26
1445	Roth Geotech	C-56	30.2433	-90.405	-26
1446	Roth Geotech	B-2U	30.1367	-89.7575	-26
1447	Roth Geotech	21-Sp	30.1433	-89.8783	-26
1448	Roth Geotech	93	30.3383	-90.1	-26
1449	Roth Geotech	MAB-12	30.1117	-90.5508	-26
1450	Roth Geotech	MAC-7	30.0717	-90.565	-26
1451	Roth Geotech	B-11	30.2802	-90.4	-26
1452	Roth Geotech	PF-23	30.2638	-90.3978	-26
1453	Roth Geotech	112-30	30.2425	-90.115	-26
1454	Roth Geotech	111-35	30.245	-90.1153	-26
1455	Roth Geotech	111-22	30.3192	-90.1017	-26
1456	Roth Geotech	F-12	30.245	-90.4033	-27
1457	Roth Geotech	F-14	30.24	-90.405	-27
1458	Roth Geotech	C-58	30.2322	-90.41	-27
1459	Roth Geotech	9-SP	30.0825	-89.8575	-27
1460	Roth Geotech	99	30.36	-90.095	-27
1461	Roth Geotech	MAC-8	30.0642	-90.5662	-27
1462	Roth Geotech	PMH-4	30.3258	-90.4087	-27
1463	Roth Geotech	B-10	30.2815	-90.4	-27
1464	Roth Geotech	F-7	30.2567	-90.4	-27
1465	Roth Geotech	F-8	30.2545	-90.4033	-27
1466	Roth Geotech	F-9	30.2517	-90.4017	-27
1467	Roth Geotech	20-R	30.1417	-89.75	-27
1468	Roth Geotech	53-66	30.2492	-90.1208	-27
1469	Roth Geotech	111-36	30.24	-90.1158	-27
1470	Roth Geotech	112-36	30.3042	-90.1033	-27
1471	Roth Geotech	111-17	30.33	-90.0992	-27
1472	Roth Geotech	13-42	30.1312	-89.9022	-27
1473	Roth Geotech	96	30.35	-90.0983	-28
1474	Roth Geotech	B-9	30.2825	-90.4	-28
1475	Roth Geotech	F-13	30.2417	-90.405	-28
1476	Roth Geotech	F-18	30.23	-90.4092	-28
1477	Roth Geotech	F-19	30.2283	-90.41	-28
1478	Roth Geotech	C-52	30.2275	-90.4117	-28
1479	Roth Geotech	53	30.1075	-89.8912	-28
1480	Roth Geotech	B-4U	30.1317	-89.7617	-28
1481	Roth Geotech	16-SP	30.1208	-89.865	-28
1482	Roth Geotech	5-USP	30.115	-89.8642	-28
1483	Roth Geotech	13-SP	30.1042	-89.8617	-28
1484	Roth Geotech	12-SP	30.0983	-89.8608	-28
1485	Roth Geotech	4-USP	30.0892	-89.8588	-28
1486	Roth Geotech	MAC-3	30.0895	-90.5533	-28
1487	Roth Geotech	MAC-18	30.0042	-90.6108	-28
1488	Roth Geotech	57	30.2217	-90.1275	-28
1489	Roth Geotech	53	30.207	-90.1308	-28
1490	Roth Geotech	31	30.1322	-90.1492	-28
1491	Roth Geotech	112-29	30.2375	-90.1158	-28
1492	Roth Geotech	111-23	30.3167	-90.1015	-28
1493	Roth Geotech	13-34	30.149	-89.8867	-28
1494	Roth Geotech	13-33	30.1512	-89.885	-28
1495	Roth Geotech	28-22	30.1173	-89.8905	-28
1496	Roth Geotech	F-22	30.22	-90.4133	-29

1497	Roth Geotech	66	30.1417	-89.86622	-29
1498	Roth Geotech	61	30.1242	-89.8758	-29
1499	Roth Geotech	50	30.1008	-89.8975	-29
1500	Roth Geotech	49	30.0983	-89.8995	-29
1501	Roth Geotech	47	30.095	-89.9033	-29
1502	Roth Geotech	G-24	30.1267	-89.7633	-29
1503	Roth Geotech	11-SP	30.0933	-89.86	-29
1504	Roth Geotech	10-SP	30.0883	-89.8583	-29
1505	Roth Geotech	MAB-15	30.1105	-90.5372	-29
1506	Roth Geotech	MAC-9	30.0612	-90.5717	-29
1507	Roth Geotech	B-2	30.2878	-90.4013	-29
1508	Roth Geotech	111-40	30.2117	-90.12	-29
1509	Roth Geotech	112-27	30.2175	-90.1183	-29
1510	Roth Geotech	111-38	30.2258	-90.1175	-29
1511	Roth Geotech	C-54	30.2388	-90.4072	-29
1512	Roth Geotech	F-23	30.2195	-90.4138	-30
1513	Roth Geotech	48	30.0967	-89.9017	-30
1514	Roth Geotech	G-3	30.12	-89.7633	-30
1515	Roth Geotech	G-4	30.1033	-89.765	-30
1516	Roth Geotech	G-19	30.0767	-89.79	-30
1517	Roth Geotech	15-SP	30.1145	-89.8642	-30
1518	Roth Geotech	100	30.3633	-90.0942	-30
1519	Roth Geotech	MAA-19	30.0133	-90.5417	-30
1520	Roth Geotech	MAB-13	30.1117	-90.5467	-30
1521	Roth Geotech	MAC-10	30.0583	-90.5683	-30
1522	Roth Geotech	MAC-17	30.0067	-90.6033	-30
1523	Roth Geotech	F-3	30.265	-90.3983	-30
1524	Roth Geotech	111-46	30.1678	-90.1283	-30
1525	Roth Geotech	112-25	30.1988	-90.1217	-30
1526	Roth Geotech	111-39	30.2162	-90.1192	-30
1527	Roth Geotech	110-14	30.2212	-90.1183	-30
1528	Roth Geotech	F-16	30.235	-90.4075	-31
1529	Roth Geotech	F-17	30.2328	-90.4083	-31
1530	Roth Geotech	C-48	30.2222	-90.4133	-31
1531	Roth Geotech	C-44	30.2142	-90.4167	-31
1532	Roth Geotech	C-42	30.21	-90.42	-31
1533	Roth Geotech	57	30.1158	-89.8833	-31
1534	Roth Geotech	56	30.1142	-89.885	-31
1535	Roth Geotech	90	30.3283	-90.1025	-31
1536	Roth Geotech	MAA-14	30.0217	-90.5733	-31
1537	Roth Geotech	MAB-14	30.1108	-90.5417	-31
1538	Roth Geotech	MAB-16	30.1103	-90.533	-31
1539	Roth Geotech	MAB-17	30.1095	-90.528	-31
1540	Roth Geotech	MAC-15	30.0158	-90.5908	-31
1541	Roth Geotech	58	30.225	-90.1267	-31
1542	Roth Geotech	112-24	30.1888	-90.1238	-31
1543	Roth Geotech	111-42	30.1972	-90.1225	-31
1544	Roth Geotech	28-19	30.0983	-89.9075	-31
1545	Roth Geotech	28-10	30.105	-89.9017	-31
1546	Roth Geotech	28-20A	30.1078	-89.8988	-31
1547	Roth Geotech	28-21A	30.1138	-89.8933	-31
1548	Roth Geotech	F-20	30.225	-90.4108	-32
1549	Roth Geotech	F-24	30.2155	-90.4156	-32
1550	Roth Geotech	52	30.1067	-89.8933	-32
1551	Roth Geotech	51	30.1033	-89.8955	-32
1552	Roth Geotech	46	30.0928	-89.905	-32
1553	Roth Geotech	9-USP	30.1467	-89.88	-32
1554	Roth Geotech	97	30.3533	-90.0968	-32
1555	Roth Geotech	MAA-15	30.0183	-90.5703	-32
1556	Roth Geotech	MAB-19	30.1083	-90.5183	-32
1557	Roth Geotech	111-49	30.1433	-90.1325	-32
1558	Roth Geotech	111-45	30.1728	-90.1275	-32
1559	Roth Geotech	111-14	30.1825	-90.1258	-32

1560	Roth Geotech	111-43	30.1867	-90.125	-32
1561	Roth Geotech	112-26	30.2095	-90.12	-32
1562	Roth Geotech	112-28	30.2278	-90.1172	-32
1563	Roth Geotech	28-21	30.1112	-89.8958	-32
1564	Roth Geotech	F-15	30.2375	-90.4067	-33
1565	Roth Geotech	F-21	30.2233	-90.4117	-33
1566	Roth Geotech	F-26	30.2122	-90.4172	-33
1567	Roth Geotech	C-28	30.205	-90.4242	-33
1568	Roth Geotech	58	30.1183	-89.8817	-33
1569	Roth Geotech	45	30.0908	-89.9067	-33
1570	Roth Geotech	MAA-20	30.0117	-90.5317	-33
1571	Roth Geotech	MAB-21	30.1075	-90.5095	-33
1572	Roth Geotech	112-21	30.1712	-90.1272	-33
1573	Roth Geotech	112-23	30.18	-90.1258	-33
1574	Roth Geotech	111-41	30.2025	-90.1217	-33
1575	Roth Geotech	110-13	30.2067	-90.1212	-33
1576	Roth Geotech	13-49	30.1158	-89.9158	-33
1577	Roth Geotech	13-48	30.1178	-89.9142	-33
1578	Roth Geotech	13-47	30.12	-89.9117	-33
1579	Roth Geotech	13-46	30.1225	-89.9095	-33
1580	Roth Geotech	28-18	30.0917	-89.9137	-33
1581	Roth Geotech	F-27	30.2075	-90.4217	-34
1582	Roth Geotech	F-30	30.2	-90.4283	-34
1583	Roth Geotech	F-32	30.195	-90.4333	-34
1584	Roth Geotech	43	30.0867	-89.91	-34
1585	Roth Geotech	39	30.0783	-89.9192	-34
1586	Roth Geotech	G-5	30.0883	-89.7783	-34
1587	Roth Geotech	MAB-18	30.1092	-90.5233	-34
1588	Roth Geotech	59	30.2287	-90.1263	-34
1589	Roth Geotech	40	30.1592	-90.1425	-34
1590	Roth Geotech	110-15	30.2358	-90.1167	-34
1591	Roth Geotech	13-45	30.1245	-89.9075	-34
1592	Roth Geotech	20-1A	30.0667	-89.9317	-34
1593	Roth Geotech	MAB-11	30.1122	-90.5558	-35
1594	Roth Geotech	30-19I	30.1067	-89.96	-35
1595	Roth Geotech	C-39	30.2017	-90.4283	-35
1596	Roth Geotech	F-37	30.1838	-90.4412	-35
1597	Roth Geotech	59	30.1208	-89.88	-35
1598	Roth Geotech	55	30.1117	-89.8867	-35
1599	Roth Geotech	41	30.0808	-89.915	-35
1600	Roth Geotech	40	30.0792	-89.9167	-35
1601	Roth Geotech	CMB-1	30.0692	-89.8033	-35
1602	Roth Geotech	CMB-3	30.0667	-89.8067	-35
1603	Roth Geotech	MAA-23	30.005	-90.52	-35
1604	Roth Geotech	MAC-14	30.0142	-90.5933	-35
1605	Roth Geotech	65	30.2467	-90.1217	-35
1606	Roth Geotech	112-22	30.175	-90.1267	-35
1607	Roth Geotech	110-12	30.1928	-90.1233	-35
1608	Roth Geotech	NOHA-319	30.0758	-89.945	-35
1609	Roth Geotech	13-58	30.0958	-89.9333	-35
1610	Roth Geotech	13-53	30.1072	-89.9233	-35
1611	Roth Geotech	13-50	30.1138	-89.9175	-35
1612	Roth Geotech	28-17	30.085	-89.9197	-35
1613	Roth Geotech	C-46	30.2175	-90.4158	-36
1614	Roth Geotech	C-40	30.2067	-90.4233	-36
1615	Roth Geotech	F-31	30.1978	-90.43	-36
1616	Roth Geotech	C-36	30.1967	-90.4325	-36
1617	Roth Geotech	C-34	30.1942	-90.435	-36
1618	Roth Geotech	44	30.0883	-89.9083	-36
1619	Roth Geotech	42	30.0842	-89.9125	-36
1620	Roth Geotech	35	30.0678	-89.9278	-36
1621	Roth Geotech	34	30.0658	-89.9292	-36
1622	Roth Geotech	33	30.0633	-89.9317	-36

1623	Roth Geotech	CMB-6	30.0683	-89.8042	-36
1624	Roth Geotech	MAA-16	30.0175	-90.565	-36
1625	Roth Geotech	MAB-20	30.1083	-90.5148	-36
1626	Roth Geotech	MAB-22	30.1075	-90.5058	-36
1627	Roth Geotech	MAC-16	30.0108	-90.5975	-36
1628	Roth Geotech	B-8	30.2833	-90.4	-36
1629	Roth Geotech	49	30.1913	-90.135	-36
1630	Roth Geotech	44	30.1733	-90.1392	-36
1631	Roth Geotech	43	30.17	-90.14	-36
1632	Roth Geotech	110-10	30.1633	-90.1283	-36
1633	Roth Geotech	110-17	30.2658	-90.1105	-36
1634	Roth Geotech	28-10	30.055	-89.9367	-36
1635	Roth Geotech	13-57	30.0978	-89.9315	-36
1636	Roth Geotech	13-51	30.1117	-89.9195	-36
1637	Roth Geotech	111-48	30.1542	-90.1308	-37
1638	Roth Geotech	F-29	30.2033	-90.4258	-37
1639	Roth Geotech	F-34	30.1905	-90.4367	-37
1640	Roth Geotech	F-35	30.1883	-90.4383	-37
1641	Roth Geotech	C-32	30.1878	-90.4405	-37
1642	Roth Geotech	54	30.11	-89.8892	-37
1643	Roth Geotech	LD-21	30.0642	-89.8467	-37
1644	Roth Geotech	63	30.2417	-90.123	-37
1645	Roth Geotech	52	30.2033	-90.1317	-37
1646	Roth Geotech	48	30.1875	-90.1355	-37
1647	Roth Geotech	46	30.18	-90.1375	-37
1648	Roth Geotech	110-9	30.1483	-90.1317	-37
1649	Roth Geotech	110-11	30.1778	-90.1267	-37
1650	Roth Geotech	30-19C	30.0762	-89.9475	-37
1651	Roth Geotech	30.19G	30.0962	-89.9555	-37
1652	Roth Geotech	13-61	30.0897	-89.9388	-37
1653	Roth Geotech	13-60	30.0917	-89.9367	-37
1654	Roth Geotech	13-59	30.0938	-89.9345	-37
1655	Roth Geotech	13-56	30.1005	-89.9292	-37
1656	Roth Geotech	13-55	30.1028	-89.9272	-37
1657	Roth Geotech	13-44	30.1292	-89.9042	-37
1658	Roth Geotech	28-16	30.0787	-89.925	-37
1659	Roth Geotech	36	30.07	-89.9258	-38
1660	Roth Geotech	32	30.065	-89.9333	-38
1661	Roth Geotech	H-58	30.0705	-89.8	-38
1662	Roth Geotech	6-USPT	30.1242	-89.8675	-38
1663	Roth Geotech	MAA-17	30.0167	-90.5617	-38
1664	Roth Geotech	B-5	30.3083	-90.405	-38
1665	Roth Geotech	60	30.2323	-90.125	-38
1666	Roth Geotech	39	30.1558	-90.1433	-38
1667	Roth Geotech	38	30.1517	-90.1442	-38
1668	Roth Geotech	37	30.1483	-90.145	-38
1669	Roth Geotech	36	30.1442	-90.1463	-38
1670	Roth Geotech	30	30.1283	-90.1497	-38
1671	Roth Geotech	20	30.0925	-90.1583	-38
1672	Roth Geotech	111-47	30.1583	-90.13	-38
1673	Roth Geotech	112-33	30.2717	-90.1097	-38
1674	Roth Geotech	111-24	30.3125	-90.1025	-38
1675	Roth Geotech	13-65	30.0858	-89.9498	-38
1676	Roth Geotech	30-19E	30.0862	-89.9512	-38
1677	Roth Geotech	30-19F	30.0912	-89.9533	-38
1678	Roth Geotech	30-17D	30.0767	-89.9608	-38
1679	Roth Geotech	13-54	30.105	-89.925	-38
1680	Roth Geotech	F-36	30.1862	-90.44	-39
1681	Roth Geotech	F-38	30.1817	-90.4417	-39
1682	Roth Geotech	C-30	30.18	-90.4433	-39
1683	Roth Geotech	F-39	30.1783	-90.4428	-39
1684	Roth Geotech	MAA-13	30.025	-90.5775	-39
1685	Roth Geotech	MAA-18	30.0167	-90.5583	-39

1686	Roth Geotech	64	30.2442	-90.122	-39
1687	Roth Geotech	47	30.1833	-90.1367	-39
1688	Roth Geotech	45	30.1767	-90.1383	-39
1689	Roth Geotech	42	30.1658	-90.1408	-39
1690	Roth Geotech	41	30.163	-90.1417	-39
1691	Roth Geotech	112-19	30.1517	-90.1305	-39
1692	Roth Geotech	30.18D	30.0788	-89.9545	-39
1693	Roth Geotech	13-64	30.0833	-89.9445	-39
1694	Roth Geotech	F-33	30.1922	-90.435	-40
1695	Roth Geotech	38	30.075	-89.9217	-40
1696	Roth Geotech	37	30.0725	-89.9233	-40
1697	Roth Geotech	31	30.0617	-89.9333	-40
1698	Roth Geotech	89	30.325	-90.1033	-40
1699	Roth Geotech	88	30.3217	-90.1042	-40
1700	Roth Geotech	84	30.3067	-90.1075	-40
1701	Roth Geotech	83	30.3033	-90.1083	-40
1702	Roth Geotech	82	30.3	-90.11	-40
1703	Roth Geotech	80	30.293	-90.1117	-40
1704	Roth Geotech	MAC-2	30.0917	-90.5517	-40
1705	Roth Geotech	MAC-13	30.045	-90.5817	-40
1706	Roth Geotech	B-6	30.285	-90.4003	-40
1707	Roth Geotech	62	30.2383	-90.1242	-40
1708	Roth Geotech	61	30.235	-90.125	-40
1709	Roth Geotech	51	30.1992	-90.1325	-40
1710	Roth Geotech	50	30.195	-90.1333	-40
1711	Roth Geotech	1121-18	30.1458	-90.1212	-40
1712	Roth Geotech	NOHA-313	30.0523	-89.9375	-40
1713	Roth Geotech	30.19-D	30.0805	-89.9492	-40
1714	Roth Geotech	30-19H	30.1017	-89.9575	-40
1715	Roth Geotech	30-19D	30.0805	-89.9492	-40
1716	Roth Geotech	13-62	30.0875	-89.9405	-40
1717	Roth Geotech	19-14A	30.0413	-89.9632	-40
1718	Roth Geotech	26-11	30.0608	-89.9367	-40
1719	Roth Geotech	C-16	30.145	-90.4483	-41
1720	Roth Geotech	F-53	30.14	-90.4492	-41
1721	Roth Geotech	C-14	30.1383	-90.45	-41
1722	Roth Geotech	30	30.06	-89.935	-41
1723	Roth Geotech	H-57	30.0712	-89.7995	-41
1724	Roth Geotech	81	30.2962	-90.1108	-41
1725	Roth Geotech	79	30.2892	-90.1125	-41
1726	Roth Geotech	78	30.2858	-90.113	-41
1727	Roth Geotech	PF-593	30.2612	-90.3983	-41
1728	Roth Geotech	32	30.1367	-90.1478	-41
1729	Roth Geotech	2G	30.0633	-90.0567	-41
1730	Roth Geotech	WB-1	30.0183	-90.0267	-41
1731	Roth Geotech	ELS-6	30.0228	-90.0003	-41
1732	Roth Geotech	NOHA-314	30.0467	-89.9372	-41
1733	Roth Geotech	30-15D	30.0728	-89.9725	-41
1734	Roth Geotech	F-40	30.1772	-90.4438	-42
1735	Roth Geotech	C-18	30.1508	-90.4475	-42
1736	Roth Geotech	F-50	30.1483	-90.4472	-42
1737	Roth Geotech	F-51	30.1462	-90.4478	-42
1738	Roth Geotech	F-54	30.1367	-90.4492	-42
1739	Roth Geotech	C-10	30.1228	-90.4462	-42
1740	Roth Geotech	4G	30.0667	-90.0442	-42
1741	Roth Geotech	WB-2	30.0183	-90.025	-42
1742	Roth Geotech	WB-5	30.0208	-90.0167	-42
1743	Roth Geotech	WB-6	30.0208	-90.0142	-42
1744	Roth Geotech	111-56	30.0967	-90.1408	-42
1745	Roth Geotech	112-20	30.1612	-90.1288	-42
1746	Roth Geotech	88-1E	30.0508	-90.0575	-42
1747	Roth Geotech	88-1F	30.0562	-90.06	-42
1748	Roth Geotech	25-1	30.0317	-89.9342	-42

1749	Roth Geotech	20.67	30.0557	-89.935	-42
1750	Roth Geotech	20-30	30.0575	-89.9353	-42
1751	Roth Geotech	28-12	30.0662	-89.9375	-42
1752	Roth Geotech	2-38M	30.0642	-89.7905	-42
1753	Roth Geotech	88-SW12	30.0622	-90.0017	-42
1754	Roth Geotech	13-63	30.0853	-89.9422	-42
1755	Roth Geotech	104-7	30.0208	-90.0115	-42
1756	Roth Geotech	PL-85-6	30.0232	-89.9938	-42
1757	Roth Geotech	28-15	30.0725	-89.9317	-42
1758	Roth Geotech	88-1H	30.0667	-90.065	-42
1759	Roth Geotech	28-11	30.0603	-89.9367	-42
1760	Roth Geotech	F-52	30.1433	-90.4483	-43
1761	Roth Geotech	F-55	30.1348	-90.4483	-43
1762	Roth Geotech	PLP-4B	30.0575	-90.25730058	-43
1763	Roth Geotech	3G	30.065	-90.05	-43
1764	Roth Geotech	WB-3	30.0192	-90.02225	-43
1765	Roth Geotech	111-50	30.1395	-90.1328	-43
1766	Roth Geotech	111-33	30.26	-90.1112	-43
1767	Roth Geotech	46-P38	30.065	-90.1195	-43
1768	Roth Geotech	95-D-3	30.0333	-90.0348	-43
1769	Roth Geotech	88-SW8	30.0572	-90.0125	-43
1770	Roth Geotech	30-16D	30.0747	-89.9667	-43
1771	Roth Geotech	104-9	30.0212	-90.0078	-43
1772	Roth Geotech	19-9	30.0522	-89.95	-43
1773	Roth Geotech	F-56	30.1325	-90.4475	-44
1774	Roth Geotech	C-12	30.1308	-90.4483	-44
1775	Roth Geotech	F-57	30.1295	-90.4467	-44
1776	Roth Geotech	F-60	30.1217	-90.445	-44
1777	Roth Geotech	PLB-5B	30.0583	-90.265	-44
1778	Roth Geotech	P4-5	30.1022	-90.485	-44
1779	Roth Geotech	B-1	30.087	-90.4052	-44
1780	Roth Geotech	JLD-1	30.0508	-90.1208	-44
1781	Roth Geotech	WB-7	30.0212	-90.0117	-44
1782	Roth Geotech	111-32	30.27	-90.11	-44
1783	Roth Geotech	46-P38	30.0612	-90.12	-44
1784	Roth Geotech	46-P37	30.0688	-90.1192	-44
1785	Roth Geotech	81A-1	29.9982	-90.0417	-44
1786	Roth Geotech	83-3-W	30.0283	-90.0367	-44
1787	Roth Geotech	88-SW7	30.0563	-90.0155	-44
1788	Roth Geotech	MH-2	30.0287	-89.975	-44
1789	Roth Geotech	F-41	30.1717	-90.4433	-45
1790	Roth Geotech	F-49	30.1517	-90.4458	-45
1791	Roth Geotech	F-58	30.1275	-90.4462	-45
1792	Roth Geotech	202	30.0883	-90.4383	-45
1793	Roth Geotech	68	30.255	-90.1217	-45
1794	Roth Geotech	MAA-12	30.025	-90.5828	-45
1795	Roth Geotech	22	30.1	-90.1567	-45
1796	Roth Geotech	WB-8	30.0217	-90.01	-45
1797	Roth Geotech	32-11	30.0295	-90.0538	-45
1798	Roth Geotech	32-3	30.0315	-90.0538	-45
1799	Roth Geotech	32-8	30.0317	-90.0532	-45
1800	Roth Geotech	32-1	30.0333	-90.0532	-45
1801	Roth Geotech	88-1D	30.0458	-90.055	-45
1802	Roth Geotech	81A-2	29.9945	-90.045	-45
1803	Roth Geotech	83-12-WT	30.0125	-90.0317	-45
1804	Roth Geotech	83-5-WT	30.0247	-90.035	-45
1805	Roth Geotech	18-271	30.011	-89.9133	-45
1806	Roth Geotech	14-26	30.0472	-89.8258	-45
1807	Roth Geotech	2-4Mu	30	-89.81	-45
1808	Roth Geotech	88-1D	30.0458	-90.055	-45
1809	Roth Geotech	81-70	30.0405	-90.2467	-45
1810	Roth Geotech	81-63	30.0383	-90.2338	-45
1811	Roth Geotech	104-6	30.0205	-90.014	-45

1812	Roth Geotech	104-8	30.0212	-90.0095	-45
1813	Roth Geotech	19-8	30.0483	-89.9567	-45
1814	Roth Geotech	F-61	30.1195	-90.4438	-46
1815	Roth Geotech	C-8	30.1175	-90.4445	-46
1816	Roth Geotech	203	30.0878	-90.4362	-46
1817	Roth Geotech	BL-16E	30.0395	-89.8442	-46
1818	Roth Geotech	BL-14E	30.0355	-89.855	-46
1819	Roth Geotech	87	30.3175	-90.1055	-46
1820	Roth Geotech	35	30.14	-90.1467	-46
1821	Roth Geotech	34	30.1375	-90.1457	-46
1822	Roth Geotech	23	30.1033	-90.155	-46
1823	Roth Geotech	WB-9	30.0217	-90.0083	-46
1824	Roth Geotech	WB-10	30.022	-90.005	-46
1825	Roth Geotech	ELS-1	30.0222	-90.0015	-46
1826	Roth Geotech	77-3-1	30.0312	-90.2183	-46
1827	Roth Geotech	111-34	30.2558	-90.1125	-46
1828	Roth Geotech	83-15-WT	30.0083	-90.0283	-46
1829	Roth Geotech	95-L-6	30.0367	-90.0355	-46
1830	Roth Geotech	234-1D	29.9917	-90.0167	-46
1831	Roth Geotech	18-274	30.0083	-89.925	-46
1832	Roth Geotech	68-647	30.0417	-90.0683	-46
1833	Roth Geotech	88-SW9	30.0592	-90.01	-46
1834	Roth Geotech	104-1	30.0167	-90.0275	-46
1835	Roth Geotech	104-10	30.0217	-90.0042	-46
1836	Roth Geotech	F-63	30.1145	-90.4442	-47
1837	Roth Geotech	LK-201	30.09	-90.4442	-47
1838	Roth Geotech	1-SP	30.0517	-89.8317	-47
1839	Roth Geotech	BL-19EU	30.0375	-89.85	-47
1840	Roth Geotech	85	30.31	-90.107	-47
1841	Roth Geotech	29	30.125	-90.15	-47
1842	Roth Geotech	21	30.0958	-90.1567	-47
1843	Roth Geotech	9W	30.0183	-90.0333	-47
1844	Roth Geotech	WB-4	30.0197	-90.0192	-47
1845	Roth Geotech	81-51	30.0322	-90.2172	-47
1846	Roth Geotech	75-1	30.0117	-90.1548	-47
1847	Roth Geotech	110-1	30.0342	-90.1517	-47
1848	Roth Geotech	112-3	30.0425	-90.15	-47
1849	Roth Geotech	111-58	30.0833	-90.1433	-47
1850	Roth Geotech	111-57	30.0883	-90.1422	-47
1851	Roth Geotech	110-5	30.0917	-90.1417	-47
1852	Roth Geotech	112-11	30.0942	-90.1408	-47
1853	Roth Geotech	111-51	30.1295	-90.1342	-47
1854	Roth Geotech	112-17	30.1367	-90.1328	-47
1855	Roth Geotech	88-1G	30.0612	-90.0623	-47
1856	Roth Geotech	28-3	30.0247	-89.9383	-47
1857	Roth Geotech	28-5	30.0275	-89.934	-47
1858	Roth Geotech	28-7	30.0367	-89.9345	-47
1859	Roth Geotech	28-9	30.0495	-89.9362	-47
1860	Roth Geotech	NOHA-311	30.0617	-89.9383	-47
1861	Roth Geotech	28-14	30.0683	-89.9378	-47
1862	Roth Geotech	NOHA-309	30.0745	-89.9412	-47
1863	Roth Geotech	28-4D	29.997	-89.9783	-47
1864	Roth Geotech	14-22	30.0417	-89.84	-47
1865	Roth Geotech	2-16M	30.0517	-89.8183	-47
1866	Roth Geotech	2-17M	30.0533	-89.8145	-47
1867	Roth Geotech	77-3-1	30.0313	-90.2183	-47
1868	Roth Geotech	81-40	30.024	-90.1908	-47
1869	Roth Geotech	NOHA-375	30.0183	-90.0983	-47
1870	Roth Geotech	104-3	30.0187	-90.0225	-47
1871	Roth Geotech	C-28	30.1745	-90.444	-47
1872	Roth Geotech	F-42	30.1695	-90.4448	-48
1873	Roth Geotech	F-59	30.125	-90.4458	-48
1874	Roth Geotech	C-6	30.1133	-90.4433	-48

1875	Roth Geotech	C-4	30.105	-90.4412	-48
1876	Roth Geotech	4-B	30.06	-90.3033	-48
1877	Roth Geotech	P4-4	30.0988	-90.4758	-48
1878	Roth Geotech	215	30.0862	-90.4317	-48
1879	Roth Geotech	217	30.0842	-90.4258	-48
1880	Roth Geotech	20	30.0783	-90.405	-48
1881	Roth Geotech	LD-2	30.0317	-89.8655	-48
1882	Roth Geotech	BL-10E	30.0255	-89.8778	-48
1883	Roth Geotech	69	30.2542	-90.1205	-48
1884	Roth Geotech	28	30.1217	-90.1508	-48
1885	Roth Geotech	26	30.1133	-90.1528	-48
1886	Roth Geotech	JLD-4	30.05	-90.135	-48
1887	Roth Geotech	1G	30.0608	-90.063	-48
1888	Roth Geotech	41609	30.02	-90.2467	-48
1889	Roth Geotech	112-2	30.0375	-90.1508	-48
1890	Roth Geotech	110-2	30.0483	-90.1492	-48
1891	Roth Geotech	112-32	30.2625	-90.1108	-48
1892	Roth Geotech	46-P2	30.0572	-90.12	-48
1893	Roth Geotech	83-10-WT	30.0167	-90.0328	-48
1894	Roth Geotech	234-2D	29.993	-90.0078	-48
1895	Roth Geotech	2-35M	30.0617	-89.795	-48
1896	Roth Geotech	2-37M	30.0625	-89.7917	-48
1897	Roth Geotech	46-B9	30.0405	-90.1428	-48
1898	Roth Geotech	46-B6	30.04	-90.1332	-48
1899	Roth Geotech	88-SW11	30.0612	-90.0045	-48
1900	Roth Geotech	81-9	30.0192	-90.1322	-48
1901	Roth Geotech	41-10WT	30.0167	-90.0333	-48
1902	Roth Geotech	104-5	30.02	-90.0167	-48
1903	Roth Geotech	GHR-3	29.9967	-90.4183	-48
1904	Roth Geotech	R-125.8	29.9933	-90.408	-48
1905	Roth Geotech	22	30.0772	-90.4025	-49
1906	Roth Geotech	LD-25	30.055	-89.8275	-49
1907	Roth Geotech	BL-13E	30.0333	-89.8617	-49
1908	Roth Geotech	BL-8EU	30.0228	-89.885	-49
1909	Roth Geotech	86	30.3133	-90.1063	-49
1910	Roth Geotech	77	30.2817	-90.1142	-49
1911	Roth Geotech	27	30.1183	-90.1517	-49
1912	Roth Geotech	19	30.0883	-90.1592	-49
1913	Roth Geotech	JLD-7	30.0663	-90.1442	-49
1914	Roth Geotech	5G	30.0683	-90.0383	-49
1915	Roth Geotech	1022	30.0175	-90.0608	-49
1916	Roth Geotech	77-3-2	30.0122	-90.2295	-49
1917	Roth Geotech	46P25	30.07	-90.1775	-49
1918	Roth Geotech	46-P1	30.0483	-90.1212	-49
1919	Roth Geotech	68-433	30.0547	-90.0247	-49
1920	Roth Geotech	4-3	30.0487	-90.2878	-49
1921	Roth Geotech	68-1808	30.0388	-90.2433	-49
1922	Roth Geotech	SR-5	29.9955	-90.4108	-49
1923	Roth Geotech	F-64	30.1117	-90.4417	-50
1924	Roth Geotech	P4-3	30.0967	-90.4692	-50
1925	Roth Geotech	P4-1	30.0917	-90.4495	-50
1926	Roth Geotech	CMB-4	30.0683	-89.805	-50
1927	Roth Geotech	BL-9ET	30.25	-89.8825	-50
1928	Roth Geotech	BL-8EU	30.233	-89.8842	-50
1929	Roth Geotech	BL-17E	30.0417	-89.8392	-50
1930	Roth Geotech	76	30.278	-90.115	-50
1931	Roth Geotech	70	30.2575	-90.12	-50
1932	Roth Geotech	110-3	30.0625	-90.1467	-50
1933	Roth Geotech	7-4	30.0372	-90.0523	-50
1934	Roth Geotech	28-8	30.0417	-89.935	-50
1935	Roth Geotech	36-5D	29.9978	-89.9678	-50
1936	Roth Geotech	18-272	30.01	-89.917	-50
1937	Roth Geotech	14-2	30.0312	-89.8658	-50

1938	Roth Geotech	2-3MU	30.0463	-89.8283	-50
1939	Roth Geotech	2-10MU	30.0607	-89.7978	-50
1940	Roth Geotech	68-652	30.0388	-90.115	-50
1941	Roth Geotech	4-6U	30.0533	-90.3117	-50
1942	Roth Geotech	4-5	30.0517	-90.3033	-50
1943	Roth Geotech	4-4	30.0512	-90.2958	-50
1944	Roth Geotech	R-125.6	29.9905	-90.4017	-50
1945	Roth Geotech	R-125.4	29.9883	-90.3983	-50
1946	Roth Geotech	GHR-8	29.975	-90.3917	-50
1947	Roth Geotech	F-62	30.1167	-90.4433	-51
1948	Roth Geotech	5-B	30.0608	-90.3133	-51
1949	Roth Geotech	2-B	30.0567	-90.2892	-51
1950	Roth Geotech	P4-2	30.0933	-90.4558	-51
1951	Roth Geotech	16	30.0795	-90.4095	-51
1952	Roth Geotech	LK-18	30.0788	-90.4078	-51
1953	Roth Geotech	75	30.275	-90.1158	-51
1954	Roth Geotech	71	30.2608	-90.1188	-51
1955	Roth Geotech	14R	30.0708	-90.1632	-51
1956	Roth Geotech	PHS-4	30.015	-90.2315	-51
1957	Roth Geotech	111-31	30.2742	-90.1092	-51
1958	Roth Geotech	83-17-W	30.0062	-90.0278	-51
1959	Roth Geotech	88-7-G	30.0733	-90.0267	-51
1960	Roth Geotech	15-8	30.0067	-89.9392	-51
1961	Roth Geotech	68-650	30.0387	-90	-51
1962	Roth Geotech	GHR-6	29.9822	-90.3938	-51
1963	Roth Geotech	GHR-7	29.9783	-90.3922	-51
1964	Roth Geotech	F-65	30.1083	-90.4408	-52
1965	Roth Geotech	F-70	30.0967	-90.4372	-52
1966	Roth Geotech	3-B	30.0583	-90.2967	-52
1967	Roth Geotech	3	30.0892	-90.4422	-52
1968	Roth Geotech	LK-38	30.0883	-90.44	-52
1969	Roth Geotech	216	30.085	-90.4283	-52
1970	Roth Geotech	CBLM-4UT	30.0133	-89.9083	-52
1971	Roth Geotech	LD-22	30.04	-89.8375	-52
1972	Roth Geotech	72	30.2642	-90.1183	-52
1973	Roth Geotech	NOA-16	29.9692	-90.1125	-52
1974	Roth Geotech	6G	30.07	-90.0333	-52
1975	Roth Geotech	PHS-5	30.0142	-90.2308	-52
1976	Roth Geotech	99-1	30.0105	-90.154	-52
1977	Roth Geotech	110-SPD	30.02	-90.1542	-52
1978	Roth Geotech	112-4	30.0517	-90.1483	-52
1979	Roth Geotech	110SPD	30.02	-90.1542	-52
1980	Roth Geotech	46-B3	30.04	-90.1217	-52
1981	Roth Geotech	83-10	30.0012	-90.0605	-52
1982	Roth Geotech	88-1C	30.0407	-90.0532	-52
1983	Roth Geotech	83-19-WT	30.005	-90.0267	-52
1984	Roth Geotech	NOHA-331	30.0445	-90.0322	-52
1985	Roth Geotech	88-8-H	30.0805	-90.0225	-52
1986	Roth Geotech	15-7	29.9983	-89.9382	-52
1987	Roth Geotech	36-7D	30	-89.95	-52
1988	Roth Geotech	36-8D	30.0072	-89.9292	-52
1989	Roth Geotech	14-24	30.0372	-89.8512	-52
1990	Roth Geotech	2-15M	30.049	-89.8233	-52
1991	Roth Geotech	LF-3	29.9692	-90.1142	-52
1992	Roth Geotech	88-2D	30.0473	-90.0492	-52
1993	Roth Geotech	88-3D	30.05	-90.0433	-52
1994	Roth Geotech	68-1021	30.0158	-90.0655	-52
1995	Roth Geotech	68-1022	30.0167	-90.0608	-52
1996	Roth Geotech	104-4	30.019	-90.0192	-52
1997	Roth Geotech	GHR-5A	29.985	-90.3958	-52
1998	Roth Geotech	F-67	30.1042	-90.4392	-53
1999	Roth Geotech	218	30.0833	-90.4228	-53
2000	Roth Geotech	219	30.0825	-90.4205	-53

2001	Roth Geotech	24	30.0758	-90.4	-53
2002	Roth Geotech	LD-27	30.0367	-89.8517	-53
2003	Roth Geotech	74	30.2717	-90.1167	-53
2004	Roth Geotech	GA-1	30.0067	-90.2017	-53
2005	Roth Geotech	1021	30.0167	-90.0665	-53
2006	Roth Geotech	76-10	29.9697	-90.1807	-53
2007	Roth Geotech	46-11	30.0328	-90.1533	-53
2008	Roth Geotech	111-62	30.0545	-90.1483	-53
2009	Roth Geotech	111-62	30.0545	-90.1483	-53
2010	Roth Geotech	112-9	30.08	-90.1433	-53
2011	Roth Geotech	111-52	30.125	-90.135	-53
2012	Roth Geotech	112-16	30.1325	-90.1333	-53
2013	Roth Geotech	46-B1	30.0238	-90.1233	-53
2014	Roth Geotech	83-9-W	30.0178	-90.0333	-53
2015	Roth Geotech	139-5A	29.992	-90.0478	-53
2016	Roth Geotech	68-1106	30.0392	-90.12	-53
2017	Roth Geotech	68-1107	30.03945	-90.114	-53
2018	Roth Geotech	88-SW10	30.0605	-90.0067	-53
2019	Roth Geotech	GHR-1	29.9972	-90.4278	-53
2020	Roth Geotech	R-121.3	29.9373	-90.37	-53
2021	Roth Geotech	C-26	30.1682	-90.4442	-54
2022	Roth Geotech	F-66	30.1067	-90.44	-54
2023	Roth Geotech	1-B	30.0558	-90.2817	-54
2024	Roth Geotech	220	30.0817	-90.4172	-54
2025	Roth Geotech	28	30.0728	-90.3958	-54
2026	Roth Geotech	BL-12EU	30.03	-89.8683	-54
2027	Roth Geotech	LD-11	30.0383	-89.8383	-54
2028	Roth Geotech	15R	30.0742	-90.1625	-54
2029	Roth Geotech	JLD-22	30.0458	-90.1867	-54
2030	Roth Geotech	7G	30.0725	-90.0278	-54
2031	Roth Geotech	TT-5	30.0108	-90.1533	-54
2032	Roth Geotech	TT-4	30.0125	-90.1553	-54
2033	Roth Geotech	111-61	30.0655	-90.1458	-54
2034	Roth Geotech	112-10	30.0875	-90.1422	-54
2035	Roth Geotech	195-1	29.9745	-90.1022	-54
2036	Roth Geotech	2-20M	30.0667	-89.7825	-54
2037	Roth Geotech	JHS-2	29.9733	-90.1033	-54
2038	Roth Geotech	68-651	30.0392	-90.1045	-54
2039	Roth Geotech	135-34	29.9917	-90.0482	-55
2040	Roth Geotech	F-45	30.1645	-90.4438	-55
2041	Roth Geotech	221	30.0812	-90.415	-55
2042	Roth Geotech	34	30.0683	-90.3883	-55
2043	Roth Geotech	BL-7E	30.0208	-89.89	-55
2044	Roth Geotech	BL-6E	30.0188	-89.8958	-55
2045	Roth Geotech	PCS-1	30.0133	-89.9667	-55
2046	Roth Geotech	LD-23	30.03	-89.8367	-55
2047	Roth Geotech	JLD-17	30.0683	-90.1633	-55
2048	Roth Geotech	OB-1	30.0058	-90.1917	-55
2049	Roth Geotech	JFK-6	30.0163	-90.0872	-55
2050	Roth Geotech	76-3	30.0125	-90.2308	-55
2051	Roth Geotech	46-P22	30.0458	-90.1855	-55
2052	Roth Geotech	46-10	30.0233	-90.155	-55
2053	Roth Geotech	110-B2	30.0395	-90.1505	-55
2054	Roth Geotech	111-63	30.045	-90.15	-55
2055	Roth Geotech	111-55	30.1022	-90.1397	-55
2056	Roth Geotech	110-6	30.1062	-90.1388	-55
2057	Roth Geotech	89-1	30.0208	-90.0827	-55
2058	Roth Geotech	15-7A	29.9958	-89.9393	-55
2059	Roth Geotech	15-2	29.9955	-89.9387	-55
2060	Roth Geotech	7-1	29.9912	-90.0428	-55
2061	Roth Geotech	104-21	30.0175	-90.0522	-55
2062	Roth Geotech	GHR-2	29.9967	-90.4223	-55
2063	Roth Geotech	R-123.7	29.9492	-90.3962	-55

2064	Roth Geotech	F-68	30.0995	-90.4378	-56
2065	Roth Geotech	26	30.0745	-90.3983	-56
2066	Roth Geotech	PIS-1	30.0095	-89.9425	-56
2067	Roth Geotech	NOA-15	29.9717	-90.1167	-56
2068	Roth Geotech	JLD-11	30.0492	-90.1542	-56
2069	Roth Geotech	112-1	30.0267	-90.1532	-56
2070	Roth Geotech	46-B2	30.0317	-90.1228	-56
2071	Roth Geotech	68-1102	30.0365	-90.12	-56
2072	Roth Geotech	68-331A	30.0267	-90.0842	-56
2073	Roth Geotech	117-19-U	29.9773	-90.0198	-56
2074	Roth Geotech	88-9-I	30.0883	-90.0188	-56
2075	Roth Geotech	84-2	29.9908	-90.0538	-56
2076	Roth Geotech	DS-1	29.97	-90.1238	-56
2077	Roth Geotech	46-P11	30.0467	-90.155	-56
2078	Roth Geotech	R-122.7	29.9623	-90.3917	-56
2079	Roth Geotech	LPL-B5	30.0633	-90.4183	-57
2080	Roth Geotech	39	30.0642	-90.383	-57
2081	Roth Geotech	NOA-13	29.97	-90.1242	-57
2082	Roth Geotech	NOA-14	29.97	-90.1225	-57
2083	Roth Geotech	NOA-18	29.9692	-90.105	-57
2084	Roth Geotech	16R	30.0783	-90.1617	-57
2085	Roth Geotech	SPD-810	30.0228	-90.1538	-57
2086	Roth Geotech	110-8	30.135	-90.1338	-57
2087	Roth Geotech	227-10	29.9917	-90.0967	-57
2088	Roth Geotech	63-1	30.0067	-90.0832	-57
2089	Roth Geotech	28-4	30.0258	-89.934	-57
2090	Roth Geotech	52-3	29.9988	-90.1922	-57
2091	Roth Geotech	14-1	30.0175	-90.1145	-57
2092	Roth Geotech	R-122.95	29.942	-90.3825	-57
2093	Roth Geotech	7-B	30.0595	-90.33	-58
2094	Roth Geotech	214	30.0872	-90.4342	-58
2095	Roth Geotech	30	30.0712	-90.3933	-58
2096	Roth Geotech	32	30.07	-90.3912	-58
2097	Roth Geotech	36	30.065	-90.384	-58
2098	Roth Geotech	CBL-8MUT	30.0095	-89.9275	-58
2099	Roth Geotech	24	30.1067	-90.1547	-58
2100	Roth Geotech	18	30.0855	-90.1597	-58
2101	Roth Geotech	5	30.038	-90.1708	-58
2102	Roth Geotech	BA-1	30.0417	-90.215	-58
2103	Roth Geotech	76-7	30.0142	-90.23	-58
2104	Roth Geotech	111-59	30.0738	-90.1445	-58
2105	Roth Geotech	111-54	30.1112	-90.1378	-58
2106	Roth Geotech	110-7	30.1208	-90.1358	-58
2107	Roth Geotech	47-1	30.0167	-90.0858	-58
2108	Roth Geotech	135-1438	29.9933	-90.0467	-58
2109	Roth Geotech	15-4A	29.9947	-89.9405	-58
2110	Roth Geotech	43-262	30.0007	-90.2005	-58
2111	Roth Geotech	84-34	29.9925	-90.0888	-58
2112	Roth Geotech	46-56	29.9682	-90.205	-58
2113	Roth Geotech	WB-19	29.978	-90.0105	-58
2114	Roth Geotech	C-2	30.1017	-90.4383	-59
2115	Roth Geotech	LK-214	30.0872	-90.4342	-59
2116	Roth Geotech	MFL-1	30.0133	-89.99	-59
2117	Roth Geotech	NOA-12	29.9692	-90.1275	-59
2118	Roth Geotech	25	30.11	-90.1533	-59
2119	Roth Geotech	65-KE-	29.9738	-90.2712	-59
2120	Roth Geotech	61-22	30.0378	-90.2117	-59
2121	Roth Geotech	84-33	29.9923	-90.086	-59
2122	Roth Geotech	47-6	30.0155	-90.0867	-59
2123	Roth Geotech	88-6-F	30.0663	-90.0303	-59
2124	Roth Geotech	43-178	30.0082	-90.2247	-59
2125	Roth Geotech	43-205	30.0072	-90.2167	-59
2126	Roth Geotech	81-45	30.0283	-90.2055	-59

2127	Roth Geotech	11-R	29.9362	-90.3622	-59
2128	Roth Geotech	LPL-B3	30.0392	-90.4395	-60
2129	Roth Geotech	95	30.0217	-90.3192	-60
2130	Roth Geotech	73	30.2675	-90.1175	-60
2131	Roth Geotech	NOA-31	29.9742	-90.0008	-60
2132	Roth Geotech	8G	30.075	-90.0222	-60
2133	Roth Geotech	9G	30.0817	-90.0183	-60
2134	Roth Geotech	68-617	30.0345	-90.0825	-60
2135	Roth Geotech	43-224	30.0035	-90.2102	-60
2136	Roth Geotech	43-234	30.0048	-90.2078	-60
2137	Roth Geotech	84-33	29.9917	-90.0867	-60
2138	Roth Geotech	6-B	30.0605	-90.3217	-61
2139	Roth Geotech	46	30.0595	-90.3763	-61
2140	Roth Geotech	48	30.0588	-90.3755	-61
2141	Roth Geotech	MAA-21	30.0095	-90.5275	-61
2142	Roth Geotech	NOA-11	29.9692	-90.1292	-61
2143	Roth Geotech	NOA-30	29.9742	-90.0033	-61
2144	Roth Geotech	NOB-14	29.96	-90.0983	-61
2145	Roth Geotech	12G	30.0897	-90.0042	-61
2146	Roth Geotech	43-187	30.0083	-90	-61
2147	Roth Geotech	81-272	29.9992	-90.1992	-61
2148	Roth Geotech	46-55	29.9678	-90.2028	-61
2149	Roth Geotech	WB-26	29.9748	-90	-61
2150	Roth Geotech	10-R	29.933	-90.3558	-61
2151	Roth Geotech	40	30.0633	-90.3817	-62
2152	Roth Geotech	LK-44	30.0617	-90.38	-62
2153	Roth Geotech	44	30.0605	-90.3775	-62
2154	Roth Geotech	59	30.0492	-90.3617	-62
2155	Roth Geotech	60	30.0485	-90.3605	-62
2156	Roth Geotech	NOB-18	29.9667	-90.0933	-62
2157	Roth Geotech	76-5	29.9858	-90.257	-62
2158	Roth Geotech	110-66	30.0262	-90.1533	-62
2159	Roth Geotech	112-5	30.0567	-90.1475	-62
2160	Roth Geotech	111-60	30.0692	-90.1458	-62
2161	Roth Geotech	112-13	30.1083	-90.1383	-62
2162	Roth Geotech	111-53	30.1158	-90.1367	-62
2163	Roth Geotech	68-384	30.026	-90.0827	-62
2164	Roth Geotech	75-6-U	29.975	-90.0208	-62
2165	Roth Geotech	24-3	29.9917	-90.0222	-62
2166	Roth Geotech	28-2	30.0183	-89.9387	-62
2167	Roth Geotech	43-110	30.0092	-90.245	-62
2168	Roth Geotech	43-229	30.0055	-90.2092	-62
2169	Roth Geotech	81-311	29.9995	-90.1842	-62
2170	Roth Geotech	84-35	29.9932	-90.0917	-62
2171	Roth Geotech	84-32	29.9922	-90.0858	-62
2172	Roth Geotech	33-15	30.0075	-89.9367	-62
2173	Roth Geotech	46-36	29.9712	-90.1792	-62
2174	Roth Geotech	WB-24	29.9747	-90.0015	-62
2175	Roth Geotech	WB-25	29.9748	-90.0005	-62
2176	Roth Geotech	222	30.08	-90.4117	-63
2177	Roth Geotech	42	30.0612	-90.3788	-63
2178	Roth Geotech	58	30.05	-90.3625	-63
2179	Roth Geotech	61	30.0478	-90.3595	-63
2180	Roth Geotech	62	30.0467	-90.3583	-63
2181	Roth Geotech	108	30.0128	-90.3072	-63
2182	Roth Geotech	NOA-19	29.9683	-90.09	-63
2183	Roth Geotech	NOB-19	29.9933	-90.0933	-63
2184	Roth Geotech	17	30.0808	-90.1608	-63
2185	Roth Geotech	JD-2	30.005	-90.2142	-63
2186	Roth Geotech	81-47P	29.9788	-90.1133	-63
2187	Roth Geotech	81-552A	29.9975	-90.1162	-63
2188	Roth Geotech	135-31	29.985	-90.0525	-63
2189	Roth Geotech	15-1A	29.9933	-89.9413	-63

2190	Roth Geotech	28-1	30.0117	-89.9388	-63
2191	Roth Geotech	81-531	29.9953	-90.1233	-63
2192	Roth Geotech	84-36	29.993	-90.0928	-63
2193	Roth Geotech	84-26	29.9915	-90.0733	-63
2194	Roth Geotech	18-275	30.0083	-89.9282	-63
2195	Roth Geotech	46-59	29.9688	-90.2067	-63
2196	Roth Geotech	ILC-6	29.97	-90.13	-63
2197	Roth Geotech	WB-17	29.9783	-90.0122	-63
2198	Roth Geotech	WB-21	29.9775	-90.0085	-63
2199	Roth Geotech	BLE-10	29.9622	-89.9655	-63
2200	Roth Geotech	64	30.0455	-90.3558	-64
2201	Roth Geotech	89	30.0272	-90.3278	-64
2202	Roth Geotech	93	30.0233	-90.3217	-64
2203	Roth Geotech	106	30.0145	-90.3095	-64
2204	Roth Geotech	NOA-10	29.97	-90.1308	-64
2205	Roth Geotech	NOA-17	29.9678	-90.1075	-64
2206	Roth Geotech	112-14	30.1183	-90.1362	-64
2207	Roth Geotech	34-10	29.9667	-90.1083	-64
2208	Roth Geotech	34-3	29.9712	-90.1097	-64
2209	Roth Geotech	81-554	29.995	-90.1158	-64
2210	Roth Geotech	134-442	29.9687	-90.1087	-64
2211	Roth Geotech	42-1	29.9862	-90.09727	-64
2212	Roth Geotech	117-3-UL	29.9635	-90.0255	-64
2213	Roth Geotech	75-2-U	29.9672	-90.0247	-64
2214	Roth Geotech	WB-15	29.9788	-90.0138	-64
2215	Roth Geotech	BLE-8	29.9642	-89.9717	-64
2216	Roth Geotech	BLE-12	29.96	-89.96	-64
2217	Roth Geotech	8-R	29.9308	-90.3458	-64
2218	Roth Geotech	WB-29	29.9745	-89.9995	-64
2219	Roth Geotech	90	30.0262	-90.3267	-65
2220	Roth Geotech	104	30.0158	-90.3117	-65
2221	Roth Geotech	NOA-29	29.9683	-90.0217	-65
2222	Roth Geotech	NOB-10	29.9383	-90.0942	-65
2223	Roth Geotech	76-1	29.9872	-90.255	-65
2224	Roth Geotech	46-40-8	29.9708	-90.1788	-65
2225	Roth Geotech	112-7	30.0717	-90.145	-65
2226	Roth Geotech	136-2	29.9583	-90.1158	-65
2227	Roth Geotech	81-552B	29.9905	-90.1162	-65
2228	Roth Geotech	139-23	29.9833	-90.058	-65
2229	Roth Geotech	135-32	29.987	-90.0508	-65
2230	Roth Geotech	24-4	29.9888	-90.0212	-65
2231	Roth Geotech	33-18	30	-89.938	-65
2232	Roth Geotech	81-541	29.9947	-90.1188	-65
2233	Roth Geotech	84-16	29.99	-90.0667	-65
2234	Roth Geotech	18-237	30.0093	-89.9205	-65
2235	Roth Geotech	WB-13	29.9792	-90.0158	-65
2236	Roth Geotech	WB-30	29.9738	-89.9978	-65
2237	Roth Geotech	BLE-11	29.9612	-89.9625	-65
2238	Roth Geotech	DLB-5	29.939	-90.3758	-65
2239	Roth Geotech	960-119.05	29.9295	-90.3325	-65
2240	Roth Geotech	4-1	30.0475	-90.28	-66
2241	Roth Geotech	57	30.0508	-90.3638	-66
2242	Roth Geotech	88	30.0278	-90.3292	-66
2243	Roth Geotech	91	30.0255	-90.3255	-66
2244	Roth Geotech	92	30.025	-90.3245	-66
2245	Roth Geotech	97	30.0205	-90.3175	-66
2246	Roth Geotech	117-21	29.9722	-90.0222	-66
2247	Roth Geotech	84-31	29.9928	-90.0783	-66
2248	Roth Geotech	84-22	29.9897	-90.0692	-66
2249	Roth Geotech	ILC-9	29.968	-90.1333	-66
2250	Roth Geotech	WB-11	29.9792	-90.0175	-66
2251	Roth Geotech	WB-22	29.9767	-90.0057	-66
2252	Roth Geotech	BLE-6	29.968	-89.9813	-66

2253	Roth Geotech	NOA-28	29.9672	-90.0242	-67
2254	Roth Geotech	NOB-13	29.9575	-90.0967	-67
2255	Roth Geotech	6	30.0417	-90.17	-67
2256	Roth Geotech	960-M-1	29.9805	-90.2572	-67
2257	Roth Geotech	46-P24	30.0562	-90.1805	-67
2258	Roth Geotech	46-40-A	29.9715	-90.1783	-67
2259	Roth Geotech	84-9	29.9913	-90.0567	-67
2260	Roth Geotech	216-1	29.9725	-90.065	-67
2261	Roth Geotech	139-3	29.9748	-90.0633	-67
2262	Roth Geotech	139-6	29.9762	-90.0617	-67
2263	Roth Geotech	81-335	29.9982	-90.1773	-67
2264	Roth Geotech	84-29	29.9923	-90.0762	-67
2265	Roth Geotech	84-25	29.9908	-90.0717	-67
2266	Roth Geotech	84-10	29.9905	-90.0588	-67
2267	Roth Geotech	24-7	29.9922	-90.0242	-67
2268	Roth Geotech	46-60	29.9717	-90.2077	-67
2269	Roth Geotech	46-51	29.9675	-90.2007	-67
2270	Roth Geotech	46-26	29.97	-90.1633	-67
2271	Roth Geotech	(PL-97)7	29.9733	-89.9958	-67
2272	Roth Geotech	BLE-9	29.9632	-89.9687	-67
2273	Roth Geotech	46-P23	30.0542	-90.1833	-67
2274	Roth Geotech	98	30.02	-90.3167	-68
2275	Roth Geotech	12R	30.063	-90.165	-68
2276	Roth Geotech	JLD-16	30.06	-90.1633	-68
2277	Roth Geotech	11R	30.0583	-90.165	-68
2278	Roth Geotech	46-P23	30.0542	-90.1833	-68
2279	Roth Geotech	84-8	29.907	-90.0592	-68
2280	Roth Geotech	139-11	29.978	-90.0535	-68
2281	Roth Geotech	139-15	29.9797	-90.0578	-68
2282	Roth Geotech	81-408	29.997	-90.1533	-68
2283	Roth Geotech	84-43	29.9942	-90.1017	-68
2284	Roth Geotech	233-27WU	29.992	-90.0272	-68
2285	Roth Geotech	46-43	29.9675	-90.1833	-68
2286	Roth Geotech	MD-1	29.9717	-90.0725	-68
2287	Roth Geotech	139-2	29.9728	-90.065	-68
2288	Roth Geotech	BLE-7	29.9665	-89.9782	-68
2289	Roth Geotech	BLE-3	29.9712	-89.9698	-68
2290	Roth Geotech	53	30.0542	-90.3675	-69
2291	Roth Geotech	140.6	30.01	-89.935	-69
2292	Roth Geotech	NOA-21	29.9678	-90.0692	-69
2293	Roth Geotech	JLD-14	30.0425	-90.1667	-69
2294	Roth Geotech	41-1	29.9817	-90.2558	-69
2295	Roth Geotech	46-49	29.9675	-90.1842	-69
2296	Roth Geotech	81-56P	29.9813	-90.1145	-69
2297	Roth Geotech	185-75	29.9767	-90.0567	-69
2298	Roth Geotech	24-5	29.9863	-90.02	-69
2299	Roth Geotech	24-2	29.9945	-90.023	-69
2300	Roth Geotech	24-1	29.9967	-90.024	-69
2301	Roth Geotech	81-346	29.998	-90.1733	-69
2302	Roth Geotech	84-42	29.9927	-90.1008	-69
2303	Roth Geotech	26-1408	30.008	-89.9367	-69
2304	Roth Geotech	50	30.0567	-90.3717	-70
2305	Roth Geotech	66	30.0442	-90.3533	-70
2306	Roth Geotech	NOA-24	29.97	-90.0505	-70
2307	Roth Geotech	13R	30.0658	-90.1642	-70
2308	Roth Geotech	9	30.0517	-90.1675	-70
2309	Roth Geotech	4	30.035	-90.1717	-70
2310	Roth Geotech	SBB-7	29.9467	-89.92	-70
2311	Roth Geotech	15-1	30.0122	-90.1178	-70
2312	Roth Geotech	185-79	29.9783	-90.0567	-70
2313	Roth Geotech	139-18	29.9798	-90.0565	-70
2314	Roth Geotech	139-19	29.9808	-90.0575	-70
2315	Roth Geotech	139-9	29.9772	-90.0603	-70

2316	Roth Geotech	185-83	29.9825	-90.055	-70
2317	Roth Geotech	9UL	29.9655	-90.0252	-70
2318	Roth Geotech	117-20-U	29.981	-90.0167	-70
2319	Roth Geotech	84-38	29.9933	-90.0948	-70
2320	Roth Geotech	2-36M	30.0633	-89.7942	-70
2321	Roth Geotech	111-3	29.9738	-90.0958	-70
2322	Roth Geotech	185-75	29.9738	-90.0562	-70
2323	Roth Geotech	17	30.01	-89.9392	-71
2324	Roth Geotech	NOA-27	29.9683	-90.0258	-71
2325	Roth Geotech	NOB-16	29.98	-90.0995	-71
2326	Roth Geotech	NOB-17	29.9648	-90.0992	-71
2327	Roth Geotech	10R	30.055	-90.1667	-71
2328	Roth Geotech	960-115	29.9695	-90.2842	-71
2329	Roth Geotech	84-44	29.9942	-90.1033	-71
2330	Roth Geotech	24-3	29.992	-90.0225	-71
2331	Roth Geotech	46-50	29.9683	-90.1917	-71
2332	Roth Geotech	13	29.9683	-90.145	-71
2333	Roth Geotech	BLE-2	29.9717	-89.9917	-71
2334	Roth Geotech	BLE-4	29.9695	-89.9862	-71
2335	Roth Geotech	70	30.0412	-90.3492	-72
2336	Roth Geotech	71	30.0403	-90.3478	-72
2337	Roth Geotech	73	30.0383	-90.3445	-72
2338	Roth Geotech	74	30.0375	-90.3433	-72
2339	Roth Geotech	132	30.0077	-90.2733	-72
2340	Roth Geotech	NOA-22	29.9683	-90.0592	-72
2341	Roth Geotech	NOA-23	29.9683	-90.055	-72
2342	Roth Geotech	NOB-3	29.8845	-90.0988	-72
2343	Roth Geotech	46-47	29.968	-90.1833	-72
2344	Roth Geotech	81-351B	29.9975	-90.1692	-72
2345	Roth Geotech	185-72	29.9733	-90.0567	-72
2346	Roth Geotech	216-4	29.9642	-90.0725	-72
2347	Roth Geotech	216-3	29.9667	-90.07	-72
2348	Roth Geotech	117-21-U	29.9587	-90.029	-72
2349	Roth Geotech	84-46	29.9948	-90.1083	-72
2350	Roth Geotech	84-30	29.9925	-90.0775	-72
2351	Roth Geotech	104-24	30.0175	-90.0483	-72
2352	Roth Geotech	67	30.0433	-90.3522	-73
2353	Roth Geotech	68	30.0428	-90.3512	-73
2354	Roth Geotech	69	30.0417	-90.35	-73
2355	Roth Geotech	72	30.0395	-90.3467	-73
2356	Roth Geotech	75	30.0367	-90.3422	-73
2357	Roth Geotech	114	30.01	-90.3	-73
2358	Roth Geotech	JLD-15	30.0517	-90.165	-73
2359	Roth Geotech	81-553	29.9922	-90.1162	-73
2360	Roth Geotech	185-68	29.9717	-90.0565	-73
2361	Roth Geotech	3-12	29.96	-89.96	-73
2362	Roth Geotech	101	30.0172	-90.3133	-74
2363	Roth Geotech	2	30.0272	-90.1733	-74
2364	Roth Geotech	185-62	29.9675	-90.056	-74
2365	Roth Geotech	84-48	29.995	-90.1108	-74
2366	Roth Geotech	84-41	29.9937	-90.1	-74
2367	Roth Geotech	46-32	29.9712	-90.1755	-74
2368	Roth Geotech	185-64	29.9692	-90.056	-74
2369	Roth Geotech	54	30.0533	-90.3667	-75
2370	Roth Geotech	76	30.0353	-90.34	-75
2371	Roth Geotech	81	30.0328	-90.3367	-75
2372	Roth Geotech	110	30.0117	-90.305	-75
2373	Roth Geotech	NOB-4	29.89	-90.0958	-75
2374	Roth Geotech	185-59	29.9638	-90.0558	-75
2375	Roth Geotech	84-45	29.9945	-90.1075	-75
2376	Roth Geotech	46-45	29.967	-90.1843	-75
2377	Roth Geotech	80	30.0333	-90.3375	-76
2378	Roth Geotech	82	30.0322	-90.3355	-76

2379	Roth Geotech	83	30.312	-90.3342	-76
2380	Roth Geotech	120	30.0075	-90.2917	-76
2381	Roth Geotech	125	30.007	-90.2838	-76
2382	Roth Geotech	NOA-6	29.9745	-90.1592	-76
2383	Roth Geotech	NOB-12	29.955	-90.0967	-76
2384	Roth Geotech	185-55	29.9617	-90.0555	-76
2385	Roth Geotech	216-2	29.9692	-90.0675	-76
2386	Roth Geotech	28-2	29.9392	-89.9678	-76
2387	Roth Geotech	46-72	29.9733	-90.2167	-76
2388	Roth Geotech	99	30.0187	-90.3153	-76
2389	Roth Geotech	52	30.055	-90.3688	-77
2390	Roth Geotech	55	30.0525	-90.3658	-77
2391	Roth Geotech	78	30.0345	-90.3385	-77
2392	Roth Geotech	131	30.0075	-90.2745	-77
2393	Roth Geotech	NOA-25	29.9692	-90.0305	-77
2394	Roth Geotech	CSS-1	30.0133	-90.1175	-77
2395	Roth Geotech	43-127B	30.0083	-90.24	-77
2396	Roth Geotech	3-14	29.9622	-89.955	-77
2397	Roth Geotech	81-356	29.9978	-90.17	-77
2398	Roth Geotech	46-28	29.971	-90.1712	-77
2399	Roth Geotech	185-51	29.9605	-90.0562	-78
2400	Roth Geotech	128	30.0072	-90.2792	-78
2401	Roth Geotech	7	30.045	-90.1692	-78
2402	Roth Geotech	KWT-1	30.005	-90.2317	-78
2403	Roth Geotech	185-41	29.9563	-90.0615	-78
2404	Roth Geotech	134-1130	29.9592	-90.0777	-78
2405	Roth Geotech	UVL-5	29.925	-89.9062	-78
2406	Roth Geotech	85	30.03	-90.3317	-79
2407	Roth Geotech	113	30.0105	-90.3012	-79
2408	Roth Geotech	129	30.0075	-90.2775	-79
2409	Roth Geotech	130	30.0073	-90.2758	-79
2410	Roth Geotech	NOA-26	29.9695	-90.0292	-79
2411	Roth Geotech	53-1	30.0242	-90.1742	-79
2412	Roth Geotech	84-49	29.995	-90.1117	-79
2413	Roth Geotech	46-P15	30.0495	-90.1647	-79
2414	Roth Geotech	84	30.0308	-90.3333	-80
2415	Roth Geotech	NOA-2	29.9772	-90.2455	-80
2416	Roth Geotech	3	30.0308	-90.1725	-80
2417	Roth Geotech	SBB-6	29.935	-89.92	-80
2418	Roth Geotech	185-27	29.9508	-90.0633	-80
2419	Roth Geotech	USL-1AU	29.9355	-89.921	-80
2420	Roth Geotech	86	30.0292	-90.3308	-80
2421	Roth Geotech	87	30.0283	-90.33	-80
2422	Roth Geotech	116	30.0083	-90.2965	-81
2423	Roth Geotech	81-494	29.9962	-90.1322	-81
2424	Roth Geotech	81-505	29.9958	-90.13	-81
2425	Roth Geotech	56	30.0517	-90.365	-82
2426	Roth Geotech	112	30.0108	-90.3028	-82
2427	Roth Geotech	115	30.0085	-90.2975	-82
2428	Roth Geotech	NOA-7	29.9755	-90.1558	-82
2429	Roth Geotech	112-8	30.0755	-90.1442	-82
2430	Roth Geotech	81-398	29.997	-90.1567	-82
2431	Roth Geotech	81-458	29.9962	-90.1462	-82
2432	Roth Geotech	84-47	29.9948	-90.11	-82
2433	Roth Geotech	UVL-3	29.9232	-89.9055	-82
2434	Roth Geotech	100	30.0178	-90.3147	-83
2435	Roth Geotech	127	30.0068	-90.2812	-83
2436	Roth Geotech	8	30.0483	-90.1683	-83
2437	Roth Geotech	207	29.939	-90.1225	-83
2438	Roth Geotech	81-468	29.9958	-90.1417	-83
2439	Roth Geotech	119	30.0075	-90.2933	-84
2440	Roth Geotech	122	30.0067	-90.2883	-84
2441	Roth Geotech	123	30.0067	-90.2867	-84

2442	Roth Geotech	124	30.0067	-90.285	-84
2443	Roth Geotech	126	30.0068	-90.2825	-84
2444	Roth Geotech	NOA-1	29.9775	-90.2467	-84
2445	Roth Geotech	117	30.0078	-90.295	-86
2446	Roth Geotech	81-473	29.9958	-90.1342	-86
2447	Roth Geotech	40	29.9363	-90.1278	-87
2448	Roth Geotech	NOB-8	29.9283	-90.095	-88
2449	Roth Geotech	R-86.1-L	29.975	-89.925	-88
2450	Roth Geotech	65-KE-8U	29.9738	-90.2633	-88
2451	Roth Geotech	141-2	29.9428	-90.12	-88
2452	Roth Geotech	82-16	29.9483	-90.065	-88
2453	Roth Geotech	463	29.9963	-90.145	-89
2454	Roth Geotech	NOA-9	29.9738	-90.1508	-90
2455	Roth Geotech	81-403B	29.997	-90.155	-90
2456	Roth Geotech	81-500	29.996	-90.1312	-94
2457	Roth Geotech	185-9	29.94	-90.0628	-95
2458	Roth Geotech	NOB-9	29.93	-90.095	-96
2459	Roth Geotech	26-4	29.9295	-90.0938	-96
2460	Roth Geotech	UVL-1	29.9208	-89.905	-96
2461	Roth Geotech	NSL-2AU	29.9205	-89.9033	-103
2462	Roth Geotech	LVL-5	29.8943	-89.8878	-107
2463	Roth Geotech	LVL-4	29.8925	-89.8858	-113
2464	Stanley Balize	MRGO-8D	29.99985538	-89.8769966	-54
2465	Stanley Balize	MRGO-1D	29.97985237	-90.0017798	-57
2466	Stanley Balize	E110.5-UT	29.94466751	-90.12531245	-91
2467	Stanley Balize	E91.09UT	29.94182654	-89.99799026	-72
2468	Stanley Balize	45	29.91140223	-90.01369438	-79
2469	Stanley Balize	NOB-5	29.87470309	-90.03696688	-78
2470	Stanley Balize	55-18	29.86979946	-90.01000727	-64
2471	Stanley Balize	6-7	29.86473497	-90.13664327	-87
2472	Stanley Balize	R72.5R	29.80635397	-90.02174789	-97
2473	Stanley Balize	75	29.77511572	-90.06534386	-87
2474	Stanley Balize	FCD-5.3	29.95110698	-89.96565298	-64
2475	Stanley Balize	R86.1-L	29.92581461	-89.92451012	-86
2476	Stanley Balize	MRGO-21D	29.90325085	-89.78882444	-72
2477	Stanley Balize	SBA-1	29.86769553	-89.98050236	-92
2478	Stanley Balize	R79.9-L	29.85936754	-89.92983635	-90
2479	Stanley Balize	SBE-2	29.85649415	-89.96030928	-89
2480	Stanley Balize	100	29.80941089	-89.75653727	-101
2481	Stanley Balize	LB	29.76540957	-89.7719038	-110
2482	Stanley Balize	MRGO-29	29.87124983	-89.71018901	-86
2483	Stanley Balize	MB-1	29.85497974	-89.63271964	-96
2484	Stanley Balize	B-17	29.84677057	-89.70442432	-92
2485	Stanley Balize	MRGO-6U	29.82364999	-89.55579554	-119
2486	Stanley Balize	BPS-1	29.71699572	-90.12444641	-91
2487	Stanley Balize	C5-1	29.53586556	-90.15742461	-140
2488	Stanley Balize	R65.6R	29.71976622	-89.99150521	-102
2489	Stanley Balize	R60.3LU	29.66334933	-89.93499236	-112
2490	Stanley Balize	R50.5-L	29.60719715	-89.83020389	-122
2491	Stanley Balize	MRGO-62D	29.74138496	-89.31833724	-129
2492	Stanley Balize	FLTB-7	29.39622807	-89.77873754	-153
2493	Stanley Balize	31-3	29.46369515	-89.3954803	-190
2494	Stanley Balize	I-U	29.34391893	-89.46587187	-212
2495	Stanley Balize	BIC-2	29.40182707	-89.12921141	-275
2496	Stanley Balize	BIB-4	29.39051198	-89.03649824	-275
2497	Stanley Balize	41-6	29.47447884	-88.97354082	-295
2498	Stanley Balize	14C-16	29.20264731	-89.56495288	-268
2499	Stanley Balize	14C-18	29.16139067	-89.6030236	-264
2500	Stanley Balize	14C-4	29.16003192	-89.57778982	-277
2501	Stanley Balize	58-3	29.03522689	-89.53956911	-328
2502	Stanley Balize	60-H	29.06977937	-88.93483065	-462
2503	SONRIS	27849	29.39571917	-90.02587487	-180
2504	SONRIS	30093	29.31792321	-89.95087309	-185

2505	SONRIS	45928	29.32462251	-90.01637553	-180
2506	SONRIS	48007	29.33982271	-89.99987381	-170
2507	SONRIS	48445	29.3917218	-90.02297508	-140
2508	SONRIS	65926	29.38801993	-89.98987245	-160
2509	SONRIS	66599	29.43521874	-90.02727324	-150
2510	SONRIS	74216	29.41971987	-89.97997409	-170
2511	SONRIS	96441	29.33742187	-89.97557216	-170
2512	SONRIS	105502	29.40462116	-90.01327455	-170
2513	SONRIS	27073	29.69551116	-89.77466615	-150
2514	SONRIS	27155	29.31261955	-89.54996087	-220
2515	SONRIS	30076	29.49810156	-89.69419656	-160
2516	SONRIS	31608	29.49621406	-89.69676443	-150
2517	SONRIS	40020	29.56810953	-89.51315776	-150
2518	SONRIS	43744	29.50161593	-89.71226675	-150
2519	SONRIS	44288	29.67690971	-89.6354607	-150
2520	SONRIS	48152	29.81130629	-90.01337111	-110
2521	SONRIS	85104	29.31661778	-89.51065927	-220
2522	SONRIS	86536	29.12332381	-89.17044883	-310
2523	SONRIS	88480	29.43741641	-89.70086621	-150
2524	SONRIS	88799	29.11912438	-89.16765123	-305
2525	SONRIS	89113	29.4435161	-89.70106537	-150
2526	SONRIS	22156	29.18692042	-89.41024751	-300
2527	SONRIS	242735	29.23818983	-89.42410267	-270
2528	SONRIS	49430	29.75790146	-89.14924212	-150
2529	USACE	LGM-PS2-1U	29.470417	-90.341944	-163
2530	USACE	MOTG-L-4U	29.512594	-90.416258	-126
2531	USACE	MTOG-A-5U	29.550389	-90.798	-142
2532	USACE	MTOG-A-9U	29.535861	-90.792111	-124
2533	USACE	MTOG-L315U	29.518856	-90.411408	-151
2534	Yu et al. 2012	I-1	29.85716365	-93.06729787	-16
2535	Yu et al. 2012	II-1	29.85806634	-93.06688434	-15
2536	Yu et al. 2012	III-1	29.85860783	-93.0668847	-13
2537	Yu et al. 2012	I-1	29.84634775	-93.02940083	-15
2538	Yu et al. 2012	II-1	29.84562567	-93.02981471	-16
2539	Yu et al. 2012	III-1	29.84508414	-93.03002159	-19
2540	Yu et al. 2012	I-1	29.83985143	-92.97867543	-7
2541	Yu et al. 2012	II-1	29.83840749	-92.97888277	-8
2542	Yu et al. 2012	III-1	29.83209056	-92.98198937	-12
2543	Yu et al. 2012	IV-1	29.82974411	-92.9819898	-16
2544	Yu et al. 2012	V-1	29.84364186	-92.97867462	-6
2545	Yu et al. 2012	VI-1	29.84364205	-92.97991688	-5
2546	Yu et al. 2012	VII-1	29.84364221	-92.98095209	-6
2547	Gonzalez and Törnqvist		29.88506212	-91.78430828	-2
2548	Gonzalez and Törnqvist		29.8839794	-91.78432142	-3
2549	Gonzalez and Törnqvist		29.88572981	-91.78430018	-1
2550	Gonzalez and Törnqvist		29.85079252	-91.73182693	-1
2551	Gonzalez and Törnqvist		29.85077448	-91.73182716	-1
2552	Gonzalez and Törnqvist		29.85063914	-91.73182887	-1
2553	Gonzalez and Törnqvist		29.85036945	-91.73193579	-2
2554	Gonzalez and Törnqvist		29.8498281	-91.73194264	-1
2555	Gonzalez and Törnqvist		29.8484767	-91.73216674	-2
2556	Gonzalez and Törnqvist		29.84838647	-91.73216788	-2
2557	Gonzalez and Törnqvist		29.84811679	-91.7322748	-1
2558	Gonzalez and Törnqvist		29.84242781	-91.71319789	-2
2559	Gonzalez and Törnqvist		29.84206892	-91.7134095	-2
2560	Gonzalez and Törnqvist		29.84170903	-91.71351762	-2
2561	Gonzalez and Törnqvist		29.84171105	-91.71372461	-2
2562	Gonzalez and Törnqvist		29.84036069	-91.71405243	-2
2563	Gonzalez and Törnqvist		29.84297723	-91.7140189	-1
2564	Gonzalez and Törnqvist		29.84305636	-91.71287931	-1
2565	Arabie Environmental		29.80751714	-93.32267334	-44
2566	Arabie Environmental		29.80846818	-93.32063759	-49
2567	Arabie Environmental		29.80682477	-93.32177698	-59

2568	Arabie Environmental		29.81162432	-93.32218009	-43
2569	Arabie Environmental		29.8085848	-93.32559384	-41
2570	FISK 1948		30.08973916	-93.32467682	-10
2571	FISK 1948		30.08683273	-93.32490423	-15
2572	FISK 1948		30.08396383	-93.3251763	-12
2573	FISK 1948		30.07581898	-93.32596301	-43
2574	FISK 1948		30.07300834	-93.32617031	-40
2575	FISK 1948		30.07019571	-93.32650931	-40
2576	FISK 1948		30.06715396	-93.32684371	-40
2577	FISK 1948		30.06434232	-93.32711681	-40
2578	FISK 1948		30.06170152	-93.32745919	-40
2579	FISK 1948		30.05906371	-93.32760401	-38
2580	FISK 1948		30.05619279	-93.32800762	-40
2581	FISK 1948		30.05326858	-93.32814669	-28
2582	FISK 1948		30.05045694	-93.32841972	-23
2583	FISK 1948		30.04494819	-93.32896804	-25
2584	FISK 1948		30.0420678	-93.32923965	-7
2585	FISK 1948		30.03977266	-93.32945711	-8
2586	FISK 1948		30.03678916	-93.32972663	-4
2587	FISK 1948		30.03374939	-93.32992915	-4
2588	FISK 1948		30.02278813	-93.33109234	-17
2589	FISK 1948		30.01980462	-93.33136177	-5
2590	FISK 1948		30.03110956	-93.33020553	-13
2591	FISK 1948		30.0282969	-93.33054427	-12
2592	FISK 1948		30.02548524	-93.33081717	-20
2593	FISK 1948		30.01699395	-93.3315688	-8
2594	FISK 1948		30.01153945	-93.33231535	-3
2595	FISK 1948		30.00872777	-93.33258815	-2
2596	FISK 1948		29.99187221	-93.33402743	0
2597	FISK 1948		29.97500323	-93.33559752	-19
2598	FISK 1948		29.97770034	-93.33532261	-18
2599	FISK 1948		29.98045573	-93.33498304	-17
2600	FISK 1948		29.98332367	-93.33477734	-16
2601	FISK 1948		29.98613433	-93.33457048	-15
2602	FISK 1948		29.988947	-93.33423201	-8
2603	FISK 1948		29.94450163	-93.33840644	-15
2604	FISK 1948		29.94645113	-93.33831404	-24
2605	FISK 1948		29.94983961	-93.33779	-25
2606	FISK 1948		29.95236189	-93.33770909	-18
2607	FISK 1948		29.95523085	-93.33743775	-11
2608	FISK 1948		29.95769986	-93.33709256	-14
2609	FISK 1948		29.95964835	-93.3370659	-24
2610	FISK 1948		29.96108433	-93.33683155	-16
2611	FISK 1948		29.96366589	-93.33662019	-16
2612	FISK 1948		29.97209891	-93.33593407	-18
2613	FISK 1948		29.96923196	-93.33607392	-17
2614	FISK 1948		29.96647656	-93.33641342	-16
2615	FISK 1948		29.9413117	-93.33868443	-40
2616	FISK 1948		29.93844073	-93.33908722	-30
2617	FISK 1948		29.92168712	-93.34059217	-40
2618	FISK 1948		29.92432598	-93.34038215	-27
2619	FISK 1948		29.92713667	-93.34017557	-23
2620	FISK 1948		29.92994837	-93.33990322	-24
2621	FISK 1948		29.93281734	-93.339632	-13
2622	FISK 1948		29.93557176	-93.33935847	-14
2623	FISK 1948		29.95896888	-93.32028595	-45
2624	FISK 1948		29.95807671	-93.30340709	-22
2625	FISK 1948		29.95732314	-93.28669579	-13
2626	FISK 1948		30.05026729	-93.31383721	-45
2627	FISK 1948		30.04469933	-93.31411416	-45
2628	FISK 1948		30.0304758	-93.3151879	-15
2629	FISK 1948		29.94482973	-93.321508	-18
2630	FISK 1948		29.98764971	-93.31827502	-10

2631	FISK 1948		29.97321517	-93.31917825	-15
2632	FISK 1948		30.00183122	-93.31700769	-16
2633	FISK 1948		29.92980578	-93.32258138	-15
2634	FISK 1948		30.01618416	-93.3160032	-45
2635	FISK 1948		30.01469716	-93.28313713	-25
2636	FISK 1948		30.08119646	-93.32531206	-40
2637	FISK 1948		29.75789453	-92.26437118	-10
2638	FISK 1948		29.75727411	-92.26228743	-12
2639	FISK 1948		29.75833235	-92.26484391	-7
2640	FISK 1948		29.75853685	-92.26428113	-7
2641	FISK 1948		29.75771303	-92.26357331	-9
2642	FISK 1948		29.75887561	-92.26668114	-6
2643	FISK 1948		29.75813135	-92.26347851	-7
2644	FISK 1948		29.75602532	-92.26477865	-18
2645	FISK 1948		29.73632988	-92.38499982	-11
2646	FISK 1948		29.76131323	-92.21052475	-24
2647	FISK 1948		29.77124233	-92.20355233	-18
2648	FISK 1948		29.73602538	-92.24333204	-10
2649	FISK 1948		29.71048245	-92.20210604	-16
2650	FISK 1948		29.70011925	-92.20796314	-17
2651	FISK 1948		29.75796644	-92.26632642	-11
2652	FISK 1948		29.73764233	-92.37573322	-14
2653	FISK 1948		29.73900555	-92.36598651	-14
2654	FISK 1948		29.74011421	-92.35824592	-25
2655	FISK 1948		29.74147317	-92.34888084	-22
2656	FISK 1948		29.74258521	-92.34056669	-16
2657	FISK 1948		29.74487131	-92.32435064	-5
2658	FISK 1948		29.74787974	-92.30424277	-6
2659	FISK 1948		29.74833694	-92.30361935	-5
2660	FISK 1948		29.74944715	-92.29841614	-10
2661	FISK 1948		29.75156013	-92.29287028	-4
2662	FISK 1948		29.7528158	-92.28725869	-8
2663	FISK 1948		29.75534857	-92.28223508	-10
2664	FISK 1948		29.75582068	-92.27620626	-10
2665	FISK 1948		29.75717014	-92.2707043	-10
2666	FISK 1948		29.75742264	-92.25858801	-10
2667	FISK 1948		29.75706476	-92.25186883	-10
2668	FISK 1948		29.75727213	-92.24603117	-8
2669	FISK 1948		29.75230257	-92.2447301	-10
2670	FISK 1948		29.75101601	-92.2385516	-10
2671	FISK 1948		29.74759817	-92.2332795	-10
2672	FISK 1948		29.74942352	-92.22759058	-12
2673	FISK 1948		29.74722575	-92.21794578	-14
2674	FISK 1948		29.74616228	-92.21313204	-13
2675	FISK 1948		29.74660324	-92.20773101	-10
2676	FISK 1948		29.72828905	-92.36795761	-30
2677	FISK 1948		29.71564294	-92.36721161	-35
2678	FISK 1948		29.72813332	-92.34190458	-10
2679	FISK 1948		29.73340798	-92.36084429	-30
2680	FISK 1948		29.74196752	-92.37430845	-10
2681	FISK 1948		29.74550158	-92.36203531	-25
2682	FISK 1948		29.74871768	-92.38997172	-25
2683	FISK 1948		29.75805022	-92.39072688	-15
2684	FISK 1948		29.75829571	-92.37792553	-10
2685	FISK 1948		29.75827477	-92.37152334	-10
2686	FISK 1948		29.76556388	-92.39146296	-10
2687	FISK 1948		29.76900045	-92.39158139	-23
2688	FISK 1948		29.77300262	-92.39260879	-10
2689	FISK 1948		29.77345979	-92.37118839	-15
2690	FISK 1948		29.77539582	-92.37088011	-5
2691	FISK 1948		29.77428137	-92.35773421	-10
2692	FISK 1948		29.76906366	-92.34717388	-15
2693	FISK 1948		29.77407821	-92.34697842	-10

2694	FISK 1948		29.75792301	-92.35239595	-10
2695	FISK 1948		29.73833005	-92.28542929	-23
2696	FISK 1948		29.74557183	-92.29975272	-25
2697	FISK 1948		29.74174802	-92.2921934	-25
2698	FISK 1948		29.73449203	-92.27804093	-24
2699	FISK 1948		29.73054835	-92.27037959	-16
2700	FISK 1948		29.72662971	-92.26333446	-21
2701	FISK 1948		29.72303761	-92.25647751	-21
2702	FISK 1948		29.71585135	-92.24290861	-25
2703	FISK 1948		29.7120825	-92.23556613	-23
2704	FISK 1948		29.7085504	-92.22845192	-25
2705	FISK 1948		29.70478216	-92.22089861	-25
2706	FISK 1948		29.70110721	-92.21360988	-24
2707	FISK 1948		29.69757387	-92.20650406	-14
2708	FISK 1948		29.69391899	-92.19967111	-16
2709	FISK 1948		29.69000325	-92.19160612	-24
2710	FISK 1948		29.68667178	-92.18539895	-21
2711	FISK 1948		29.68266255	-92.17781616	-18
2712	FISK 1948		29.67508867	-92.16292261	-9
2713	FISK 1948		29.67158138	-92.15598468	-9
2714	FISK 1948		29.66364774	-92.13999143	-9
2715	FISK 1948		29.69948046	-92.28026021	-21
2716	FISK 1948		29.69701316	-92.24429319	-21
2717	FISK 1948		29.72089494	-92.24967944	-21
2718	FISK 1948		29.69216224	-92.25187707	-21
2719	FISK 1948		29.70342501	-92.24910935	-19
2720	FISK 1948		29.66891932	-92.236261	-20
2721	FISK 1948		29.65230227	-92.23139681	-18
2722	FISK 1948		29.65304538	-92.22744064	-20
2723	FISK 1948		29.66597797	-92.25591455	-20
2724	FISK 1948		29.66804277	-92.20520718	-23
2725	FISK 1948		29.74478636	-92.20739616	-10
2726	FISK 1948		29.73423842	-92.20511587	-12
2727	FISK 1948		29.72348822	-92.1972961	-14
2728	FISK 1948		29.76926198	-92.98968051	-19
2729	FISK 1948		29.77006741	-92.98088293	-20
2730	FISK 1948		29.77008462	-92.98065336	-23
2731	FISK 1948		29.77010244	-92.98037454	-25
2732	FISK 1948		29.77009459	-92.97985724	-20
2733	FISK 1948		29.7691649	-92.97402415	-20
2734	FISK 1948		29.769004	-92.9675101	-18
2735	FISK 1948		29.77240142	-92.98276938	-19
2736	FISK 1948		29.76930477	-92.98032389	-18
2737	FISK 1948		29.76235346	-93.01530132	-20
2738	FISK 1948		29.76455057	-93.01371122	-20
2739	FISK 1948		29.76769803	-93.0118116	-20
2740	FISK 1948		29.75582494	-93.01306022	-20
2741	FISK 1948		29.75389988	-93.00958055	-20
2742	FISK 1948		29.75267612	-93.00726184	-20
2743	FISK 1948		29.75191147	-93.00544333	-23
2744	FISK 1948		29.75119251	-93.0028459	-35
2745	FISK 1948		29.74249526	-93.01652935	-28
2746	FISK 1948		29.74305863	-93.0200678	-30
2747	FISK 1948		29.7435067	-93.02365523	-30
2748	FISK 1948		29.74386117	-93.02727229	-35
2749	FISK 1948		29.74519529	-93.0304464	-20
2750	FISK 1948		29.74653273	-93.03335802	-25
2751	FISK 1948		29.7492549	-93.03993739	-30
2752	FISK 1948		29.75059042	-93.04298056	-28
2753	FISK 1948		29.75158474	-93.04582102	-35
2754	FISK 1948		29.76128998	-93.0616164	-30
2755	FISK 1948		29.76330315	-93.09553649	-25
2756	FISK 1948		29.76277607	-93.09211241	-25

2757	FISK 1948		29.762196	-93.08835909	-30
2758	FISK 1948		29.76150039	-93.08466946	-28
2759	FISK 1948		29.75927314	-93.09697571	-30
2760	FISK 1948		29.78099938	-93.09927382	-26
2761	FISK 1948		29.78074833	-93.09574589	-22
2762	FISK 1948		29.77487096	-93.09564215	-20
2763	FISK 1948		29.77185723	-93.09562316	-30
2764	FISK 1948		29.76609873	-93.09555573	-29
2765	FISK 1948		29.86674448	-93.08281229	-9
2766	FISK 1948		29.7429001	-93.0614018	-30
2767	FISK 1948		29.74252914	-93.05783906	-20
2768	FISK 1948		29.73293746	-93.02900711	-30
2769	FISK 1948		29.72884741	-93.01522053	-30
2770	FISK 1948		29.72796974	-93.01151323	-30
2771	FISK 1948		29.72705691	-93.00821569	-28
2772	FISK 1948		29.72607998	-93.00525903	-32
2773	FISK 1948		29.72229107	-92.99672388	-25
2774	FISK 1948		29.72374253	-92.99992756	-25
2775	FISK 1948		29.72498766	-93.00292276	-30
2776	FISK 1948		29.73439506	-93.00468672	-29
2777	FISK 1948		29.7342288	-93.00133309	-31
2778	FISK 1948		29.73435907	-92.99812116	-30
2779	FISK 1948		29.73755974	-93.00456859	-30
2780	FISK 1948		29.7351073	-92.97422608	-30
2781	FISK 1948		29.73200361	-92.97424358	-28
2782	FISK 1948		29.72887135	-92.97415805	-25
2783	FISK 1948		29.72562019	-92.97403638	-30
2784	FISK 1948		29.72272448	-92.97412567	-32
2785	FISK 1948		29.72483255	-92.9821263	-28
2786	FISK 1948		29.7276085	-92.98206945	-30
2787	FISK 1948		29.73709989	-92.98191805	-25
2788	FISK 1948		29.7404427	-92.98187052	-25
2789	FISK 1948		29.74318751	-92.98191573	-26
2790	FISK 1948		29.72081195	-92.99334206	-30
2791	FISK 1948		29.71982777	-92.99093261	-30
2792	FISK 1948		29.71761907	-92.96954646	-30
2793	FISK 1948		29.74908269	-92.98202994	-28
2794	FISK 1948		29.75174014	-92.9819028	-23
2795	FISK 1948		29.75499599	-92.98164878	-23
2796	FISK 1948		29.75759333	-92.98155488	-30
2797	FISK 1948		29.76061178	-92.98119432	-23
2798	FISK 1948		29.76432914	-92.9807837	-23
2799	FISK 1948		29.76397535	-92.87100612	-35
2800	FISK 1948		29.76382725	-92.86733738	-30
2801	FISK 1948		29.76377834	-92.86334183	-32
2802	FISK 1948		29.76367966	-92.85950969	-30
2803	FISK 1948		29.78455621	-92.8772893	-40
2804	FISK 1948		29.78450376	-92.87362126	-45
2805	FISK 1948		29.78411897	-92.86978391	-26
2806	FISK 1948		29.78285716	-92.85924466	-30
2807	FISK 1948		29.78256932	-92.85524471	-30
2808	FISK 1948		29.7825112	-92.85201455	-28
2809	FISK 1948		29.78231231	-92.84856332	-25
2810	FISK 1948		29.78230302	-92.84522444	-30
2811	FISK 1948		29.78210395	-92.84177324	-28
2812	FISK 1948		29.78214347	-92.83832564	-30
2813	FISK 1948		29.78203782	-92.83504006	-20
2814	FISK 1948		29.77287626	-92.85531583	-24
2815	FISK 1948		29.76977849	-92.85565169	-28
2816	FISK 1948		29.76681818	-92.85566127	-26
2817	FISK 1948		29.76347535	-92.85571974	-32
2818	FISK 1948		29.7613724	-92.85590655	-30
2819	FISK 1948		29.75826825	-92.85596865	-28

2820	FISK 1948		29.7634694	-92.85210793	-34
2821	FISK 1948		29.76336535	-92.84871352	-24
2822	FISK 1948		29.76331084	-92.84515571	-24
2823	FISK 1948		29.7631595	-92.84170588	-30
2824	FISK 1948		29.7572308	-93.0913865	-19
2825	FISK 1948		29.75481489	-93.08234941	-20
2826	FISK 1948		29.77302364	-92.92047189	-19
2827	FISK 1948		29.84414625	-92.86970314	-16
2828	FISK 1948		29.81573058	-92.99757488	-13
2829	FISK 1948		29.81710123	-92.99773464	-14
2830	FISK 1948		29.85444646	-93.06368899	-12
2831	FISK 1948		29.81214058	-92.99735073	-19
2832	FISK 1948		29.8162384	-92.94922289	-16
2833	FISK 1948		29.77368799	-92.35356245	-15
2834	FISK 1948		29.68517111	-92.20766114	-20
2835	FISK 1948		29.71767577	-92.24648469	-12
2836	Flock USACE		29.61392	-91.73184	-30
2837	Flock USACE		29.60076	-91.70987	-31
2838	Flock USACE		29.59374	-91.69353	-34
2839	Flock USACE		29.9	-91.93142	-3
2840	Flock USACE		29.87803	-91.91898	-5
2841	Flock USACE		29.95886	-91.81568	10
2842	Flock USACE		29.80755	-91.77226	-24
2843	Flock USACE		29.77458	-91.77463	-30
2844	Flock USACE		29.87847	-91.66415	-8
2845	Flock USACE		29.87468	-91.65204	-8
2846	Flock USACE		29.87112	-91.64298	-9
2847	Flock USACE		29.86861	-91.63754	-10
2848	Flock USACE		29.67433	-91.93411	-29
2849	Flock USACE		29.67097	-91.92223	-26
2850	Flock USACE		29.64806	-91.90932	-31
2851	Flock USACE		29.59287	-91.87408	-42
2852	Flock USACE		29.55961	-91.88845	-51
2853	Flock USACE		29.71872	-91.86909	-35
2854	Flock USACE		29.6835	-91.79852	-43
2855	Flock USACE		29.68057	-91.79868	-43
2856	Flock USACE		29.67703	-91.79678	-44
2857	Flock USACE		29.67175	-91.79323	-39
2858	Flock USACE		29.66884	-91.79147	-36
2859	Flock USACE		29.65053	-91.78573	-36
2860	Flock USACE		29.61559	-91.7961	-44
2861	Poche and Vutera		29.62500996	-91.87895	-35
2862	Poche and Vutera		29.62411069	-91.87877848	-34
2863	Poche and Vutera		29.58710586	-91.87175397	-43
2864	Poche and Vutera		29.57091609	-91.95786461	-49
2865	Poche and Vutera		29.5502206	-91.91472813	-48
2866	Poche and Vutera		29.57354659	-92.00070123	-46
2867	USACE		29.935219	-91.844083	-5
2868	USACE		29.930789	-91.839944	-5
2869	USACE		29.924044	-91.836886	-4
2870	USACE		29.917517	-91.837911	-3
2871	USACE		29.909731	-91.836839	-4
2872	USACE		29.903425	-91.839497	-5
2873	USACE		29.896364	-91.837978	-10
2874	USACE		29.889983	-91.839367	-15
2875	USACE		29.882003	-91.83835	-20
2876	USACE		29.875283	-91.839217	-20
2877	USACE		29.868311	-91.838183	-20
2878	USACE		29.864761	-91.838783	-22
2879	USACE		29.854939	-91.837656	-24
2880	USACE		29.849581	-91.835696	-25
2881	USACE		29.843772	-91.839939	-28
2882	USACE		29.8455	-91.847139	-20

2883	USACE		29.845733	-91.862694	-17
2884	USACE		29.845753	-91.878539	-15
2885	USACE		29.846053	-91.893842	-25
2886	USACE		29.846067	-91.909917	-14
2887	USACE		29.84625	-91.925286	-5
2888	USACE		29.843867	-91.941836	-7
2889	USACE		29.840992	-91.956972	-10
2890	USACE		29.838289	-91.972675	-10
2891	USACE		29.83453	-91.986725	0
2892	USACE		29.828578	-92.005492	-2
2893	USACE		29.824647	-92.017494	-4
2894	USACE		29.820233	-92.0327	-5
2895	USACE		29.815317	-92.047917	-8
2896	USACE		29.809464	-92.063083	-7
2897	USACE		29.804256	-92.078983	-2
2898	USACE		29.799842	-92.092994	-3
2899	USACE		29.795661	-92.108056	-4
2900	USACE		29.790942	-92.122861	-5
2901	USACE		29.785683	-92.137547	-4
2902	USACE		29.788111	-92.145719	-3
2903	USACE		29.778056	-92.168636	-20
2904	USACE		29.772122	-92.179675	-7
2905	USACE		29.764658	-92.190428	-7
2906	USACE		29.756581	-92.203383	-7
2907	USACE		29.750484	-92.213303	-16
2908	USACE		29.740892	-92.229036	-13
2909	USACE		29.732494	-92.241497	-14
2910	USACE		29.719994	-92.246775	-15
2911	USACE		29.706353	-92.248992	-20
2912	USACE		29.692681	-92.251948	-19
2913	USACE		29.679783	-92.254508	-21
2914	USACE		29.639111	-92.267342	-39
2915	USACE		29.626633	-92.272289	-27
2916	USACE		29.614908	-92.281139	-28
2917	USACE		29.603681	-92.289428	-32
2918	USACE		29.590994	-92.298325	-40
2919	USACE		29.576931	-92.30165	-39
2920	USACE		29.563381	-92.304142	-44
2921	USACE		29.843911	-91.855822	-18
2922	USACE		29.844058	-91.871067	-17
2923	USACE		29.843861	-91.886617	-21
2924	USACE		29.843992	-91.902001	-15
2925	USACE		29.843814	-91.917443	-14
2926	USACE		29.842764	-91.936073	-8
2927	USACE		29.840958	-91.945694	-13
2928	USACE		29.837794	-91.963789	-10
2929	USACE		29.834409	-91.979933	-15
2930	USACE		29.829653	-91.995069	-10
2931	USACE		29.82465	-92.009606	-10
2932	USACE		29.819892	-92.024619	-8
2933	USACE		29.815314	-92.038656	-6
2934	USACE		29.809272	-92.055094	-6
2935	USACE		29.804981	-92.070058	-1
2936	USACE		29.799711	-92.086608	-4
2937	USACE		29.795519	-92.099872	-5
2938	USACE		29.790548	-92.114439	-8
2939	USACE		29.786206	-92.129175	-9
2940	USACE		29.779481	-92.159969	-20
2941	USACE		29.772806	-92.173219	-13
2942	USACE		29.767042	-92.181767	-7
2943	USACE		29.7597	-92.194472	-7
2944	USACE		29.750978	-92.208006	-16
2945	USACE		29.742469	-92.221722	-15

2946	USACE		29.734738	-92.233679	-15
2947	USACE		29.725439	-92.241667	-20
2948	USACE		29.713114	-92.245483	-16
2949	USACE		29.699089	-92.246886	-24
2950	USACE		29.685726	-92.250384	-25
2951	USACE		29.67185	-92.252672	-22
2952	USACE		29.658328	-92.257644	-30
2953	USACE		29.645853	-92.261917	-23
2954	USACE		29.632933	-92.266706	-30
2955	USACE		29.6191	-92.272992	-32
2956	USACE		29.608586	-92.282581	-31
2957	USACE		29.597106	-92.291283	-37
2958	USACE		29.583306	-92.297183	-37
2959	USACE		29.56995	-92.30049	-40
2960	USACE		29.559247	-92.302054	-43
2961	USACE		29.553511	-92.301572	-45
2962	USACE		29.546386	-92.304069	-45
2963	USACE		29.540544	-92.305669	-45
2964	Törnqvist et al.	I	30.09874861	-90.68422603	-6
2965	Törnqvist et al.	II	30.09856827	-90.68423024	-6
2966	Törnqvist et al.	III	30.0984781	-90.68423234	-6
2967	Törnqvist et al.	IV	30.09712737	-90.68436758	-9
2968	Törnqvist et al.	V	30.09694703	-90.68437179	-8
2969	Törnqvist et al.	VI	30.09667743	-90.68442995	-8
2970	Törnqvist et al.	VII	30.09649709	-90.68443415	-8
2971	Törnqvist et al.	VIII	30.09622658	-90.68444046	-7
2972	Törnqvist et al.	IX	30.09154592	-90.68501641	-9
2973	Törnqvist et al.	X	30.09127449	-90.68497087	-10
2974	Törnqvist et al.	XI	30.09060917	-90.68560878	-10
2975	Törnqvist et al.	XII	30.09042883	-90.68561299	-11
2976	Törnqvist et al.	XIII	30.08822238	-90.68582	-11
2977	Törnqvist et al.	I	30.06780352	-90.68401381	-16
2978	Törnqvist et al.	II	30.06726797	-90.68433742	-18
2979	Törnqvist et al.	III	30.06699563	-90.68424005	-19
2980	Törnqvist et al.	IV	30.0659081	-90.68395426	-21
2981	Törnqvist et al.	V	30.06554558	-90.68385899	-21
2982	Törnqvist et al.	VI	30.0649089	-90.6835627	-22
2983	Törnqvist et al.	VII	30.062916	-90.6830906	-20
2984	Törnqvist et al.	VIII	30.06219098	-90.68290008	-20
2985	Törnqvist et al.	IX	30.07829078	-90.68532527	-12
2986	Törnqvist et al.	X	30.07738541	-90.68513891	-12
2987	Törnqvist et al.	XI	30.07674873	-90.68484258	-12
2988	Törnqvist et al.	XII	30.07421115	-90.68417567	-13
2989	Törnqvist et al.	XIII	30.07258259	-90.68390246	-14
2990	Törnqvist et al.	XIV	30.07177105	-90.68392137	-15
2991	Törnqvist et al.	XV	30.07113254	-90.68352139	-16
2992	Törnqvist et al.	IV	30.0388848	-90.71195528	-24
2993	Törnqvist et al.	V	30.03751777	-90.71115726	-27
2994	Törnqvist et al.	VI	30.03687934	-90.71075722	-30
2995	Törnqvist et al.	VII	30.03669719	-90.71065773	-31
2996	Törnqvist et al.	VIII	30.03596678	-90.71015614	-34
2997	Törnqvist et al.	I	29.80596552	-91.65810235	-16
2998	Törnqvist et al.	II	29.80869114	-91.65992843	-22
2999	Törnqvist et al.	III	29.77942813	-91.67521383	-33
3000	USACE		29.6215539	-91.88255991	-38
3001	USACE		30.78552368	-92.1489869	-32
3002	USACE		30.90546989	-92.16953945	-28
3003	USACE		30.95070088	-92.17208097	21
3004	USACE		30.85075419	-92.00555141	13
3005	USACE		30.89047768	-92.12138311	1
3006	USACE		30.91510877	-92.21561781	-20
3007	USACE		30.92101394	-92.23248401	-47
3008	USACE	P-1	30.97987604	-92.2592129	33

3009	USACE		30.95394929	-92.27934882	-8
3010	USACE		30.95119448	-92.28710811	3
3011	USACE		30.6948468	-92.0507837	-66
3012	USACE		30.54627016	-92.00826126	-29


Louisiana Geological Survey
Earth Science
Serving Louisiana
1934